

**QUANTUM MECHANICAL AND FTIR-FTRAMAN  
SPECTRAL ANALYSIS OF CERTAIN  
BIOLOGICALLY ACTIVE AROMATIC COMPOUNDS**

Thesis submitted to the Bharathidasan University in partial fulfillment  
for the award of the degree of  
**DOCTOR OF PHILOSOPHY IN PHYSICS**

By

**M. GOVINDARAJAN**

*Under the supervision of*

**Dr. K. GANESAN**

Reader and HOD of Physics

T.B.M.L. College, Porayar-609 307.



**BHARATHIDASAN UNIVERSITY**

**TIRUCHIRAPPALI - 620 024**

**MARCH - 2011**

6489

530

Q12

C1

## CERTIFICATE

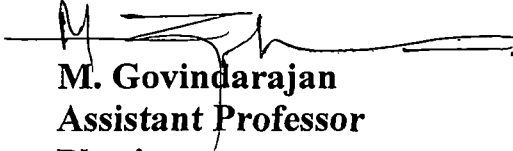
Certified that this thesis entitled “**QUANTUM MECHANICAL AND FTIR-FT-RAMAN SPECTRAL ANALYSIS OF CERTAIN BIOLOGICALLY ACTIVE AROMATIC COMPOUNDS**” submitted for the award of degree of Doctor of Philosophy in Physics, in Bharathidasan University, Tiruchirappali, is an authentic record of the investigation carried out by **Shri. M.Govindarajan** under my supervision and guidance. This thesis or any part thereof has not been submitted elsewhere for the award of any Degree, Diploma, Associateship, Fellowship or any other similar titles.

*K. Ganesan*  
C  
27.02.2011

**Dr. K. GANESAN**  
**Reader and HOD of Physics**  
**T.B.M.L College,**  
**Porayar – 609 307.**

## DECLARATION

I hereby declare that the thesis entitled “**QUANTUM MECHANICAL AND FTIR-FT-RAMAN SPECTRAL ANALYSIS OF CERTAIN BIOLOGICALLY ACTIVE AROMATIC COMPOUNDS**” submitted for the award of Ph.D Degree is the original work carried out under the supervision of **Prof. K. GANESAN, Ph.D.**, Reader and HOD of Physics, T.B.M.L College, Porayar.



**M. Govindarajan**  
Assistant Professor  
Physics,  
MGGA.College, Mahe  
UT of Pondicherry  
India.

## ACKNOWLEDGEMENT

The words fail to express my deep sense of regards and gratitude to **Prof. K. GANESAN, Ph.D** Reader and HOD of Physics, T.B.M.L College, Porayar, Tamilnadu, for his dedicated effort, advice, timely suggestions, excellent guidance and encouragement for this thesis work. This work would not have been satisfactorily accomplished but for his genuine cordiality, patience, encouragement and motivation.

I convey my sincere thanks to **The Principal and the HOD and Professors** of Department of Physics, T.B.M.L College, Porayar for providing me the opportunity to carry out the investigation in their Research center.

I also thank **Dr. S. PERIANDY**, Associate Prof.Physics, Tagore Arts College, Puducherry for his kind constant help and critical suggestions. I also thank **Dr. R.MADIVANANE**, Associate Prof.Physics, Bharathidasan Govt. College for Women, Puducherry, for his inspiring words, constant help and critical suggestions.

My heartfelt thanks are due to Mr. S.Ramalingam for his help in drawing. I also acknowledge his technical help in bringing this thesis and my sincere thanks to Mr. G.Nagabalasubramanian who helped me in technical work. I also thank to all my co-researchers, friends and relatives who helped me towards the successful completion of the work. It is my foremost bound duty to thank my parents, family for their blessings and my wife and daughters for their affectionate co-operation.

  
(M.GOVINDARAJAN)

**Dedicated to**  
**My Parents**

## CONTENTS

	Page No.
<b>PREFACE</b>	<b>I - VII</b>
<b>CHAPTER – 1</b>	
<i>VIBRATIONAL SPECTROSCOPY THEORY AND TECHNIQUES</i>	<b>1-82</b>
<b>CHAPTER – 2</b>	
<i>SPECTRAL AND THEORETICAL VIBRATIONAL ANALYSIS OF 2-BROMOBENZOIC AND ANTHRANILIC ACIDS</i>	<b>83-96</b>
<b>CHAPTER – 3</b>	
<i>FTIR – FT-RAMAN SPECTRAL AND QUANTUM MECHANICAL VIBRATIONAL ANALYSIS OF 2, 5-DIBROMO PYRIDINE AND 2, 6-DIBROMO PYRIDINE</i>	<b>97-106</b>
<b>CHAPTER – 4</b>	
<i>FTIR – FT-RAMAN SPECTRAL AND GUASSIAN VIBRATIONAL ANALYSIS OF 2, 5-DIMETHYL ANILINE AND 2, 6-DIMETHYL ANILINE</i>	<b>107-118</b>
<b>CHAPTER – 5</b>	
<i>QUANTUM MECHANICAL AND FTIR &amp; FTRAMAN SPECTRAL ANALYSIS OF 1-AMNIO-4-BROMONAPHTHALENE</i>	<b>119-130</b>
<b>CHAPTER – 6</b>	
<i>EXPERIMENTAL (FTIR and FT-Raman) AND DFT STUDIES OF 1-METHOXYNAPHTHALENE</i>	<b>131-145</b>
<b>CHAPTER – 7</b>	
<i>LSDA, B3LYP and B3PW91 COMPARATIVE VIBRATIONAL SPECTROSCOPIC ANALYSIS OF <math>\alpha</math>-ACETONAPHTHONE</i>	<b>146-157</b>
<b>CHAPTER-8</b>	
<i>BIBLIOGRAPHY</i>	

## PREFACE

Vibrational spectroscopy, which consists of the techniques and principles of infrared spectroscopy and Raman spectroscopy, is used to investigate substances and materials, generally non-destructively, for the purpose of both qualitative and quantitative analysis. The study of vibrational spectroscopy could provide wealth of data on the vibration of polyatomic molecules which when properly interpreted yields information regarding molecular structure, bonds holding the structure, forces behind the bonds, interplay between the intermolecular forces, molecular dynamics, etc. It is not only a powerful tool in the elucidation of molecular structure and in the understanding of molecular forces but also an excellent technique to analyze catalysis, fast reaction dynamics, charge transfer complexes, molecular orientation, polymer chemistry, polymerization, crystallization, etc.

Infrared spectroscopy has been a common laboratory technique for more than four decades and become an indispensable tool because of its simplicity and accuracy. Raman spectra are complementary, but mostly not identical, to infrared spectra. Now it becomes customary to use both the methods to analyze vibrational energy of a molecule. The two methods are based on quite different physical principles. Infrared absorption spectroscopy is mainly concerned with the absorption of energy by a molecule from a continuum. Infrared energies are absorbed with varying intensities and at different frequencies by inter-

atomic bonds depending on the different environment in the molecular structure. Thus, IR spectroscopy involves collection of absorbed frequencies and intensities.

The Infrared and Raman techniques are applied to samples in all the three states; gaseous, liquid and solid states, and to a wide variety of problems, which yield not only the desired knowledge such as inter-nuclear distances, vibrational frequencies and force constants, etc, but also certain vital thermodynamical quantities such as entropy, free energy, specific heat capacity, enthalpy etc. Thus in the modern era of sciences, the Infrared and Raman spectroscopy, which constitute the core of the vibrational spectroscopy, have found wide applications in the precise identification and analysis of the compounds. Vibrational spectroscopies also act as an important tool for spectroscopists to identify the Organic, Inorganic, Crystalline and Coordination compounds.

## **DEFINITION OF THE PROBLEM**

Under the background of established and standard experimental and theoretical techniques and effective utility of vibrational study in the present thesis a thorough vibrational analysis has been attempted for nine biologically and structurally important molecules, and the entire works along with the techniques have been presented in eight chapters. The first chapter gives a brief account of the experimental and theoretical aspect of vibrational spectroscopy.

The basic principles of the classical and quantum mechanical methods; particularly the Normal coordinate analysis, Hartree-Fock, and Density functional theory (DFT) methods with relevant force fields and basis sets have been explained. The theory of Infrared spectroscopy, Raman scattering, and the principles of the respective spectrometers have also been presented. The underlying principle of Fourier transformation of the spectra is also discussed. The remaining six chapters except last one are dedicated to discuss in detail the vibrational study on the nine important molecules. The last chapter deals with literature survey and bibliography.

### **SCOPE OF THE RESEARCH WORK**

The usage of any material is based on the characteristics or the physical and chemical properties of the atoms and molecules, which constitute the material. The life saving materials like drugs or very strong materials like synthetic polymers differ in their properties only due to the inner dynamics of the molecules which constitute them. The vibrational spectroscopy which accurately predicts the inner modes of vibration study the major part of molecular dynamics. The rest is only the translational and rotational motions, which can also be studied by extending the work to their energy levels. Hence, the proposed vibrational study on nine biologically active molecules certainly provides lot of knowledge about the dynamics of these molecules and wide

scopes in the field of pharmaceutical industry as many potential drugs can be prepared in future based on the reports of this study.

## METHODOLOGY

The instrumentation technology has also grown to such an extent that infrared and Raman spectrometers are now available commercially in a single package like Bruker IFS 66V FT-IR spectrometer. All the compounds are used in this thesis for investigation are purchased from Sigma-Aldrich chemicals, USA with spectroscopic grade and it is used as such without any further purification. The FTIR spectra of the compounds have been recorded in Perkin-Elmer 180 Spectrometer in the range of  $4000\text{--}100\text{ cm}^{-1}$ . The spectral resolution is  $\pm 2\text{ cm}^{-1}$ . The FT-Raman spectrum of the compounds are also recorded in the same instrument with FRA 106 Raman module equipped with Nd: YAG laser source operating at  $1.064\text{ }\mu\text{m}$  line widths with 200 mW powers. The spectra are recorded with scanning speed of  $30\text{ cm}^{-1}\text{ min}^{-1}$  of spectral width  $2\text{ cm}^{-1}$ . The frequencies of all sharp bands are accurate to  $\pm 1\text{ cm}^{-1}$ .

Recently, a very substantial progress has been made to calculate quantum mechanically the vibrational modes, and other structurally related parameters of the molecules which are generally called as HF, DFT and Hybrid methods with the help of Gaussian 03W software package, which provides all the different quantum mechanical methods and necessary basis sets. The quantum calculations performed previously were limited by the speed and

storage capacity of the computers based on the sizes of the molecules. As the larger and faster computers are now available, it becomes easier to treat such larger molecules also.

## ORIGINAL CONTRIBUTION

In the case of 2-bromobenzoic acid, it is observed that the other vibrations can hinder the C–Br vibrations due to its weak force constant. The influence of COOH on both stretching and deformation bands is found to be predominant in this compound. The C–H vibrations in  $\alpha$ -acetoneaphthone indicate aromatic nature of the compound.

The position of bromine atom in 2, 5 and 2, 6-dibromo pyridine molecules is found producing a slight difference in frequencies between the two molecules. Also, the variation of the position of Br has not influenced C–H out-of-plane bending modes whereas C–H in-plane bending vibration is found to be suppressed by this substitution

In case of 2, 5 and 2, 6-dimethyl aniline which belongs to  $C_s$  point group symmetry, the N–H stretching and deformation frequencies are found relatively high when compared to the literature values. The abnormalities may be due to the presence of the methyl groups in the vicinity. All the vibrations of methyl group are completely influenced by the position of the amino group in these

two molecules. Among the symmetric and antisymmetric bands of N-H vibrations, symmetric bands are found to be more intense.

The vibrational analysis of the 1-methoxynaphthalene indicates that the skeletal and C–H vibrations of the naphthalene are almost identical with that of benzene except very small changes. Even the substitution OCH<sub>3</sub> has not influenced these modes much.

### **PAPERS PUBLISHED**

Parts of the material presented in this thesis have been published in the form of papers in various reputed national/international journals as follows:

1. Scaled quantum FTIR and FTRAMAN spectral analysis of 1-amnio-4-bromonaphthalene. *Journal of current sciences* 14 (1), 129-136 (2009)
2. FTIR –FT Raman spectral and theoretical vibrational analysis of 2, 5-dimethylaniline and 2, 6-dimethylaniline, *Journal of current sciences*, 14 (1), 137-136 (2009)
3. Scaled quantum FTIR and FT-Raman Spectral analysis of 1-Methoxynaphthalene, *E- Journal of Chemistry*, 7(2), 457-464 (2010)
4. DFT (LSDA, B3LYP and B3PW91) comparative vibrational spectroscopic analysis of  $\alpha$ -acetonephthone, *Spectrochimica Acta, Part A*, 76, 12-21 (2010)

### **PAPERS SUBMITTED FOR PUBLICATION**

5. Density functional theory calculations of vibrational spectra of 2, 5 and 2, 6-dibromopyridine, *Spectrochimica Acta, Biomolecular spectroscopy*

6. Vibrational Spectroscopic Analysis of 2-bromobenzoic and anthranilic acids: A combined experimental and theoretical study, *Spectrochimica Acta*, Biomolecular spectroscopy

## CHAPTER – I

### VIBRATIONAL SPECTROSCOPY THEORY AND TECHNIQUES

#### INTRODUCTION

Spectroscopy deals with interaction of matter with electromagnetic energy and spectroscopists harvest wealth of information, about the matter, from these interaction. Molecular spectroscopy aims to understand the interaction of molecular energy with electromagnetic radiation. A molecule possesses various forms of energy due to its different kinds of motion and intermolecular interactions. For instance, it possesses translational energy, Rotational energy, vibrational energy, etc., and these energies are quantized and interactions between them are very weak. Electromagnetic radiations can be allowed to interact with the molecular energy levels and investigation of these interactions can provide various information regarding their rotation, charge localization, molecular structure, symmetry, vibration, etc. It is an established fact that the interaction of electromagnetic energy with the vibrational energy levels of a molecule provide amazing information on the molecular dynamics [1] and vibrational spectroscopy emerged with theories and techniques to deal with such interactions.

The frontiers of vibrational spectroscopy are very wide, as the technique is applicable to solids, crystals, powder; liquids, solutions, melt, gases, films and absorbed species. Its important application are: Molecular

structural determinations, calculation of intra molecular & inter molecular forces, computation of degree of association in condensed phases, elucidation of molecular symmetries, identification and characterization of new molecules, deducing thermo dynamical properties of molecular systems, etc. [2]. Vibration spectroscopy has also contributed significantly to the growth of other areas such as polymer chemistry, catalysis, fast reaction dynamics, charge-transfer complexes, etc [3].

Vibrational spectroscopy involves different methods, the most important of which are infrared and Raman spectroscopy. Molecular vibrations, which modulate the molecular dipole moment, are visible in the infrared spectrum, while those vibrations, which modulate the polarizability, appear in the Raman spectrum. These two techniques yield complementary and / or confirmatory information regarding molecular vibrations. Thus both these methods should necessarily be used for a complete vibrational analysis of a molecule [4]. The present thesis is entirely devoted to the proper use of infrared and Raman spectroscopy in the vibrational analysis of some important poly atomic and substituted benzene molecules. Thus important topics relevant to this dissertation, including theoretical background, instrumentation and sample handling for infrared and Raman spectroscopy, group theoretical approach in vibrational analysis, various force fields and theory of normal coordinate analysis are presented here.

## INFRARED SPECTROSCOPY

### MOLECULAR VIBRATIONS

A molecule is not a rigid assembly of atoms; it can be viewed as a system of balls and springs of varying strengths, corresponding to the atoms and chemical bonds of the molecule. There are two kinds of fundamental vibrations for molecules: stretching, in which the distance between two atoms decreases or increases, but the atoms remain in the same bond axis, and bending (or deformation), in which the position of the atom changes relative to the original bond axis. Each of the vibrational motions of a molecule occurs with a certain frequency, which is characteristic of the molecule and of the particular bond. The energy involved in a particular vibration is characterized by the amplitude of the vibration, so that the higher the vibrational energy, the larger the amplitude of the motion [5].

According to the results of quantum mechanics, only certain vibrational energies are allowed to the molecule, and thus only certain amplitudes are allowed. Associated with each of the vibrational motions of the molecule, there is a series of energy levels (or vibrational energy states). The molecule may be made to go from lower energy level to a higher energy level by absorption of a quantum of electromagnetic radiation, such that

$$E_{\text{final}} - E_{\text{initial}} = nh\nu \quad \rightarrow 1.1$$

In undergoing such a transition, the molecule gains vibrational energy, and this is manifested in an increase in the amplitude of the vibration. The frequency of light required to cause a transition for a particular vibration is equal to the frequency of that vibration, so that we may measure the vibrational frequencies by measuring the frequencies of light, which are absorbed by the molecule. Since most vibrational motions in molecules occur at frequencies of about  $10^{14}\text{sec}^{-1}$ , then light of wavelength  $= c/\lambda = 3 \times 10^{10} \text{ cm/sec}/10^{14}\text{sec}^{-1} = 3 \times 10^{-4} \text{ cm} = 3 \text{ microns}$  will be required to cause transitions [6]. As it happens, light of this wavelength lies in the infrared region of the spectrum, IR spectroscopy deals with such transitions between vibrational energy levels in molecules and is therefore constitute a part of vibrational spectroscopy.

## VIBRATIONAL DEGREES OF FREEDOM

A molecule has as many degrees of freedom as the total degrees of freedom of its individual atoms. Each atom has 3 degrees of freedom in the Cartesian coordinates (x, y, z), necessary to describe its position with respect to a fixed point in the molecule. A molecule of n atoms therefore has 3n degrees of freedom. Of the 3n degrees of freedom, for non-linear molecules, 3 degrees of freedom describe translation and 3 describe rotation and the remaining  $3n-6$  degrees of freedom describe vibrational degrees of freedom. Linear molecules have only  $3n-5$  vibrational degrees of freedom, since only 2 degrees of freedom are required to describe rotation. In the case of polymers the

number of vibrational degrees of freedom becomes  $3n-4$ , as rotation is constrained to only one axis [7]. Of the  $3n-6$  vibrational modes,  $(n-1)$  modes are bond stretching vibrations and the other  $2n-5$  [ $(2n-4)$  for a linear molecule] modes are angle-bending vibrations [8]. The number of vibrational degrees of freedom gives the number of fundamental vibrational frequencies of the molecule, or in other words, the number of normal modes of vibrations [1].

### **NORMAL MODES OF VIBRATION**

A molecule may consist of many numbers of atoms and the atomic nuclei may be regarded as mass points in the potential field due to the bonding. When the atoms of a molecule are slightly displaced from their equilibrium position and released, they perform vibrations of complicated nature. In the absence of other normal modes, each normal mode is nothing but the simple harmonic motion of every nucleus about its equilibrium position and all these oscillations are in phase.

### **INFRARED VIBRATION SPECTRA**

During the vibrational motion of a molecule the charge distribution undergoes a periodic change, and therefore in general the dipole moment changes periodically. For a particular vibrational mode, in order to directly absorb infrared electromagnetic radiation, the vibrational motion associated with that mode must produce a change in the dipole moment of the molecule.

Normal vibrations that are connected with a change of dipole moment and therefore, appear in the infrared spectrum are called infrared active modes, while vibrations for which the change of charge distribution is such that no change of dipole moment arises and which, therefore, do not appear in the infrared spectrum are called infrared inactive modes [4].

Let  $\mu_x$ ,  $\mu_y$  and  $\mu_z$  are the three components of the dipole moment  $\mu$  of the molecule in the direction of the axes, of a Cartesian coordinate system fixed in the molecule, in a displaced position of the nuclei. If  $\mu_x^0$ ,  $\mu_y^0$  and  $\mu_z^0$  are the components of the dipole moment  $\mu^0$  in the equilibrium position, then, for sufficiently small displacements, we can expand  $\mu_x$  as

$$\mu_x = \mu_x^0 + \sum_k \left[ \left( \frac{\partial \mu_x}{\partial x_k} \right)_0 x_k + \left( \frac{\partial \mu_x}{\partial y_k} \right)_0 y_k + \left( \frac{\partial \mu_x}{\partial z_k} \right)_0 z_k \right] + \dots \rightarrow 1.2$$

Where the  $x_k$ ,  $y_k$  and  $z_k$  are the displacements coordinates of nucleus  $k$ . Similar relations hold for  $\mu_y$  and  $\mu_z$ . If we use normal coordinates  $q_1, q_2, q_3 \dots q_k$  we have

$$\mu_x = \mu_x^0 + \left( \frac{\partial \mu_x}{\partial q_k} \right)_0 q_k + \frac{1}{2} \left( \frac{\partial^2 \mu_x}{\partial q_k^2} \right)_0 q_k^2 + \dots \rightarrow 1.3$$

With 
$$q_k = q_k^0 \cos(2\pi\nu_k t + \varphi_k) \rightarrow 1.4$$

and similarly we can express  $\mu_y$  and  $\mu_z$ .

Thus generally we can write the molecular dipole moment

$$\mu = \mu^0 + \left( \frac{\partial \mu}{\partial q_k} \right)_0 q_k + \frac{1}{2} \left( \frac{\partial^2 \mu}{\partial q_k^2} \right)_0 q_k^2 + \dots \quad \rightarrow 1.5$$

According to equation (1.4) and (1.5), the dipole moment  $\mu$  of the molecule will change with the frequency  $\nu_k$  of a normal vibration  $k$  if and only if at least one of the derivatives  $\left( \frac{\partial \mu_x}{\partial q_k} \right)_0$ ,  $\left( \frac{\partial \mu_y}{\partial q_k} \right)_0$ ,  $\left( \frac{\partial \mu_z}{\partial q_k} \right)_0$  is different from zero. The intensity of this infrared fundamental band is proportional to the square of the vector representing the change of the dipole moment for the corresponding modes of vibration near the equilibrium position; that is,

$$I \propto \left( \frac{\partial \mu_x}{\partial q_k} \right)_0^2 + \left( \frac{\partial \mu_y}{\partial q_k} \right)_0^2 + \left( \frac{\partial \mu_z}{\partial q_k} \right)_0^2 \quad \rightarrow 1.6$$

The above discussion is based on the assumption that the vibration of the molecule is simple harmonic. If the anharmonicity is taken into account, the vibrational motion contain also the frequencies  $2\nu_k, 3\nu_k, \dots$ , and furthermore  $\nu_k + \nu_i, \nu_k - \nu_i, 2\nu_k + \nu_i, \dots$ . Therefore, in the infrared spectrum in addition to the fundamentals, overtones and combination vibrations may also occur, if they are connected with a change of dipole moment. However, they will, be much weaker than the fundamentals, since the anharmonicities in general are slight, except for very large amplitudes of the nuclei [1].

## INFRARED SELECTION RULE

Selection rule for the infrared activity can be obtained by expressing equation (1.5) using the transition moment integral, as

$$[\mu_{ij}] = \mu_o \int \psi_i \psi_j d\tau + \sum_k \left[ \left( \frac{\partial \mu}{\partial q_k} \right)_o \int \psi_i q_k \psi_j d\tau \right] \quad \rightarrow 1.7$$

neglecting the higher order terms. As  $\mu_o$  is a constant and also due to the orthogonal of the wave functions the first integral is zero except for  $i = j$ . Since we are considering a transition from state  $i$  to  $j$ , the first term vanishes. Consequently, the permanent dipole moment of the molecule has no effect on the vibrational transitions.

The second term gives the transition probability for the infrared absorption. In this term, there is a factor  $\left( \frac{\partial \mu}{\partial q_k} \right)_o$ , which gives a change in dipole moment  $\mu$  around the equilibrium position during a vibration. For at least one of the components  $q_k$  of  $\mu$ , the dipole moment must be non-zero. Accordingly,  $\frac{\partial \mu}{\partial q_o} \neq 0$ , then a normal mode  $q_k$  will be active in the infrared absorption spectrum [3].

## RAMAN SPECTROSCOPY

### RAMAN EFFECT

When electromagnetic radiation of energy content  $h\nu$  irradiates a molecule the energy may be transmitted, absorbed or scattered. The scattering mechanisms can be classified on the basis of the difference between the energies of the incident and scattered photons. If the energy of the incident photon is equal to that of the scattered one, the process is called *Rayleigh scattering*. If the energy of the incident photon is different to that of the scattered one, the process is called *Raman scattering*. When the substance is illuminated by monochromatic light, the spectra of the scattered light consists of a strong line (the exciting line) of the same frequency as the incident light together with weaker lines on either side shifted from the strong line by frequencies ranging from a few  $\text{cm}^{-1}$  to about  $3500 \text{ cm}^{-1}$ . The lines of frequency less than that of exciting line are called Stokes lines, the others anti-Stokes lines. [9].

### CLASSICAL THEORY

The classical theory of Raman effect, while not wholly adequate, is worth consideration since it leads to an understanding of the concept – the polarizability of a molecule. For a molecular vibration to be Raman active there must be a change in the polarizability of the molecule. A hypothetical atom

with an spherically symmetrical electron cloud has no permanent dipole moment. When such an atom is irradiated by an electromagnetic radiation the electric field of the radiation displaces the electron and positively charged nucleus in opposite directions. This separation is called polarization and the atom now has an induced dipole moment. If  $E$  represents the electric field of the radiation and  $\mu'$  represents the induced dipole moment oriented parallel to the direction of  $E$ , which can be described by its components

$$\begin{aligned}\mu'_x &= \alpha_{xx} E_x + \alpha_{xy} E_y + \alpha_{xz} E_z \\ \mu'_y &= \alpha_{yx} E_x + \alpha_{yy} E_y + \alpha_{yz} E_z \\ \mu'_z &= \alpha_{zx} E_x + \alpha_{zy} E_y + \alpha_{zz} E_z\end{aligned} \quad \rightarrow 1.8$$

All  $\alpha_{ij}$  are components of a tensor  $\alpha$ , which projects one vector, the electric fields vector  $E$  to produce another vector  $\mu'$ , the induced dipole moment. This can be written in matrix notation as

$$\begin{bmatrix} \mu'_x \\ \mu'_y \\ \mu'_z \end{bmatrix} = \begin{bmatrix} \alpha_{xx} & \alpha_{xy} & \alpha_{xz} \\ \alpha_{yx} & \alpha_{yy} & \alpha_{yz} \\ \alpha_{zx} & \alpha_{zy} & \alpha_{zz} \end{bmatrix} \cdot \begin{bmatrix} E_x \\ E_y \\ E_z \end{bmatrix} \quad \rightarrow 1.9$$

or as 
$$\mu' = \alpha E \quad \rightarrow 1.10$$

Since the electric field associated with the incident radiation of frequency  $\nu_0$  alternates the induced dipole moment also alternates at the same frequency  $\nu_0$ .

Thus the molecule emits electromagnetic radiation of the frequency  $\nu_0$ . Rayleigh scattering is due to this process [4].

A molecule is not static; it continuously vibrates (also rotate) when radiations fall on it. This vibratory motion of the molecule is capable of modulating the polarizability of the molecule. Consequently, the induced dipole moment and therefore also the amplitude of the emitted field is modulated by the frequency of the vibration. The modulation of the polarizability of a molecule, vibrating with the frequency  $\nu_k$  is

$$\alpha_k = \alpha_0 + \left( \frac{\partial \alpha}{\partial q_k} \right)_0 q_k^0 \cdot \cos 2\pi \nu_k t + \dots \quad \rightarrow 1.11$$

Here  $q_k^0$  represent the normal coordinates. As a consequence of irradiation, molecular polarizability get modulated with the frequency of electric field  $\nu_0$  of incident light and gives the induced dipole moment as

$$\mu'_k = \alpha_0 E_0 \cos 2\pi \nu_0 t + \left( \frac{\partial \alpha}{\partial q_k} \right)_0 q_k^0 E_0 \cdot \cos 2\pi \nu_0 t \cdot \cos 2\pi \nu_k t \quad \rightarrow 1.12$$

This is equivalent to

$$\mu'_k = \alpha_0 E_0 \cos 2\pi \nu_0 t + \left( \frac{\partial \alpha}{\partial q_k} \right)_0 q_k^0 E_0 [\cos 2\pi (\nu_0 - \nu_k) t + \cos 2\pi (\nu_0 + \nu_k) t] \quad \rightarrow 1.13$$

According to this equation, the induced dipole moment acquires three components  $\nu_0$ ,  $(\nu_0 - \nu_k)$  and  $(\nu_0 + \nu_k)$ . When light is emitted by these induced

dipoles, the emitted light also possesses the above frequencies. The first term in equation (1.12) describes Rayleigh scattering, the second term concerns Stokes, and the third anti-Stokes Raman scattering [2]. The intensity of the emitted radiation is proportional to the square of the absolute value of the second derivative of the induced dipole moment:

$$S \propto \langle |\ddot{u}'_k|^2 \rangle \quad \rightarrow \quad 1.14$$

Just as in case the infrared spectrum, if the anharmonicity is taken into account, in addition to the fundamentals, overtone and combination vibrations may also appear as Raman shifts if they are connected with a change of polarizability. When the anharmonicity is small, the intensity of Raman lines corresponding to overtone and combination vibrations will be very small compared to those corresponding to fundamentals.

## QUANTUM THEORY

The description of Raman Effect will be complete if we use quantum theory [9]. Suppose a molecule is initially in state  $|i\rangle$  with the energy  $E_i$  and after interaction with monochromatic radiation of angular frequency  $\nu_0$  goes to state  $|f\rangle$  with energy  $E_f$ . From the conservation of energy

$$E_i + h\nu_0 = E_f + h(\nu_0 \pm \nu_{fi}) \quad \rightarrow \quad 1.15$$

Where  $h\nu_{fi} = E_f - E_i$

and  $h(\nu_0 \pm \nu_{fi}) = h\nu_s$ , the energy of the scattered photon..

If  $E_f > E_i$ ,  $\nu_s = \nu_0 - \nu_{fi}$  (stokes)  $\rightarrow$  1.16

If  $E_f < E_i$   $\nu_s = \nu_0 + \nu_{fi}$  (anti-stokes)  $\rightarrow$  1.17

The stoke lines are more intense than the anti-stokes lines, a consequence of the different populations of molecule in the ground and first excited vibrational state, as described by the Boltzmann distribution. Application of the Boltzmann distribution law shows that the ratio of the intensities for the Stokes and the corresponding anti-Stokes Raman lines is given by

$$\frac{I_{AS}}{I_S} = \left( \frac{\nu_0 + \nu_{fi}}{\nu_0 - \nu_{fi}} \right)^4 \exp\left( \frac{-h\nu_{fi}}{kT} \right) \rightarrow 1.18$$

where  $\nu_{fi}$  is the magnitude of the Raman shift and  $\nu_0$  is the frequency of the incident beam. Thus the intensity of anti-stokes lines decreases greatly at higher vibrational frequencies [3].

## RAMAN SELECTION RULES

The induced transition moment associated with a transition from the initial state final state  $j$  and  $I$  are given by

$$\mu'_{ij} = \int \psi_i \mu' \psi_j d\tau \rightarrow 1.19$$

$$\mu'_{ij} = \int (\psi_i \alpha_y \psi_j d\tau) E \rightarrow 1.20$$

where  $\mu'_{ij}$  is the induced dipole moment,  $\psi_i$  and  $\psi_j$  are the wave functions of the lower and final excited vibrational states respectively [10]. Using equations (1.11) and (1.20) we obtain

$$\mu'_{ij} = E\alpha_0 \int \psi_i \psi_j d\tau + E \sum_k \left( \frac{\partial \alpha}{\partial q_k} \right) \int \psi_i q_k \psi_j d\tau \quad \rightarrow \quad 1.21$$

where  $q_k$  is given by the equation (1.4). The first term of the above equation (1.21) disappears for all values, except for  $\psi_i = \psi_j$  due to mutual orthogonal of the wave functions. This first term accounts for Rayleigh scattering. The components of  $\alpha_0$  are nonzero for all molecules and hence it follows that the Rayleigh scattering is never forbidden. The second term shows that the transition probability depends on the transition moment integrals involving the components of the molecular polarizability matrix element  $\alpha_{ij}$  which transform with the normal coordinate  $q_k$ .

## MUTUAL EXCLUSION PRINCIPLE

To understand the presence and absence of lines in IR and Raman spectra, the understanding of the *Mutual exclusion principle* is necessary. It gives the relation between the symmetry of the molecular structure and their infrared and Raman activity. The rule is: *For molecules with a centre of symmetry, transitions that are allowed in the infrared are forbidden in the Raman spectrum; conversely, transitions that are allowed in the Raman*

*spectrum are forbidden in the infrared.* This rule implies that *if there is no centre of symmetry then some (but not necessarily all) vibrations may be both Raman and infrared active.* It should be realized that the above rule does not imply that all transitions that are forbidden in the Raman scattering active in the infrared.

The rule can also be explained as follows: in the infrared, only transitions between states of opposite symmetry with respect to the centre of symmetry  $i$  are allowed ( $g \leftrightarrow u$ ) whereas in the Raman spectrum, only transitions between states of same symmetry with respect to  $i$  can take place ( $g \leftrightarrow g, u \leftrightarrow u$ ). This rule arises mainly due to the fact that all the components of magnetic dipole moment  $\mu$ , change sign for a reflection at the centre of symmetry, but the components of polarizability  $\alpha$ , which behave as the product of two components of induced dipole moment  $\mu'$  remain unchanged [1]. From the mutual exclusion rule, we can conclude that the observance of Raman and infrared spectra showing no common lines implies that the molecule has centre of symmetry. But, it has to be done cautiously because some times a vibration may be Raman active but too weak to be observed. However, if some vibrations are observed to give coincident infrared and Raman bands it is certain that the molecule has no centre of symmetry.

## **VIBRATIONAL SPECTROSCOPY OF POLYMERS**

Structural study of polymers based on vibrational spectroscopic technique does not attract many due to the inherent difficulties present in the polymers. Thus the unique technique, precautions, extra-care required in the study of polymers needs special mention.

### **I. INFRARED SPECTROSCOPY**

For the study of polymers, among the available spectroscopic techniques infrared spectroscopy is proved to be the best technique because the majority of functional groups present in the polymers give rise to bands in the infrared region [11]. The success of infrared spectroscopic method for the polymer analysis also lies in its easy sampling techniques and the fast and sensitive spectrophotometers. As in polyatomic molecules, characteristic group frequencies present in the infrared spectra of polymers makes the vibrational analysis effective. The advantage of characteristic group frequencies is that they generally appear in the same region for polymers as for other molecules [12]. When chemical groups of the same structure and energy are present in a polymer, their vibrational motions often produce coupling or resonance. This may lead to new modes, as a characteristic of the length of the polymer chain and it is confirmed from the spectra of ordered polymers [13].

Polymers usually contain a large number of additives, fillers, pigments, lubricants, and mold release agents, etc and many of these substances may result in interference in the infrared spectrum [12]. Thus many of the polymers require prior removal of impurities or special sample preparative techniques. It is also possible that the infrared sample preparation techniques sometimes destroy or modify the characteristics of interest.

It is well known that there are many preparative methods available for the same polymer and different manufacturers use different methods. This may lead to the same polymer having similar but different characteristics, which may appear in the spectrum [14]. Recording infrared spectra of a polymer can also pose some problems like background noise. The main source of this noise in polymers is the partial non-absorbing scattering of the infrared radiation from in-homogeneities in the polymer sample. FTIR spectrometer eliminates this by spectral subtraction technique [13]. Bands introduced by artifacts, solvents and other impurities can also be removed by this technique.

## **II. RAMAN SPECTROSCOPY**

Till the advent of FT Raman spectrometers, Raman method was rarely used in the polymer vibrational study. The basic reason for this practical limitation is due to the occurrence of fluorescence but the FT technique combined with Nd: YAG laser as source removed this problem to a greater extent. Raman spectrometers are capable of covering lower wave numbers, up

to  $100\text{ cm}^{-1}$  or lower, than those of infrared and so can reveal information relating to polymer structures which are not easily available using other techniques [14]. As already mentioned infrared and Raman methods are often provide complementary information. These differences in the vibrational patterns of infrared and Raman can be used to a grater advantage in the determination of structure of molecules. Often in the Raman spectra of polymers, the skeletal vibrations give characteristic bands which are usually very weak and not of much use for characterization in the infrared.

Since water is a highly polar molecule, it is a strong infrared absorber, but it can be studied using Raman spectroscopy. Thus water-soluble polymers such as surfactants can be successfully carried out with Raman technique. Filled polymers can be easily studied by using Raman spectroscopy because fillers such as silica, clay and glass are weak Raman scatters and do not interfere with the Raman spectrum of the polymer matrix [13]. In contrast to infrared the Raman does not require elaborate sample preparatory techniques. Care should be taken that the polymer sample should not get heated by the laser radiation as it may lead to poor Raman spectra, phase change, decomposition, etc. Heating can be avoided by rotating the sample while the spectrum is recorded [14].

## INSTRUMENTATION – INFRARED SPECTROSCOPY

Infrared spectrometers generally falls under two categories namely: dispersive and interferometer instruments. Conventional spectrometers are *dispersive instruments* using prism or grating as dispersive elements. In order to overcome shortcomings of these devices spectrometers based on interferometer technique were developed. This type of instruments records the interferogram of the signal and later with the help of Fourier transformation methods, it is converted into conventional spectrum and these instruments are called FTIR spectrometers.

### A. CONVENTIONAL IR SPECTROMETERS

It essentially consists of a *source* which generates light of desired wave numbers, a *monochromater* (either a salt prism or a grating with finely spaced etched lines) separates the source radiation into its constituent wavelengths and a *slit* selects the collection of wavelengths that shine through the sample at any given time. In double beam operation, a *beam splitter* separates the incident beam in two; half goes through the sample, and half to a reference. The *sample* absorbs light according to its chemical properties. A *detector* collects the radiation that comes out of the sample, and in double-beam operation, compares its energy with that of the reference. The detector generates an electrical signal proportional to the collected radiation and sends to an analog *recorder*. A link between the monochromater and the recorder allows us to

record energy as a function of frequency or wavelength, depending on how the recorder is calibrated [15].

Although very accurate instruments can be designed on these principles, there are several important limitations. First, the monochromator/slit limits the amount of signal that can be obtained at a particular resolution. To improve resolution, the slit must be narrow but it decreases intensity. Second, there is no easy way to run multiple scans to build up signal-to-noise ratios. Finally, the instrument must be repetitively calibrated, because the analog connection between the monochromator position and the recording device is subject to misalignment and wear [2].

## **B. FOURIER TRANSFORM IR SPECTROMETER**

A Fourier transform infrared spectrometer consists of a source, an interferometer (an addition which makes the instrument unique) and a detector.

### **SOURCES**

Most of the FT instruments use a heated ceramic source. The composition of the ceramic and the method of heating vary from instrument to instrument but the idea is always the same a ceramic is heated to suitable temperature to obtain IR radiations of required range. Modern FTIR instruments use a conducting ceramic or a wire heater coated with ceramic as source. The advantage with the heated ceramics is that at high temperature

they emit IR radiation of all wavelengths with reasonable intensity. Care should be taken to maintain the temperature of the heater at constant value and this is achieved by monitoring the source output, and using part of the output signal as feedback to control the electrical power [16].

In recent years, tunable dye lasers are emerging as very precise sources with resolution of  $10^{-6} \text{ cm}^{-1}$ . The wave number range of tunable dye lasers is however restricted and hence their applicability is limited. The use of carbondioxide laser and Semiconductor lasers in the infrared spectroscopic analysis has also been reported [3].

## **INTERFEROMETERS**

The interferometer is the heart of any FTIR instrument. It is this part which analyses the infrared radiation and hence enables us to generate a spectrum. The classical Michelson Interferometer involves a beam splitter – which sends the light in two directions at right angles. One beam goes to a stationary mirror then returns back to the beam splitter. The other goes to a moving mirror. The motion of the mirror produces path difference with respect to the stationary mirror. When the two beams meet again at the beam splitter, they recombine, but the difference in path lengths creates constructive and destructive interference producing an interferogram

The recombined beam passes through the sample. The sample absorbs all the different wavelengths characteristic of its spectrum, and this subtracts

specific wavelengths from the interferogram. The detector now reports variation in energy versus time for all wavelengths simultaneously. A laser beam (usually a He-Ne Laser having a wavelength near 632.8nm) is superimposed to provide a reference for the instrument operation i.e for the measurement of path difference. Thus the output of the detector is an interferogram.

A mathematical function called a Fourier transform allows us to convert this intensity-vs.-time spectrum into an intensity-vs.-frequency spectrum [17]. The Fourier theorem states that any complex wave can be viewed as a superposition of series of sine and cosine waves. The Fourier Transform uses the above concept to convert an interferogram into constituent vibrations. The Fourier transformations connects two physical descriptions using the integral

$$f(t) = \frac{1}{2\pi} \int_{-\infty}^{+\infty} F(\omega) e^{-i\omega t} d\omega \quad \rightarrow 1.22$$

This relates an  $f(t)$  - a function of time with  $F(\omega)$  - a function of frequency. We can also express the relation as,

$$F(\omega) = \int_{-\infty}^{+\infty} f(t) e^{i\omega t} dt \quad \rightarrow 1.23$$

The  $F(\omega)$  function gives the frequencies at which the signal is non-zero and the  $f(t)$  function gives the corresponding time of the signal. Both of these functions are suitable descriptions of a waveform or physical system. If one is known the other function can be obtained from it [18]. An interferogram, as mentioned

earlier, is a function of time and hence it can be transformed into a function of frequency using the above equation. The intensity detected by the detector of a FTIR instrument can be mathematically expressed as

$$I(x) = \int_0^{\infty} S(\bar{\nu}) [1 + \cos 2\pi\bar{\nu}x] d\bar{\nu} \quad \rightarrow 1.24$$

The above equation can also be written as

$$S(\bar{\nu}) = 2 \int_0^{+\infty} I(x) [1 + \cos 2\pi\bar{\nu}x] dx \quad \rightarrow 1.25$$

where  $x$  is the path difference. Thus using  $I(x)$  and  $S(\bar{\nu})$  as the Fourier transform pair, a Fourier transformation can be performed using the above equation on the interferogram and a spectrum as a plot of percentage transmission against the wave numbers can be obtained [3]. Since, all modern FT instruments are computer-interfaced, a small computer program will do the transformation in a matter of seconds (or less) and the output of the detector is digitized. The Discrete Fourier-Transform (DFT) is an algorithm for doing the transform with discrete data, which was used previously. The DFT is an order  $N^2$  calculation, meaning that the number of multiplications is equal to the square of the number of data points. This algorithm has been supplanted by Fast Fourier-Transform (FFT) algorithms, which reduce redundancies and take much less computer time. The order of this calculation is  $N \log(N)$  [18].

## DETECTORS

Various detectors are encountered in FTIRs and the majority of which

are photo resistors i.e. they have a very high resistance in the dark and this falls as light falls on them. The most sensitive are the Ge and InGaAs semi-conductor devices and others are Golay cell, thermocouple, and pyroelectric detectors. Some of detectors give adequate performance (an acceptable useful S:N ratio) at room temperature but others must be cooled. Cooling detectors invariably reduces the amount of noise they develop, but unfortunately cooling shifts the absorption edge towards shorter wavelength. In an FTIR, one normally finds a TGS or similar detector for ordinary use. If better results are required, one then resorts to the use of a cryogenically cooled mercury cadmium telluride semi-conductor detector [16]. Thus, these are invariably used in infrared microscopy and very often in diffuse reflection experiments.

### **There are several advantages in the modern FTIR instruments**

All of the source energy gets to the sample, improving the inherent signal-to-noise ratio. This is usually called as *energy advantage*.

- Resolution is limited by the design of the interferometer. The longer the path of the moving mirror, the higher the resolution. Even the least expensive FT instrument provides better resolution than all the best CW instruments were capable of.
- During spectral acquisition all the frequencies were recorded simultaneously during the whole period of the detection and it is called

multiplexing. This method gives rise to *multiplex advantage* or *Fellgett advantage* [19].

- The radiation from the source reaching the detector in an interferometer is not limited by the entrance and exit slits as in a dispersive spectrometer thus the brightness of the detected signal increases enormously which is called as *Jacquinot's advantage* or *throughput advantage* [20].
- The digitization and computer interface allows multiple scans to be collected, also dramatically improving the signal-to-noise ratio.
- Most of the computer programs today allow further mathematical refinement of the data: you can subtract a reference spectrum, correct the baseline, edit spurious peaks or otherwise correct for sample limitations.

## **INSTRUMENTATION - RAMAN SPECTROSCOPY**

The problem facing the development of Raman spectroscopic instrumentation is the inherent weakness of the inelastic scattering. Therefore to produce a detectable Raman signal a high-powered light source is required. In addition, Raman requires a spectrometer with a very high degree of discrimination against the Rayleigh elastic scattered light. Finally, since very few Raman photons are generated, the detection system must be very sensitive

to detect the Raman signal over the dark noise background [2]. The above facts delayed the use of Raman technique in research and industrial laboratories.

It was not until early sixties that the Modern renaissance took place with the development of commercial continuous wave visible lasers. In recent years, micro electronics revolution has further improved the technique with the developments of stepper motor drives, photon counting devices, digital data acquisition techniques and computer data processing and provided the Chemists and physicists a technique which is more useful and versatile than infrared spectroscopy [14]. Some of the advantages of Raman over infrared technique are: Raman spectroscopy is a scattering process, so samples of any size or shape can be examined; Very small amounts of materials can be examined; glass and closed containers can be used for sampling; fiber optics can be used for remote sampling; aqueous solution can be analyzed. Recent development in Fourier transform instrumentation now made these advantages available to researchers.

## **SOURCES**

Before the inventions of lasers, radiation emitted by the mercury arc, especially at 435.8 and 404.7 nm, has been used for exciting Raman spectra [4]. Today, most types of lasers, like continuous wave (CW) and pulsed, gas, solid state, semiconductor lasers, etc., with emission lines from the UV to the near-IR region, are used as radiation sources for the excitation of Raman

spectra. Especially argon ion lasers with lines at 488 and 515 nm are presently employed. Near-IR Raman spectra are excited mainly with a neodymium doped yttrium-aluminum garnet laser (Nd:YAG), emitting at 1064 nm [2]. The main advantage of a laser light source for Raman spectroscopy are: (i) directionality which makes focusing simple, (ii) coherency which enhances the usable power, (iii) intensity which yields a high power density and (v) monochromatic which eliminates multiple Raman lines.

### **CONVENTIONAL RAMAN SPECTROMETERS**

Raman spectroscopy until recently relayed on conventional single-channel spectrometers. They are designed to generate Raman signal and differentiate it from the unwanted stronger Raleigh-scattered light from the weaker Raman signal and count the Raman photons. These conventional Raman spectrometers are the simplest and are readily available for routine work when interfering fluorescence is not a major problem. It is essentially consists of a powerful laser irradiating in the visible region, an illuminating chamber for the sample, a high performance light dispersion system to resolve the more intense, elastically scattered light from the weak, in-elastically scattered Raman signal, a light detection and amplification system capable of detecting weak light levels and a recorder [4].

## FOURIER TRANSFORM RAMAN SPECTROMETER

FT-Raman spectrometers are designed to eliminate the fluorescence problem encountered in conventional Raman spectroscopy [21]. The FT-Raman instrument has the following components: (1) A near IR Laser excitation source, generally an Nd: YAG laser working at 1.06  $\mu\text{m}$ . (2) An interferometer equipped with an appropriate beam splitter, made of glass, and a detector for the near IR region. The detector is usually InGaAs or Ge semiconductor detector. (3) A sample chamber with scattering optics that match the input port of the Fourier transform instrument. (4) An optical filter rejection of the Raleigh –scattered light.

Utilizing an excitation frequency well below the threshold for any fluorescence process eliminates fluorescence. To focus and align the invisible Nd:YAG laser beam a visible He:Ne laser beam is co-aligned with the Nd:YAG beam. Another method of optical alignment can be realized by using fiber optics [16]. With fiber-optic components, optical alignment is virtually eliminated which allows rapid switching from one sample to another.

One of the advantages of FT instrument is that it can collect all the scattered radiation over the entire range of frequencies simultaneously during the whole period of the detection and it is called multiplexing. This becomes a disadvantage, as the intense Rayleigh line is the primary source of noise. Multiplexing redistributes the noise associated with Rayleigh line across the

entire spectrum by the FT-process and this is called as *multiplex disadvantage* [22]. Interferometer can be combined with Rayleigh line filters (notch filters) in order prevent the consequences of the multiplex disadvantage. The Rayleigh line filters minimizes the amount of Rayleigh scattered light entering the interferometer [23] and is essential for FT-Raman spectroscopy.

## **DUAL INSTRUMENTS**

Due to the rapid developments in the instrumentation techniques, nowadays both infrared and Raman spectrometers are incorporated into a single instrument assembly and available commercially as a single package. The main advantages of such instruments are: switching over from one technique to other is simple; they are compact, and comparatively cheaper. Bruker's FTIR spectrometers IFS 66/S fitted with FRA 106/S, Thermo Nicolet's Nexus/Magna FTIR & FTR systems, ABB Bomen MB157 series these are some of the commercially available dual instrument packages. Figure-1.5 shows the schematic diagram of Bruker's FTIR spectrometers IFS 66/S fitted with Raman module FRA 106/S, which was used in the present work.

## **SAMPLE HANDLING**

### **I. INFRARED SPECTROSCOPY**

One of the advantages of infrared spectroscopy is that it can be applied to nearly all types of substances. The infrared spectra of samples can be

measured in gas, liquid or solids. The spectra obtained may, however, to some extent, depend on the physical state of the system. A wide range of sampling technique is available for mounting the sample in the infrared instruments. The technique depends on whether the sample is a gas, a liquid, a solid or a polymer.

## SOLIDS

Solids are usually examined as a mull, a pressed disc, or as a deposited glassy film. Mulls are prepared by thoroughly grinding 2-5 mg of a solid in a smooth agate mortar. Grinding is continued after the addition of one or two drops of the mulling oil. Care must be taken in grinding to achieve particles of size less than 2  $\mu\text{m}$  so that excessive scattering of radiation can be avoided. The mull is examined as thin film between flat salt plates. Nujol, high boiling point petroleum oil, is commonly used as a mulling agent. The mull technique has the advantage of non-reactivity with samples, reproducibility of results and rapidity of preparation. But the Nujol shows strong absorption near  $2915\text{ cm}^{-1}$  and medium bands around  $1462$  and  $1376\text{ cm}^{-1}$  so it can not be used if bands in the C-H stretching or  $\text{CH}_3$  deformation region are to be observed [24]. Preparing a second mull using perfluoro-kerosene, halocarbon oil or hexachloro-butadiene as the mulling agent can circumvent this. The disadvantages with this technique are: if the sample concentration is too low, the spectrum will be that of the mull, but if too much sample is used the mull

will not transmit the radiation. Also excess mull lead to poor transmission of radiation but little quantity of mull leads to very weak spectrum [4].

The pressed disc technique depends upon the fact that dries, powdered potassium bromide or other alkali halides, can be pressed in an evacuated die under high pressure to form transparent discs. The sample is thoroughly mixed with about 100 mg of dry powdered potassium bromide. The mixture is pressed with special dies under a pressure of about 10,000 – 15,000 pounds per square inch into a transparent disk. Since the making of good pellet requires expertise and its use is often avoided. Such KBr technique can be less formidable through the Mini-press that affords a simple procedure and greatly simplified the task of making discs [24]. The main advantage of pressed disc technique is that the concentration of the sample and thickness of the disk can be controlled easily. It is also possible to store the disc for future reference. The limitations of the technique are: sample grinding with KBr may lead to polymorphism and the high pressure applied can bring physical and chemical changes in the sample.

## **LIQUIDS**

In most instances the spectra of liquids are measured in either a demountable type cell or in fixed thickness or sealed cells. The spectra of pure samples can be measured as very thin films squeezed between two alkalis halide windows of a demountable cell. This technique can produce a film of

thickness 0.01 mm or less. This method is most useful for qualitative work only because sample thickness cannot be controlled. Liquid cells consists of two alkali halide windows, usually NaCl or KBr, separated by a spacer of suitable thickness made of Teflon or lead which limits the volume of the cell. Capillary dropper or hypodermic syringe is used to fill or emptying such cells [4].

Solutions are handled in cells of 0.1 – 1 mm thickness. Usually solutions of 1 to 10 % can be used in commercially available cavity cells of path length 0.01 to 0.1 m. commonly used solvents for infrared spectra are  $\text{CCl}_4$ ,  $\text{CHCl}_3$ ,  $\text{CS}_2$ ,  $\text{CH}_2\text{Cl}_2$ ,  $\text{C}_6\text{H}_6$  and n-heptane. The solvents selected must not chemically react with the solute and it should not exhibit intense absorption with the frequency range of interest. For obtaining spectrum in a wide frequency range several solvents must be used [24].

## **POLYMERS**

The technique used in the study of organic and inorganic polyatomic molecular samples can, in many cases, is simply applied to polymers. For recording infrared spectra, liquids may be studied in thin cells having transparent IR windows. Liquids may also be studied as thin films stretched by surface tension between transparent plates. Using suitable solvents solids can be dissolved and examined. Polymeric samples in powder form may be examined by preparing discs and mulls [14]. Brittle solid polymers can be ground to powder form, of suitable particle size, and then used as discs or

mulls. Thermoplastic polymers or elastomers can be studied by cooling them below its glass transition temperature before grinding. If the polymer is in the form of thin film it can be examined directly [13]. Thermoplastic polymers can be made to thin films using hot press.

## **II. RAMAN SPECTROSCOPY**

Raman spectrometer but the important thing to be taken care of while preparing sample is that they should be dust free can study gases, liquids and solids. Glass is almost transparent in the Raman frequency region and thus samples in different phases can be measured in glass or silica containers or capillaries [4].

### **LIQUIDS**

Liquids may be examined neat or in solution and normally liquids of about 0.3 ml enclosed in glass or silica containers or capillaries may be required for obtaining good spectrum. Even though water cannot be used as solvent in IR studies, in the Raman studies water is one of a good solvent. Thus spectra of aqueous solutions can be easily studied and also spectra of water-soluble biological material can be easily recorded [2].

### **SOLIDS**

Solid as poly crystalline material or as a single crystal can be studied with the help of Raman technique. Solvents or alkyl halides or mull are not

required for recording the spectra. Solids in the form of fine powder enclosed in a glass or silica fiber can be used. When the measurement is made as a single crystal, depending on the orientation of the crystal axis and polarization of the incident radiation the spectra may vary. Raman spectra can also be recorded for adsorbed species. Samples can also be studied using the Raman technique at various pressures and temperatures [4].

## **POLYMERS**

Polymers do not require elaborate sample preparation techniques for Raman study. Polymers samples often produce fluorescence due to contaminants on their surface. Wiping the sample with a solvent like acetone or alcohol can reduce the fluorescence [14]. Even very small amount of polymeric samples can be studied. Polymeric sample containing Glass fibers can be examined without prior treatment [2]. A simple technique to determine the inorganic fillers incorporated in polymers is simply burn the sample and examines the residue in spectrometer [13].

## **APPLICATION OF GROUP THEORY TO VIBRATIONAL SPECTROSCOPY**

Symmetry is a visual concept as reflected by the geometrical shapes of molecules such as ammonia, benzene, etc. The link between molecular symmetry and quantum mechanics is provided by the group theory. In

vibrational spectroscopy, group theory can be effectively used for: (1) determining the symmetry types of normal mode vibrations of the molecule, (2) predicting the infrared and Raman activity of a normal mode of vibration of a particular symmetry types and (3) simplification of method of obtaining the relation between force constants and vibrational frequencies [10]. The group theory was used, first time by Wigner (1930), for the study of molecular vibrations [25].

The molecular symmetry is systematized quantitatively by introducing the concept of 'symmetry operation'. A symmetry operation transforms the molecular framework into an equivalent configuration or identical configuration. A symmetry element is a geometrical entity such as point, an axis or a plane about which one or more symmetry operations are carried out. Five kinds of fundamental symmetry operations are utilized in specifying molecular symmetry. (i) Proper axis of symmetry ( $C_n$ ) it is rotation once or several times by an angle  $\theta = (2\pi/n)$  about the axis, (ii) Plane of symmetry ( $\sigma$ ) one or more reflections in the plane, (iii) Improper axis of symmetry ( $S_n$ ) rotation about an axis followed by reflection in a plane perpendicular to the rotation axis, (iv) centre of symmetry (I) inversion of all atoms through the centre of symmetry, (v) identity element (E) rotation of the molecule through  $0^\circ$  or  $360^\circ$  which leaves the molecule unchanged [8].

All the symmetry operations present in a molecule form a group and such groups are called point groups. In a point group all the elements of symmetry present in the molecule intersect at a common point and this point remains fixed under all the symmetry operations of the molecule. Although theoretically large numbers of such groups are possible, most molecules fall under a dozen point groups. Some of the common molecular point groups are  $C_s$ ,  $C_n$ ,  $C_{nv}$ ,  $C_{nh}$ ,  $C_{\infty v}$ ,  $D_n$ ,  $D_{nh}$ ,  $D_{nd}$ ,  $S_n$ ,  $T$ ,  $T_d$ ,  $O$ ,  $O_h$ ,  $I_h$ ,  $D_{\infty h}$ , etc. Molecules can be fixed to point groups using the following steps [26].

I. For a linear molecule:

No centre of symmetry :  $C_{\infty v}$  Group

Centre of symmetry present :  $D_{\infty h}$  Group

II. For a molecule of Octahedral shape :

No  $i$  present :  $O$  Group

$i$  present :  $C_{\infty v}$  Group

III. For a molecule of Tetrahedral shape:

No  $\sigma_d$  present :  $T$  group

$6\sigma_d$  present :  $T_d$  group

If the molecule does not belong to any of the above categories, look for the  $C_n$  axis of highest order present.

IV. If  $n=1$  and

- |  |                           |               |
|--|---------------------------|---------------|
|  | No other elements present | : $C_1$ group |
|  | i present                 | : $C_1$ group |
|  | $\sigma$ present          | : $C_s$ group |
- V.  $C_n$  with  $n > 1$  exists and there are no  $C'_2$  axis perpendicular to  $C_n$  and if
- |  |                                       |                  |
|--|---------------------------------------|------------------|
|  | No other elements present             | : $C_n$ group    |
|  | $\sigma_h$ exists                     | : $C_{nh}$ group |
|  | $n\sigma'_v$ exists but no $\sigma_h$ | : $C_{nv}$ group |
- VI.  $C_n$  with  $n > 1$  exists and there are  $C'_2$  axis perpendicular to  $C_n$  and if
- |  |                                       |                  |
|--|---------------------------------------|------------------|
|  | No $\sigma$ exists                    | : $D_n$ group    |
|  | $\sigma_h$ exists                     | : $D_{nh}$ group |
|  | $n\sigma'_d$ exists but no $\sigma_h$ | : $D_{nd}$ group |
- VII.  $C_n$  with  $n > 1$  exists and there exists a  $S_{2n}$  coincident with  $C_n$  and no other element of symmetry (sometimes i may present) exists
- :  $S_{2n}$  group

Any symmetry operation about a symmetry element in a molecule involves the transformation of a set of coordinates  $x, y$  &  $z$  of an atom into a set of new coordinates  $x', y'$  &  $z'$ . The two sets of coordinates can be related with the help set of equations or a matrix. The matrix is referred as the

*transformation matrix* and a specific transformation matrix can represent each symmetry operation. Such matrices for the various symmetry operations of a point group form a representation. Representations can be divided into two types: Reducible representation and irreducible representation.

Let A, B, C and S is the matrices in the representation T of a group. Let S be the similarity transformation matrix in this group. By similarity transformation the matrices A, B, C and S are changed to A', B', C' and S' as

$$S^{-1}AS = A' ; \quad S^{-1}BS = B' ; \quad S^{-1}CS = C' ; \quad S^{-1}DS = D'$$

If the resulting matrices can be blocked into smaller matrices, then the representation T is called a reducible representation. If it is not possible to find a similarity transformation matrix, which will reduce the matrices of representation T, then the presentation is said to be irreducible [8]. Every point group consists of a certain number of irreducible representations. The characters of matrices in the different irreducible representations of a point group can be listed in a table known as character table. Character table plays a vital role in solving problems such as molecular vibrations. The character table for a point group can be constructed with the knowledge of properties of irreducible representations.

The construction of character table requires practice, expertise and knowledge of theorems in group theory such as orthogonal theorems, theorems

of representation theory, etc. Without elaborating the procedure, the character table for two point groups [10]  $C_s$  and  $C_{2v}$  (the molecules chosen for the present thesis falls under these groups) are given below:

In the tables A and B represents representation which is symmetric and anti-Symmetric with respect to the main axis of rotation, ' , ' -represents symmetric and anti-symmetric with respect to a plane of symmetry, and 1,2 (as subscripts) represents symmetric and anti-symmetric with respect to a rotation axis ( $C_n$ ). The last two columns of each character table list the infrared and Raman activity of the particular species. Polarizability components are listed for Raman activity and translational and rotational components are listed for infrared activity.

Based on the character table the selection rules for infrared and Raman activity can be obtained with the help of group theory and quantum mechanics.

### Character Table for $C_s$ point Group

$C_s$	E	$\sigma_{2v}$	Activity	
			Infrared	Raman
A'	1	1	$T_z, T_y, R_z$	$\alpha_{xx}, \alpha_{yy}, \alpha_{zz}, \alpha_{xy}$
A''	1	- 1	$T_z, R_x, R_y$	$\alpha_{yz}, \alpha_{xz}$

**Character Table for  $C_{2v}$  point Group**

$C_{2v}$	E C <sub>2</sub> $\sigma_v(xz)$ $\sigma_v(yz)$				Activity	
	Infrared	Raman				
A <sub>1</sub>	1	1	1	1	T <sub>z</sub>	$\alpha_{xx}, \alpha_{yy}, \alpha_{zz}$
A <sub>2</sub>	1	1	-1	-1	R <sub>z</sub>	$\alpha_{xy}$
B <sub>1</sub>	1	-1	1	-1	T <sub>x</sub> , R <sub>y</sub>	$\alpha_{xz}$
B <sub>2</sub>	1	-1	-1	1	T <sub>y</sub> , R <sub>x</sub>	$\alpha_{yz}$

### INFRARED-ACTIVE VIBRATIONS

The point group of a molecule will have a definite number of symmetry operations. These operations are of two types: *Proper Rotations* – a rotation through an angle  $\pm \phi$  about some axis of symmetry and *Improper Rotations* – rotation followed by a reflection in a plane perpendicular to the axis of rotation. A quantity called character is necessary for the determination of the selection

rules and number of fundamentals of each vibration type. For a given vibration type there is a separate character for each class of symmetry operations. These characters can be found from the character table.

Vibrations active in infrared spectra are determined by character  $\chi_M$  of the dipole moment given by

$$\chi_M = \pm 1 + 2 \cos \varphi \quad \rightarrow 1.26$$

The + sign is for proper rotations and – sign for improper rotations. The character  $\chi_M$  for a given class is always a linear combination of the characters of the vibration types for that class. This linear combination is done by means of the reduction formulae

$$N_i = \frac{1}{g} \sum n_M \chi_M \chi_i \quad \rightarrow 1.27$$

Where  $g$  is the number of elements in a point group,  $\chi_M$  the number of elements in each class,  $\chi_i$  is the character of the vibration type,  $N_i$  the number of times the character  $\chi_i$  of the vibration appear in  $\chi_M$ . The value of  $N_i$  if equal to zero than that vibration type is infrared inactive otherwise active [10].

## **RAMAN ACTIVE VIBRATIONS**

Vibrations active in Raman spectra are determined by character  $\chi_\alpha$  of the polarizability  $\alpha$  given by

$$\chi_\alpha = (2 \pm 2 \cos \varphi) + (2 \cos 2\varphi) \quad \rightarrow 1.28$$

The character  $\chi_\alpha$  must likewise be some linear combination of the  $\chi_i$  using the reduction formulae 1.27. Here also if the  $N_i$  is equal to zero then that vibration type is Raman inactive otherwise active [8].

### NUMBER OF FUNDAMENTALS IN EACH SYMMETRY TYPE

The number of vibrations of each type depends upon the geometry of the molecule. To find the number of fundamentals of each type a quantity  $\xi(R)$  for every symmetry operation required.  $\xi(R)$  is given by:

$$\xi(R) = \begin{cases} (U_R - 2)(1 + 2 \cos \varphi) & \text{for proper rotation} \\ U_R (-1 + 2 \cos \varphi) & \text{for improper rotation} \end{cases} \quad \rightarrow 1.29$$

where  $U_R$  is the number of nuclei unchanged by the symmetry operation.

Knowing  $\xi(R)$  the number of frequencies of each type is determined by using the relation [10]:

$$n_i = \frac{1}{g} \sum n \xi(R) \chi_i \quad \rightarrow 1.30$$

### NORMAL COORDINATE ANALYSIS

The problem of finding the normal modes of vibrations of a polyatomic molecule can be solved by the method of classical mechanics. For carrying out the normal coordinate analysis first the vibrational frequencies observed in the infrared and Raman spectra must be assigned to individual normal modes of vibration. The next step is the calculation of the relative amplitudes of the

normal (or symmetry) coordinates in any normal mode. The main technique behind this is framing the vibrational secular equations and solving these equations. The theoretical background of the normal coordinate analysis is briefed below:

The technique of normal coordinate analysis is highly helpful and essential for complete assignment of the vibrational frequencies of the spectra of a polyatomic molecule and it also leads to a quantitative description of the vibrations. Intermolecular force constants, which hold the structure, can be obtained and used for the understanding of the molecular vibrational frequencies of other molecules. The force constants supply alternative ways of probing bonding and structural characteristics and they can be correlated with inter-atomic repulsions and bond nature. It is also useful in the quantitative study of vibrational band intensities and to study interaction between vibration and rotation levels.

## **FRAMING THE SECULAR EQUATIONS**

Consider a molecule undergoing vibrational motion and let there be many number of normal modes of vibration. The centre of gravity of the molecules in its equilibrium configuration may be chosen as the origin of the coordinate system so as to express the displacement in each normal vibration in terms of Cartesian coordinates. The total kinetic energy is given by the formula,

$$2T = \sum_{i=1}^n m_i (\dot{X}_i^2 + \dot{Y}_i^2 + \dot{Z}_i^2) \quad \rightarrow 1.31$$

This equation can be simplified by using a new set of Cartesian coordinates called the reduced displacement coordinates

$$q_1 = \sqrt{m_1} X_1, \quad q_2 = \sqrt{m_2} X_2, \quad q_3 = \sqrt{m_3} X_3, \quad q_4 = \sqrt{m_4} X_4, \quad \dots \quad \rightarrow 1.32$$

now the equation 1.31 can be written as

$$2T = \sum_{i=1}^{3n} a_{ij} \dot{q}_i \dot{q}_j \quad \rightarrow 1.33$$

If the vibrations are simple harmonic then the potential energy, in reduced coordinates, can be written as

$$2V = \sum_{i,j}^{3n} b_{ij} q_i q_j \quad \rightarrow 1.34$$

The  $b_{ij}$  values are constants and the  $a_{ij}$  values are functions of the atomic masses.  $q_i$  and  $q_j$  are the  $i^{\text{th}}$  and  $j^{\text{th}}$  coordinates.

The classical equation of motion for the  $i^{\text{th}}$  mass by using the Newton's equation in the Lagrange form is:

$$\frac{\partial}{\partial t} \left( \frac{\partial T}{\partial \dot{q}_i} \right) + \frac{\partial V}{\partial q_i} = 0 \quad \rightarrow 1.35$$

Using equations 1.33 and 1.34 in 1.35 we get

$$\sum_j (a_j \ddot{q}_j + b_j q_j) = 0 \quad \rightarrow 1.36$$

The general solutions of the above equation is given by.

$$q_j = A_j \sin(\lambda^{1/2} t + \varphi) \quad \rightarrow 1.37$$

which is an equation characteristic of wave motion with  $\lambda = 4\pi^2 \nu^2$  where  $\nu$  is the frequency, and  $A$  &  $\varphi$  are amplitude and phase constant respectively. From equations 1.36 and 1.37, we can write

$$\sum_{j=1}^{3n} (b_{i,j} - a_{i,j} \lambda) A_j = 0 \quad \rightarrow 1.38$$

Where  $j = 1, 2, 3, \dots, 3n$ . For non-trivial solution the determinant of the coefficients must be equal to zero i.e.,

$$|b_{i,j} - a_{i,j} \lambda| = 0 \quad \rightarrow 1.39$$

The equation 1.39 is called as the secular determinant. It has  $3n$  roots,  $\lambda_i$  for which the above equation is satisfied. Each of these  $\lambda$  values expresses the harmonic vibration of a mass particle with frequency  $\nu$ . These  $\nu$  values are the normal frequencies of the vibrations. The values of  $\lambda$  can be substituted back in equation 1.38 and  $A_j$  can be calculated which will describe the vibration [27].

## EVALUATION OF THE SECULAR DETERMINANT

The evaluation of the secular determinant is simplified by the transformation to a new set of coordinates  $Q_i$ , such that the cross product terms in 1.33 and 1.34 disappears. The old and new coordinates can be related by an orthogonal transformation

$$q_k = \sum_{i=1}^{3n} B_{ki} Q_i \quad \rightarrow 1.40$$

The coordinates  $Q_i$  are called the normal coordinates for the molecular system. Based on the equation 1.29 the kinetic and potential energies can be written as

$$2T = \sum_i \dot{Q}_i^2 \quad \rightarrow 1.41$$

$$2V = \sum_i \lambda_i Q_i^2 \quad \rightarrow 1.42$$

Employing equations 1.40 and 1.41 in 1.35, we get,

$$\ddot{Q}_i + \lambda_i Q_i = 0 \quad \rightarrow 1.43$$

The solution of this expression is given by, similar to equation 1.26,

$$Q_i = B_i \sin(\lambda_i^{1/2} t + \varphi) \quad \rightarrow 1.44$$

The vibrational problem is much easier to describe by means of matrix algebra.

Thus the expression for kinetic and potential energies in matrix notation is

$$2T = \dot{Q}^T \dot{Q} \quad \rightarrow 1.45$$

and 
$$2V = Q^T \Lambda Q \quad \rightarrow 1.46$$

where  $\Lambda$  is the diagonal matrix with element  $\lambda_i$  and  $Q^T$  represents the transpose of the column matrix  $Q$  of the normal coordinates. The simplified form of the secular equation can now be written as

$$|\Lambda - E\lambda| = 0 \quad \rightarrow 1.47$$

This equation will have  $3n - 6$  roots  $\lambda_i$  and each value of  $\lambda$  corresponds to a normal vibrational frequency of the molecule. All the atoms vibrate with the same frequency and phase in each normal mode  $Q_i$  [3].

### **SOLUTION OF SECULAR EQUATION IN INTERNAL COORDINATES**

If internal coordinates are used as the initial coordinates the solution of the secular determinant 1.47 is greatly simplified. The internal coordinates are defined as the increments in bond lengths and bond angles. The principle advantage of internal coordinates is the representation of the potential energy or force constant matrix in terms of bond stiffness and resistance to bond angle deformations, which make these coordinates physically comprehensible. The size of the secular equation in internal coordinates is smaller and hence easier to solve.

The kinetic energy in terms of internal coordinates is given by the expression

$$2T = \sum_{i,j} G_{ij}^{-1} \dot{r}_i \dot{r}_j \quad \rightarrow 1.48$$

Where  $G_{ij}^{-1}$  the inverse kinetic energy element for each pair of coordinates  $r_i$  and  $r_j$ . Similarly, the potential energy in internal coordinates is

$$2V = \sum_{i,j} f_{ij} r_i r_j \quad \rightarrow 1.49$$

where  $f_{ij}$  are the harmonic force constants.

In matrix notation, the equation 1.48 and 1.49 can be suitably expressed by the equations,

$$2T = \dot{R}^T G^{-1} \dot{R} \quad \rightarrow 1.50$$

and 
$$2V = R^T F R \quad \rightarrow 1.51$$

where  $G^{-1}$  is the inverse kinetic energy matrix and  $F$  is the potential energy matrix comprises of the intermolecular force constants. Using equations 1.50 and 1.51 in the Newton's equation in Lagrange form given by equation 1.35 and simplifying we get the secular determinant as

$$|GF - E\lambda| = 0 \quad \rightarrow 1.52$$

where E is the unit matrix. The expression 1.52 expresses the secular equation by involving the product term GF. Wilson first described this method of expressing the secular equation and so it is often referred as Wilson's FG matrix method [9].

In order to frame a secular equation 1.52 for a polyatomic molecule it is necessary to select suitable set of internal coordinates and then set up the F and G matrix. At least  $3n - 6$  internal coordinates are necessary to describe the vibration of an n-atom molecule. Sometimes it necessary to include more than  $3n-6$  internal coordinates and this will result in redundancies. These redundancies (interdependence of internal coordinates) can be removed later by a suitable coordinate transformation. While choosing the internal coordinates the rules given by Decius [28] will be much helpful.

## **SOLUTION OF SECULAR EQUATION IN SYMMETRY COORDINATES**

After setting up the F and G matrix, the secular determinant 1.52 can be solved for Eigen values and Eigen vectors. But the size of the determinant is very high for most of the polyatomic molecules. It is therefore be advantageous to reduce the order of the determinant by taking advantage of the molecular symmetry. The simplification can be effected by the use of symmetry coordinates [29] and they are simple linear combinations of internal coordinates. For introducing symmetry coordinates the first step is to classify

the normal vibrations according to the irreducible representation of the point group to which the molecule belongs. The symmetry coordinates are next selected so as to transform according to the appropriate irreducible representations of the molecular point group. These coordinates block diagonalise the secular determinant. Hence the problem of solving the determinant of the order  $3n - 6$  is reduced to the problem of solving several independent determinants of smaller order [27].

By using an orthogonal coordinate transformation internal coordinates  $R$  can be transformed to symmetry coordinates  $S$  and such an operation is written as,

$$S = UR \quad \rightarrow 1.53$$

where  $U$  is an orthogonal matrix. The  $G$  and  $F$  matrices in internal coordinates can be block-diagonalised using the  $U$ -matrix as below

$$UGU^T = G_s \quad \rightarrow 1.54$$

$$UFU^T = F_s \quad \rightarrow 1.55$$

The above equations give the  $G$  and  $F$  matrices in symmetry coordinates. Now the secular determinant in terms of symmetry coordinates is

$$|G_s F_s - E\lambda| = 0 \quad \rightarrow 1.56$$

the normal vibrations according to the irreducible representation of the point group to which the molecule belongs. The symmetry coordinates are next selected so as to transform according to the appropriate irreducible representations of the molecular point group. These coordinates block diagonalise the secular determinant. Hence the problem of solving the determinant of the order  $3n - 6$  is reduced to the problem of solving several independent determinants of smaller order [27].

By using an orthogonal coordinate transformation internal coordinates  $R$  can be transformed to symmetry coordinates  $S$  and such an operation is written as,

$$S = UR \quad \rightarrow 1.53$$

where  $U$  is an orthogonal matrix. The  $G$  and  $F$  matrices in internal coordinates can be block-diagonalised using the  $U$ -matrix as below

$$UGU^T = G_s \quad \rightarrow 1.54$$

$$UFU^T = F_s \quad \rightarrow 1.55$$

The above equations give the  $G$  and  $F$  matrices in symmetry coordinates. Now the secular determinant in terms of symmetry coordinates is

$$\left| G_s F_s - E\lambda \right| = 0 \quad \rightarrow 1.56$$

This expression has the same roots as the secular equation 1.52 in terms of internal coordinates and thus the Eigen values and Eigen vectors of both 1.56 and 1.52 are the same.

When the Eigen values  $\lambda$  are determined, the Eigen vectors  $L$  for each of the Eigen values can be evaluated from

$$|G_s F_s - E\lambda| L = 0 \quad \rightarrow 1.57$$

The  $L$  matrix consisting of the Eigen vectors which are normalized. It provides the transformation from internal coordinates to the normal coordinates [3].

## POTENTIAL ENERGY DISTRIBUTION

In the normal coordinate analysis, potential energy distribution (PED) plays an important role in obtaining a detailed understanding about the nature of the normal modes. Morino and Kuchitsu [30] have shown that the potential energy distribution rather than the normalized amplitudes is a more satisfactory quantity to use in band assignments.

The normal coordinates ( $R_i$ ) are related to the normal coordinates ( $Q_k$ ) as follows

$$R_i = \sum_{k=1}^{3n-6} L_{ik} Q_k \quad \rightarrow 1.58$$

where  $L_{ik}$  is the component of the L-matrix. Substitution of equation 1.58 to the potential energy expression 1.44 yields the potential energy of the molecule, for a vibration of frequency  $\nu_k$ , associated with a normal coordinate  $Q_k$ ,

$$2V = Q_k^2 \sum_{i,j} f_{ij} L_{ik} L_{jk} \quad \rightarrow 1.59$$

Such terms are large only when  $i = j$ , since the diagonal force constants  $f_{ij}$  are much greater than the off-diagonal constants  $f_{ij}$ . Consequently to get the PED, only the terms  $f_{ii} L_{ik}^2$  need to be calculated. The normalization condition  $L^T f L = A$ , gives the relation of the form,

$$\sum_{i,j} f_{ij} L_{ik} L_{jk} = \lambda_k \quad \rightarrow 1.60$$

neglecting the cross terms yields

$$\sum_i f_{ii} L_{ik}^2 = \lambda_k \quad \rightarrow 1.61$$

We can therefore get a normalized potential energy distribution (PED), whose terms are

$$PED = V_{ik} = \frac{f_{ii} L_{ik}^2}{\lambda_k} \quad \rightarrow 1.62$$

It is the contribution of the  $i^{\text{th}}$  symmetry coordinates to the potential energy of the vibration whose frequency is  $\nu_k$  [31]. The contribution of the potential energy from the individual diagonal elements gives rise to a conceptual link

between the empirical analysis of the vibration spectra of complex molecules dealing with the characteristic group frequencies and the theoretical approach from the computation of the normal modes.

## **FORCE FIELD APPROXIMATIONS**

The primary aim of vibrational analysis is to theoretically calculate the vibrational frequencies of a molecule from the force constants. But the vibrational frequencies are easily observable from IR and Raman spectra. With some difficulty it is possible to compute the force constants from the observed frequencies. To achieve this, the observed vibrational frequencies should be first correctly assigned to the symmetry species of a molecular point group. Force constants can also be calculated from molecular data like Coriolis coupling constants, centrifugal distortion constants and mean amplitude of vibration.

For many molecules it is not possible to evaluate all the force constants from the experimental data and it becomes necessary to reduce the force constants. This is accomplished by making assumptions about the nature of the potential energy function. Some of the important restrictive force fields are:

## COMPUTER PROGRAMS FOR SOLVING THE SECULAR EQUATIONS

The advent of computers has certainly aided the normal coordinate analysis of molecules since computers can compensate some of the inherent difficulties and problems in the method. The multiplication of matrices and the solving of secular equations become highly simplified and completed in least time. With the developments of high-level computer languages, a large number of programs are developed for the normal coordinate treatment. Schachtschneider (1965) [30], Shimanouchi (1968) [31], Fuhrer et al (1976) [32], are some of the notable program developers for normal coordinate analysis. Many such programs are also available commercially for instance, Vibratz by Eric Dowty (1998) [33]. Some programs, under public domain, are also available in Internet like Prometheus by Martin Jursch (1997) [34].

After introducing necessary modifications in the program developed by Fuhrer et al, was used for the normal coordinate analysis in the present thesis. The necessary information that is needed for the calculation is an initial vibrational force field and the structural parameters of the molecules. These parameters may be both the bond lengths and bond angles or the Cartesian coordinates of the atoms with respect to an arbitrarily chosen origin. Force constants from structurally similar molecules can be transferred as initial values and if necessary some additional force constants can be added. The program is

designed to consist of modules so that the output from one calculation serves as a part of the input to the next. The vibrational frequencies of normal modes and potential energy distribution are obtained as output. With the help of the program the initial set of force constants can be refined to give an excellent fit between the calculated and observed frequencies. Least squares procedure is used to refine the force field calculations.

## **EXPERIMENTAL DETAILS**

All the compounds are used in this thesis for investigation are purchased from Sigma-Aldrich chemicals, USA with spectroscopic grade and it is used as such without any further purification. The FTIR spectra of the compounds have been recorded in Perkin-Elmer 180 Spectrometer in the range of 4000–100  $\text{cm}^{-1}$ . The spectral resolution is  $\pm 2 \text{ cm}^{-1}$ . The FT-Raman spectrum of the compounds are also recorded in the same instrument with FRA 106 Raman module equipped with Nd: YAG laser source operating at 1.064  $\mu\text{m}$  line widths with 200 mW powers. The spectra are recorded with scanning speed of 30  $\text{cm}^{-1} \text{ min}^{-1}$  of spectral width 2  $\text{cm}^{-1}$ . The frequencies of all sharp bands are accurate to  $\pm 1 \text{ cm}^{-1}$ .

## **COMPUTATIONAL DETAILS**

The quantum calculations were performed with Gaussian 03W program [35] using Hatree-Fock(HF), DFT and Hybrid fundamentals, supplements with

different basis sets. Initial geometry of the molecules were generated from standard geometrical parameters were minimized without any constraint in the potential energy surface at Hartree-Fock level, adopting the standard basis sets. The geometries were then reoptimised at B3LYP level using basis sets. The optimized structural parameters were then used for the vibrational frequency calculations to characterize all stationary points as minima. Then vibrationally averaged nuclear positions of the molecules were used for predicting IR intensities and Raman depolarization ratios. Vibrational frequencies are scaled by 0.9067 in HF calculations and the range of wave numbers above  $1700\text{ cm}^{-1}$  by 0.958 and for the range below  $1700\text{ cm}^{-1}$  scaled by 0.983 in B3LYP [36]. The results of the GAUSSVIEW program [37] with symmetry considerations, vibrational frequency assignments were made with a high degree of accuracy introduced by using a least-square optimization of the computed to the experimental data. The assignments of certain modes have been made by calculating PEDs. The PEDs are computed quantum chemically from calculated vibrational frequencies using VEDA program [38]. Gauss view program has been used to get visual animation and for the verification of the normal modes.

## **GAUSSIAN**

Gaussian [39-40] is a computational software program initially released in 1970 by John Pople and research group at Carnegie-Mellon University. It has been continuously updated since then. The recent version is Gaussian 09.

The name originates from the word Gaussian function or orbital, a choice made to improve the computing capacity of then existing software which used a function or orbital called Slater type. Gaussian functions are widely used in statistics where they describe the normal distributions. In this Quantum computation, it represents the wave function of the ground state of a harmonic oscillator. The linear combinations of such Gaussian functions for a molecular orbital is called as Gaussian orbital. The Gaussian software program is used by Physicists, Chemists, Chemical engineers, Biochemists and others for research in established and emerging areas of molecular physics or chemistry. Starting from the basic laws of quantum mechanics, Gaussian predicts the energies, molecular structures, vibrational frequencies and other molecular properties derived from these basic quantities. It can be used to study molecules and reactions under a wide range of conditions, including both stable and short lived intermediate compounds.

Computational techniques consist of three areas: Ab-initio methods, semi-empirical methods, and molecular mechanics. Molecular mechanics utilizes classical physics to solve large systems of molecules and is considered the least accurate due to the fact that no electron behavior is factored in. Semi-empirical methods are more accurate because of utilization of quantum physics to account for some of the electron behavior, but its scope is still limited since it relies on extensive approximations and empirical parameters. Ab-initio methods are based purely on quantum physics and use no approximations from

classical physics to describe the electronic structure of the molecule very accurately. The drawback of using ab-initio methods is that the computations are extremely taxing and so is limited to much smaller systems such as individual molecules. However, ab-initio methods give a lot of information on the electronic structure without having to actually synthesize the molecule experimentally. The fundamental idea behind ab-initio calculations is to solve Schrodinger's equation with a set of mathematical functions called a "basis set".

## BASIC THEORY

In many body electronic structure calculations, the nuclei of the molecules or clusters are treated as fixed, in abeyance with the Born-Oppenheimer approximation, and that generate a static potential  $V$  in which electrons are moving. A stationary electronic state is described by a wave function  $\psi(r_1, r_2 \dots r_n)$ , satisfying the many electron time independent Schrödinger Equation [36]

$$\hat{H}\Psi = [\hat{T} + \hat{V} + \hat{U}] \psi = \left[ \sum_i^N -\frac{\hbar^2}{2m} \nabla_i^2 + \sum_{i>j}^N V(i) + \sum_{i>j}^N U(\vec{r}_i, \vec{r}_j) \right] \Psi = E\Psi$$

Where  $H$  is the Hamiltonian,  $E$  is the total energy,  $T$  is the kinetic energy,  $V$  is the potential energy from the external field due to positively charged nuclei and  $U$  is the electron- electron interaction energy. The operators

T and U are called Universal operators as they are the same for any N- electron system, while V is system dependent.

In theory, solving the Schrödinger equation yields wave functions  $\psi$  that describe the system fully. Unfortunately the Schrödinger equation cannot be solved analytically for many body systems, so approximations are to be made. Typical solution algorithms therefore is to fix the atomic positions and then solve the Schrödinger equation for a specific value of the atomic coordinates  $r_i$ . This is repeated many times to obtain the energy of the system as a function of the atomic coordinates.

The complicated many particle equations are not separable into simpler single particle equations because of the interaction term U. However the single-particle approximation simplifies calculations notably, as it does not account for electron-electron interaction. This method is known as Hartree-Fock method.

#### **HARTREE – FOCK (HF) METHOD**

The origin of the Hartree–Fock method dates back to 1927, soon after the derivation of the Schrödinger equation. D.R.Hartree introduced a procedure to calculate the approximate wave functions and energies for atoms and ions. Hartree was guided by some earlier, semi-empirical methods of the early 1920s (by E. Fues, R. B. Lindsay, and himself) based on the old quantum theory of Bohr. In the Bohr model of the atom, the energy of a state with principal

quantum number  $n$  is given in atomic units as  $E = -1/n^2$ . It was observed from atomic spectra that the energy levels of many-electron atoms are well described by applying a modified version of Bohr's formula. By introducing the quantum defect  $d$  as an empirical parameter, the energy levels of a generic atom was well approximated by the formula  $E = -1/(n + d)^2$ . The existence of a non-zero quantum defect was attributed to electron-electron repulsion, which clearly does not exist in the isolated hydrogen atom. This repulsion resulted in partial screening of the bare nuclear charge. These early researchers later introduced other potentials containing additional empirical parameters with the hope of better reproducing the experimental data. Hartree sought to do away with empirical parameters and solve the many-body time-independent Schrödinger equation from fundamental physical principles, i.e., **ab-initio**. His first proposed method of solution became known as the **Hartree method**.

This method is an approximate method for the determination of the ground-state wave function and ground-state energy of a quantum many-body system. This method assumes that the exact,  $N$ -body wave function of the system can be approximated by a single Slater determinant (in the case where the particles are fermions) or by a single permanent (in the case of bosons)  $N$  spin-orbitals. By invoking the variational principle, one can derive a set of  $N$ -coupled equations for the  $N$  spin orbitals. Solution of these equations yields the Hartree–Fock wave function and energy of the system, which are approximations of the exact ones.

The **Slater type of orbitals (STO)** is of the general form

$$STO = \frac{\xi^3}{\pi^{0.5}} e^{-\xi r}$$

where  $\xi$  is orbital exponent which reflects the spatial extent of the orbital. The HF method is also called, especially in the older literature, the **self-consistent field method (SCF)** as the solutions to the resulting non-linear equations behave as if each particle is subjected to the mean field created by all other particles. The equations are almost universally solved by means of an iterative, fixed-point type algorithm.

It is important to remember that STO leads to very tedious calculations. Thus S.F.Boys developed an alternative type of orbital called **Gaussian type orbital (GTO)** for calculations, which are of the form

$$GTO = \frac{2\chi}{\pi^{0.75}} e^{-\chi r^2}$$

The difference between STO and GTO lies in the spatial coordinate  $r$ . The GTO has square of  $r$  so that the product of one Gaussian gives another Gaussian. Ultimately it is found that more the combination of Gaussians, more the accuracy of the equations.

This solution scheme is not the only one possible and is not an essential feature of the HF method. For molecules, Hartree–Fock is the central starting

point for most ab-initio quantum chemistry methods. The above discussion is only for the Restricted Hartree–Fock method, where the atom or molecule is a closed-shell system with all orbitals (atomic or molecular) are doubly occupied. Open-shell systems, where some of the electrons are not paired, can be dealt with by either restricted open-shell Hartree–Fock (ROHF) or Unrestricted Hartree–Fock (UHF) method.

## **OTHER METHODS**

Additional modifications have been implemented with the previous Hartree-Fock approximations to account for electron correlation. There are three methods, among several, that account for electron correlation: Configuration-Interaction, Moller-Plesset perturbation, and Density Functional Theory.

## **CONFIGURATION INTERACTION (CI) METHOD**

In Hartree–Fock, it is assumed that a wave function can be written as a product of one–electron wavefunctions. In Configuration interaction (CI) method (2), some multi–electron wave functions are added back into the basic Hartree–Fock method to account for their coordinated motion. This is done systematically by constructing multi–electron wave functions as a sum of the Hartree–Fock wavefunctions for different electronic states. A slight

improvement of this method is CISD where one or two electron is assumed to be in excited states. S and D stand for single and double.

**Couple cluster (CC)** methods are conceptually similar but differ mathematically in the construction of multi electron wave functions. Unlike in CI, CC uses an exponential ansatz to guarantee size extensivity of the solution. The calculations may also include single, double and triple excitations, leading to CCSD and CCSDT methods.

### **MOLLER–PLESSET PERTURBATION THEORY (MPPT)**

The alternative to multi–electron wavefunctions is to choose an approximation for the correlation energy. In this theory, an additional term is added to the total energy and is treated as a perturbation. The perturbed wave function and perturbed energy are expressed as a power series to the  $n^{\text{th}}$  order (MP $n$ ) such as MP2, MP4 etc, although it is not always convergent with increasing the power  $n$ .

### **DENSITY FUNCTIONAL THEORY (DFT)**

The previous methods are fundamentally based on the wavefunction approach. They scale poorly the complexity of the molecule with a number of basis functions the atomic s, p, d etc., orbitals are used to describe the molecular orbitals. Instead of solving for the wavefunction in order to calculate

the energy of the molecule, density functional theory calculates the energy directly from the ground state electron density  $n(\vec{r})$

Here DFT provides an appealing alternative, being much more versatile as it provides a way to systematically map the many-body problem, with  $\hat{U}$ , onto a single-body problem without  $\hat{U}$ . In DFT the key variable is the particle density  $n(\vec{r})$  which for a normalized  $\Psi$  is given by

$$n(\vec{r}) = N \int d^3 r_2 \int d^3 r_3 \dots \int d^3 r_N \Psi^* (\vec{r}, \vec{r}_2, \dots, \vec{r}_N) \Psi (\vec{r}, \vec{r}_2, \dots, \vec{r}_N)$$

This relation can be reversed, i.e. for a given ground-state density  $n_0(\vec{r})$  it is possible, in principle, to calculate the corresponding ground-state wavefunction  $\psi_0(\vec{r}_1, \dots, \vec{r}_N)$ . In other words,  $\psi_0$  is a unique functional of  $n_0$ ,

$$\psi_0 = \psi_{n_0}$$

and consequently the ground-state expectation value of an observable  $\hat{O}$  is also a functional of  $n_0$

$$O[n_0] = \langle \psi[n_0] | \hat{O} | \psi[n_0] \rangle$$

In particular, the ground-state energy is a functional of  $n_0$

$$E_0 = E [n_0] = \langle \psi [n_0] | \hat{T} + \hat{V} + \hat{U} | \psi [n_0] \rangle$$

where the contribution of the external potential  $\langle \psi [n_0] | \hat{V} | \psi [n_0] \rangle$  can be written explicitly in terms of the ground-state density  $n_0$

$$V [n_0] = \int V(\vec{r}) n_0(\vec{r}) d^3r$$

More generally, the contribution of the external potential  $\langle \psi | \hat{V} | \psi \rangle$  can be written explicitly in terms of the density  $n$ ,

$$V [n] = \int V(\vec{r}) n(\vec{r}) d^3r$$

The functionals  $T [n]$  and  $U [n]$  are called universal functionals, while  $V [n]$  is called a non-universal functional, as it depends on the system under study. Having specified a system, i.e., having specified  $\hat{V}$ , one then has to minimize the functional

$$E [n] = T [n] + U [n] + \int V(\vec{r}) n(\vec{r}) d^3r$$

with respect to  $n(\vec{r})$ , assuming one has got reliable expressions for  $T [n]$  and  $U [n]$ . A successful minimization of the energy functional will yield the ground-state density  $n_0$  and thus all other ground-state observables.

The variational problems of minimizing the energy functional  $E[n]$  can be solved by applying the Lagrangian method of undetermined multipliers. First, one considers an energy functional that doesn't explicitly have an electron-electron interaction energy term,

$$E_s[n] = \langle \psi_s[n] | \hat{T}_s + \hat{V}_s | \psi_s[n] \rangle$$

where  $\hat{T}_s$  denotes the non-interacting kinetic energy and  $\hat{V}_s$  is an external effective potential in which the particles are moving. Obviously,  $n_s(\vec{r}) \stackrel{def}{=} n(\vec{r})$  if  $\hat{V}_s$  is chosen to be

$$\hat{V}_s = \hat{V} + \hat{U} + (\hat{T} - \hat{T}_s)$$

Thus, one can solve the so-called Kohn-Sham equations of this auxiliary non-interacting system,

$$\left[ -\frac{\hbar^2}{2m} \nabla^2 + V_s(\vec{r}) \right] \phi_i(\vec{r}) = \epsilon_i \phi_i(\vec{r})$$

which yields the orbital's  $\phi_i$  that reproduce the density  $n(\vec{r})$  of the original many-body system

$$n(\vec{r}) \stackrel{def}{=} n_s(\vec{r}) = \sum_i^N |\phi_i(\vec{r})|^2$$

The effective single-particle potential can be written in more detail as

$$V_s(\vec{r}) = V(\vec{r}) + \int \frac{e^2 n_s(\vec{r}')}{|\vec{r} - \vec{r}'|} d^3 r' + V_{XC} [n_s(\vec{r})]$$

where the second term denotes the so-called Hartree term describing the electron-electron Coulomb repulsion, while the last term  $V_{XC}$  is called the exchange-correlation potential. Here,  $V_{XC}$  includes all the many-particle interactions. Since the Hartree term and  $V_{XC}$  depend on  $n(\vec{r})$ , which depends on the  $\phi_i$ , which in turn depend on  $V_s$ , the problem of solving the Kohn-Sham equation has to be done in a self-consistent way. Usually one starts with an initial guess for  $n(\vec{r})$ , then calculates the corresponding  $V_s$  and solves the Kohn-Sham equations for the  $\phi_i$ . From these one calculates a new density and starts again. This procedure is then repeated until convergence is reached. A non-iterative approximate formulation called Harris functional DFT is an alternative approach to this.

## **APPROXIMATIONS (EXCHANGE-CORRELATION FUNCTIONALS)**

The major problem with DFT is that the exact functionals for exchange and correlation are not known except for the free electron gas. However, approximations exist which permit the calculation of certain physical quantities

quite accurately. In physics the most widely used approximation is the local-density approximation (LDA), where the functional depends only on the density at the coordinate where the functional is evaluated:

$$E_{XC}^{LDA}[n] = \int \epsilon_{XC}(n) n(\vec{r}) d^3r$$

The local spin-density approximation (LSDA) is a straightforward generalization of the LDA to include electron spin:

$$E_{XC}^{LSDA}[n_{\uparrow}, n_{\downarrow}] = \int \epsilon_{XC}(n_{\uparrow}, n_{\downarrow}) n(\vec{r}) d^3r$$

Highly accurate formulae for the exchange-correlation energy density  $\epsilon_{XC}(n_{\uparrow}, n_{\downarrow})$  have been constructed from quantum Monte Carlo simulations of a free electron model. Generalized gradient approximations (GGA) are still local but also take into account the gradient of the density at the same coordinate:

$$E_{XC}^{GGA}[n_{\uparrow}, n_{\downarrow}] = \int \epsilon_{XC}(n_{\uparrow}, n_{\downarrow}, \vec{\nabla}n_{\uparrow}, \vec{\nabla}n_{\downarrow}) n(\vec{r}) d^3r$$

Using the latter (GGA) very good results for molecular geometries and ground-state energies have been achieved. Potentially more accurate than the GGA functionals are the meta-GGA functionals. These functionals include a further term in the expansion, depending on the density, the gradient of the density and the Laplacian (second derivative) of the density. Difficulties in expressing the exchange part of the energy can be relieved by including a component of the

exact exchange energy calculated from Hartree-Fock theory. Functionals of this type are known as hybrid functionals.

## HYBRID METHODS

Indeed, it is common to use calculations that are a hybrid of the two methods the popular B3LYP scheme is one such hybrid functional method. The mixture of exact HF exchange and approximate DFT exchange is commonly employed to increase performance. Several different mixing ratios have been advocated. Becke Half-and-Half LYP uses a 1:1 ratio of HF and DFT exchange energies. ie

$$E_{XE} = \frac{1}{2} E_X(\text{HF}) + \frac{1}{2} E_X(\text{Becke88}) + E_C(\text{LYP})$$

The most commonly employed hybrid method is the Becke 3- parameter scheme (B3). The scheme is represented as

$$E_{XE} = 0.2 E_X(\text{HF}) + 0.8 E_X(\text{LSDA}) + 0.72 E_X(\text{Becke88}) + 0.81 E_C(\text{LYP}) + 0.19 E_C(\text{LYP})$$

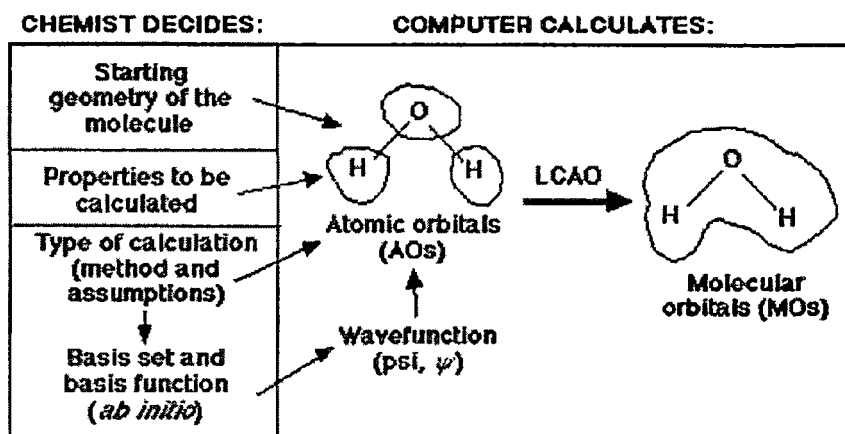
Becke derived the parameters by fitting to a set of thermo chemical data, the G1 molecule set. When B3 is paired with a correlation function other than LYP, the LYP coefficients are retained. Becke also developed a one parameter fit (B). Another option is to use modern valence bond methods. The MPW1PW91 method was developed by Barone and Adamo. It employs a

modified PW91 exchange functional with original PW91 correlation functional and employs a HF and DFT exchange ratio of 0.25: 0.75.

## BASIS SETS

A **basis set** [41] is a set of functions used to create the molecular orbitals, which are expanded as a linear combination of similar functions with the weights or coefficients to be determined.

One characteristic of a molecule that explains a great deal about the properties is their molecular orbitals. The following diagram must be considered in order to



calculate the molecular orbitals.

One of the three major decisions is which of the basis set to use. There are two general categories of basis sets:

### **Minimal basis sets**

A basis set that describes only the most basic aspects of the orbitals.

### **Extended basis sets**

A basis set with a much more detailed description.

Basis sets were first developed by J.C. Slater. Slater fit linear least-squares to data that could be easily calculated. The general expression for a basis function is given as:

$$\text{Basis Function} = N * e^{(-\alpha * r)}$$

where:

N = normalization constant

alpha = orbital exponent

r = radius in angstroms

All basis set equations in the form STO-NG (where N represents the number of GTOs combined to approximate the STO) are considered to be "minimal" basis sets. The "extended" basis sets, then, are the ones that consider the higher orbitals of the molecule and account for size and shape of molecular charge distributions.

There are several types of extended basis sets:

- Double-Zeta, Triple-Zeta, Quadruple-Zeta
- Split-Valence
- Polarized Sets
- Diffuse Sets

### Double-Zeta, Triple-Zeta, Quadruple-Zeta

Previously with the minimal basis sets, all orbitals are approximated to be of the same shape. However, this is not true. The **double-zeta basis set** is important because it allows treating each orbital separately when Hartree-Fock calculation is conducted. This gives us a more accurate representation of each orbital. In order to do this, each atomic orbital is expressed as the sum of two Slater-type orbitals (STOs). The two equations are the same except for the value of  $\zeta$  (zeta). The zeta value accounts for how diffuse (large) the orbital is. The two STOs are then added in some proportion. The constant 'd' determines how much each STO will count towards the final orbital. Thus, the size of the atomic orbital can range anywhere between the value of either of the two STOs. For example, let's look at the following example of a 2s orbital:

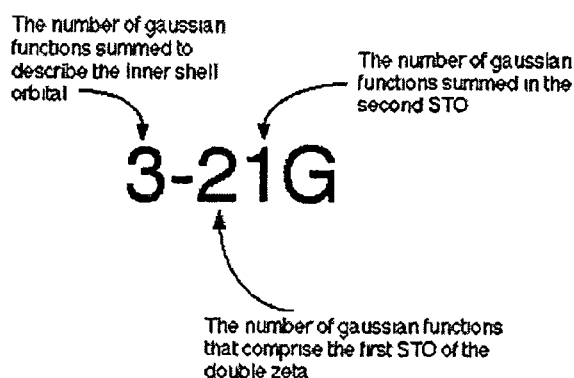
$$\phi_{2s}(r) = \phi_{2s}^{STO}(r, \zeta_1) + d\phi_{2s}^{STO}(r, \zeta_2)$$

In this case, each STO represents a different sized orbital because the zetas are different. The 'd' accounts for the percentage of the second STO to add in. The linear combination then gives the atomic orbital. Since each of the two equations is the same, the symmetry remains constant.

The triple and quadruple-zeta basis sets work the same way, except the use of three and four Slater equations instead of two. The typical trade-off applies here as well, better accuracy for more time or work.

### Split-Valence

Often it takes too much effort to calculate a double-zeta for every orbital. Instead, it can be simplified by calculating a double-zeta only for the valence orbital. Since the inner-shell electrons aren't as vital to the calculation, they are described with a single Slater Orbital. This method is called a **split-valence basis set**. A few examples of common split-valence basis sets are 3-21G, 4-31G, and 6-31G.



An example is given below. It will be of help to understand the subject. Here, a 3-21G basis set is used to calculate for the carbon atom. This means 3 summing Gaussians for the inner shell orbital, two Gaussians for the first STO of the valence orbital and 1 Gaussian for the second STO. Here is the output file from the Gaussian Basis Set Order Form for carbon given a 3-21G basis set.

```

CARBON    (6S,3P)->[3S,2P]
S 3
1    172.256000    0.617669000E-01
2    25.9109000    0.358794000
3    5.53335000    0.700713000
L 2
1    3.66498000    -0.395897000    0.23640000
2    0.770545000    1.21584000    0.860619000
L 1
1    0.195857000    1.00000000    1.00000000

```

Atom	$\alpha_{1s}$	$d_{1s}$	$\alpha_{2s} = \alpha_{2p}$	$d_{2s}$	$d_{2p}$	$\alpha'_{2s} = \alpha'_{2p}$
C	172.256000	0.617669000E-01	3.66498000	-0.395897000	0.23640000	0.195857000
	25.9109000	0.358794000	0.770545000	1.21584000	0.860619000	
	5.53335000	0.700713000				

There is another common method of displaying data. Notice the numbers are labeled so it is easy to match this data with the corresponding data in the output file.

Once a basis set output file is retrieved, these numbers can be used to calculate equations. For a carbon, three equations will be needed: 1s orbital, 2s orbital, and 2p orbital.

This equation combines the 3 GTO orbitals that define the 1s orbital.

$$\begin{aligned}\phi_{1s}(r) &= \sum_{i=1}^3 d_{1si} \phi_{1s}^{GF}(r, \alpha_{1si}) \\ &= 0.6176 \phi_{1s}^{GF}(r, 172.256) + 0.3587 \phi_{1s}^{GF}(r, 25.910) \\ &+ 0.7007 \phi_{1s}^{GF}(r, 5.533)\end{aligned}$$

This equation combines the 2 GTO orbitals that make up the first STO of the double-zeta, plus the 1 GTO that represents the second STO for the 2s orbital.

$$\begin{aligned}\phi_{2s}(r) &= \sum_{i=1}^3 d_{2si} \phi_{2s}^{GF}(r, \alpha_{2si}) + d'_{2s} \phi_{2s}^{GF}(r, \alpha'_{2s}) \\ &= -0.395 \phi_{2s}^{GF}(r, 3.664) + 1.215 \phi_{2s}^{GF}(r, 0.771) \\ &+ 1.000 \phi_{2s}^{GF}(r, 0.195)\end{aligned}$$

This equation combines the 2 GTO orbitals that make up the first STO of the double-zeta, plus 1 GTO that represents the second STO for the 2p orbital.

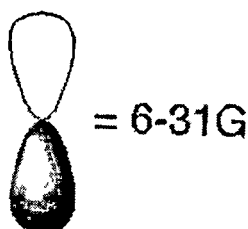
$$\begin{aligned}\phi_{2s}(r) &= \sum_{i=1}^3 d_{2pi} \phi_{2p}^{GF}(r, \alpha_{2pi}) + d'_{2p} \phi_{2p}^{GF}(r, \alpha'_{2p}) \\ &= -0.395 \phi_{2p}^{GF}(r, 3.664) + 1.215 \phi_{2p}^{GF}(r, 0.771) \\ &+ 1.000 \phi_{1s}^{GF}(r, 0.195)\end{aligned}$$

Now, using these three equations, the LCAO can be calculated for the carbon atom.

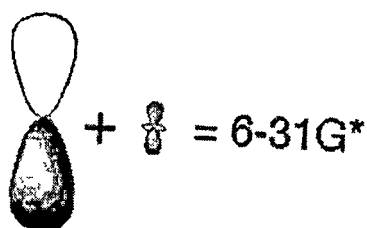
## Polarized Sets

In the previous basis sets atomic orbitals are treated as existing only as 's', 'p', 'd', 'f' etc. Although those basis sets are good approximations, a better approximation is to acknowledge and account for the fact that sometimes orbitals share qualities of 's' and 'p' orbitals or 'p' and 'd', etc. and not necessarily have characteristics of only one or the other. As atoms are brought close together, their charge distribution causes a polarization effect (the positive charge is drawn to one side while the negative charge is drawn to the other) which distorts the shape of the atomic orbitals. In this case, 's' orbitals begin to have a little of the 'p' flavor and 'p' orbitals begin to have a little of the 'd' flavor. One asterisk (\*) at the end of a basis set denotes that polarization has been taken into account in the 'p' orbitals. Notice in the graphics below the difference between the representation of the 'p' orbital for the 6-31G and the 6-31G\* basis sets. The polarized basis set represents the orbital as more than just 'p', by adding a little 'd'.

Original 'p' orbital

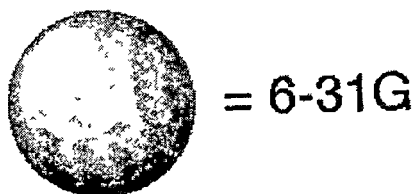


Modified 'p' orbital

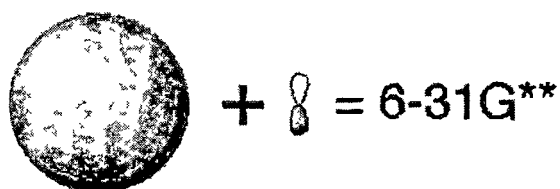


Two asterisks (\*\*) means that polarization has taken into account the 's' orbitals in addition to the 'p' orbitals. Below is another illustration of the difference of the two methods.

#### Original 'S' orbital

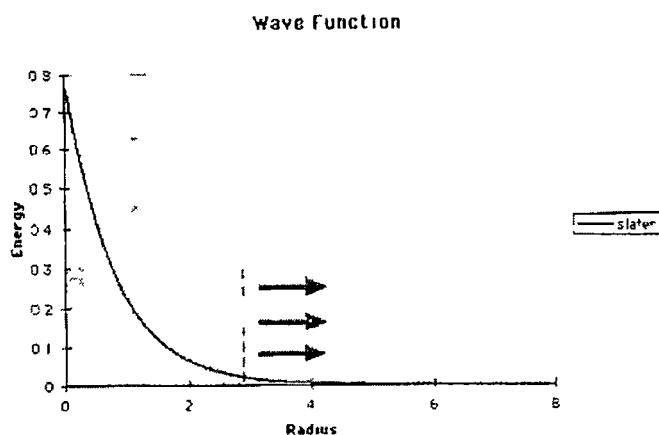


#### Modified 's' orbital



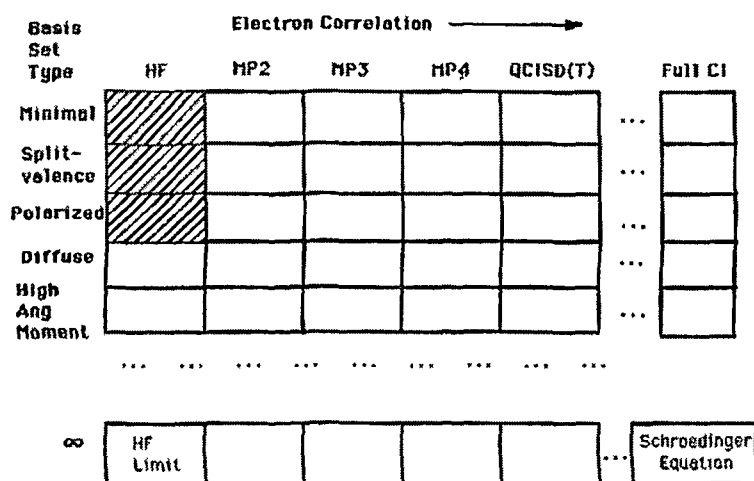
#### Diffuse Sets

In chemistry the valence electrons are the main concern which interacts with other molecules. However, many of the basis sets that are talked about previously concentrate on the main energy located in the inner shell electrons. This is the main area under the wave function curve. In the graphic below, this area is that to the left of the red dotted line. Normally the tail (the area to the right of the dotted line), is not really a factor in calculations.



However, when an atom is in an anion or in an excited state, the loosely bound electrons, which are responsible for the energy in the tail of the wave function, become much more important. To compensate for this area, computational scientists use **diffuse** functions. These basis sets utilize very small exponents to clarify the properties of the tail. Diffuse basis sets are represented by the '+' signs. One '+' means the 'p' orbitals are accounted, while '++' signals mean both 'p' and 's' orbitals, (much like the asterisks in the polarization basis sets).

The tradeoff/relationship between basis sets and accuracy is represented in the diagram below. The ultimate goal is to calculate an answer to the Schrödinger's Equation (right bottom corner). However, we are still a long way from being able to complete this calculation. Right now we are in the top left corner of the chart. In that first box, we are treating each electron independently of the others. As moved across to the right, we can find calculations that account for the interactions of electrons. As moved down the column, more complex and more accurate basis set calculations can



be found.

There are other trade-offs for using each type of basis set. The more complex basis sets are more accurate but, they use up a great deal of computing time. Thus, it is important to choose the correct basis set that can be run fastest without compromising desired level of accuracy.

**REFERENCES**

- [1] G.Herzberg, *Molecular Spectra & Molecular Structure*, Vol-II, Von Nostrand Reinhold Company, New York, (1945).
- [2] Bernhard Schrader, *Infrared & Raman Spectroscopy*, VCH publishers, Inc., New York, (1995).
- [3] D.N.Sathyanaryana, *Vibrational Spectroscopy*, New Age International (P) Ltd., Publishers, New Delhi, (1996).
- [4] B.Norman, Colthup, H.Lawrence, Daly and E.Stephen, Wiberley, \ Introduction to Infrared and Raman Spectroscopy, Academic Press, New York (1964).
- [5] G.Fogarasi,P. Pulay , *Vibrational Spectra &Structure*, Vol.14, (edited by J.R.Durig), Elsevier, Amsterdam, (1983).
- [6] <http://www.wpi.edu/Academics/Depts/Chemistry/Courses/CH2670/infrared.html>
- [7] Stewart J. J. P, *MOPAC 2002 Manual*, Fujitsu Ltd. (2001)
- [8] Sindhu P.S, *Molecular spectroscopy*, Tata McGraw-Hill Publishing Company Ltd, New Delhi, I ed., (1990).
- [9] Wilson E.B Jr., Decius J.C & cross P.C, *Molecular Vibrations*, McGraw-Hill, New York, (1955).
- [10] F.Albert Cotton, *Chemical Applications of Group Theory*, Wiley eastern Ltd., New Delhi, II-Ed., (1986).
- [11] D.I.Bower, W.F.Maddams, *The Vibrational Spectroscopy of Polymers*, Cambridge University Press, Cambridge, (1992).
- [12] Haslam J et al., *Identification and Analysis of Plastics*, Iliffe, London, (1972).
- [13] L.J.Koenig, *Spectroscopy of Polymers*, II Ed., Elsevier, New York, (1999).
- [14] George Socrates, *Infrared and Raman Characteristic Group Frequencies – Tables and Charts*, 3<sup>rd</sup> ed., John Wiley & Sons Ltd., England, (2001).

- [15] N.L.Alpert, W.E. Keiser, H.A.Szymanski, Theory and Practice of Infrared Spectroscopy, Plenum/Rosetta Ed., (1973).
- [16] P.J.Hendra, Int.J.Vibr.Spec., [www.ijvs.com] 5, 5, 2 (2001).
- [17] Gable.K, [http:// www. chem. orst.edu/ch361-464/ch362/irinstrs.htm](http://www.chem.orst.edu/ch361-464/ch362/irinstrs.htm)., (2000).
- [18] Brian M.Tissue, <http://www.chem.vt.edu/chem-ed/data/fourier.html>, (2000).
- [19] P.R.Griffiths, J.A.& de Haseth, Fourier Transform Infrared Spectroscopy, John Wiley & Sons New York, (1986).
- [20] P.Jacquinot, J. Opt. Soc. Am., 44, 761, (1954).
- [21] S.F.Parker, K. Williams, A.J.Turner, P.J.Hendra, Appl. Spectrosc., 42, 796, (1988)
- [22] D.Cutler.J, Spectrochim Acta., 46A, 123, (1990).
- [23] T.Hirschfeld, B.Chase, Appl. Spectrosc., 40, 133, (1986).
- [24] R.M.Silverstein, G.C.Bassier. & Terrence C. Morrill, Spectrometric Identification of Organic Compounds, John Wiley & Sons, Singapore, (1981).
- [25] E.Wigner, G. Nachrichten, 133, (1930).
- [26] V.Ramakrishnan, M.S.Gopinathan, Group Theory in Chemistry, Vishal Publications, Jalandhar, (1988).
- [27] G.M.Barrow, Introduction to molecular spectroscopy, McGraw-Hill International, Singapore, (1964).
- [28] Y.Morino, K.Kuchitsu, J. Chem. Phys. 20, 1809 (1952).
- [29] S.D.Ross, Inorganic Infrared and Raman Spectra, McGraw-Hill International, England, (1972).
- [30] J.H.Schachtschneider, Snyder R.G, Spectrochim Acta., 21, 169 (1965)

- [31] T.Shimanouchi, Computer program for Normal Coordinate Treatment of Polyatomic Molecules, the University of Tokyo, Tokyo, (1968).
- [32] H. Fuhrer, V.B.Kartha, K.G.Kidd, P.J.Matsch. Computer Program for Infrared Spectrometry, Normal Coordinate Analysis, (Ottawa, national Research Council, Canada), 5 (1976).
- [33] Eric Dowty, Vibratz, Version 1.0, (1998).
- [34] Martin Jursch, Prometheus, Version-5.1, ([ftp.anachem.ruhr-uni-bochum.de/ pub/ Prometheus/](ftp://anachem.ruhr-uni-bochum.de/pub/Prometheus/)), (1997).
- [35] Gaussian 03, Gaussian, Inc., Pittsburgh, PA, 2003.
- [36] M.Karabacak, M. Kurt , Spectrochim. Acta A 71 (2008) 876
- [37] M.H.Jamróz, Vibrational Energy Distribution Analysis, VEDA4, Warsaw, 2004.
- [38] R.I.Dennington, T.Keith, J.Millam, K. Eppinnett, W.Hovell, Gauss View Version 2003.
- [39] Wikipedia, the free encyclopedia. (2010)
- [40] CET IIB Research Project. (2010)
- [41] The Schodor Education Foundation, Inc. (2010)

## CHAPTER – II

### SPECTRAL AND THEORETICAL VIBRATIONAL ANALYSIS OF 2-BROMOBENZOIC AND ANTHRANILIC ACIDS

#### INTRODUCTION

Benzoic acid [1] is a simple aromatic carboxylic acid containing carboxyl group bonded directly to benzene. It occurs naturally in many plants and resins. It is also found in animals. Its derivatives are the constituent parts of many enzymes and other biologically important molecules. It also occurs widely in plants and animals tissues along with Vitamin-B complex and is used in miticides, contrast media in urology, cholecystographic examinations and in the manufacture of pharmaceuticals. The amino benzoic acid belongs to the aromatic amino acids, which is biologically active substance. 2-aminobenzoic acid is known as Vitamin-L. The compound N-phenylanthranilic acid is used as a common intermediate in the synthesis of pharmaceutically important molecules such as anti-malarials, anti-inflammatory and anti-neoplastics. The derivatives of benzoic acid are known to enhance the action of local anaesthetics, as evaluated by measuring the pain sensibility of human skin and the action potentials from the crayfish giant axon and the rat cervical vagus in vitro.

Benzoic acid derivatives, such as bromo/chloro benzoic acid and amino benzoic acid [anthranilic acid], have active bacteriostatic and fragrant

properties, hence they are used in pharmaceutical and perfumery industry. They are also used as intermediate for many other pharmaceutical products, especially for antipyretic analgesic and anti-rheumatism and other organic synthesis. Hence a lot works have been reported in the literature [2–23] from time to time on these molecules. However, no vibrational study based on HF and B3LYP has been reported either on anthranilic acid or on 2-bromobenzoic acid, in particular the comparative vibrational analysis of these molecules. Hence in this present work, a complete and detailed vibrational analysis has been carried out on 2-bromobenzoic and anthranilic acids with the help of both experimental and theoretical data.

## RESULTS AND DISCUSSION

### Molecular geometry

The structure of the title molecules 2-bromobenzoic acid (2BrAD) and anthranilic acid (AAD) are presented in Figures 2.1a and 2.1b respectively. Since the molecules do not possess any rotational, reflection and inversion symmetries, both the molecules are considered under  $C_s$  point group symmetry, which divide the entire modes of vibrations into two category : planar  $A'$  and non-planar  $A''$ . The 39 fundamental vibrations possible in 2BrAD and 45 vibrations in AAD, in terms of irreducible form of representation are distributed as follows:

$$\Gamma_{\text{vib}} = 27 A' + 12 A'' \quad -2\text{BrAD}$$

$$\Gamma_{\text{vib}} = 31 A' + 14 A'' \quad -\text{AAD}$$

All vibrations are active in both IR and Raman spectra. The optimized parameters of bond length and bond angle are given in Table 2.1. The observed wavenumbers from IR and Raman spectra, calculated wavenumbers and the assignments for the molecules 2BrAD and AAD are shown in Table 2.2 and 2.3. The FTIR and FT-Raman spectra of these compounds are given in the Figures 2.2 and 2.3 respectively. Computed vibrational spectral IR intensities and Raman activities of the title molecules for corresponding wavenumbers by HF and B3LYP methods with 6-311++G (d, p) basis set are given in Table 2.4.

Both the molecules are acid groups and are slightly different by the substitutions Br and NH<sub>2</sub>. Both the aromatic rings (2BrAD and AAD) appear little distorted and angles are slightly out of perfect hexagonal ring structure. It is due to the substitutions of Br, NH<sub>2</sub> and COOH groups with different masses in the place of H atoms. The breakdown of hexagonal symmetry of the benzene ring is obvious from the elongation of C-C bond lengths due to the replacement of bromine atom, amino group and acid group with different masses. The order of the bond length of 2BrAD is C5-C6 < C3-C4 < C4-C5 < C2-C3 < C6-C1 < C1-C2, whereas bond length of AAD is C3-C4 < C5-C6 < C4-C5 < C6-C1 < C2-C3 < C1-C2. The orders of bond length of these

molecules are entirely different, since the substitutions between the molecules are different.

The substitution of bromine atom is not so much affected the geometry of benzoic acid ring (2BrAD) and it is evident from the difference of calculated bond length of C1–C2 (1.406 Å) from the evaluated bond length C1–C6 (1.405 Å) whereas in the case of AAD, the introduction of NH<sub>2</sub> has much affected the geometry of benzoic acid ring and it is evident from the difference of calculated bond length C1–C2 (1.424 Å) from the evaluated bond length (1.409 Å). The bond length of C–Br (cal. 1.912), 0.027 Å is larger than the experimental value (1.885 Å) [19]. The bond length of C=O (1.204 Å) of 2BrAD 0.018 Å is shorter than the bond length of C=O (1.222 Å) of AAD. According to the experimental value [20], the C–H bond length of AAD is larger than the 2BrAD. Several authors [21–22] have explained the changes of vibrational frequency and bond length of the COOH due to the charge distribution on the carbon atom of the benzene ring. The ring carbon atoms in substituted benzene exert a large attraction on the valence electron cloud of the hydrogen atom and this leads to the increment of COOH force constant and decrement of the corresponding bond length.

In the ring C–H attachment, HF technique reproduces the bond length, which is about 0.01Å larger than normal value. However, B3LYP yield the corresponding bond lengths close to experimental results. The large deviation

from experimental bond length value of C6–H10 may arise due to low scattering of hydrogen atoms in X–ray diffraction. The bond distance of C–Br is 0.011Å [23] greater than experimental value. The C=O bond of the acid group show significant elongation for B3LYP method with respect to the standard value. The bond angle of C2–C1–C11 shows significant variation in HF and B3LYP methods due to the substitutions. The C5–C6 bond lengths (1.38 Å) in both the molecules are not affected with the bromine and amino group substitutions. The bond length of C2–Br15 is greater than C–N15. The O–H bond length in two molecules is nearly equal. Comparison of bond lengths and bond angles calculated by HF and B3LYP at 6–311++G(d, p) levels with experimental values exposes the variation of bond lengths and bond angles. In both molecules, the values of HF are found to be higher than B3LYP.

The global minimum energy obtained for structure optimization of 2BrAD with B3LYP/6–311++G (d, p) basis set is about –2990 a.u and –2993 a.u. for both HF and B3LYP. Similarly, the energy for AAD is –473 a.u and –476 a.u. for both HF and B3LYP methods respectively. The difference in energy between the methods is about 3 a.u. only. Vibrational frequencies are scaled as 0.9067 for HF and the range of wavenumbers above 1700  $\text{cm}^{-1}$  are scaled as 0.958 and below 1700  $\text{cm}^{-1}$  scaled as 0.983 for B3LYP [24]. After scaled with the scaling factor, the deviation from the observed wave numbers is reduced by less than 10  $\text{cm}^{-1}$  with a few exceptions.

## C–H Vibrations

The aromatic C–H stretching vibrations of 2BrAD give the bands at 3087, 3050 and 3025  $\text{cm}^{-1}$  in Raman with medium and weak intensities and at 3000  $\text{cm}^{-1}$  in IR with strong intensity. In AAD these modes are obtained as strong and medium bands in IR at 3070, 3055, 3032 and 3010  $\text{cm}^{-1}$ . The first three bands are very strong and the last band is very weak. However, the important observation is that all the four bands are IR bands and no band is present in Raman spectrum for C–H vibrations. Thus the change in the intensities of the bands between the two molecules is purely due to the different substitution which in turn shows the impact of mass and the interaction of N–H vibration. In both the molecules, the range of C–H stretching vibrations lies within the expected range and almost identical, which shows that the substitutions in both the molecules have not disturbed the frequency of C–H stretching much. The calculated wavenumbers are in very good agreement with B3LYP/6–311++G (d, p) basis set with mean difference 4 and 3  $\text{cm}^{-1}$  in 2BrAD and AAD respectively. All the above vibrations are observed in the expected range [25].

Substitution sensitive C–H in–plane bending vibrations lie in the region 1000 – 1300  $\text{cm}^{-1}$  [26]. In 2BrAD, two medium and weak infrared bands at 1180 and 1120  $\text{cm}^{-1}$  and two Raman bands at 1030 and 1000  $\text{cm}^{-1}$  with medium and strong intensities are assigned to C–H in–plane bending

vibrations. However, in the same vibrations in AAD, one Raman band at  $1164\text{ cm}^{-1}$  with weak intensity and three infrared bands at  $1075$ ,  $965$  and  $950\text{ cm}^{-1}$  are observed. All these bands are in the expected range. The upper limits of vibration of the two compounds are slightly elongated with literature values which may be due to the halogen compounds. Bands involving the out-of-plane C-H vibrations appear in the range  $1000 - 675\text{ cm}^{-1}$  [27]. The bands at  $976$  and  $781$  in infrared are very weak intensity for 2BrAD and  $875$ ,  $700$  and  $650\text{ cm}^{-1}$  in IR with weak and strong intensity and  $840$  and  $810\text{ cm}^{-1}$  Raman with very weak intensity for AAD are assigned to C-H out-of-plane vibrations. Most of the bands are observed to be weak in intensity.

### C-C Vibrations

The carbon-carbon stretching modes of the benzene ring are expected in the range from  $1650$  to  $1200\text{ cm}^{-1}$  [28]. The bands at  $1588$ ,  $1274$  and  $1210\text{ cm}^{-1}$  in infrared and  $1584$ ,  $1476$  and  $1364\text{ cm}^{-1}$  in Raman for 2BrAD and the bands at  $1605$ ,  $1585$ ,  $1484$ ,  $1455$ , and  $1347\text{ cm}^{-1}$  in Raman for AAD are observed for C-C stretching. The first three bands are assigned to C=C stretching and the rest to C-C stretching in both the molecules. In AAD, all the bands are in Raman and one band is missing may be due to the interaction of N-H and C-H bending modes which also lie in this range. Thus, it may be concluded that the substitutes COOH and NH<sub>2</sub> have considerably influenced the skeletal

vibrations. The calculated frequencies are in very good agreement with B3LYP/6-311++G(d, p) basis set in 2BrAD and AAD.

### **C–Br Vibrations**

According to early works [29], strong characteristic absorptions due to the C–X stretching vibrations are to be observed with the position of the band being influenced by neighbouring atoms or groups, the smaller the halide atom, the greater the influence of the neighbour. Bands of weak to medium intensity are also observed due to overtones of the C–X stretching vibrations. In Raman spectrum, the vibrational bands result as strong bands for Cl, Br and I atoms, but for F the bands are weaker.

The C–Cl and C–Br stretching vibrations are appeared as strong bands in the regions  $760 - 505 \text{ cm}^{-1}$  and  $650 - 485 \text{ cm}^{-1}$  [30] respectively. In contradiction to above observation, C–Br stretching is observed at  $475 \text{ cm}^{-1}$  with weak intensity and the deformation bands are found at  $295$  and  $200 \text{ cm}^{-1}$ , for in-plane and out-of-plane bending respectively, which show that the other vibrations can hinder the C–Br vibrations due to its weak force constant. The influence of other substitution on both stretching and deformation bands is significant in this compound.

## COOH Vibrations

According to early reports, due to the presence of strong intermolecular hydrogen bonding carboxylic acids normally exist as dimers. The infrared spectra exhibit a broad band at  $3300 - 3000 \text{ cm}^{-1}$  due to O–H stretching vibrations, a strong band at  $1740 - 1700 \text{ cm}^{-1}$  due to C=O stretching vibrations and strong band at  $1320 - 1210 \text{ cm}^{-1}$  due to C–O stretching vibrations. Carboxylic acid monomers have a weak and sharp band at  $3580 - 3500 \text{ cm}^{-1}$ . Usually monomers exist only in vapour phase [31, 32]. This observation by the previous workers is found to be true in the present case also. In 2BrAD, a very weak infrared band is present in O–H stretching at  $3550 \text{ cm}^{-1}$  and a very strong IR band is present at  $3505 \text{ cm}^{-1}$  for the same mode in AAD. The comparison of the magnitude of wavenumbers of two molecules clearly shows a large difference, which is obviously due to the presence of N–H vibrations in the second molecule.

The C=O and C–O stretching vibrations are observed at 1691 and 1023  $\text{cm}^{-1}$  in 2BrAD and the bands at 1671 and 1321  $\text{cm}^{-1}$  in AAD. All these bands are observed in infrared region with strong and weak intensities. The presence of C=O bands at these high wavenumbers has already been observed in some of the early reports [33, 34]. The difference in wavenumbers, both for C=O and C–O, between the two molecules is naturally due to the amino group. The deformation modes for both C=O and C–O are also observed in the present

work whose range coincides with the range cited in the literature cited above [35].

### **Amino group vibrations**

The AAD possesses one  $\text{NH}_2$  group and hence one symmetric and one asymmetric N–H stretching can be expected in its spectra. In N–H stretching frequency, in most of the primary aromatic amines, appears in the region  $3000 - 3500 \text{ cm}^{-1}$  [36]. Thus the IR bands at  $3485$  and  $3366 \text{ cm}^{-1}$  with medium and very strong intensity are assigned to N–H stretching vibrations, the first one to asymmetric and second to symmetric modes. These observations agree well with the earlier work. The characteristic frequency of the  $\text{NH}_2$  scissoring vibration is usually located in the region  $1650 - 1600 \text{ cm}^{-1}$ . In the present work, the  $\text{NH}_2$  scissoring mode is observed at  $1626 \text{ cm}^{-1}$  in Raman with strong intensity. Some more bands are also observed for  $\text{NH}_2$  group;  $\text{NH}_2$  rocking at  $375 \text{ cm}^{-1}$ , wagging at  $263 \text{ cm}^{-1}$  and twisting at  $255 \text{ cm}^{-1}$ . Almost all these modes are in the same range as in some of the previous works, which indicate that the amino group vibrations are least disturbed by substituent groups.

### **CONCLUSION**

The present investigation thoroughly analyzed the vibrational spectra, both infrared and Raman of 2BrAD and AAD. All the vibrational bands observed in the FTIR and FT–Raman spectra of these compounds are assigned

to the various modes of vibrations. Vibrational frequencies calculated by B3LYP/6-311++G (d, p) method agree very well with the experimental results. With this level, the deviations between calculated and experimental values are quite small for a given type of vibrations. The influence of bromine atom and amino group were discussed in the title molecules. The assignments of the fundamentals are confirmed by the qualitative agreement between the calculated and observed frequencies. The theoretically constructed FTIR and FT-Raman spectra exactly coincide with experimentally observed FTIR and FT-Raman solid phase spectra.

**REFERENCES:**

- [1] [http://en.wikipedia.org/wiki/Benzio\\_acid](http://en.wikipedia.org/wiki/Benzio_acid).
- [2] I. Chalakkal Jose, A.Anagha, Belhkar and S.Mangala Agashe, *Spectrochim Acta A Molecular spectroscopy*, 44, (1988) 899
- [3] M.Pagannone, B.Formari, G.Matt G el, *Spectrochim Acta A Molecular spectroscopy*, 43, (1987) 621
- [4] K.Yesook, Katsunosuke Machida, *Spectrochim Acta A Molecular spectroscopy*, 42, (1986) 881
- [5] Masui, *Coord. Chem. Rev.* 957 (2001) 219.
- [6] S. Shaik, A. Skurki, D. Danovich, P.C. Hiberty, *Chem. Rev.* 101(2001) 1501.
- [7] N.Sundaraganesan, B.Anand, B.Dominic Joshua, *Spectrochim Acta A5* (2006) 1053–62
- [8] Y. Akkaya, S.Akyuz, *Vibrational Spectroscopy* 42 (2006) 292–301.
- [9] C.S.Jean, S.Costa, S.Denise. Cordeiro, C.Antonio. Sant'Ana, Liane M.Rossi, S.Paulo, Santos, Paola Corio, *Vibrational Spectroscopy* 54 (2010) 133–136
- [10] Y.Ye , M. Ruan, Y.Song , YY.Li , W.Xie, *Spectrochim Acta A68* (2007) 85–93
- [11] M.Karabacak , M.Kurt, *Spectrochim Acta A* 71(2008) 876–83
- [12] Y. Sarrafi, M. Mohadeszadeh, K. Alimohammadi, *Chin. Chem. Lett.* 20 (2009) 784.
- [13] W. Zhang, G. Pugh, *Tetrahedron* 59 (2003) 3009
- [14] G.Rauhut, P. Pulay, *J. Phys. Chem.* 99 (1995) 3093–3100.
- [15] A.P. Scott, L. Radom, *J. Phys. Chem.* 100 (1996) 16502–16513.
- [16] P.K. Verma, A. Rashid, S. Tariq, *Ind. J. Pure Appl. Phys.* 25 (1987) 203.

- [17] S. Mohan, D. Arul Dhass, *Ind. J. Phys.* 67B (1993) 403.
- [18] J. Swaminathan, M. Ramalingam, H. Saleem, V. Sethuraman, M.T. Noorul Ameen, *Spectrochimica Acta Part A* 74 (2009) 1247–1253
- [19] M.Samsonowicz, T.Hrynaszkiewicz, R.Swisłocka, E.Regulska, W. Lewandowski, *Journal of Molecular Structure* 744–747 (2005) 345–352
- [20] Mehmet Karabacak, Dilek Karagoz, Mustafa Kurt, *Spectrochim. Acta* 72A (2009) 1076–1083.
- [21] G. Ferguson, G.A. Sim, *Acta Crystallography*, 15 (1962) 346–349.
- [22] A.C. Dros, R.W.J. Zijlstra, P.T. Van Duijnen, A.L. Spek, H.Kooijman, R.M. Kellogg, *Tetrahedron letter*, 54 (1998) 7787.
- [23] B.G. Johnson, P.M. Gill, J.A. Pople, *J. Chem. Phys.* 98 (1993) 5612.
- [24] M.K. Ahmed, B.R. Henry, *J. Phys. Chem.* 90 (1986) 1737.
- [25] M.Silverstein, G.C.Basseler, C.Morill, *Spectrometric Identification of Organic Compounds*, Wiley, New York, 1981.
- [26] M. Karabacak, M. Kurt, *Spectrochim. Acta A* 71 (2008) 876–883.
- [27] M. Fox, *J. Chem. Soc.* (1939) 318.
- [28] N.P. Sing, R.A. Yadav, *Ind. J. Phys. B* 75 (4) (2001) 347.
- [29] V.Arjunan, I. Saravanan, P.Ravindran, S. Mohan , *Spectrochimica Acta Part A* 74 (2009) 642–649
- [30] M. Chaman, P.K. Verma, *Ind. J. Phys.* 77B (3) (2003) 315.
- [31] D.A.Long, D.Stecke, *Spectrochim Acta* 19 (1963) 1947.
- [32] George Socrates, “Infrared and Raman Characteristic Group frequencies”, Third edition, John wiley & sons Ltd. 126 (2001).

- [33] R.Matheammal, S.Muthunatesan, V.Krishnakumar, *Spectrochim Acta PartA* 70 (2008) 210–220
- [34] S.Ramasamy, V. Krishnakumar, *Spectrochim Acta Part A* 72 (2008) 465–470.
- [35] N.Dheivamalar, V.Krishnakumar, *Spectrochim Acta PartA* 69 (2008) 8–17
- [36] L.J. Bellamy, R.L. Williams, *Spectrochim. Acta* 9 (1957) 311.

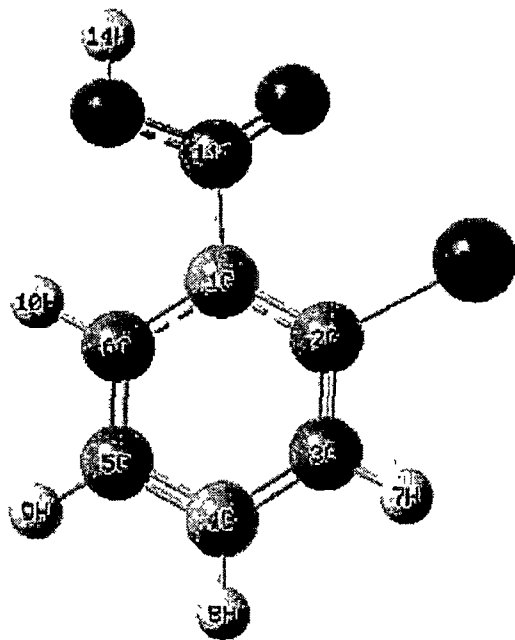


**Fig 2.1a** Molecular structure of 2-bromobenzoic acid (2BrAD)

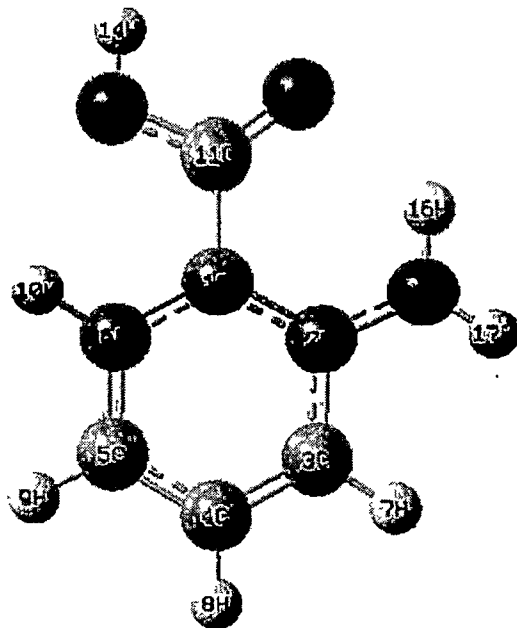


**Fig 2.1b** Molecular structure of anthranilic acid (AAD)

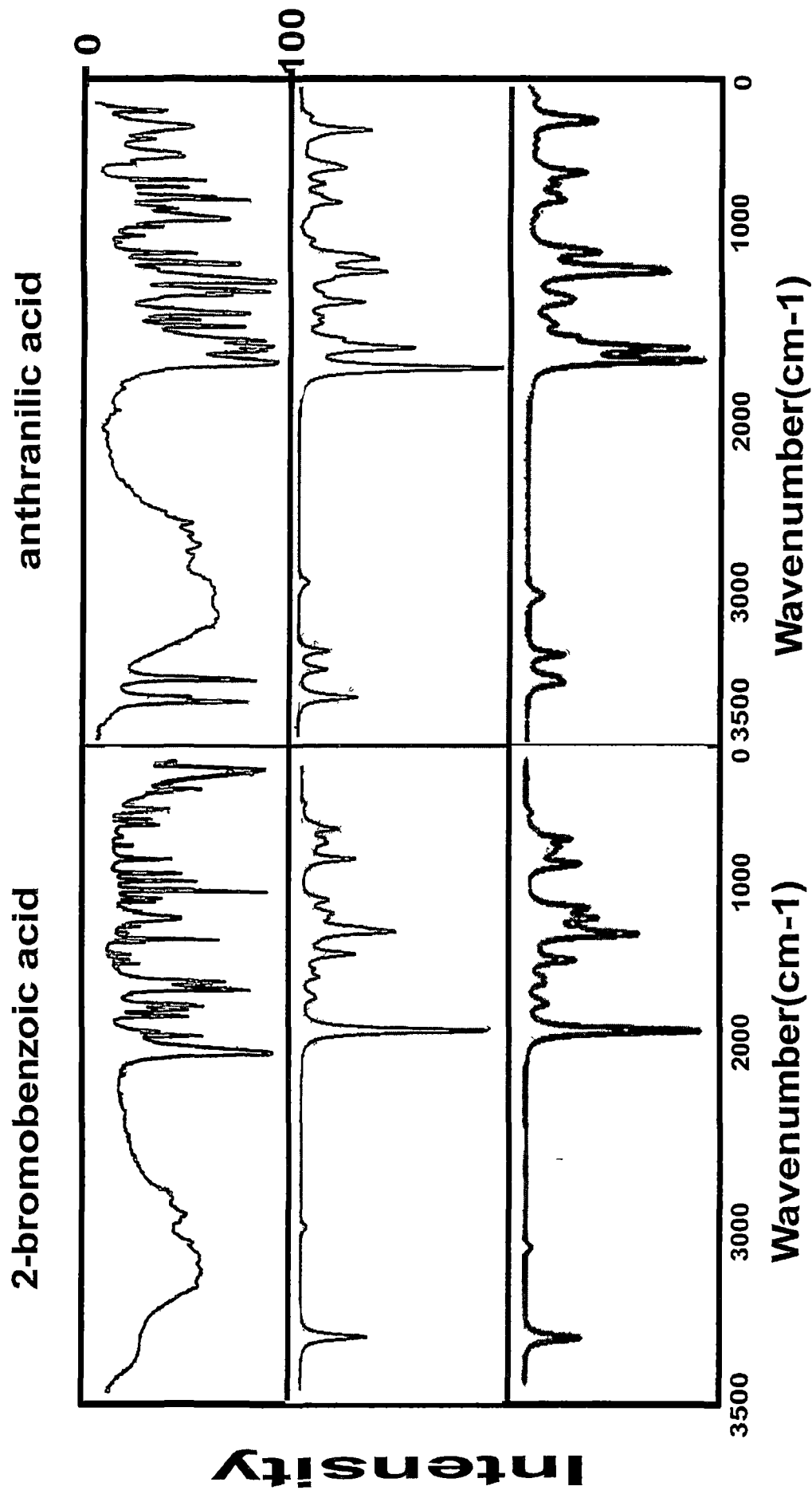


**Figure 2.2: Experimental and Simulated Infrared spectra**

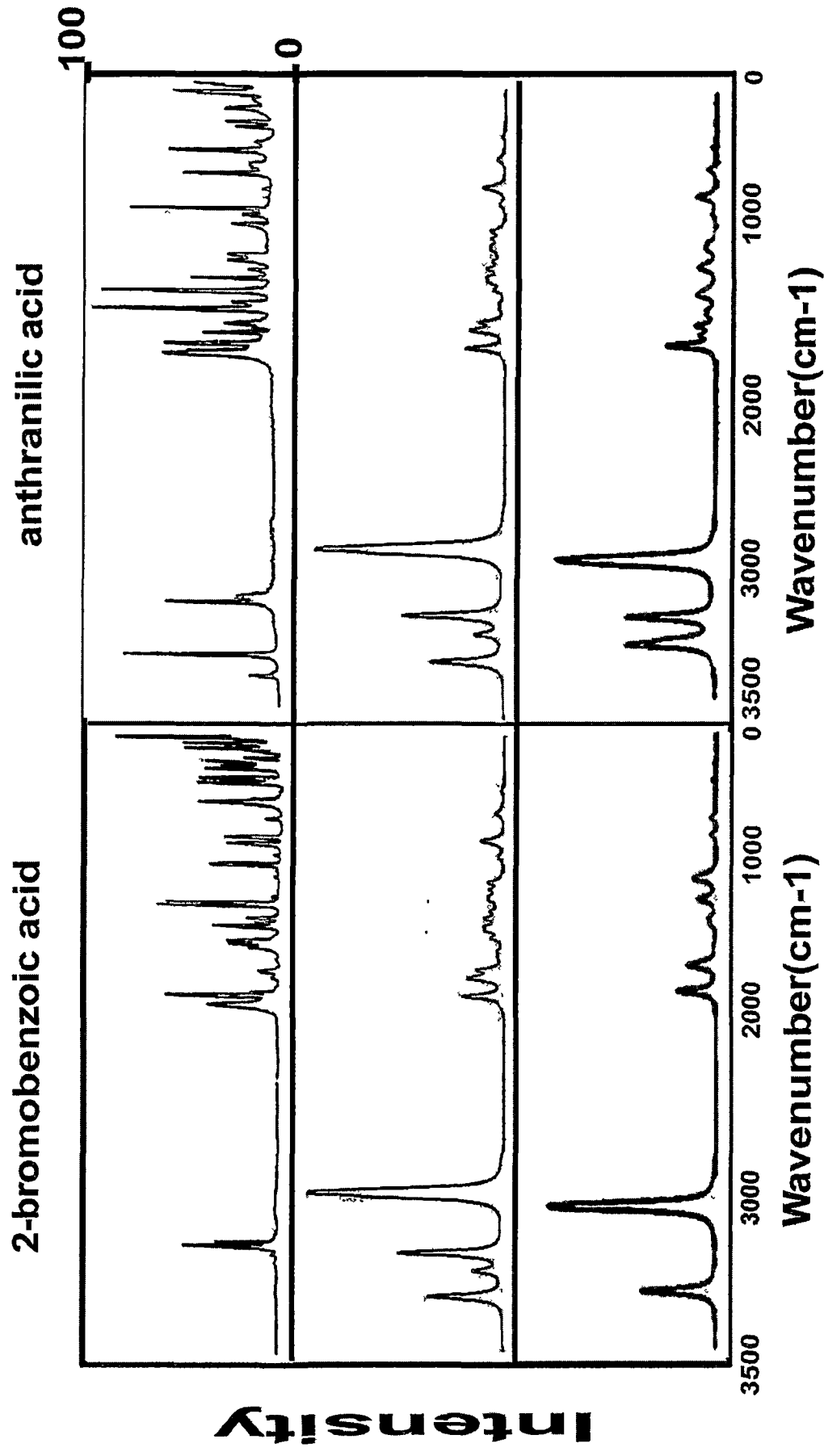


Figure 2.3: Expermental and Simulated Raman spectra

**Table.2.1 .Optimized parameters of 2BrAD and AAD, bond length (Å) and bond angle (°)**

#Parame ters	2BrAD				AAD				#Parameters	2BrAD				AAD			
	HF/ 6-311 ++ G(d,p)	B3LY P/ 6-311 ++ G(d,p)	Expt value	HF/ 6-311 ++ G(d,p)	HF/ 6-311 ++ G(d,p)	B3LYP/ 6-311 ++ G(d,p)	Expt value	HF/ 6-311 ++ G(d,p)		HF/ 6-311 ++ G(d,p)	B3LYP/ 6-311 ++ G(d,p)	Expt value	HF/ 6-311 ++ G(d,p)	HF/ 6-311 ++ G(d,p)	B3LYP/ 6-311 ++ G(d,p)	Expt value	
	Bond length(Å)									Bond angle(°)							
R(1,2)	1.3946	1.4065	1.362	1.4079	1.4249	1.411	A(2,1,6)	118.42	118.04	120.2	119.50	119.41	120.2	119.50	119.67		
R(1,6)	1.3935	1.4057	1.384	1.4021	1.409	1.403	A(2,1,11)	123.51	123.40	123.4	120.78	120.30	123.4	120.78	121.22		
R(1,11)	1.4965	1.4927	1.487	1.4735	1.4656	1.464	A(6,1,11)	118.04	118.54	116.4	119.71	120.29	116.4	119.71	119.11		
R(2,3)	1.3853	1.3944	1.427	1.4069	1.4133	1.411	A(1,2,3)	120.24	120.42	120.8	117.91	117.90	120.8	117.91	117.39		
R(2,15)	1.8972	1.9126	1.885	1.3628	1.3639	1.364	A(1,2,15)	123.64	123.61	124.9	123.29	122.48	124.9	123.29	122.91		
R(3,4)	1.3829	1.3909	1.385	1.3702	1.3809	1.366	A(3,2,15)	116.08	115.94	114.4	118.77	119.61	114.4	118.77	121.56		
R(3,7)	1.0728	1.0819	1.363	1.0758	1.0864	0.919	A(2,3,4)	120.34	120.37	119.9	121.18	121.28	119.9	121.18	115.66		
R(4,5)	1.3831	1.3928	1.363	1.3959	1.4026	1.385	A(2,3,7)	119.42	119.26	119.26	118.71	118.66	119.26	118.71	115.66		
R(4,8)	1.0752	1.0841	1.440	1.0762	1.0858	0.399	A(4,3,7)	120.24	120.37	119.3	120.11	120.05	119.3	120.11	120.93		
R(5,6)	1.3806	1.3876	1.440	1.3712	1.3817	1.374	A(3,4,5)	120.16	120.09	119.3	121.13	120.90	119.3	121.13	120.19		
R(5,9)	1.0744	1.0833	1.202	1.0737	1.0840	0.882	A(3,4,8)	119.43	119.41	121.4	119.07	119.17	121.4	119.07	120.19		
R(6,10)	1.0723	1.0813	1.346	1.0725	1.0826	0.989	A(5,4,8)	120.41	120.50	121.4	119.80	119.92	121.4	119.80	119.05		
R(11,12)	1.1803	1.2048	1.202	1.1943	1.2221	1.229	A(4,5,6)	119.40	119.51	118.5	118.41	118.83	118.5	118.41	119.05		
R(11,13)	1.3308	1.3618	1.346	1.3293	1.3586	1.320	A(4,5,9)	120.60	120.53	118.5	120.83	120.63	118.5	120.83	119.52		
R(13,14)	0.9459	0.9684	0.946	0.9454	0.9690	0.924	A(6,5,9)	120.00	119.96	120.4	120.76	120.54	120.4	120.76	120.35		
R(15,16)				0.9930	1.0093	0.968	A(1,6,5)	121.42	121.57	118.5	121.88	121.68	118.5	121.88	120.35		
R(15,17)				0.9918	1.0056	0.879	A(1,6,10)	118.73	118.29	118.5	118.32	118.19	118.5	118.32	120.35		
							A(5,6,10)	119.85	120.14	126.0	119.80	120.13	126.0	119.80	121.51		
							A(1,11,12)	126.00	126.60	113.7	125.76	126.07	113.7	125.76	116.46		
							A(1,11,13)	112.03	111.78	120.4	113.85	113.88	113.7	113.85	116.46		
							A(12,11,13)	121.94	121.61	120.4	120.40	120.05	120.4	120.40	122.03		
							A(11,13,14)	108.14	106.32	107.92	107.92	106.70	107.92	107.92	118.51		
							A(2,15,16)			118.64	118.64	119.02	118.64	118.64	118.84		
							A(2,15,17)			117.67	117.67	119.50	117.67	117.67	118.84		
							A(16,15,17)			117.54	117.54	119.00	117.54	117.54	199.08		

# refer Fig.1 and 2 for numbering of atom; <sup>a</sup>refer reference 23

**Table 2.2 Detailed assignment of fundamental vibrations of 2-bromobenzoic acid (2BrAD) based on the HF/6-311++G (d, p) and B3LYP/6-311++G (d, p) basis sets**

Symmetry species	Observed frequencies (cm <sup>-1</sup> )		Calculated frequencies HF/6-311++G(d,p) (cm <sup>-1</sup> )		Calculated frequencies B3LYP/6-311++G (d, p) (cm <sup>-1</sup> )		Assignments
	IR	Raman	unscaled	scaled	unscaled	scaled	
A'	3550vw		4123	3738	3771	3613	γO-H
A'		3087m	3387	3071	3218	3083	γC-H
A'		3050m	3371	3056	3206	3071	γC-H
A'		3025vw	3352	3039	3190	3056	γC-H
A'	3000s		3333	3022	3174	3041	γC-H
A'	1691vs		2015	1827	1800	1724	γC=O
A'	1588vs		1779	1613	1627	1599	γC=C
A'		1584vs	1750	1587	1601	1574	γC=C
A'		1476w	1633	1481	1497	1472	γC=C
A'		1440w	1582	1434	1460	1435	βO-H
A'		1364w	1488	1349	1355	1332	γC-C
A'	1274w		1398	1268	1318	1296	γC-C
A'	1210m		1337	1212	1290	1268	γC-C
A'	1180m	1180vw	1306	1184	1198	1178	βC-H
A'		1120m	1248	1132	1190	1170	βC-H
A'	1023		1213	1100	1157	1137	γC-O
A'		1055m	1191	1080	1100	1081	βC-H
A'	1030m	1030m	1139	1033	1064	1046	βC=O
A'			1122	1017	1038	1020	βC-H
A''		1000vs	1121	1016	1005	988	βC-H
A''	976vw		1094	992	980	963	φC-H

A''		880vw	991	899	888	873	φC-H
A''	781vw	781vw	902	818	809	795	φC-H
A'		775m	849	770	785	772	βC-O
A'	750vs		840	762	757	744	βCCC
A'	681m		771	699	700	688	βCCC
A'		657m	728	660	674	663	βCCO
A'	623m		694	629	641	630	βCCC
A''	560m		624	566	590	580	φC=O
A''		530w	579	525	532	523	φC-O
A'	475vs		523	474	479	471	γC-Br
A'	415s		457	414	422	415	βCCC
A''	407vw		442	401	414	407	φCCC
A'		295s	320	290	296	291	βC-Br
A'		225vw	296	268	276	271	φCCC
A''		200vw	217	197	198	195	φC-Br
A''		150vw	175	159	162	159	φCCC
A''		110vw	122	111	110	108	φCCC
A''			35	32	31	30	φCCC

vs – very strong; s – strong; m- medium; w – weak; vw-very weak; HF/6-311++G(d,p) scale factor is 0.9050 and B3LYP/6-311++G(d, p) scale factor is 0.950 for the wavenumbers from 4000 to 1700  $\text{cm}^{-1}$  and 0.983 for wavenumbers below 1700  $\text{cm}^{-1}$ .  $\gamma$ -stretching,  $\beta$ -in-plane bending,  $\phi$ -out-of-plane bending

**Table 2.3 Detailed assignment of fundamental vibrations of Anthranilic acid (AAD) based on the HF/6-311++G (d, p) and B3LYP/6-311++G (d, p) basis sets**

Symmetry species	Observed frequencies (cm <sup>-1</sup> )		Calculated frequencies HF/6-311++G(d,p) (cm <sup>-1</sup> )		Calculated frequencies B3LYP/6-311++G(d,p) (cm <sup>-1</sup> )		Assignments
	IR	Raman	unscaled	scaled	unscaled	scaled	
A'	3505vs		4130	3745	3742	3585	γO-H
A'	3485m		3941	3573	3707	3551	γN-H
A'	3366vs		3815	3459	3565	3415	γN-H
A'	3070s		3381	3066	3214	3079	γC-H
A'	3055m		3351	3038	3189	3055	γC-H
A'	3032vs		3334	3023	3172	3039	γC-H
A'	3010m		3315	3006	3154	3022	γC-H
A'	1671vs		1948	1766	1743	1670	γC=O
A'		1636s	1806	1638	1670	1642	βNH <sub>2</sub> scissoring
A'		1605s	1786	1619	1644	1616	γC=C
A'		1585w	1741	1579	1599	1572	γC=C
A'		1484m	1641	1488	1523	1497	γC=C
A'		1455vw	1599	1450	1490	1465	γC-C
A'		1347vs	1510	1369	1390	1366	γC-C
A'		1330w	1449	1314	1368	1345	βO-H
A'	1321vs		1417	1285	1346	1323	γC-O
A'		1240vs	1361	1234	1310	1288	βN-H
A'		1175m	1310	1188	1211	1190	βN-H
A'		1170s	1266	1148	1189	1169	γC-NH <sub>2</sub>
A'	1164vs		1228	1113	1180	1160	βC-H
A'	1075vw		1201	1089	1095	1076	βC-H
A'		1052w	1155	1047	1074	1056	γC-COOH

A'	1015w	1108	1005	1045	1027	$\beta$ C=O
A'	965w	1104	1001	979	962	$\beta$ C-H
A'	950vw	1097	995	961	945	$\beta$ C-H
A''	875w	951	862	867	852	$\phi$ C-H
A''	840w	921	835	857	842	$\phi$ C-H
A''	810vw	897	813	810	796	$\phi$ C-H
A'	775vs	841	763	759	746	$\beta$ C-O
A''	745s	810	734	749	736	$\phi$ C-H
A''	700s	788	714	718	706	$\phi$ C-H
A'	650s	705	639	653	642	$\beta$ C-NH <sub>2</sub>
A''	570w	614	557	600	590	$\phi$ C=O
A'	565s	612	555	575	565	$\beta$ C-COOH
A'	535m	589	534	571	561	$\beta$ CCC
A'	510m	563	510	537	528	$\beta$ CCC
A'	499vw	547	496	512	503	$\beta$ CCC
A''	430s	467	423	431	424	$\phi$ C-NH <sub>2</sub>
A''	385w	444	403	419	412	$\phi$ C-COOH
A''	375vw	396	359	372	366	NH <sub>2</sub> rocking
A''	263w	368	334	267	262	NH <sub>2</sub> wagging
A''	255w	268	243	247	243	NH <sub>2</sub> twisting
A''	130w	256	232	236	232	$\phi$ CCC
A''		146	132	123	121	$\phi$ CCC
A''		79	72	82	81	$\phi$ CCC

vs – very strong; s – strong; m – medium; w – weak; vw – very weak; HF/6-311++G(d, p) scale factor is 0.9050 and B3LYP/6-311++G(d, p) scale factor is 0.950 for the wavenumbers from 4000 to 1700 cm<sup>-1</sup> and 0.983 for wavenumbers below 1700 cm<sup>-1</sup>.  $\gamma$ -stretching,  $\beta$ -in-plane bending,  $\phi$ -out-of-plane bending



1.7	0.1	2.1	0	126.8	7.9	121	8.5
0.9	0.3	0.3	0.1	3.8	8.7	53.2	10.9
7.2	0.9	2.4	0.4	0.6	0	5.1	10.6
20.5	5.1	10.7	9	30.2	9.9	0	0.1
111	0.5	92.6	0.3	0.6	0.4	0.5	0.1
21.7	0.4	17.6	0.3	19.3	0.7	6.4	6
49.2	7.6	29.4	10.3	9.6	5.1	5.9	0.5
39.8	2.1	42.5	0.7	20.8	0.4	3.6	0.2
86.3	3.8	75.9	2.9	95.1	0.1	58.5	0.5
14.9	1.9	11.4	1.9	31.3	21.5	12.1	33.5
3	0.4	2.4	0.3	30.8	0.2	47.9	0.3
6.8	0.8	6.2	0.4	63.5	0.4	49.8	0.7
4.7	8.4	3.1	7.5	34.3	7.8	28.7	0.4
0.9	4.6	0.7	4.1	71.6	4.5	107.3	2.3
0.8	1	1.2	1	9.1	0.6	3.9	10.8
2.8	1.9	2.4	1.3	63.6	0.9	9.3	0.2
0.8	0.8	0.9	0.6	27.2	1.4	5.8	1.5
0.1	4.1	0	2.7	6.9	0.7	7	0.6
1.4	0.4	1	0.6	2.4	2.9	1.8	5.6
				49.7	1.9	10.1	1.8
				176.3	1.4	99.1	1.1
				3.5	0.2	76.8	0.8
				16.8	1.1	25.7	0.5
				1.2	2.7	15.6	1.5
				0.7	0.4	0.8	0.2

## CHAPTER – III

### FTIR – FT RAMAN SPECTRAL AND QUANTUM MECHANICAL VIBRATIONAL ANALYSIS OF 2, 5–DIBROMO PYRIDINE AND 2, 6–DIBROMO PYRIDINE

#### INTRODUCTION

Pyridine [1] is a heterocyclic aromatic compound characterized by a six membered ring structure composed five carbon atoms and one nitrogen atom. It is the simplest member of the pyridine family, colorless, flammable, and toxic liquid with an unpleasant odor and miscible with water and most organic solvents. Many drugs are found with pyridine compounds. Bromopyridine finds wide application in pharmacological industry and in chemical laboratories. The basicity becomes strongly indicated when electron donating groups are present in the pyridine ring at 2– and 6–positions because they alter the electron availability on the nitrogen atom by resonance. But in 2– and 5–positions act by inductive effects and their effect is less pronounced. Thus the spectral and vibrational analyses of substituted pyridines have been subjected to several investigations. The spectroscopic investigations with the help of quantum chemistry calculations are also available for pyridine and its other derivatives in recent years because of their applications [2–18].

However, no comparative spectral and quantum mechanical vibrational analysis was reported for 2, 5–dibromopyridine (25DBP) and 2, 6–dibromopyridine (26DBP) so far. Hence, the present investigation was carried

out to do a complete vibrational analysis on the basis of experimental as well as theoretical calculations. The aim was also to determine the impact of the bromine substitution in the vibrational pattern of the pyridine ring and observe the influence of the position of bromine in the ring.

## RESULTS AND DISCUSSION

### Molecular geometry

The labeling of atoms of the titled compounds is shown in Fig 3.1a and 3.1b and the optimized geometrical parameters at HF and B3LYP with 6-311++G (d, p) basis set are listed in Table 3.1. The global minimum energies obtained by the DFT structure optimization for 25DBP was  $-5395.43578007$  hartress and for 26DBP was  $5395.43576576$  hartress. The corresponding zero point vibrational energies were found to be  $42.59485$  and  $42.53276$  kcal/mol respectively.

Both the compounds 25DBP and 26DBP belong to Cs point group of symmetry and the optimized geometrical parameters were calculated according to labeling of atoms. Each molecule has 11 atoms; hence there can be 27 normal modes of vibrations, of which 19 are in-plane vibrations ( $A'$  species) and 8 out-of-plane vibrations ( $A''$  species). They can be distributed as:

$$\Gamma_{\text{vib}} = 19 A' + 8 A''$$

All vibrations are to be active collectively in FTIR and FT-Raman spectra. The vibrational assignments of all the fundamental modes of 25DBP and 26DBP along with the calculated frequencies, IR intensities and Raman activities were reported in the Tables 2.3 and 3.3 respectively.

The observed and simulated FTIR and FT-Raman spectra were presented in Figs 3.2 and 3.3 for the molecules 25DBP and 26DBP respectively. The optimized bond lengths and bond angles are slightly smaller as well as longer than the experimental values with HF and B3LYP with 6-311++G(d, p) basis set for 25DBP and 26DBP. The optimized bond length of C-C in phenyl ring falls between the range 1.395 – 1.390 Å at B3LYP/6-311++G(d, p) and 1.387 – 1.379 Å at HF/6-311++G (d, p) methods show good agreement with experimental data. The N1-C2 bond distance of 25DBP is shorter by 0.015 Å than that in 26DBP. The other bond distance N1-C6 is longer by 0.038 Å in 25DMP. The values of the optimized C-N bond lengths 1.382 and 1.378 Å are calculated by HF methods for 2A5MP and 2A6MP, respectively are overestimated by 0.018 and 0.014 Å with that of crystal data of 2A5MP(1.364 Å).

### **C-H vibrations**

The 25DBP and 26DBP molecules possess three C-H bonds in the ring. Generally, in hetro aromatic compounds, the C-H stretching vibrations appear in the region 3000 – 3100  $\text{cm}^{-1}$  [19, 20]. In 3, 5-dibromopyridine, the bands

were reported to have values at 3096, 3044 and 3007  $\text{cm}^{-1}$  [21]. In this case, the bands are observed at 3095, 3075 and 3050  $\text{cm}^{-1}$  in 25DBP and 3095, 3080 and 3040  $\text{cm}^{-1}$  in 26DBP. The bands are appeared with weak and very weak intensities in both molecules. All the above vibrations are observed within the expected range. The observed frequencies are in very good agreement with the calculated values of B3LYP/6-311++G (d, p). The frequencies are within the expected range which shows that the substituent N atoms in the benzene ring and the presence of two Bromine atoms have not much influenced the C-H stretching vibrations. The slight difference in frequencies between the two molecules purely indicates the positional influence of Br atoms on such modes.

The bands which appeared at 1130, 1090 and 1075  $\text{cm}^{-1}$  are assigned to C-H in-plane bending vibrations in 25DBP, while the same are observed at 1135, 1095 and 1070  $\text{cm}^{-1}$  for 26DBP. These bands are located in very low region when compared to the expected literature range 1300 – 1150  $\text{cm}^{-1}$  [19–21]. This observation clearly indicates that, the C-H in-plane bending vibrations are suppressed by the substitutions whereas the position of Br has no effect.

The C-H out-of-plane bending vibrations are observed at 810, 740 and 710  $\text{cm}^{-1}$  in 25DBP and at 780, 740 and 710  $\text{cm}^{-1}$  in 26DBP. These bands are in the expected range according to the above cited literature. The first frequency is only having difference 30  $\text{cm}^{-1}$ . The remaining two frequencies are same. It is purely due to the variation of Br atom position. The C-H in-

plane and out-of-plane bending vibrations are in good agreement with calculated values by B3LYP/6-311++G (d, p).

### **CC vibrations**

The CC stretching vibrations have generally occurred in the region 1430 – 1750  $\text{cm}^{-1}$ , particularly between 1759 – 1590  $\text{cm}^{-1}$  for pure benzene [22–24], of which C=C stretching lies between 1600 – 1300  $\text{cm}^{-1}$  and that of C–C below 1600  $\text{cm}^{-1}$ . In the present case, four bands are observed for these modes in both the molecules, at 1560, 1555, 1425 and 1345  $\text{cm}^{-1}$  in 25DBP and at 1570, 1560, 1415 and 1380  $\text{cm}^{-1}$  in 26DBP. The first two bands in each molecule are assigned to C=C stretching and the last two for C–C stretching respectively.

For both C=C and C–C stretching, the observed values are lesser than the expected literature values. This difference in values between the two molecules indicates the substitutions of N and Br on the ring have considerable impact on these vibrations. The position variation of Br atom has also altered the vibrations of these modes. The theoretically calculated values by B3LYP/6-311++G (d, p) coincide well with the experimental values.

### **CN vibrations**

The CN vibrations are generally difficult to be identified due to the mixing up of various modes of vibrations that are possible in this region [25–28]. But using the force field calculations and Gaussian view program, these

modes can be identified easily. The C=N stretching vibration bands are observed at 1280 and 1260  $\text{cm}^{-1}$  both in 25DBP and 26DBP. But the C–N vibrations are observed at 1240  $\text{cm}^{-1}$  in 25DBP and at 1170  $\text{cm}^{-1}$  in 26DBP. The range of the values is in agreement with the cited literature values. But the values observed in the present case are relatively low. The CN in-plane and out-of-plane bending vibrations are absent as they are suppressed by CC and CH modes of vibrations.

### **C–Br vibrations**

The vibrations belonging to C–X, bonds which are formed between the ring and the halogen atoms, are interesting since mixing of vibrations are possible due to the lowering of molecular symmetry and the presence of heavy atoms [29]. The assignments of C–Br vibrations have been made by comparison with p-bromophenol and the halogen substituted benzene derivatives [30, 26, and 27]. The stretching vibrations of C–X group (X=Cl, Br, I) usually lie in the frequency range 480 – 800  $\text{cm}^{-1}$  [31]. Bromine compounds absorb strongly in the region 650 – 450  $\text{cm}^{-1}$  due to the C–Br stretching vibrations [32]. In the present case, The C–Br stretching appeared as strong bands at 625 and 480  $\text{cm}^{-1}$  in 25DBP and at 645 and 560  $\text{cm}^{-1}$  in 26DBP. The C–Br in-plane bending and out-of-plane bending vibrations are also observed at 320  $\text{cm}^{-1}$  and 220  $\text{cm}^{-1}$  in 25DBP and at 310  $\text{cm}^{-1}$  and 170  $\text{cm}^{-1}$  in 26DBP. The values differ between the two molecules for all the three modes which can be purely due to the position variation of the Br atoms among the molecules.

The deviation is  $5\text{ cm}^{-1}$  between experimental and calculated (B3LYP/6-311++G (d, p)) values of 25DBP and 26DBP.

## CONCLUSION

From the vibrational analysis of the FTIR and FT-Raman spectra of 25DBP and 26DBP, with the help of HF and B3LYP calculations and in comparison with the cited early works on the halogen substituted aromatic molecules and other pyridine molecules, the following observations are made:

The C-H stretching frequencies show that the substituent N atoms in the benzene ring and the presence of two Bromine atoms have not much influenced. The slight difference in frequencies between the two molecules indicates purely the positional influence of Br atoms on such modes. The variation of the position of Br has not influenced on C-H out-of-plane bending modes whereas C-H in-plane bending vibration is suppressed by the substitutions. For both C=C and C-C stretching, the observed values are lesser than the expected literature values.

There is also difference between the values of the two molecules which indicate the substitutions of N and Br atoms on the ring. The position variation of Br atom has also altered the vibrations of these modes. The vibrations of C=N and C-N bonds are suppressed by other modes, particularly by CC and CH modes. The absence of CN in-plane and out-of-plane bending vibrations also supports this observation. The C-Br vibration values lie in the expected

range. But the difference between the two molecules for all the three modes can be purely due to the position variation of the Br atoms between the molecules.

**REFERENCES**

- [1] R.C.Smith, H.H.Emmen, F.W.Bertels Mann, B.M. Kulig, A.C.Van Loenen, C.H.Polman C.H, *Neurology*, 44(9) (1994) 1701.
- [2] J.H.S.Green, D.J.Harrison, M.R.Kipis, *Spectrochim. Acta*, 29A (1973) 1177.
- [3] B.K.Wiberg , A.V.Waltrus, N.K.Wong, D.S.Colson, *J. Phys. Chem.*, 88 (1984).
- [4] G.Ponger, P.Pulay, G.Fogarsi, E.J.Boggs, *J. Am. Chem. Soc.*, 106, 2765 (1984) 6067.
- [5] R.K.Goel, M.L.Agarwal, *Indian J. Pure & Appl. Phys.*, 20 (1982)164 .
- [6] R.N. Medhi, R Barman, K.C. Medhi , S.S. Jois, *Spectrochimica Acta Part A* 56 (2000) 1523–1532.
- [7] S.Gunasekaran, R.S.Vardhan, K.Manoharan, *Indian J. Phys.*, 67B(1) (1993) 95.
- [8] Li–Ran Wang, Yan Fang, *J.Chemical Physics* 323 (2006) 376.
- [9] N.Sundaraganesan, S.Ilakiamani, B.Anand, H.Saleem, B.Dominic Joshua *Spectrochimica Acta* , A 64 (2006) 586
- [10] Adnan Saglam, Fatih Ucun, Vesile G"uc,l"u ,*Spectrochimica Acta A* 67 (2007) 465.
- [11] Z.Zhuang, *Spectrochim. Acta*, 72 (2009) 954.
- [12] V.Krishnakumar, R.John Xavier, *Spectrochim acta A*61 (2005) 253.
- [13] M.K.Subramanian, P.M.Anbarasan, S.Manimegalai, *Spectrochim acta A*73 (2009) 642.
- [14] J.Swaminathan, M.Ramalingam, V.Sethuraman, N.Sundaraganesan, S.Sebastian, *Spectrochimica Acta A* 73 (2009) 593.
- [15] Yu–Xi Sun, Qing–Li Hao, Zong–Xue Yu ,Wen–Jun Jiang, Lu–De Lu, XinWang *Spectrochimica Acta* , A73,892, (2009).

- [16] Yunusa Umar, *Spectrochimica Acta* , A71 (2009) 1907.
- [17] V.Karthikeyan, *Indian journal of chemistry*, 46A (2007) 929.
- [18] B.S.Yadav, I.Ali, Pradeep Kumar, Preeti Yadav, *Indain Journal of Pure and Applied Physics* 45,979,(2007).
- [19] George W.O and McIntyre P.S *Infrared Spectroscopy*, John Wiley, New York (1987)
- [20] M.Siverstein, G.Clayton Basseler, C.Morill, *Spectrometric Identification of Organic compounds* ,Wiley, New York, (1981)
- [21] R.John Xavier and V. Krishnakumar, *Spectrochim Acta A* 61 (2005).253
- [22] Varsanyi G, *Vibrational spectra of Benzene Derivatives*, Academic Press, New York, (1969).
- [23] N.Surumbarkazhali, V.Krishnakumar, S.Muthunatesan, *Spectrochim Acta A* 71 (2009) 1813.
- [24] R.Nagalakshmi, V.Krishnakumar, S.Manohar, *Spectrochim Acta A* 71 110 (2008) 110.
- [25] N.Prabavathi, V.Krishnakumar, *Spectrochim Acta A* 72, (2009) 743–747.
- [26] R.Ramasamy, V.Krishnakumar, *Spectrochim Acta A* 69, (2008) 8–17.
- [27] S.Shadri, V.Krishnakumar, S.Muthunatesan, *Spectrochim Acta A* 68, 811 (2007) 811–816
- [29] J.N.Roy, *Indian J.Phys* B 65, (1991) 364.
- [30] S.Lee, W.Yang, R.G.Parr, *Phys Rev B*, 37, (1988) 785.
- [31] M.Bakiler, I.V.Maslov, S.Akyliz, *J Mol Struct*, 475 (1999) 83.
- [31] E.F.Mooney, *Spectrochim Acta*, 20,(1964)1024.
- [32] Socrates.G, *Infrared and Raman characteristic, Group Frequencies Tables and Charts* .third ed.J.Wiley and Sons Chichester. (2001).

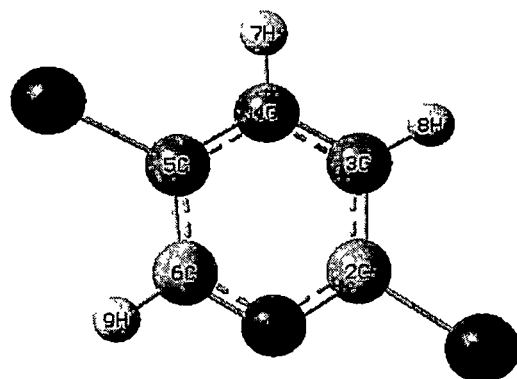


**Fig 3.1a Molecular structure of 2, 5-dibromopyrdine (25DBP)**

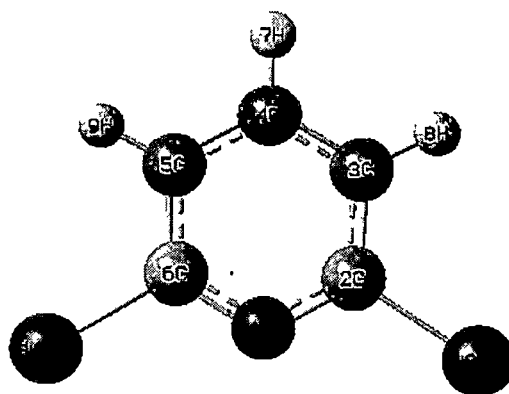


**Fig 3.1b Molecular structure of 2, 6-dibromopyrdine (26DBP)**

# 2,5-dibromopyridine

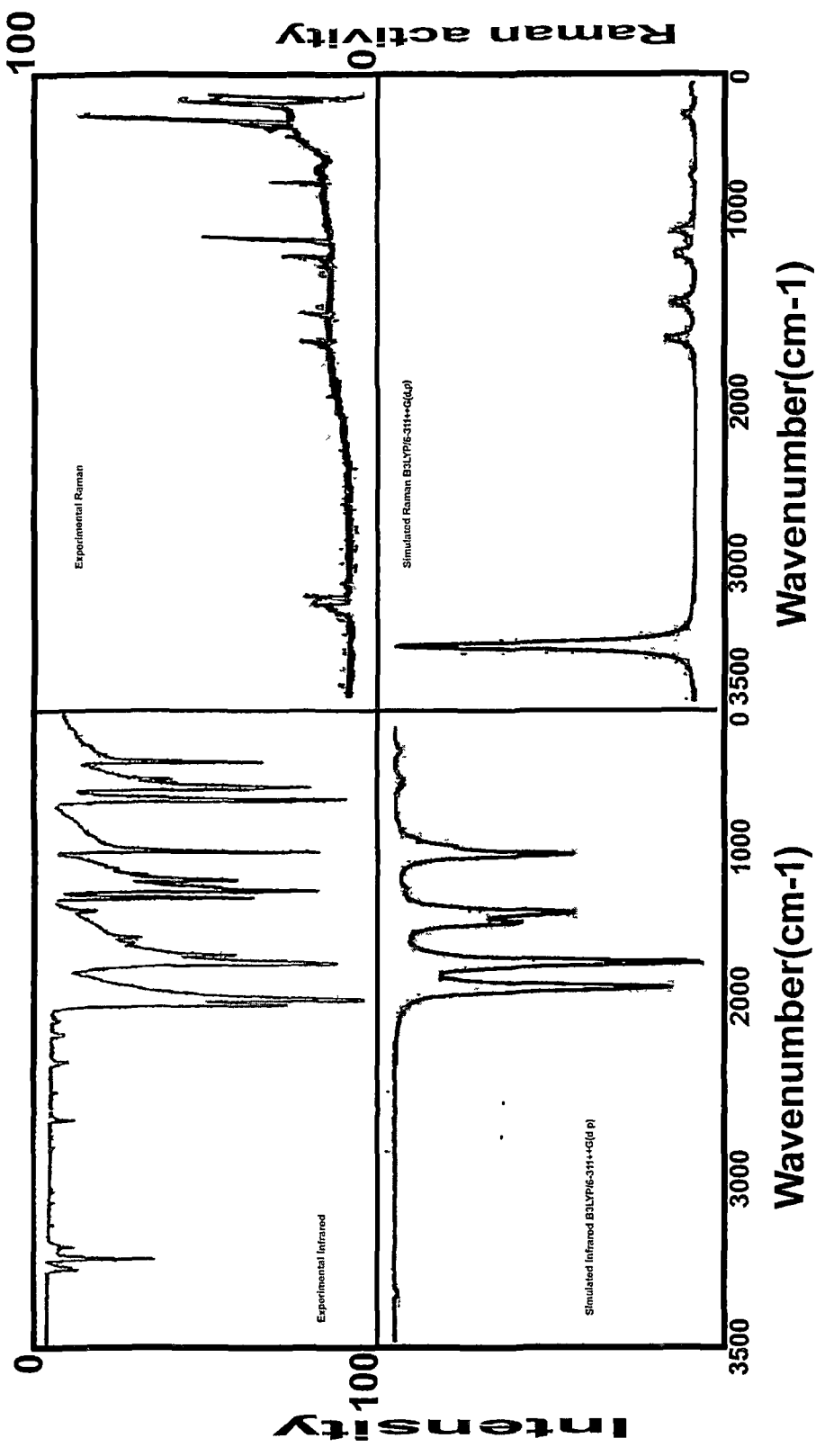


Figure 3.2: Experimental and Simulated IR and Raman spectra

## 2,6-dibromopyridine

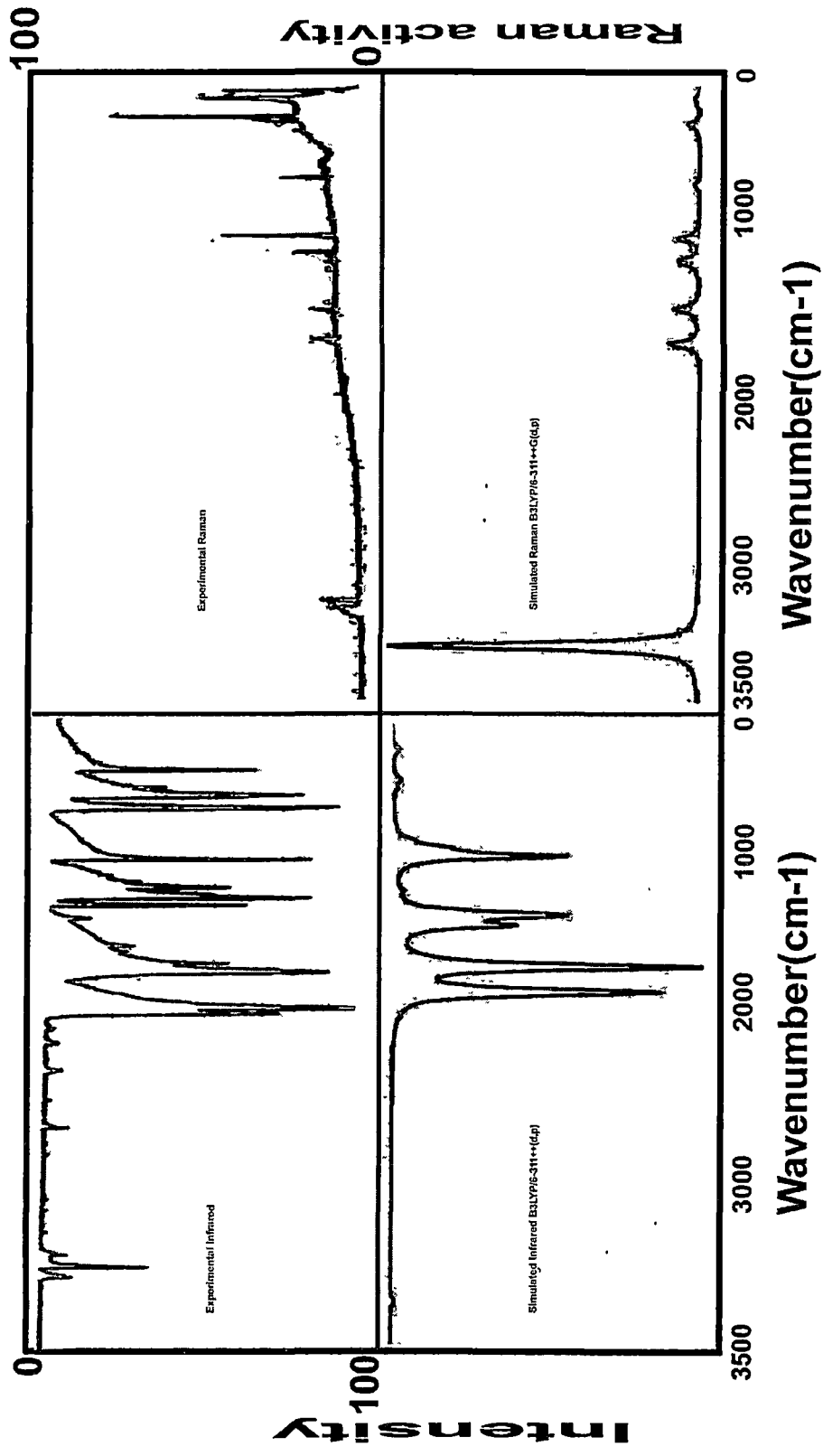


Figure 3.3: Experimental and Simulated IR and Raman spectra

**Table 3.1 Optimized geometrical parameters for 2, 5-dibromopyridine (25DBP) and 2, 6-dibromopyridine (26DBP)**

Parameters	25DBP		26DBP		25DBP		26DBP	
	HF/6-311++G(d,p)	HF/6-311++G(d,p)	B3LYP/6-11++G(d,p)	B3LYP/6-11++G(d,p)	B3LYP/6-311++G(d,p)	B3LYP/6-311++G(d,p)	EXPT VALUES	
Bond length value (Å°)								
N1-C2	1.302	1.308	1.315	1.315	1.320	1.320	1.338	
N1-C6	1.322	1.308	1.338	1.338	1.320	1.320	1.352	
C2-C3	1.387	1.383	1.395	1.395	1.390	1.390	1.401	
C2-Br10	1.899	1.896	1.924	1.924	1.920	1.920		
C3-C4	1.379	1.383	1.390	1.390	1.392	1.392	1.406	
C3-H8	1.072	1.072	1.081	1.081	1.081	1.081	0.950	
C4-C5	1.384	1.383	1.393	1.393	1.392	1.392	1.370	
C4-H7	1.074	1.075	1.083	1.083	1.084	1.084	0.980	
C5-C6	1.380	1.383	1.391	1.391	1.393	1.393	1.370	
C5-H9(Br11)	1.892	1.072	1.909	1.909	1.081	1.081	0.990	
C6-Br11(H11)	1.302	1.308	1.084	1.084	1.920	1.920	0.950	
Bond angle value(°)								
C2-N1-C6	118.3	117.7	118.2	118.2	117.7	117.7	115.0	
N1-C2-C3	124.3	124.3	124.5	124.5	124.3	124.3	125.1	
N1-C2-Br10	116.7	116.3	116.9	116.9	116.6	116.6		
C3-C2-Br10	118.9	119.2	118.7	118.7	119.1	119.1	119.4	
C2-C3-C4	117.4	116.9	117.5	117.5	116.9	116.9	119.4	
C2-C3-H8	121.0	121.0	121.2	121.2	121.1	121.1	122.8	
C4-C3-H8	121.4	122.0	121.3	121.3	122.0	122.0	121.0	
C3-C4-C5	118.5	119.7	118.5	118.5	119.9	119.9	119.4	
C3-C4-H7	120.6	120.1	120.6	120.6	120.0	120.0	122.0	
C5-C4-H7	120.8	120.1	120.9	120.9	120.0	120.0	121.0	
C4-C5-C6	119.0	116.9	119.4	119.4	116.9	116.9	119.4	
C4-C5-H9	120.8	122.0	120.6	120.6	122.0	122.0	122.0	
C6-C5-H9	120.1	121.0	120.0	120.0	121.1	121.1	121.0	
N1-C6-C5	122.3	124.3	122.0	122.0	124.3	124.3	124.7	
N1-C6-H11(Br11)	116.6	116.3	116.8	116.8	116.6	116.6		
C5-C6-Br11(H11)	121.0	119.2	121.2	121.2	119.1	119.1		

Table 3.2 Detailed assignment of observed and theoretical wavenumbers of 2, 5-dibromopyridine with HF/6-311++G (d, p) and B3LYP/6-311++G (d, p) basis sets

Symmetry species	Observed frequencies (cm <sup>-1</sup> )		Calculated frequencies HF/6-311++G(d,p) (cm <sup>-1</sup> )		Calculated frequencies B3LYP/6-311++G(d,p) (cm <sup>-1</sup> )		IR intensity	Raman activity	Assignments
	IR	Raman	unscaled	scaled	unscaled	scaled			
A'	3095vw		3384	3062	3217	3082	0.07	122.54	γC-H
A'		3075w	3361	3042	3198	3064	0.09	57.69	γC-H
A'		3050w	3359	3040	3185	3051	4.41	79.15	γC-H
A'	1560vs		1754	1588	1591	1564	18.50	12.58	γC-C
A'	1555vs		1742	1577	1583	1556	19.36	26.27	γC-C
A'	1425vs		1608	1455	1470	1445	157.34	1.65	γC-C
A'	1345m		1497	1355	1380	1357	34.89	3.49	γC-C
A'		1280vw	1415	1281	1308	1286	0.94	4.31	γC-N
A'		1240vw	1255	1136	1270	1248	0.47	2.14	γC-N
A'	1130m		1214	1099	1153	1133	5.01	1.77	βC-H
A'	1090vs	1090m	1185	1072	1109	1090	178.27	0.16	βC-H
A'	1075m		1150	1041	1093	1074	20.95	44.66	βC-H
A'	985vs		1103	998	1014	997	63.55	1.70	βCCC
A'	950vw		1101	996	979	962	0.01	0.05	βCCC
A'		920vw	1057	957	938	922	3.03	0.22	βCCC
A''		810vw	932	843	835	821	28.23	0.09	φC-H
A''		740vs	809	732	750	737	1.10	17.32	φC-H
A''	710m		805	729	731	719	2.16	0.13	φC-H
A'	625vw	625w	685	620	630	619	3.96	5.19	γC-Br
A'	480vw		540	489	485	477	7.30	0.03	γC-Br
A''	418vw		461	418	419	412	0.14	4.55	φCCC
A''	410vw		460	416	416	409	25.04	0.06	φCCC
A'	320w	320w	347	314	319	314	1.60	1.04	βC-Br
A''	278w	278w	300	272	271	266	0.14	0.74	φCCC
A'	220vs	220vs	234	212	214	210	0.28	9.02	βC-Br
A''	160vw	160vw	178	161	164	161	0.10	0.04	φC-Br
A''			83	75	72	71	0.12	0.01	φC-Br

HF/6-311++G(d,p) scale factor is 0.9050 and B3LYP/6-311++G(d, p) scale factor is 0.950 for the wavenumbers from 4000 to 1700 cm<sup>-1</sup> and 0.983 for wavenumbers below 1700 cm<sup>-1</sup>; γ-stretching, β-in-plane bending, φ-out-of-plane bending

**Table 3.3 Detailed assignment of observed and theoretical wavenumbers of 2, 6-dibromopyridine with HF/6-311++G (d, p) and B3LYP/6-311++G (d, p) basis sets**

Symmetry species	Observed frequencies (cm <sup>-1</sup> )		Calculated frequencies HF/6-311++G(d,p) (cm <sup>-1</sup> )		Calculated frequencies B3LYP/6-311++G(d,p) (cm <sup>-1</sup> )		IR intensity	Raman activity	Assignments
	IR	Raman	unscaled	scaled	unscaled	scaled			
A'	3095w		3387	3065	3221	3086	0.12	160.08	γC-H
A'		3080vw	3384	3062	3219	3084	0.00	58.55	γC-H
A'	3040w		3342	3025	3182	3048	4.42	117.07	γC-H
A'	1570s		1746	1580	1593	1566	207.43	19.68	γC-C
A'	1560vs		1745	1579	1589	1562	68.52	11.69	γC-C
A'	1415vs		1567	1418	1435	1411	238.19	1.47	γC-C
A'	1380s		1552	1404	1420	1396	10.57	18.51	γC-C
A'		1260vw	1312	1187	1292	1270	7.12	0.24	γC-N
A'	1170vs		1251	1132	1184	1164	50.33	0.04	γC-N
A'	1135vs		1218	1102	1152	1132	89.33	0.12	βC-H
A'	1095s		1177	1065	1118	1099	55.92	8.11	βC-H
A'	1070m		1150	1041	1096	1077	5.95	11.48	βC-H
A'		980w	1121	1014	1000	983	0.02	0.10	βCCC
A'	975vs		1082	979	994	977	9.07	29.71	βCCC
A'		895vw	1008	912	906	891	0.00	0.18	βCCC
A''	780vs		883	799	794	781	45.24	0.02	φC-H
A''	740vs		817	740	748	735	130.14	0.03	φC-H
A''	710m		806	729	727	715	4.17	0.00	φC-H
A'		645w	705	638	655	644	6.36	4.71	γC-Br
A'	560vw		628	569	570	560	0.00	0.02	γC-Br
A''	440vw		483	437	444	436	0.01	0.24	φCCC
A''		365vw	405	366	365	359	2.76	1.23	φCCC
A'	310vw		342	310	314	309	8.57	1.57	βC-Br
A''	285vs		320	290	287	282	1.11	10.26	φCCC
A'	170m		186	168	158	155	0.00	1.81	βC-Br
A''	150m		171	155	153	150	3.48	0.55	φC-Br
A''			143	129	131	129	0.03	3.22	φC-Br

HF/6-311++G(d,p) scale factor is 0.9050 and B3LYP/6-311++G(d, p) scale factor is 0.950 for the wavenumbers from 4000 to 1700 cm<sup>-1</sup> and 0.983 for wavenumbers below 1700 cm<sup>-1</sup>; γ-stretching, β-in-plane bending, φ-out-of-plane bending

## CHAPTER IV

### FTIR – FT-RAMAN SPECTRAL AND GUASSIAN VIBRATIONAL ANALYSIS OF 2, 5–DIMETHYL ANILINE AND 2, 6–DIMETHYL ANILINE

#### INTRODUCTION

Aniline and its derivatives have been widely used as parent materials in a large amount of pharmaceutical, electro–optical and other industrial processes. They are also used for the synthesis of the technological materials with non–linear optical responses. Aniline based compounds play a very important role in designing organic materials for molecular electronics. The understanding of their molecular properties as well as natures of reaction mechanisms they undergo has great importance. Hence, the investigation on the structures and the vibrations of aniline and substituted anilines are still being carried out, increasingly. The inclusion of a substituent in aniline leads to the variation of charge distribution in the molecule, and consequently affects the structural, electronic and vibrational parameters.

The methyl and amino groups are generally referred to as electron donating substituents in aromatic ring systems. The electron donating methyl group interacts with nearby  $\pi$  systems through hyper conjugation, while the  $\text{NH}_2$  shares its lone pair electrons with the ring. Both the effects imply electronic delocalisation and are taken into account by the molecular orbital approach. The position of the substituents in the benzene ring as well as its

electron a donor/acceptor capability plays a very important role on the structural and electronic properties of the molecules. Because of their spectroscopic properties and chemical significance, aniline and its derivatives were studied extensively by spectroscopic and theoretical methods [1]. Hence, considerable numbers of works [3–25] have been reported on aniline and substituted anilines.

However, the Gaussian vibrational study has not been reported on 2, 5–dimethyl aniline (25DMA) and 2, 6–dimethyl aniline (26DMA), particularly the comparative analysis. Hence the present work has been undertaken to carry out a complete vibrational analysis on these molecules, based on both experimental and theoretical study.

## **RESULTS AND DISCUSSION**

### **Molecular geometry**

The optimized geometrics of the 25DMA and 26DMA compounds with atom numbering are shown in Figs 4.1a and 4.1b respectively. The molecules do not possess any rotational, reflection or inversion symmetry. So the molecules are considered under  $C_s$  point group symmetry. The optimized parameters (bond lengths and bond angle) by HF and B3LYP with basis set 6–311++G(d, p) of this compounds were calculated and shown in Table 4.1. The optimized bond lengths of C–C phenyl ring fall in the range of 1.3827 – 1.4019

Å for HF/6-311++G(d, p) method and 1.3933 – 1.4102 Å for B3LYP/6-311++G (d, p) method for 25DMA. Similarly, for the molecule of 26DMA is observed in the range 1.399 – 1.3829 Å for HF/6-311++G (d, p) method and 1.4106 – 1.3921 Å for B3LYP/6-311++G (d, p) method. The SCF converges to total energy about –363 hartrees approximately in HF level in both molecules. Similarly the same energy converges at –366 hartrees in B3LYP level.

The 54 fundamental vibrations are possible in each compound as they have same symmetry and number of atoms. These modes can be ordered in terms of irreducible form representation distributed as:

$$\Gamma_{\text{vib}} = 38 A' + 16 A''$$

$$\Gamma_{\text{vib}} = 38 A' + 16 A''$$

In agreement with  $C_s$  point group symmetry, all vibrations are active in FT-Raman and infrared spectra. The observed frequencies from IR and Raman spectra, calculated frequencies by HF and B3LYP with basis set 6-311++G (d, p), IR and Raman relative intensities and the assignments of frequencies for 25DMA and 26DMA are presented in the Tables 4.2 and 4.3 respectively. The FTIR and FT-Raman spectra of these compounds are given in Figs 4.2 and 4.3 respectively.

### **Aromatic C–H vibrations**

Most of the mono and poly nuclear aromatic compounds [23–26] have three or four peaks in the region  $3080 - 3010 \text{ cm}^{-1}$  in the IR and Raman spectra which are due to the stretching vibrations of the ring C–H bonds. In the present case, three bands are observed at  $3055, 3010$  and  $3003 \text{ cm}^{-1}$  in 25DMA and at  $3040, 3020$  and  $3010 \text{ cm}^{-1}$  in 26DMA. The corresponding calculated values are  $3038, 3018$  and  $3006 \text{ cm}^{-1}$  and  $3051, 3026$  and  $3022 \text{ cm}^{-1}$  in both the molecules by B3LYP/6–311++G (d, p) method, which clearly shows the close agreement of calculated and experimental values. The optimized bond lengths are nearly equal in both compounds.

Only three bands are expected for aromatic C–H stretching mode in both the molecules. All the three bands are lie within the expected range. But the observed bands are of medium to weak intensities, which should have been strong and medium respectively. This indicates that the substitutions influence the benzene ring; two methyl and amino groups have very less influence on the stretching vibrations of the ring C–H bonds.

### **Aromatic C–C vibrations**

Ring CC stretching vibrations are expected in the range  $1680 - 1400 \text{ cm}^{-1}$  [27, 28], C=C stretching usually lie between  $1800$  to  $1600 \text{ cm}^{-1}$  and C–C stretching in the range  $1600 - 1400 \text{ cm}^{-1}$ . In some molecules, it even extends

up to  $1400\text{ cm}^{-1}$  [29, 30]. In the present study, the C=C stretchings are observed at  $1630$  and  $1590\text{ cm}^{-1}$  and at  $1620$  and  $1605\text{ cm}^{-1}$  in 25DMA and 26DMA respectively. The frequency difference found between the two molecules indicates the positional variation of methyl group has influenced the skeleton C=C vibrations. One band for C=C stretching is found missing in both the molecules which has been predicted in calculations. A very strong IR band is observed at  $1596\text{ cm}^{-1}$  in 25DMA and at  $1491\text{ cm}^{-1}$  in 26DMA for C=C stretching. It shows the position of methyl group has undoubtedly affected the intensity of these modes also.

Only two bands are expected for aromatic C–C stretching vibrations at  $1516$  and  $1462\text{ cm}^{-1}$  in 25DMA. But five bands are present in 26DMA at  $1491$ ,  $1485$ ,  $1465$ ,  $1456$  and  $1450\text{ cm}^{-1}$ . This result is not quite expected. The intensity of these bands is completely suppressed in 25DMA, which shows the 5<sup>th</sup> position of the methyl group is not favouring these modes. The mean difference between experimental and calculated values in these modes is  $\pm 4.7\text{ cm}^{-1}$ . It is notable in this study that both C=C and C–C stretching values are very much low when compared to pure benzene which also shows the substitutions have considerable influence on the skeleton vibrations.

### **Methyl functional group vibrations**

Residual alkane groups are found in a very large number of compounds and hence, there is an extremely important class in aromatic vibration [31].

Three types of vibration are normally observed, namely stretching, in-plane and out-of-plane bending vibrations of C–H bonds. The C–H vibration frequencies of methyl and methylene groups fall in narrow ranges of saturated hydrocarbons. However, atoms directly attached to  $-\text{CH}_3-$  and  $-\text{CH}_2-$  may result in relatively large shifts in the absorption frequencies.

The C–H stretching vibrations in these groups occur in the region  $2975 - 2840 \text{ cm}^{-1}$  [32, 33]. In the present study, the bands at 2960, 2920, 2910, 2880 and  $2865 \text{ cm}^{-1}$  in 25DMA and at 2965, 2910, 2908, 2866 and  $2848 \text{ cm}^{-1}$  in 26DMA have been observed for C–H stretching. In both the molecules, the first three are asymmetrical and the remaining are symmetrical vibrations. All the bands are within the expected range but the comparison between the molecules clearly shows that only band  $2910 \text{ cm}^{-1}$  is identical in both the molecules, whereas all other bands differ from one another, particularly the last two bands. The deviation is purely due to the positional variation of the methyl groups in these two molecules.

### **Aromatic and Methyl C–H deformation vibrations**

In Raman spectra, the bands due to the C–H in-plane deformation vibrations, which occur in the region  $1390 - 990 \text{ cm}^{-1}$ , are very useful for characterisation [17]. Generally, a very strong band in the Raman spectra of mono, di and tri substituted benzenes is observed near  $1000 \text{ cm}^{-1}$  which may be the strongest band in the spectrum. In the infrared, a number of C–H in-plane

deformation bands occur in the region  $1390 - 900 \text{ cm}^{-1}$ . Although these bands are usually sharp, they are of weak to medium intensity [29]. In the present molecules, all the nine bands are observed between  $1390 - 925 \text{ cm}^{-1}$  in 25DMA and  $1383 - 985 \text{ cm}^{-1}$  in 26DMA, for C-H in-plane bending vibrations. The out-plane bending vibrations are observed between  $945 - 446 \text{ cm}^{-1}$  and  $967 - 339 \text{ cm}^{-1}$  for the first and second molecules respectively. Most of the vibrations are observed only in infrared spectrum.

The comparison of these deformation modes between the molecules and also with other methyl substituted benzenes [30] clearly indicates the delicate nature of these bands. There is a lot of interaction of these modes as noted in the earlier works with the other modes such as  $\Phi\text{N-H}$ ,  $\beta\text{C-CH}_3$ ,  $\beta\text{C-NH}_2$  etc, whose frequencies also lie in these ranges. The change of position of the methyl group also caused appreciable variation in the frequencies of vibration of these bands.

### **N-H vibrations**

In solids and liquids where hydrogen bonding occur the N-H stretching appear in the region  $3450 - 3160 \text{ cm}^{-1}$  with a broad band of medium intensity, whereas in aromatic cases the bands occurs at  $3520 - 3340 \text{ cm}^{-1}$  with medium or strong intensity. This observation made by the early researchers has also been found true in the present case. In these compounds, two N-H stretching frequencies are observed at  $3483$  and  $3390 \text{ cm}^{-1}$  in 25DMA and at  $3493$  and

3393  $\text{cm}^{-1}$  in 25DMA, with strong and medium intensities in both the cases. In each molecule, one asymmetric and one symmetric vibration are observed. It is also observed that symmetric band is more intense than asymmetric one.

The N–H in–plane deformation bands occur usually at 1300 – 1150  $\text{cm}^{-1}$  with weak intensity [34]. The N–H in–plane bending vibrations in these cases are found at 1395  $\text{cm}^{-1}$  in 25DMA and at 1392  $\text{cm}^{-1}$  in 26DMA. One band is found missing in each case. The frequency is also relatively high when compared to the cited literature. These abnormalities may only be due to the influence of the presence of the methyl groups in the vicinity. The out–of–plane bending N–H vibrations are found at 570  $\text{cm}^{-1}$  in 25DMA and at 540  $\text{cm}^{-1}$  in 26DMA which is also in line with the previous work on dimethyl benzimidazole [34].

## CONCLUSION

From the vibrational analysis of the 25DMA and 26DMA with the help of the calculations performed by HF and B3LYP methods and compared with the literatures of the amino and methyl substituted aromatic molecules, the following observations are made.

The influence of the substituents in the benzene ring; two methyl groups and one amino group, have very less influence on the stretching vibrations of ring C–H bonds. Both C=C and C–C stretching frequency values are very

much less when compared to pure benzene, which shows the substitutions have considerable influence on these skeleton vibrations.

All the bands of C–H stretching in methyl groups are within the expected range but the comparison between the molecules clearly shows that only band  $2910\text{ cm}^{-1}$  is identical in both the molecules, whereas all other bands differ from one another, particularly the last two bands. The deviation is purely due to the positional variation of the methyl groups between the two molecules. The comparison of C–H deformation modes between the molecules clearly indicates the delicate nature of these bands. There is a lot of interaction of these modes as noted in the earlier works with the other modes such as  $\Phi\text{N–H}$ ,  $\beta\text{C–CH}_3$ ,  $\beta\text{C–NH}_2$  etc, whose frequencies also lie in these ranges. The change of position of the methyl group also caused appreciable variation in the frequencies of vibration of these bands.

The N–H stretching and deformation frequencies are more relative when compared to the literatures. The abnormalities may only be due to the presence of the methyl groups in the vicinity

**REFERENCES**

- [1] M.Critchley, "Butter worths Medical dictionary" II edition, (1986).
- [2] <http://www.p-chloroaniline.com/>(2007).
- [3] R.B.Sing and D.R.Rai, Indian J. Pure and Appl.Phys. 20 (1982) 596
- [4] J.A.Faniran and H.F.Sharvell, Spectrochim acta, part A 38A (1982) 1155.
- [5] R.A.Kydd and A.R.C.Dunham, J. Mol. Struct. 98 (1983) 39.
- [6] P.K.Mallick and S.B.Banergee, J. Pure and Appl.Phys. 12 (1974) 296.
- [7] E.Allenstein, P.Kimle, E.Schlipf and W.Podzun, Spectrochim acta, 34A, (1978) 423.
- [8] S.L Srivastava, Specroscopic studies of some distr. Substituibuted benzenes, Ph.d. Thesis , Gorkhapur university , Gorkhapur.
- [9] Y.Anantharama, Spectrochim Acta 34 A, (1978) 825.
- [10] Y.Abdulla, Obaid, S.Mamdouh and Soliman, Spectrochim acta, 46A (1990)1779.
- [11] R.B.Sing and D.K.Ray, Indian J. Pure and Appl.Phys. 20 (1982) 330.
- [12] I.Krishnan, Indian J. Pure and Appl.Phys. 12 (1974) 598.
- [13] E.Allenstein, P.Kimle, E.Schlipf and W.Podson, J. Spectrochim Acta A(GB) 34 (1978) 423.
- [14] G.Quillard, G.Lourn and S.Lefrant, Phys.Rev.B50 (1994) 12496.
- [15] K.Sree Ramulu and Ramana Rao, Indian J pure and Appl Phys, 20, (1982) 372.
- [16] E.Krishnamoorthy and Ramana Rao, J. Raman Spectrosc. 19 (1988), 359.
- [17] N. G. Dongre, B. P. Asthana, P. C. Mishra and Chandra M. Pathak Molecular Spectroscopy 47(1991) 673.

- [18] Piotr M. Wojciechowski and Danuta Michalska *Spectrochim acta* 68 (2007) 948.
- [19] Elif Akalin and Sevim Akyüz Structure and vibrational spectra of benzidine *Journal of Molecular Structure*, 651( 2003) 571.
- [20] A. R. Shukla, B. P. Asthana, N. G. Dongre, Chandra M. Pathak *Vibrational Spectroscopy*, 3( 1992) 245.
- [21] I. López– Tocón, M. Becucci, G. Pietraperzia, E. Castellucci and J. C. Otero *Journal of Molecular Structure*, 565( 2001) 421.
- [22] M.Karabacak, D.Karagöz, M.Kurt, *Spectrochimica Acta* 72 ( 2009) 1076.
- [23] George.Socrates, *Infrared and Raman Characteristic Group Frequencies*, Third ed., John Wiley & sons, Ltd., Chichester, 2001.
- [24] B.S.Yadav,Israt Ali,Pradeep Kumar and Preeti Yadav,*Indian Journal of Pure and Applied Physics* 45 (2007) 979
- [25] N.Sundaraganesan, G.Elango, S.Sebastian and P.Subramani ,*Indian Journal of Pure and Applied Physics* 47 (2009) 481
- [26] R.B.Singh and D.K.Rai, *Indian Journal of Pure and Applied Physics* 20 (1982) 330
- [27] V.Krishnakumar and V.Balachandran, *Spectrochim Acta* 61(2005) 1811
- [28] T.F.Ardyukova, *Atlas of spectra of Aromatic and Hetrocyclic compounds*, Nauka Sib. Otd., Novosibirsk, (1973).
- [29] A.R.Katrizky, *J. Chem. Soc.*, (1959) 2058.
- [30] C.J.Pouchert, *The Aldric Library of FT IR spectra*, Aldrich Chemicals Co, Milwaukee, WI, (1985).
- [31] J.E.Stewart, *J. Chem. Phys.* 30 (1959) 1259

- [32] J.R.Durig, *J Raman spectrosc.*, 20 (1989) 311.
- [33] S.Shadri, S.Muthunatesan and V. Krishnakumar, *Spectrochim Acta PartA* 68 (2007) 811.
- [34] R.Ramasamy and V. Krishnakumar, *Spectrochim Acta PartA* 66 (2007) 503.

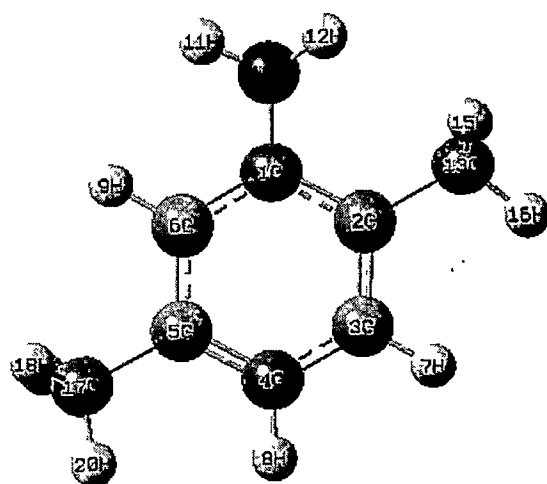


**Fig 4.1a Molecular Structure of 2, 5-Dimethyl aniline (25DMA)**

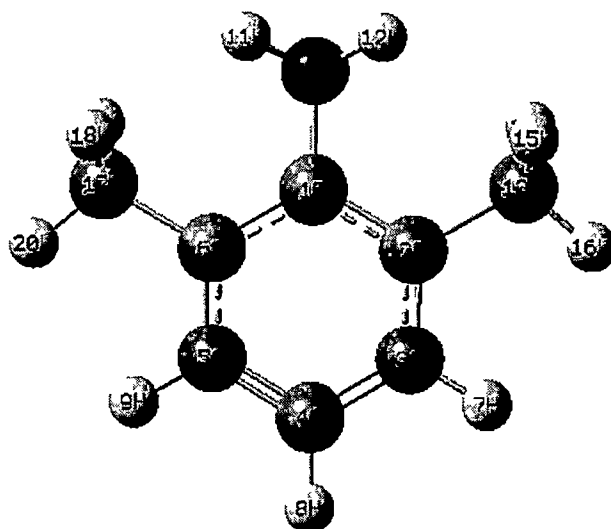


**Fig 4.1b Molecular Structure of 2, 6-Dimethyl aniline (26DMA)**

### 2,5-dimethylaniline

### 2,6-dimethylaniline

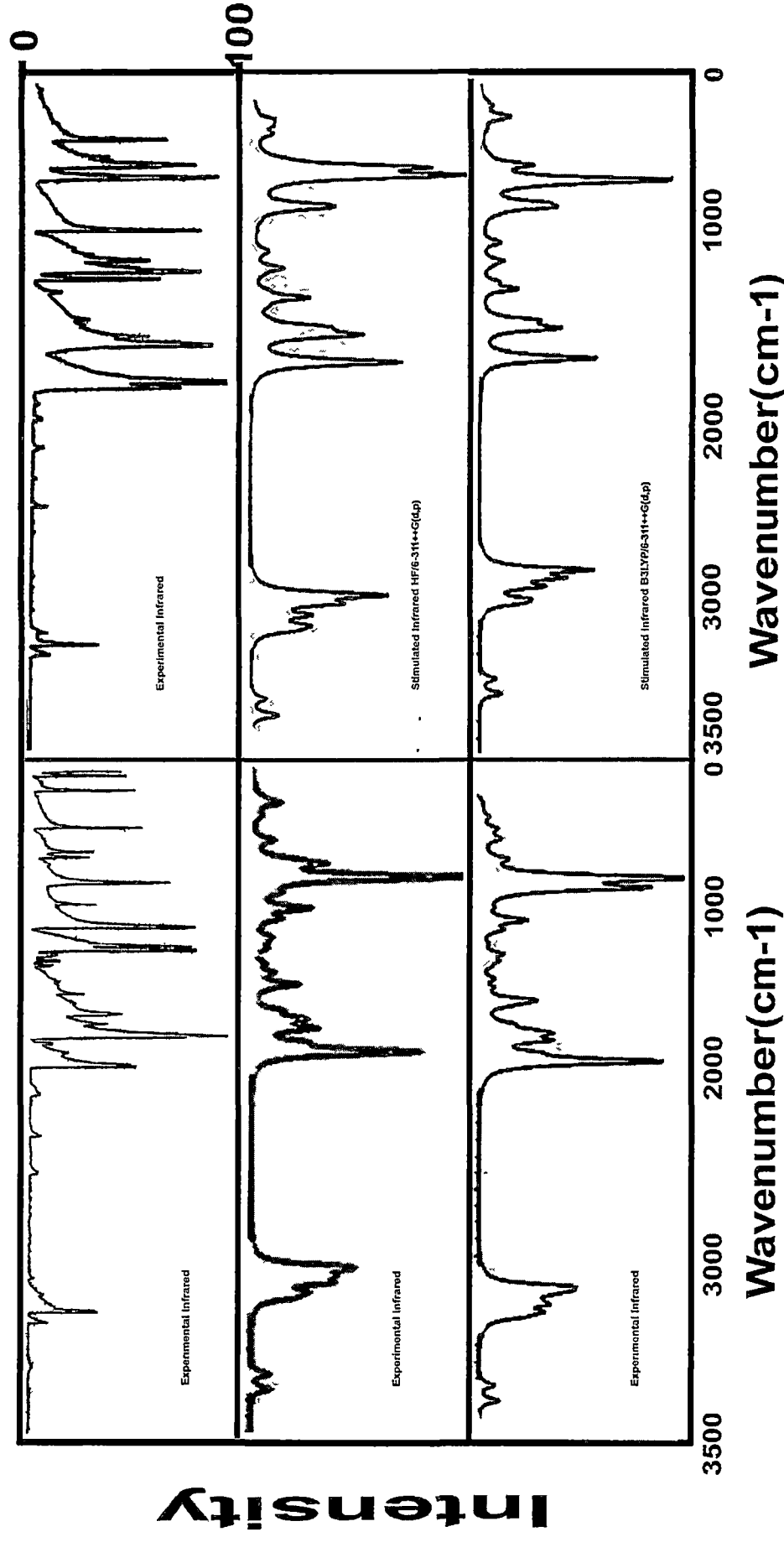
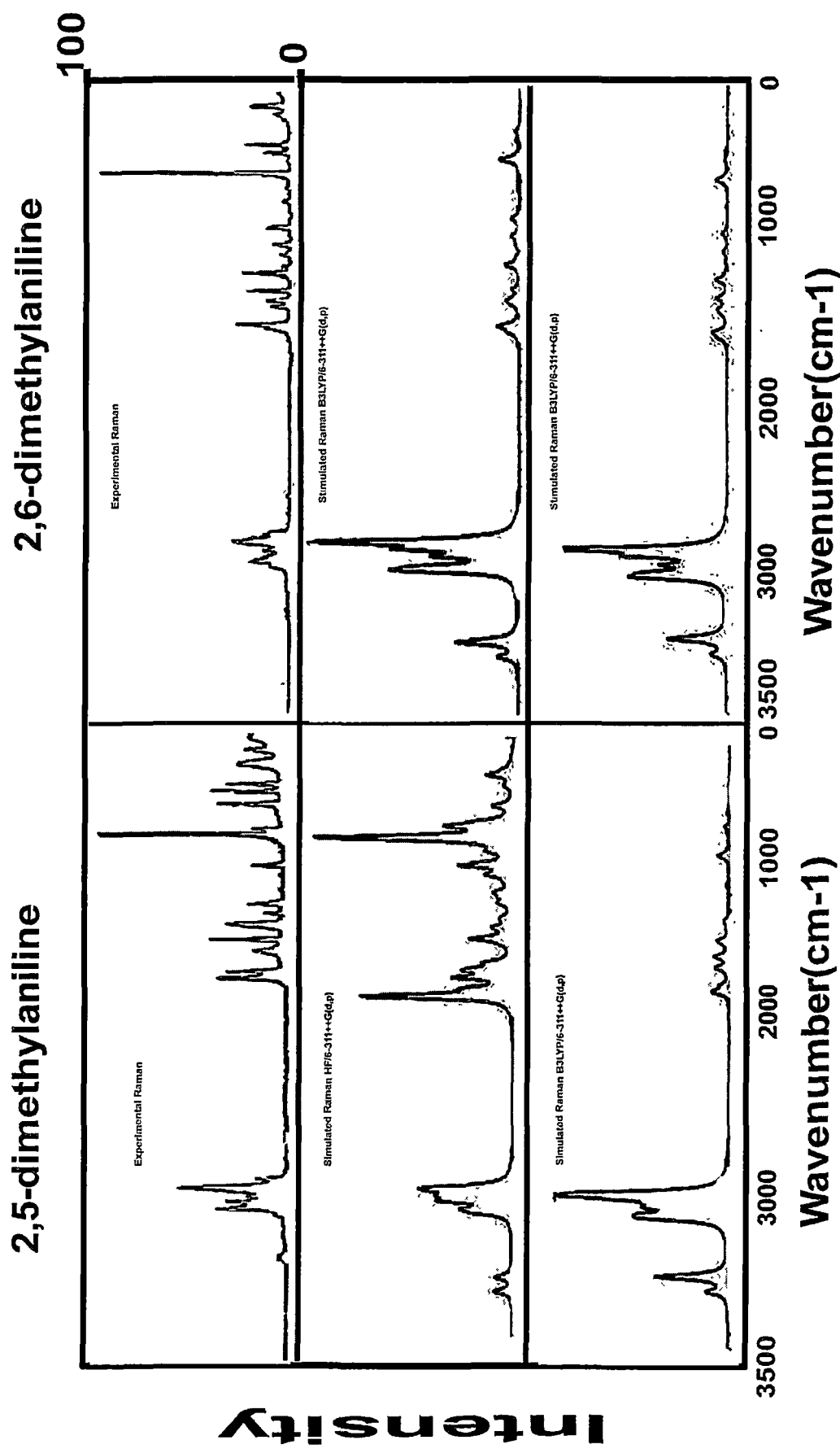


Figure 4.2: Experimental and Simulated Infrared spectra



**Figure 4.3: Experimental and Simulated Raman spectra**

Table 4.1 Optimized parameters of 25DMA and 26DMA, bond length (Å), bond angle (°)

#Parameters	25DMA			26DMA			Expt	25DMA			26DMA			Expt
	HF/6-311 ++G(d,p)	B3LYP/ 6-311 ++G(d,p)	B3LYP/ 6-311 ++G(d,p)	HF/ 6-311 ++G(d,p)	B3LYP/ 6-311 ++G(d,p)	B3LYP/ 6-311 ++G(d,p)		HF/ 6-311 ++G(d,p)	B3LYP/ 6-311 ++G(d,p)	B3LYP/ 6-311 ++G(d,p)	HF/ 6-311 ++G(d,p)	B3LYP/ 6-311 ++G(d,p)	B3LYP/ 6-311 ++G(d,p)	
R(1,2)	1.4019	1.4102	1.4105	1.3990	1.3990	1.4105	1.39	A(2,1,6)	119.81	119.68	120.43	120.38	120.3	
R(1,6)	1.3872	1.4009	1.4106	1.3990	1.3990	1.4106	1.36	A(2,1,10)	120.18	120.25	119.75	119.78		
R(1,10)	1.3991	1.4007	1.4012	1.4010	1.4010	1.4012	1.43	A(6,1,10)	119.96	120.01	119.76	119.77		
R(2,3)	1.3821	1.3945	1.3950	1.3863	1.3863	1.3950	1.40	A(1,2,3)	117.85	117.96	118.87	118.83	119.2	
R(2,13)	1.5097	1.5075	1.5084	1.5106	1.5106	1.5084	1.55	A(1,2,13)	120.87	120.62	120.61	120.30		
R(3,4)	1.3887	1.3933	1.3920	1.3829	1.3829	1.3920	1.39	A(3,2,13)	121.28	121.42	120.52	120.86		
R(3,7)	1.0769	1.0859	1.0855	1.0764	1.0764	1.0855	1.08	A(2,3,4)	122.26	122.13	121.40	121.41		
R(4,5)	1.3838	1.3974	1.3921	1.3829	1.3829	1.3921	1.40	A(2,3,7)	118.79	118.57	118.98	118.78		
R(4,8)	1.0756	1.0847	1.0836	1.0750	1.0750	1.0836	1.08	A(4,3,7)	118.95	119.30	119.63	119.81		
R(5,6)	1.3899	1.3950	1.3949	1.3863	1.3863	1.3949	1.39	A(3,4,5)	119.89	120.06	119.04	119.13		
R(5,17) (5,9)	1.5105	1.5102	1.0855	1.0764	1.0764	1.0855	1.55(1.08)	A(3,4,8)	119.76	119.90	120.48	120.44		
R(6,9) (6,17)	1.0782	1.0872	1.5084	1.5106	1.5106	1.5084	1.08(1.55)	A(5,4,8)	120.35	120.03	120.48	120.43		
R(10,11)	0.9956	1.0095	1.0087	0.9945	0.9945	1.0087	1.02	A(4,5,6)	118.41	118.33	121.40	121.41	120.5	
R(10,12)	0.9953	1.0092	1.0087	0.9945	0.9945	1.0087	1.02	A(4,5,17)	121.50	121.08	119.63	119.80		
R(13,14)	1.0868	1.0959	1.0961	1.0870	1.0870	1.0961	1.09	A(6,5,17)	120.09	120.58	118.98	118.79		
R(13,15)	1.0891	1.0981	1.0980	1.0890	1.0890	1.0980	1.09	A(1,6,5)	121.77	121.84	118.86	118.83		
R(13,16)	1.0834	1.0913	1.0911	1.0831	1.0831	1.0911	1.09	A(1,6,9)	118.85	118.78	120.62	120.30		
R(17,18)	1.0862	1.0930	1.0980	1.0890	1.0890	1.0980	1.09	A(5,6,9)	119.38	119.39	120.51	120.86		
R(17,19)	1.0864	1.0957	1.0960	1.0870	1.0870	1.0960	1.09	A(1,10,11)	114.20	115.13	115.05	115.91		
R(17,20)	1.0839	1.0925	1.0911	1.0831	1.0831	1.0911	1.09	A(1,10,12)	115.19	116.06	115.05	115.91		
								A(11,10,12)	111.01	111.92	110.81	111.94		
								A(2,13,14)	111.34	111.61	111.44	111.69		
								A(2,13,15)	111.88	112.11	111.83	112.07		
								A(2,13,16)	110.64	110.84	110.61	110.81		
								A(14,13,15)	107.55	107.13	107.64	107.20		
								A(14,13,16)	107.98	107.81	107.86	107.73		
								A(15,13,16)	107.26	107.12	107.27	107.11		
								A(5,17,18)	111.06	111.55	111.83	112.06		
								A(5,17,19)	110.93	111.00	111.44	111.69		
								A(5,17,20)	111.12	111.29	110.61	110.81		
								A(18,17,19)	107.63	107.36	107.64	107.20		
								A(18,17,20)	108.00	108.04	107.28	107.11		
								A(19,17,20)	107.96	107.41	107.85	107.73		

#Refer Fig.1a and 1b for numbering of atom

Table 4.2 Detailed assignment of fundamental vibrations of 25DMA based on the HF/6-311++G (d, p) and B3LYP/6-311++G (d, p)

Symmetry species	Observed frequencies (cm <sup>-1</sup> )		Calculated frequencies HF/6-311++G(d,p) (cm <sup>-1</sup> )		Calculated frequencies B3LYP/6-311++G (d, p) (cm <sup>-1</sup> )		Assignments
	IR	Raman	unscaled	scaled	unscaled	scaled	
A'	3483vw		3887	3518	3664	3510	γ (N - H)
A'	3390vw		3791	3431	3568	3418	γ (N - H)
A'	3055vw		3333	3016	3171	3038	γ (C - H)
A'		3010m	3310	2996	3150	3018	γ (C - H)
A'	3003vs		3295	2982	3138	3006	γ (C - H)
A'	2960vw		3242	2934	3101	2971	γ(C - H) CH <sub>3</sub>
A'			3241	2933	3098	2968	γ(C - H) CH <sub>3</sub>
A'		2920vw	3213	2908	3072	2943	γ(C - H) CH <sub>3</sub>
A'	2910vw		3194	2891	3041	2913	γ(C - H) CH <sub>3</sub>
A'	2880w		3164	2863	3019	2892	γ(C - H) CH <sub>3</sub>
A'		2865vw	3144	2845	2996	2870	γ(C - H) CH <sub>3</sub>
A'			1816	1643	1665	1637	γ (C = C)
A'		1630s	1798	1627	1651	1623	γ (C = C)
A'	1590vs	1590vs	1755	1588	1615	1588	γ (C = C)
A'	1516w		1672	1513	1544	1518	γ (C - C)
A'			1624	1470	1507	1481	γ (C - C)
A'			1610	1457	1491	1466	γ (C - C)
A'			1605	1453	1490	1465	γ (C - CH <sub>3</sub> )
A'	1462m		1605	1453	1486	1461	γ (C - CH <sub>3</sub> )
A'	1420vs		1564	1415	1450	1425	β (CH <sub>3</sub> ) WAG
A'		1395vw	1538	1392	1413	1389	β (N - H)
A'	1390m		1534	1388	1412	1388	β (C - H)
A'	1305vw		1433	1297	1341	1318	β (C - H)
A'	1275m		1393	1261	1324	1301	γ (C - N)
A'	1216vw	1200vw	1335	1208	1307	1285	β (C - H)
A'	1175vw		1314	1189	1230	1209	β (C - H)
A'	1150m		1261	1141	1182	1162	β (C - H)
A'			1240	1122	1171	1151	β (C - H)
A'			1159	1049	1092	1073	β (C - H)
A'			1154	1044	1059	1041	β (C - H)
A'	1045s		1148	1039	1055	1037	β (C - H)
A'	1015vw		1111	1005	1024	1007	β (C - C)
A'	985vs		1079	976	1013	996	β (C - C)
A''	945m		1060	959	948	932	φ (C - H)
A''		925vw	1011	915	946	930	φ (C - H)
A''	877vw		961	870	863	848	φ (C - H)
A''	800s		897	812	806	792	φ (C - H)
A'		732vw	809	732	764	751	β (N - H)
A''		728vw	803	727	734	722	φ (C - H)
A''	703m		772	699	727	715	φ (C - H)
A''			712	644	617	607	φ (C - H)
A''		570vw	634	574	577	567	φ (N - H)

A'			605	548	560	550	$\beta$ (C CC)
A'	480vs		524	474	488	480	$\beta$ (CCC)
A''	446vw		494	447	454	446	$\phi$ (C - H)
A'			475	430	447	439	$\beta$ (C CC)
A''		320s	355	321	340	334	$\phi$ (C - H)
A'			333	301	308	303	$\beta$ (CCN)
A''			307	278	291	286	$\phi$ (CCC)
A''			271	245	282	277	$\phi$ (CCC)
A''			232	210	215	211	$\phi$ (C CC)
A''			191	173	175	172	$\phi$ (CCC)
A''			145	131	130	128	$\phi$ (CCC)
A''			35	32	24	24	$\phi$ (CCN)

HF/6-311++G(d,p) scale factor is 0.9050 and B3LYP/6-311++G(d, p) scale factor is 0.950 for the wavenumbers from 4000 to 1700  $\text{cm}^{-1}$  and 0.983 for wavenumbers below 1700  $\text{cm}^{-1}$

$\gamma$ -stretching,  $\beta$ -in-plane bending,  $\phi$ -out-of-plane bending

**Table 4.3 Detailed assignment of fundamental vibrations of 26DMA based on the HF/6-311++G (d, p) and B3LYP/6-311++G (d, p)**

Symmetry species	Observed frequencies (cm <sup>-1</sup> )		Calculated frequencies HF/6-311++G(d,p) (cm <sup>-1</sup> )		Calculated frequencies B3LYP/6-311++G (d, p) (cm <sup>-1</sup> )		Assignments
	IR	Raman	unscaled	scaled	unscaled	scaled	
A'	3493vw		3901	3530	3672	3518	γ (N - H)
A'	3393vw		3808	3446	3577	3427	γ (N - H)
A'		3040vw	3344	3026	3185	3051	γ (C - H)
A'	3020vs		3320	3005	3159	3026	γ (C - H)
A'		3010s	3312	2997	3154	3022	γ (C - H)
A'		2965	3245	2937	3104	2974	γ(C - H) CH <sub>3</sub>
A'			3245	2937	3104	2974	γ(C - H) CH <sub>3</sub>
A'	2910vw		3194	2891	3040	2912	γ(C - H) CH <sub>3</sub>
A'		2908vw	3194	2891	3040	2912	γ(C - H) CH <sub>3</sub>
A'		2866vw	3146	2847	2996	2870	γ(C - H) CH <sub>3</sub>
A'	2848vw		3145	2846	2995	2869	γ(C - H) CH <sub>3</sub>
A'			1819	1646	1667	1639	γ (C = C)
A'	1620vs		1785	1615	1635	1607	γ (C = C)
A'		1605vs	1775	1606	1633	1605	γ (C = C)
A'		1491s	1637	1481	1518	1492	γ (C - C)
A'	1485w		1634	1479	1514	1488	γ (C - C)
A'	1465vw		1612	1459	1490	1465	γ (C - C)
A'		1456vw	1608	1455	1488	1463	γ (C - CH <sub>3</sub> )
A'	1450m		1607	1454	1487	1462	γ (C - CH <sub>3</sub> )
A'	1435vs		1582	1432	1466	1441	β (CH <sub>3</sub> ) WAG
A'	1392s		1539	1393	1414	1390	β (N - H)
A'		1383s	1537	1391	1414	1390	β (C - H)
A'	1275m		1412	1278	1349	1326	β (C - H)
A'	1240vw		1381	1250	1300	1278	γ (C - N)
A'			1334	1207	1297	1275	β (C - H)
A'			1332	1205	1249	1228	β (C - H)
A'	1140vs		1256	1137	1186	1166	β (C - H)
A'			1228	1111	1157	1137	β (C - H)
A'	1090vs		1195	1081	1118	1099	β (C - H)
A'			1156	1046	1057	1039	β (C - H)
A'	1045vw	1016vw	1152	1043	1055	1037	β (C - H)
A'	985vs		1087	984	1022	1005	β (C - C)
A'			1080	977	1005	988	β (C - C)
A''	967vs		1075	973	959	943	φ (C - H)
A''			1017	920	903	888	φ (C - H)
A''	855vw		959	868	901	886	φ (C - H)
A''			899	814	845	831	φ (C - H)
A'		769s	853	772	768	755	β (N - H)
A''	740vs		825	747	751	738	φ (C - H)
A''			719	651	679	667	φ (C - H)
A''	627s		687	622	587	577	φ (C - H)
A''	540vw		594	538	551	542	φ (N - H)

*	A'		587	531	542	533	$\beta$ (C CC)
	A'	490vw	556	503	507	498	$\beta$ (CCC)
	A''		525	475	495	487	$\phi$ (C - H)
	A'	445vw	511	462	479	471	$\beta$ (C CC)
	A''		373	338	355	349	$\phi$ (C - H)
	A'		319	289	310	305	$\beta$ (CCN)
	A'		307	278	298	293	$\phi$ (CCC)
	A''		295	267	278	273	$\phi$ (CCC)
	A''		231	209	223	219	$\phi$ (C CC)
	A''	195m	208	188	186	183	$\phi$ (CCC)
	A''	145m	195	176	174	171	$\phi$ (CCC)
	A''		40	36	29	29	$\phi$ (CCN)

HF/6-311++G(d,p) scale factor is 0.9050 and B3LYP/6-311++G(d, p) scale factor is 0.950 for the wavenumbers from 4000 to 1700  $\text{cm}^{-1}$  and 0.983 for wavenumbers below 1700  $\text{cm}^{-1}$

$\gamma$ -stretching,  $\beta$ -in-plane bending,  $\phi$ -out-of-plane bending

**Table 4.4 Comparative values of IR intensities and Raman Activities between HF/6-31++G (d, p) and B3LYP/6-311++G (d, p) of 25DMA and 26DMA**

25DMA				26DMA			
HF/6-311++ G(d,p) (cm <sup>-1</sup> )		B3LYP/6-311++ G(d,p) (cm <sup>-1</sup> )		HF/6-311++ G(d,p) (cm <sup>-1</sup> )		B3LYP/6-311++ G(d,p) (cm <sup>-1</sup> )	
IR intensity	Raman activity	IR intensity	Raman activity	IR intensity	Raman activity	IR intensity	Raman activity
17.4	41.8	15.2	49.3	20.1	33.3	19.2	36.9
16.5	129.5	11.7	191.2	14.6	114.5	10.1	163.6
23.8	138.9	18.8	160.6	25.3	179.5	20.3	203.6
14.5	65.1	12.7	79.2	32.4	66.1	27.9	76.3
25.9	74.5	24.8	84.2	0.6	67.9	1.3	87
26.3	55.7	15.9	59.3	22.3	65.2	13	69.5
24.0	61.8	17.8	65.9	25.7	49.5	19.2	54.1
27.5	81.5	21.3	88.4	56.1	118.8	37.9	126.7
31.1	90.6	24.1	111.4	5.4	46	9.4	75.6
42.5	207.6	36.4	275.2	49.3	325.9	42.7	407.9
56.0	190.6	49.5	255.4	47	34.5	44.3	57.2
133.3	25.6	130.1	27.4	107.7	17	102.6	21.8
20.2	14.8	10.3	19.6	0	13.7	3	22
32.2	17.5	25	17.7	3.6	24.4	0.1	13.9
48.6	1.4	41.7	0.9	13.1	3.5	11.5	4
24.0	3.7	30.9	3.8	51.2	6.2	53.3	5.9
8.4	8.5	8.6	10.1	1.3	1.2	2.1	4.1
10.8	5.7	6.1	10.5	0	17.7	0.1	16.7
2.5	13.3	7.4	10	14.8	0.5	17.1	0.4
20.2	0.5	15.5	0.3	41	1.8	33.8	2.2
0.2	13	0.2	34.6	0.5	7.7	1.4	18.3
0.2	1.9	1.6	1.2	0.1	4.9	1.7	11.2
4.2	1.1	10.4	2.0	0.1	0.1	4.9	1.2
38.5	22.2	8.8	3.7	32.9	26.8	1.8	0.1
4.3	4.3	34.8	27	4	2	36	33.2
13.8	2.6	6.7	5.4	8.4	2.5	5	3.9
7.4	2.8	1	9.6	0.4	5.2	0.3	3.7
3.8	5.5	8.3	4.1	4.9	3	3.5	1.4
2.7	0.1	5.1	2.1	18.9	13	20.3	12.9
0.7	0.3	7.1	0.3	0.1	0.3	0.1	0.1
8.3	1.4	3	1.4	0.3	0.6	1.3	0.4
7.2	1.3	1.7	1	1.8	14.5	8.3	0.5
13.5	0.9	13.9	1	0.8	0.2	3.3	14
1.2	0.1	2.8	7.4	16	0.2	0.5	0.1
3.1	11.4	0.6	0.4	0.1	0.3	0.1	0.2

20.5	0.1	13.8	0.2	1	0.2	1.6	0.1
47.7	1.4	33.1	0.7	4.3	2.7	2.3	2.9
3.3	29.9	0.1	28.7	53.3	1.4	35	0.5
11.7	2.7	2.3	1.4	41.2	0.4	30	0.2
2.5	1.5	1	1.5	14.6	35.7	0.9	32
190.8	5.5	112.9	4.6	176.7	2.1	130.8	2.3
48.5	3.5	25.1	10	39.3	1.1	2.1	4.8
20	4.7	135	0.1	2.1	5.1	101	2.7
0.2	6.2	0.4	6.8	0	0.6	0.1	0.2
17.2	0.1	15.3	0.3	2.8	7.2	6.6	6.7
0.1	5.1	0.1	3.2	0.1	0.1	0.1	0.1
6	2	13.3	0.8	4.1	0	11.1	0.1
2.5	0.3	1.7	0.8	0.9	0.6	9.4	1
0.6	0.5	2	1	14.7	0.7	0.2	0.8
23.8	0.8	8.7	0.7	14.4	0.8	12.9	0.5
6.5	0.6	5.7	0.6	8.8	1.8	2.6	2.3
1.7	0.6	1.1	0.7	1.4	0	1.1	0
1.7	0.3	1.5	0.2	2.8	0.5	0.7	0.5
0.1	0.2	0.2	0.8	0.5	0.1	0.3	0.1

## FTIR - FT Raman spectral and theoretical vibrational analysis of 2-5 dimethyl aniline and 2-6 dimethyl aniline

M. Govindarajan \*, K. Ganasan # ,S. Periandy @, and R. Madivanan &

\*Department of Physics, Avvaiyar Govt College for Women, Puducherry, Karaikal-609 605

#Department of Physics, T.B.M.L. College, Tamilnadu, Porayar-609 307

@Department of Physics, Tagore Arts College Women, Puducherry, 605 001

& Department of Physics, BGCW, Puducherry, 605 001

### ABSTRACT

---

FT-Raman and FT-IR spectra of 2-5 Dimethyl aniline and 2-6 Dimethyl aniline have been recorded in the solid phase. In this work, we will report a combined experimental and theoretical study on molecular and vibrational structures of titled compounds. The equilibrium geometry, harmonic vibrational frequencies, infrared intensities and Raman scattering activities are calculated by ab initio HF/6-31G (d) basis set. The scaled theoretical wave numbers showed very good agreement with the experimental values. A complete assignment of the infrared and Raman spectra of 2-5 Dimethyl aniline and 2-6 Dimethyl aniline are reported. The experimental and stimulated spectrograms of the title molecules have been constructed.

---

Keywords: FT-IR and FT-Raman spectra, DFT, 2-5 Dimethyl aniline, 2-6 Dimethyl aniline, Vibrational analysis

### INTRODUCTION

Aniline is used as the parent of many synthetic drugs and dyes stuff. It has an antipyretic action (Critchley.M, 1986). They are toxic if inhaled, ingested, or absorbed through the skin. The aniline derivatives are used in the production of antioxidants, agricultural, pharmaceutical, rubber chemicals and other target organic molecules (Dimethylaniline.com, 2009). Methyl aniline can also affect human when breathed in or by passing through skin. Several workers have studied the spectra of large number of mono, di, tri and tetra substituted anilines and related molecules studied the near UV spectrum of aniline derivatives in vapour phase (Sing et al 1982). The vibrational spectrum was analysed assuming that the molecules belongs to Cs point group symmetry. The spectrum was analysed interms of frequencies observed in Infrared and Raman spectra.

## MATERIALS AND METHODS

The compounds under investigations namely 2-5 Dimethyl aniline and 2-6 Dimethyl aniline were purchased from M/S Aldrich chemicals, U.S.A which are of spectroscopic grade and hence used for recording the spectra as such without any further purification. The FTIR spectra of the compounds were recorded in Bruker IFS 66V spectrometer in the range of 4000 to 200  $\text{cm}^{-1}$ . The spectral resolution is  $\pm 2 \text{ cm}^{-1}$ . The FT Raman spectra of these compounds were also recorded in the same instrument with FRA 106 Raman module equipped with Nd: YAG laser source operating at 1.064  $\mu\text{m}$  line width with 200 mW power. The spectra were recorded with scanning speed of 30  $\text{cm}^{-1} \text{ min}^{-1}$  of spectral width 2  $\text{cm}^{-1}$ . The frequencies of all sharp bands are accurate to  $\pm 1 \text{ cm}^{-1}$ .

The general molecular structure of 2-5 Dimethyl aniline and 2-6 Dimethyl aniline are shown in fig.1 and 2 respectively. Since the molecules do not possess any rotational, reflection or inversion symmetry, all the molecules are considered under  $C_s$  point group symmetry, which divide the entire modes of vibrations into two category : planar  $a'$  and non – planar  $a''$ . The 54 fundamental vibrations are possible in each compound as they have same symmetry and number of atoms. These modes can be, in terms of irreducible form representation, distributed as

$$\tilde{\nu}_{\text{vib}} = 38 a' + 16 a''$$

$$\tilde{\nu}_{\text{vib}} = 38 a' + 16 a''$$

All vibrations are active both in IR and Raman.

## RESULTS AND DISCUSSION

The observed frequencies from IR and Raman spectra, calculated frequencies by HF/6-31G(d) using GAUSSION 03 program and with the assignments, relative intensities IR and Raman activities for the titled molecules are observed. The optimized bond lengths and bond angles are used for the calculation of vibrational frequencies at the HF levels for the molecule 2-5 Dimethyl aniline is shown in Table.1. The same have been given in Table.2 respectively for the molecule 2-6 Dimethyl aniline. The FTIR and FT Raman experimental and stimulated spectra of these compounds are given fig.3 and 4 respectively. The SCF converges to total energy about -363.804468339 hartrees and the rotational constants values are 3.05115, 1.30337 and 0.92456 for the molecule 2-5 Dimethyl aniline. In 2-6 Dimethyl aniline the same SCF converges to total energy about -363.802802853 hartrees and the rotational constants values are 2.29046, 1.75911 and 1.00834. GAUSSVIEW program is very helpful for visual interpretation of vibrational frequencies assignments with normal mode of vibration.

**Aromatic C-H & C-C vibrations:** For simplicity, modes of vibrations of aromatic compounds are considered as separate C-H or ring C-C vibrations. In infrared spectra, most mono nuclear and poly nuclear aromatic compounds have three or four peaks in the region 3000 – 3100  $\text{cm}^{-1}$  (Lee C. Yang W and Parr R.G et al 1988) due to the stretching vibrations of the ring C-H bonds. In present study three bands are observed at 3055, 3010 & 3003  $\text{cm}^{-1}$  in 2-5 Dimethyl aniline compound and 3040, 3020 & 3010  $\text{cm}^{-1}$  in 2-6 Dimethyl aniline. All the bands are within the range. But these vibrations are appeared in the lower range 3055-3000  $\text{cm}^{-1}$  due to the influence of substituents. The upper bands of the compounds are deviated more with the other two, due to the presence of ortho and meta methyl groups. Ring C-C stretching vibrations occur in the region 1600 – 1400  $\text{cm}^{-1}$  (Gunasekaran et al, 2007). The decreasing number of strong C-H stretching bands with increasing mass of the substituents clearly indicates the impact of the mass on vibrations.

Five bands are observed at 1630, 1590, 1516, 1480 & 1420  $\text{cm}^{-1}$  of 2-5 Dimethyl aniline, but six bands observed at 1620, 1605, 1491, 1485, 1465 & 1435  $\text{cm}^{-1}$  in 2-6 Dimethyl aniline for C-C stretching. When compared to the literature range cited above, there is a considerable increase in magnitude of the frequencies and the number of bands is also different between the compounds. This is due to the interaction of N-H bending vibrations whose values also lie between the above ranges. This effect had already been observed in the early work. (Periandy. S and Mohan et al, 1998).

**Alkane functional group vibrations:** The C-H vibration frequencies of methyl and methylene groups fall in narrow ranges of saturated hydrocarbons. However, atoms directly attached to - $\text{CH}_3$ - and - $\text{CH}_2$ - may result in relatively large shifts in the absorption frequencies. In general, the effect of electronegative groups or atoms is to increase the C-H absorption frequency.

For aliphatic hydrocarbons, with the exception of small ring compounds, the C-H stretching vibrations occur in the region 2975–2840  $\text{cm}^{-1}$  (Katrizky A R, et al, 1959). In the present work, the bands at 2960, 2925, 2920, 2910, 2880 & 2865  $\text{cm}^{-1}$  in 2-5 Dimethyl aniline and bands at 2965, 2950, 2910, 2908, 2866 & 2848  $\text{cm}^{-1}$  in 2-6 Dimethyl aniline have been observed to be due C-H stretching. It also shows four asymmetrical vibrations and two symmetric vibrations in 2-5 Dimethyl aniline. The same trend in 2-6 Dimethyl aniline. The bands are observed within range. This shows that these bands are not much affected by their positions of alkene group.

**Aromatic & Alkane C-H deformation vibrations:** In Raman and Infrared spectra, the bands due to the C-H in-plane deformation vibrations, which occur in the region 1350–900  $\text{cm}^{-1}$  (Whiffen et al, 1955) are very useful for characterisation purposes and may be very strong indeed. Generally, a very strong band in the Raman spectra of mono, di and tri

**Table 1:** Observed and HF/6-31G (d) level calculated vibrational frequencies of 2-5 Dimethyl.

Symmetry Species	Experimental Frequency		Calculated Frequency		IR	Raman Intensity	Assignments Activity
	IR	Raman	Unscaled	Scaled			
A'	3483		3885	3492	10.8577	55.1423	$\tilde{a}$ (N-H)
A'	3390		3788	3405	11.7416	115.5353	$\tilde{a}$ (N-H)
A'	3055		3396	3053	31.2870	142.1714	$\tilde{a}$ (C-H)
A'		3010	3346	3008	17.0571	65.3565	$\tilde{a}$ (C-H)
A'	3003		3330	2993	29.4048	72.6239	$\tilde{a}$ (C-H)
A'	2960		3281	2949	24.9964	57.8599	$\tilde{a}$ (C-H)
A'	2925		3280	2948	24.7160	63.9686	$\tilde{a}$ (C-H)
A'		2920	3252	2923	33.9384	95.7642	$\tilde{a}$ (C-H)
A'	2910		3236	2909	33.9542	89.6215	$\tilde{a}$ (C-H)
A'	2880		3201	2877	41.7829	162.6564	$\tilde{a}$ (C-H)
A'		2865	3180	2858	56.0208	147.9182	$\tilde{a}$ (C-H)
A'	1660		1848	1661	110.3852	18.0541	$\hat{a}$ (N-H)
A'		1630	1821	1637	19.4355	23.9862	$\tilde{a}$ (C-C)
A'	1590	1590	1776	1596	27.7158	14.3641	$\tilde{a}$ (C-C)
A'	1516		1691	1520	45.0557	1.3775	$\tilde{a}$ (C-C)
A'		1480	1651	1484	16.9099	7.4697	$\tilde{a}$ (C-C)
A'			1638	1472	7.7549	17.7068	$\tilde{a}$ (C-C)
A'	1465		1633	1468	9.5625	9.1187	$\hat{a}$ (CH <sub>3</sub> ) wag
A'	1450		1632	1467	0.1109	31.9974	$\hat{a}$ (CH <sub>3</sub> ) wag
A'	1420		1586	1425	22.7920	0.8683	$\tilde{a}$ (C-C)
A'		1395	1567	1408	0.1842	28.8039	$\hat{a}$ (N-H)
A'	1390		1562	1404	1.3583	1.5793	$\hat{a}$ (C-H)
A'	1305		1450	1303	3.9553	1.2742	$\hat{a}$ (C-H)
A'	1275		1410	1267	28.9799	12.1370	$\tilde{a}$ (C-N)
A'	1216	1200	1351	1214	5.8759	2.0616	$\hat{a}$ (C-C)
A'	1175		1328	1193	11.0573	2.0723	$\hat{a}$ (C-H)
A'	1150		1276	1147	5.3216	3.7116	$\hat{a}$ (C-H)
A'	1120		1254	1127	4.4997	3.0080	$\hat{a}$ (C-C)
A''	1045		1171	1052	3.5153	0.8554	$\ddot{o}$ (C-H)
A''		1040	1167	1049	1.1020	1.5663	$\ddot{o}$ (C-H)
A'	1045		1166	1048	7.8010	1.1309	$\hat{a}$ (C-H)
A'	1015		1124	1010	5.6755	4.6528	$\hat{a}$ (C-H)
A'	985		1091	980	9.5492	0.5045	$\hat{a}$ (C-H)
A''	945		1063	955	0.7628	1.7431	$\ddot{o}$ (C-H)
A'		925	1022	918	2.6074	8.3106	$\hat{a}$ (C-H)
A''	877		969	871	25.9543	3.7757	$\ddot{o}$ (C-H)

A''	800		905	813	41.6923	0.6003	ö (C-H)
A'		732	818	735	37.0102	19.0485	â (N-H)
A''		728	810	728	43.6343	6.9800	ö (C-H)
A''	703		777	698	6.2523	1.4663	ö (C-H)
A''		670	747	671	204.3443	5.5382	ö (C-H)
A''		570	639	574	28.7132	1.9731	ö (N-H)
A'	535		609	547	11.3610	6.0656	â (CCC)
A'	480		526	472	0.1706	5.0383	â (CCC)
A''	446		496	445	10.6788	0.1008	ö (C-H)
A'	425		476	427	0.1674	4.4214	â (CCC)
A''		320	356	320	5.6669	2.8011	ö (C-H)
A'		295	335	301	3.5265	0.5148	â (CCC)
A'			307	275	0.3751	0.5011	â (CCC)
A''		240	266	239	28.9939	1.7621	ö (CCC)
A''			235	211	5.1009	1.1262	ö (CCC)
A''		155	189	169	3.0028	1.0122	ö (CCC)
A''		140	146	131	1.2464	0.3793	ö (CCC)
A''			31	27	0.1132	0.1751	ö (CCC)

**Table 2:** Observed and HF/6-31G (D) level calculated vibrational frequencies of 26 Dimethyl aniline.

Symmetry Species	Experimental Frequency		Calculated Frequency		IR	Raman Intensity	Assignments Activity
	IR	Raman	Unscaled	Scaled			
A'	3493		3902	3507	13.1406	45.3579	ã (N-H)
A'	3393		3807	3422	11.4673	100.4144	ã (N-H)
A'		3040	3380	3038	35.7693	188.0012	ã (C-H)
A'	3020		3356	3017	39.6256	71.4525	ã (C-H)
A'		3010	3348	3009	0.7704	69.8726	ã (C-H)
A'		2965	3284	2952	22.1909	64.0195	ã (C-H)
A'	2950		3283	2951	24.2514	51.0046	ã (C-H)
A'	2910		3235	2908	64.5017	124.0167	ã (C-H)
A'		2908	3234	2907	5.2070	40.9440	ã (C-H)
A'		2866	3182	2860	50.9547	252.6745	ã (C-H)
A'	2848		3181	2859	45.9801	25.1707	ã (C-H)
A'	1676		1855	1667	93.5646	11.9793	â (N-H)
A'	1620		1803	1620	0.3393	10.2181	â (C-C)
A'		1605	1798	1616	4.3770	22.2501	â (C-C)

J. Curr. Sci.

A'		1491	1660	1492	15.0891	4.3149	$\tilde{a}(C-C)$
A'	1485		1659	1491	35.2376	13.3399	$\tilde{a}(C-C)$
A'	1465		1637	1471	0.4033	3.1082	$\tilde{a}(C-C)$
A'		1456	1635	1469	0.0749	36.9776	$\hat{a}(CH_2)_{wag}$
A'	1450		1634	1468	11.1039	0.8563	$\hat{a}(CH_2)_{wag}$
A'	1435		1606	1443	50.6358	3.9691	$\tilde{a}(C-C)$
A'	1395		1567	1408	0.4728	14.4037	$\hat{a}(C-H)$
A'		1383	1566	1407	0.3023	10.4147	$\hat{a}(N-H)$
A'	1275		1429	1284	0.0512	0.2011	$\hat{a}(C-H)$
A'	1240		1397	1255	25.0655	14.2764	$\tilde{a}(C-N)$
A'	1215		1349	1212	3.9172	2.6580	$\hat{a}(CCC)$
A'	1199		1342	1206	6.6302	2.9315	$\hat{a}(C-H)$
A'	1140		1273	1144	0.2127	6.9169	$\hat{a}(C-H)$
A'	1110		1243	1117	5.8299	5.0197	$\hat{a}(CCC)$
A''	1090		1210	1087	13.0928	6.8166	$\ddot{o}(C-H)$
A''	1070		1169	1050	0.1958	1.2643	$\ddot{o}(C-H)$
A'		1045	1163	1045	0.5344	1.3038	$\hat{a}(C-H)$
A'		990	1099	988	2.1208	10.3453	$\hat{a}(C-H)$
A'	980		1089	979	13.7869	0.0805	$\hat{a}(C-H)$
A''	967		1083	973	0.7848	0.0255	$\ddot{o}(C-H)$
A'		900	1023	919	0.0918	2.5390	$\hat{a}(C-H)$
A''	855		969	871	0.9366	0.4550	$\ddot{o}(C-H)$
A''	795		907	815	9.6742	1.8323	$\ddot{o}(C-H)$
A'		769	863	775	40.2129	0.9523	$\hat{a}(N-H)$
A''	740		826	742	69.3465	0.4268	$\ddot{o}(C-H)$
A''		675	739	664	162.4751	14.7392	$\ddot{o}(C-H)$
A''	627		716	643	70.5358	17.1447	$\ddot{o}(C-H)$
A''	540		598	537	23.7734	0.7592	$\ddot{o}(N-H)$
A'		525	589	529	2.3842	5.4272	$\hat{a}(CCC)$
A'	490		555	498	0.0162	0.1622	$\hat{a}(CCC)$
A''		470	527	473	2.0708	6.7295	$\ddot{o}(C-H)$
A'	445		513	461	0.0223	0.0876	$\hat{a}(CCC)$
A''			378	339	5.0791	0.0706	$\ddot{o}(C-H)$
A'		290	320	287	1.0236	0.8540	$\hat{a}(CCC)$
A'			309	277	10.4218	1.9580	$\hat{a}(CCC)$
A''		240	289	259	12.3409	0.5888	$\ddot{o}(CCC)$
A''			227	204	7.6753	3.1153	$\ddot{o}(CCC)$
A''		195	212	190	1.2293	0.0966	$\ddot{o}(CCC)$
A''		145	180	161	11.4102	1.8549	$\ddot{o}(CCC)$
A''			141	126	0.5016	0.0310	$\ddot{o}(CCC)$

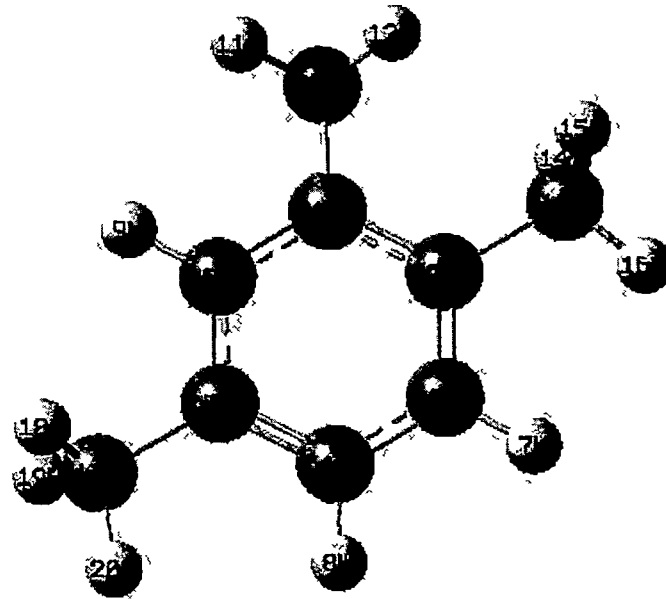


Fig.1: Structure Of 2-5 Dimethyl Aniline

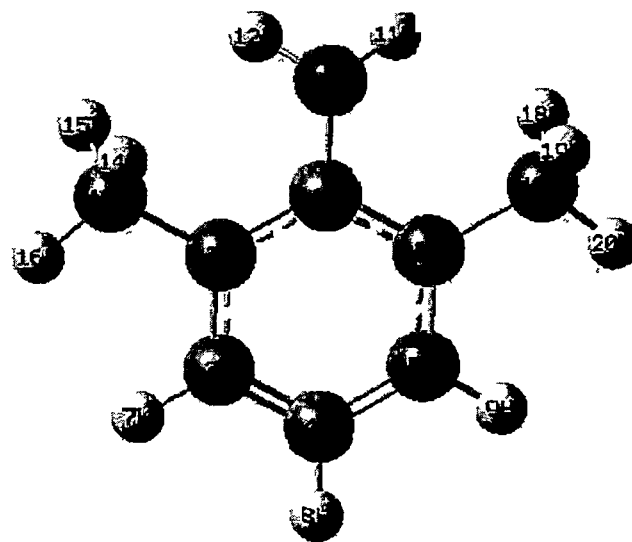


Fig.2: Structure Of 2-6 Dimethyl Aniline

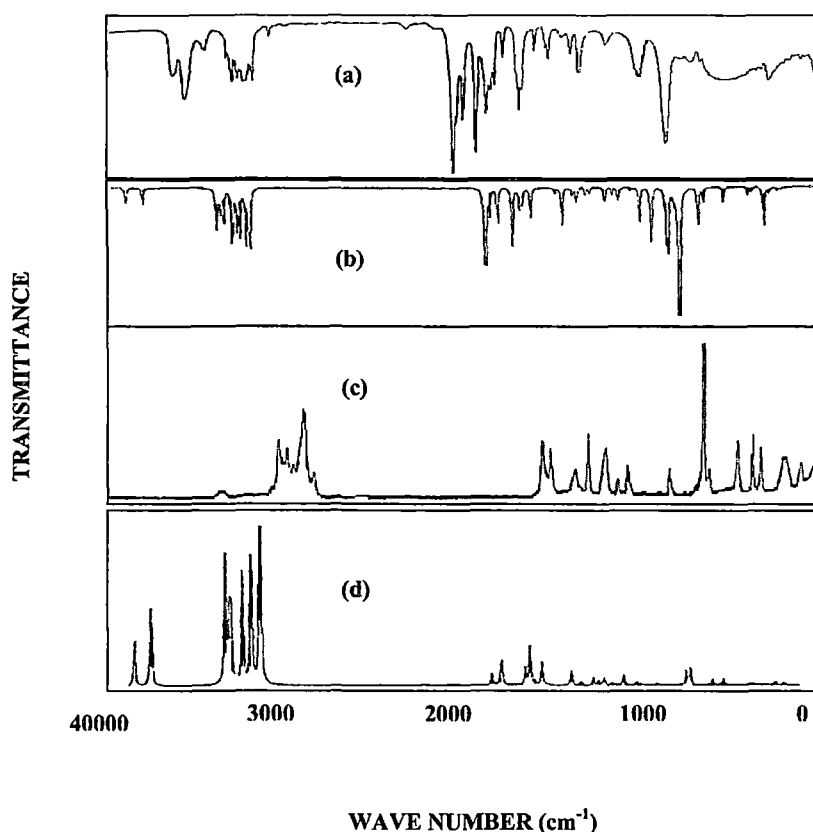
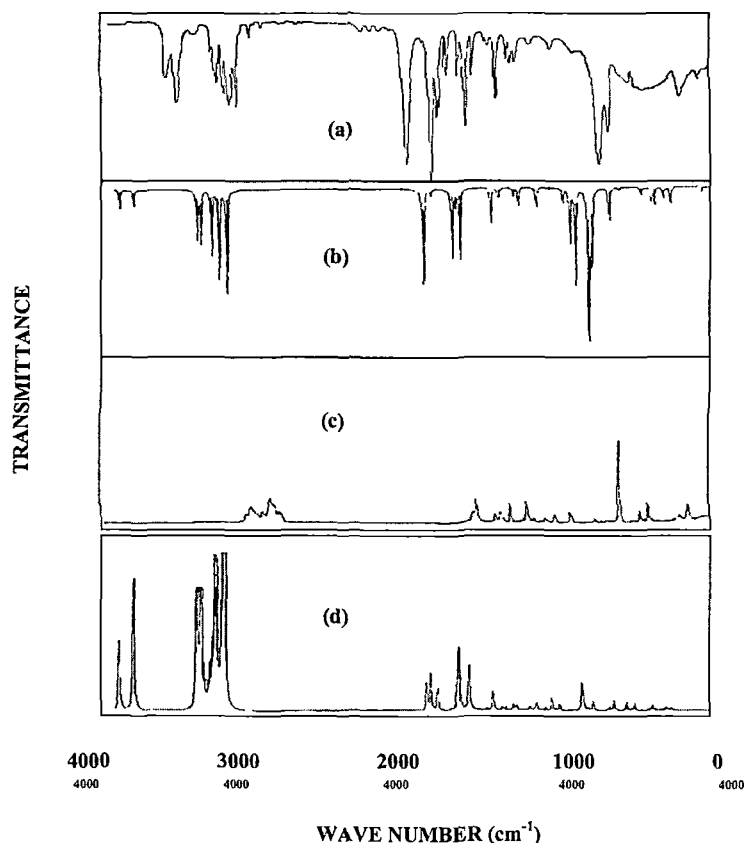


Fig. 3: Ftir and framan spectrum of 2-5 dimethyl aniline (a) experimental (b) stimulated (c) experimental (d) stimulated

substituted benzenes is observed near  $1000\text{ cm}^{-1}$  which may be the strongest band in the spectrum. Although these bands are usually sharp, they are weak to medium intensity. These bands are not normally of importance for interpretation purposes although they can be used. Besides a number of interactions are also possible which needs a careful interpretation of these bands. Polar ring substituents may result in an increase in intensity of these bands. Additional difficulties may also arise due to the presence of other bands in this region such as C-C & N-H stretching vibrations (Arduykova T F, 1973).

In the present work, the bands are observed at  $1395, 1390, 1305, 1175, 1150, 1045, 1015, 985$  &  $945\text{ cm}^{-1}$  in 2-5 Dimethylaniline and  $1395, 1384, 1275, 1140, 1045$  &  $985\text{ cm}^{-1}$  in 2-6 Dimethyl aniline due to C-H in-plane deformation. Even though the required number of in plane and out of plane deformation bands have been observed but the frequencies are pushed



**Fig. 4:** FTIR and Ftraman Spectrum of 2,6-Dimethyl Aniline (a) Experimental (b) Stimulated (c) Experimental (d) Stimulated

beyond the range mentioned above on upper side. This clearly indicates the substitutional effect of the aniline and the position of methyl group. This observation is also in agreement with other halogen substituted early works (Abdulla. Y, et al, 1990).

The frequencies of the C-H out of plane deformation vibrations are mainly determined by the number of hydrogen atoms on the ring and position of the substitution and not much affected by the nature of substituents (McKean D C, et al, 1973), although strongly electron attracting groups such as nitro, can result in an increase of about  $30\text{ cm}^{-1}$  in the frequency of vibration. In the present work, this trend has been observed but in 2-5 Dimethyl aniline. In 2-5 Dimethyl aniline nine C-H out of plane deformation bands have been observed and the same number of bands present in 2-6 Dimethyl aniline. All bands are weak due to presence of alkene stretching and N- H deformation in this range.

**N-H vibrations:** As solids and liquids in which hydrogen bonding may occur, primary aliphatic amines absorb in the region  $3450 - 3160 \text{ cm}^{-1}$  with a broad band of medium intensity, whereas in aromatic cases, one band occurs at  $3520 - 3420 \text{ cm}^{-1}$  and other at  $3420 - 3340 \text{ cm}^{-1}$  with medium or strong intensity. Secondary amines show only one band at  $3500 - 3300 \text{ cm}^{-1}$  (Varsanyi G, book vol.1 1974). The N-H in plane deformation bands occur at  $1650 - 1600 \text{ cm}^{-1}$  with weak intensity (Bellamy L.J, book 1959). This observation made by the early workers has also been found in the present case. Two N-H stretching frequencies are observed at  $3483$  and  $3390 \text{ cm}^{-1}$  in 2-5- Dimethyl aniline and at  $3493$  and  $3393 \text{ cm}^{-1}$  in 2-6 Dimethyl aniline, with strong and medium intensity in both the cases. The N-H in plane bending vibrations are found at  $1395 \text{ cm}^{-1}$  in 2-5 Dmethyl aniline and at  $1383 \text{ cm}^{-1}$  in 2-6 Dimethyl aniline but the intensity of bands are medium in both the molecules unlike in the literatures cited above. The C-N stretching vibrations are present at  $1275 \text{ cm}^{-1}$  and  $1240 \text{ cm}^{-1}$  both 2-5 and 2-6 Dimethyl aniline molecules, with strong intensity band. This is in agreement with the literatures (Durig J R, et al, 1989).

## CONCLUSION

Complete vibrational analysis of 2, 5 Dimethyl aniline and 2, 6 Dimethyl aniline were performed on the basis of HF/6-31G (d) level of theory. The roles of amino and methyl groups in the vibrational frequencies of the title compounds were discussed. The various modes of vibrations were unambiguously assigned on the results from normal coordinate analysis. The difference between the observed and scaled wave number values of most of the fundamentals is very small.

## REFERENCES

- Abdulla.Y, Obaid and Mamdouh S. Soliman. . Spectrochim acta, 46A, 1779, (1990).  
Ardyukova T F, Atlas of spectra of Aromatic and Hetrocyclic ompounds, Nauka Sib. Otd., Novosibirsk, (1973).  
Bellamy L.J, The infrared spectra of complex molecules ,John Wiley & Sons ,London ( 1959)  
Critchley.M, " Butter worths Medical dictionary" II edition, (1986).  
Durig J R, J Raman spectrosc., 20, 311 (1989)  
Gunusekeran .S, Seshadri.S, Muthu.S, Spectrochim acta, part A , (2007).  
Katrizky A R, J. Chem. Soc., (1959) 2058  
McKean D C, Spectrochim Acta 29A (1973) 1037  
Lee C. Yang W and Parr R.G Phys rev .B 37(1988)785  
Periandy. S and Mohan. S. Proc. Nat. Acad. Sci. India, 68(A), IV, (1998)  
Sing.R.B, Rai.D.R, Indian J. Pure and Appl.Phys. 20, 596, (1982).  
Varsanyi G, Assignments for vibrational spectra of Benzene Derivatives, Vol.1 1974  
Wiffen D H, Spectrochim Acta 7 (1955) 253.

## CHAPTER – V

### QUANTUM MECHANICAL AND FTIR & FTRAMAN SPECTRAL ANALYSIS OF 1-AMNIO-4-BROMONAPHTHALENE

#### INTRODUCTION

1-amnio-4-bromonaphthalene is also called as 4-bromo-1-naphthylamine. It is used to make azo dyes. It is a known human carcinogen and has largely been replaced by less toxic compounds. It is considered to be very important molecule because of method of preparations, pharmaceutical compositions and methods of disease treatment etc. The compounds also are used as novel therapeutic agents for the treatment of cancer, diabetes, metabolic diseases and skin disorders in mammalian subjects. These compounds are also useful as modulators of gene expression. Their activities are exerted by interfering with certain cellular signal transduction cascades, thus are also useful for regulating cell differentiation and cell cycle processes, controlled or regulated by various hormones or cytokines.

Vibrational analyses of molecules are very much essential in organic chemistry for the study and confirmation of functional groups, molecular structure, and reaction kinetics. Naphthalene sulfonic acids are used in the manufacture of naphthalene sulfonate polymer plasticizers which are used to produce concrete and plasterboard. They are also used as dispersants in

synthetic and natural rubbers, and as tanning agents in leather industries, agricultural formulations, dyes and as a dispersant in lead–acid battery plates. The naphthalene and its derivatives are the most important class of organic compounds containing two condensed rings. Hence, a few works [1–16] have been reported on these molecules.

However, no vibrational study based on B3LYP has been reported on 1–amino–4–bromonaphthalene (abbreviated as 1A4BNAP) in spite of its wide applications and importance. Hence, in this present work, a complete and detailed vibrational analysis has been carried out on 1–amino–4–bromonaphthalene with the help of both experimental and theoretical data.

## **RESULTS AND DISCUSSION**

### **Molecular geometry**

The most optimized geometries are performed by HF and B3LYP of 1A4BNAP molecule with atoms numbering are shown in Fig 5.1, and optimized bond lengths, bond angles and dihedral angles of title compounds, which are calculated by using HF and B3LYP methods with 6–311++G(d, p) basis set are shown in Table 5.1. In this present work, geometry optimization parameters for 1A4BNAP have been employed without symmetry constrain. From the theoretical values, we can find that most of the optimized bond

lengths are slightly larger than the experimental values, due to that the theoretical calculations belong to isolated molecules in gaseous phase and the experimental results belong to molecules in solid state.

Comparing bond angles and bond lengths of B3LYP with those of HF, as a whole the formers are bigger than later and the B3LYP calculated values correlate well compared with the experimental data. It is found that bond angles and dihedral angles calculated by B3LYP method are consistent with those by HF method, but the bond lengths calculated by HF method are a little shorter than those by B3LYP method. The C–Br bond length is relatively longer due to the electron–withdrawing effect depending on the presence of the carbonyl groups linked to these bonds.

The aromatic C–H bond distances of 1A4BNAP are found to have higher values in case of B3LYP/6–311++G(d, p) calculation with respect to HF/6–311++G (d, p). The same trend reflects in the amino group and bromine atom. The bond lengths C3–C4 and C4–C5 are longer than the experimental bond lengths. This shows the impact due to bromine atom. Most of the C–C calculated bond lengths by HF/6–311++G (d, p) are less deviation with experimental values. The C–C aromatic bond distances of the title compounds are found to have higher values in case of B3LYP calculation with respect to those of HF method. A similar trend has also been observed in case of the C–Br

bonds. Moreover, the calculated values of C–H bond lengths according to B3LYP and HF methods are also in good agreement.

The geometric parameters of B3LYP/6–311++G (d, p) are much closer to experimental values. Because of these reasons we take into account B3LYP/6–311++G(d, p) level for geometric parameter, while the introduction of the substituent group causes slight difference between them. The breakdown of hexagonal symmetry of the benzene ring is obvious from the negative deviation of C1–C2 (~1.3822Å), C3–C4 (~1.3714Å), C7–C10 (~1.3743Å) and C8–C9 (~1.3751Å) from the normal value of 1.390Å. The asymmetry of the naphthalene ring is also evident from the negative deviation of C2–C1–C6 (119.1°), C5–C7–C10 (118.6°) and positive deviation of C3–C4–C5 (121.2°), C6–C8–C9 (121.5°) from the normal value of 120°. The bond angles C2–C1–C6 and C4–C5–C6 are shorter by 0.9 and 1.9 Å from hexagonal angle.

The values of some thermodynamic parameters (such as zero-point vibrational energy, thermal energy, specific heat capacity, rotational constants, entropy, etc.) of 1A4BNAP are listed in Table 5.1. The variation in Zero Point Vibrational Energies (ZPVEs) seems to be significant. The ZPVE is much lower by the B3LYP method than by the HF method. The biggest value of ZPVE of 1A4BNAP is 102.25881 kJ/mol obtained with HF/6–311++G(d, p), whereas the smallest values is 96.31388 kJ/mol obtained with B3LYP/6–

311++G(d, p). The specific heat at constant volume, entropy and dipole moment are biggest values with B3LYP/6-311++G (d, p) method.

1A4BNAP molecule consists 20 atoms therefore it has got 54 normal modes of vibrations. The sixty normal modes of vibrations of 1A4BNAP are distributed by symmetry species as  $\Gamma_{3N-6} = 37A'$  (in-plane) +17A'' (out-of-plane). It is in agreement with  $C_s$  point group symmetry, all vibrations are active both in Raman scattering and infrared absorption. Here A' represents symmetric planer and A'' asymmetric non-planer vibrations. The detailed vibrational assignment of the experimental wavenumbers is based on normal mode analyses and a comparison with theoretically scaled wavenumbers by different DFT methods. Since the scaled wavenumbers by following B3LYP/6-311++G (d, p) method is found closest to experimental data than the results obtained using other methods.

The calculated wavenumbers are usually higher than the corresponding experimental quantities, due to the combination of electron correlation effects and basis set deficiencies. After applying, the different scaling factors, the theoretical wave numbers are good in agreement with experimental wave numbers. The observed (FTIR and FT-Raman) spectra of 1A4BNAP are shown in Fig 5.2. The observed and scaled theoretical frequencies using HF and DFT (B3LYP) methods with 6-311++G (d, p) basis sets and infrared

intensities and reduced mass of B3LYP/6-311++G(d, p) basis set and assignments are listed in Table 5.2.

### **C-H vibrations**

Since 1A4BNAP is a disubstituted naphthalene molecule, it has six C-H moieties. Hence it is expected to give six C-H stretching vibrations. In 2-naphthalenol C-H vibrations has appeared in the region 3085 – 3040  $\text{cm}^{-1}$  [17] and 3070 – 3030  $\text{cm}^{-1}$  in 2, 4-diisopropylnaphthalene [18]. In pure naphthalene, the same has occurred in the region 3080 – 3000  $\text{cm}^{-1}$ . In the present case, the C-H stretching vibrations are observed at 3070, 3050 and 3030  $\text{cm}^{-1}$  in IR and 3060, 3040 and 3025 in Raman  $\text{cm}^{-1}$ . These six vibrations are observed with very weak intensities and in the expected range. They are not appreciably affected by the nature of the substituents. All the computed bands for C-H vibrations by B3LYP/6-311++G(d, p) method shows excellent agreement with recorded spectrum as well as literature data

The bands due to C-H in-plane bending vibrations which interact with C-C stretching vibrations are to be observed in the region 1300 – 1000  $\text{cm}^{-1}$  and the C-H out-of-plane bending vibrations in the region 900 – 667 $\text{cm}^{-1}$  [19, 20]. In the present investigation, the bands are observed at 1201, 1125, 1025 and 995  $\text{cm}^{-1}$  in IR and 1115 and 1040  $\text{cm}^{-1}$  in Raman for C-H in-plane

bending. The C–H out-of-plane bending vibrations are observed at 955, 925, 850, 810, 790 and 760  $\text{cm}^{-1}$  in infrared spectrum.

### **C=C and C–C vibrations**

Generally the C=C stretching vibrations in benzene compounds lie in the region 1500 – 1650  $\text{cm}^{-1}$  [21]. In the present case, the bands are observed at 1640, 1625, 1575, 1520 and 1460  $\text{cm}^{-1}$  for C=C stretching modes. The values show that except the last one, all lie in the expected range which indicate that C=C skeletal modes is strongest and are not affected by the changes. In 1-bromo-4-fluronaphthalene the same bands are observed between the range 1667 – 1560  $\text{cm}^{-1}$  [22] which shows that the position and substitution slightly affects the range of C=C stretching.

The C–C stretching vibrations generally appear [21] in the range 1350 – 900  $\text{cm}^{-1}$  and interact with C–H in-plane bending vibrations. In this molecule, C–C stretching vibrations are observed at 1390, 1360 and 1250  $\text{cm}^{-1}$  in IR and at 1440 and 1340  $\text{cm}^{-1}$  in Raman. The range of these vibrations indicates that C–C modes are also not much influenced by the substitutions.

The in-plane bending CCC vibrations generally occur at higher frequencies than of out-of-plane bending [23]. In the present study, the bands are observed at 750, 580, 550, 525, 510 and 480  $\text{cm}^{-1}$  assigned to CCC in-

plane bending modes. The CCC out-of-plane bending modes of frequencies are attributed to 420, 295, 240 and 180  $\text{cm}^{-1}$ . The maximum numbers of bands are almost observed in Raman spectrum. The theoretically calculated CCC in-plane and out-of-plane bending vibrations have been found to be consistent with the recorded spectral values. The calculated values in ring vibrations are in good agreement with B3LYP/6-311++G(d, p) method.

### **N-H vibrations**

As solids and liquids in which hydrogen bonding may occur, primary aliphatic amines absorb in the region 3450 – 3160  $\text{cm}^{-1}$  with a broad band of medium intensity, whereas in aromatic cases, one band occurs at 3520 – 3420  $\text{cm}^{-1}$  and other at 3420 – 3340  $\text{cm}^{-1}$  with medium or strong intensity. Secondary amines show only one band at 3500 – 3300  $\text{cm}^{-1}$ . The N-H in-plane deformation bands occur at 1650 – 1580  $\text{cm}^{-1}$  in primary amines and at 1650 – 1580  $\text{cm}^{-1}$  in secondary amines with weak intensity. This observation made by the early workers [24–28] has also been found in the present case.

Two N-H stretching vibrations are observed at 3510 and 3420  $\text{cm}^{-1}$  in the present case, which is assigned to the N-H asymmetric and symmetric stretching modes respectively. This shows the aromatic nature of the naphthalene compounds. But, unlike in the literature, the N-H in-plane bending vibration in the present case is found at 1280  $\text{cm}^{-1}$  in Raman and 1115

$\text{cm}^{-1}$  in IR and the N–H out-of-plane bending vibrations are observed at 879 and  $725 \text{ cm}^{-1}$ . Both N–H out-of-plane bending vibrations are observed in IR region.

### **NH<sub>2</sub> scissoring vibrations**

The characteristic frequency of the NH<sub>2</sub> scissoring is usually located in the region  $1650 - 1600 \text{ cm}^{-1}$  [29]. On this basis, the NH<sub>2</sub> scissoring mode is assigned at  $1620 \text{ cm}^{-1}$  in this compound which is in line with Carmona et al [30]. The rocking and wagging vibrations are observed at  $1160 \text{ cm}^{-1}$  in IR and  $640 \text{ cm}^{-1}$  in Raman. But the twisting and torsion vibrations are observed at  $330$  and  $109 \text{ cm}^{-1}$  in Raman. All these vibrations are weak except scissoring mode. The above ranges of vibrations are not deviated much due to the presence of double ring.

### **C–Br vibrations**

The vibrations due to C–Br bond are delicate as mixing of vibrations are possible due to the presence of heavy atoms [31]. Usually, strong absorption peaks observed due to halogen substituted compound. But in this compound, the C–Br bond shows weak absorption when compared to N–H bond due to the decreased force constant and increased reduced mass. The C–Br stretching, in-plane bending and out-of-plane bending modes are observed at 630, 465 and

175  $\text{cm}^{-1}$  respectively in the present case. For all the three vibrations when compared with literature values [31], the frequencies are slightly greater than the literature which indicates that these vibrations are favoured by the amino group.

## CONCLUSION

A complete vibrational analysis of 1A4BNAP was carried out with the help of both experimental and theoretical data. The influences of bromine, amino group in the vibrational frequencies of the compound were discussed. All the C–H stretching vibrations are observed in IR region. The bands are within the expected range which shows that, these modes are not affected by the substitutions. The scaled vibrations are in good agreement with the experimental values. The observed and stimulated spectra are in agreement, showing a good frequency fit. The difference between theoretical and experimental wave numbers lies within 15  $\text{cm}^{-1}$  which supports the validity of the theory.

**REFERENCES**

- [1] E. Clar, Polycyclic Hydrocarbons Academic Press, London. 1964.
- [2] J. Baran, A. PawlukojÄ, I. Majerz, Z. Malarski, L. Sobczyk, E. Grech. Spectrochim Acta A 56(2000) 1801
- [3] A PawlukojÄ, I. Natkaniec, G. Bator, L. Sobczyk, E. Grech, J. Nowicka–Scheibe, Spectrochim Acta A 63(2006) 766
- [4] V. Balachandran and V.Krishnakumar, Spectrochim Acta A 61(2005)1811.
- [5] R.Mathammal, V.Krishnakumar and S.Muthunatesan, Spectrochim Acta A70 (2008) 210
- [6] D. Sajan, J. Binoy, B. Pradeep, K. Venkata Krishna, VB. Kartha, I. Hubert Joe, VS. Jayakumar, Spectrochim Acta A60 (2004)173
- [7] RJ. Xavier, V. Krishnakumar, Spectrochim Acta A 61(2005)1799
- [8] R.John Xavier, V.Krishnakumar, Spectrochim Acta A63( 2006) 454
- [9] N.Prabavathi, V.Krishnakumar, S.Muthunatesan, Spectrochim Acta A 70(2008) 991
- [10] R.Mathammal, S.Muthunatesan and V.Krishnakumar, Spectrochim Acta A 70 (2008) 201
- [11] Krishnakumar V, Prabavathi N, Muthunatesan S Spectrochim Acta A69 (2008) 528
- [12] M.Karabacak, D.Karagöz and M.Kurt, Spectrochim Acta A 72(2009)1076
- [13] G.Keresztury, V.K.Kumar and T.Sundius and R.J.Xavier, Spectrochim Acta A 61(2005)261.
- [14] V.Krishnakumar, N.Prabavathi and S.Muthunatesan, Spectrochim Acta A 69(2008)853
- [15] V.Balachandran and V.Krishnakumar, Spectrochim Acta A 63(2006)464

- [16] S.Muthunatesan, V.Krishnakumar and N.Prabavathi, *Spectrochim Acta A* 70 (2008) 991
- [17] Michal. H.Jamroz , Jan.Cz.Dobrowolski and Robert Brzozowski *J. Mol. Structure*, 787 (2006)
- [18] Jag Mohan, *Organic Spectroscopy—Principles and applications*, second ed., Narosa publishing House, New Delhi., 2001.
- [19] W.D.Bowman and T.G.Spiro, *J.Chem.Phys.*,73 (1980) 5482
- [20] G.Varasanyi, *Vibrational Spectra of Benzene Derivatives*, Academic Press, New York., 1969.
- [21] N.Prabavathi,S.Muthunatesan and V.Krishnakumar, *Spectrochim acta A* 70 (2008) 991
- [22] G. Socrates, *Infrared and Raman Characteristic Group Frequencies*, 3<sup>rd</sup> Ed., John Wiley & Sons, Ltd., Chichester., 2001.
- [23] V.Krishnakumarar, V.S.muthunatesan, GaborKeresztury and TomSundius,*Spectrochimica Acta Part A* 62 (2005) 1081
- [24] V.Balachandraen and V.Krishnakumar, *Spectrochim acta A*61 (2005)1811.
- [25] N. Puviarasan, V. Arjunan and S. Mohan, *J. Chem.* 28 (2004) 53. (40)
- [26] D.N. Singh, R. Shanker, R.A. Yadev and I.S. Singh, *J. Raman Spectrosc.* 27 (1996) 177.
- [27] R.K. Gupta, R. Prasad and H.L. Bhatnagar, *Indian J. Pure Appl. Phys.* 28 (1990) 533
- [28] L.J.Bellamy, *The infrared spectra of complex molecules*, John, wiley, Newyork 1959
- [29] P.Carmona, M.Molina and R.Escobar, *Spectrochimica Acta Part A*1 (1993) 49
- [30] M. Bakiler, I.V. Maslov and S. Akyiiz, *J. Mol. Struct.* 475 (1999) 83
- [31] V.Balachandraen, V.Krishnakumar and T.Chitambarathanu, *Spectrochim acta A*62 (2005) 918

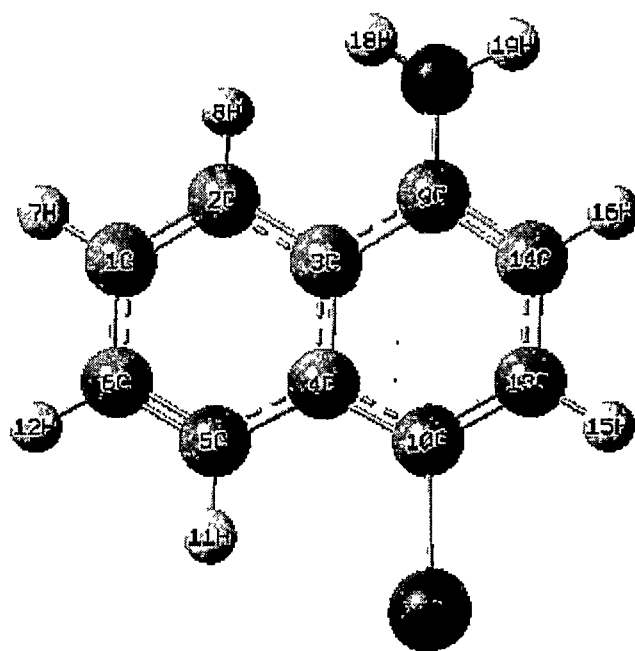


**Fig 5.1 Molecular structure of 1-amino-4-bromo naphthalene**

# 1-amnio-4-bromonaphthalene

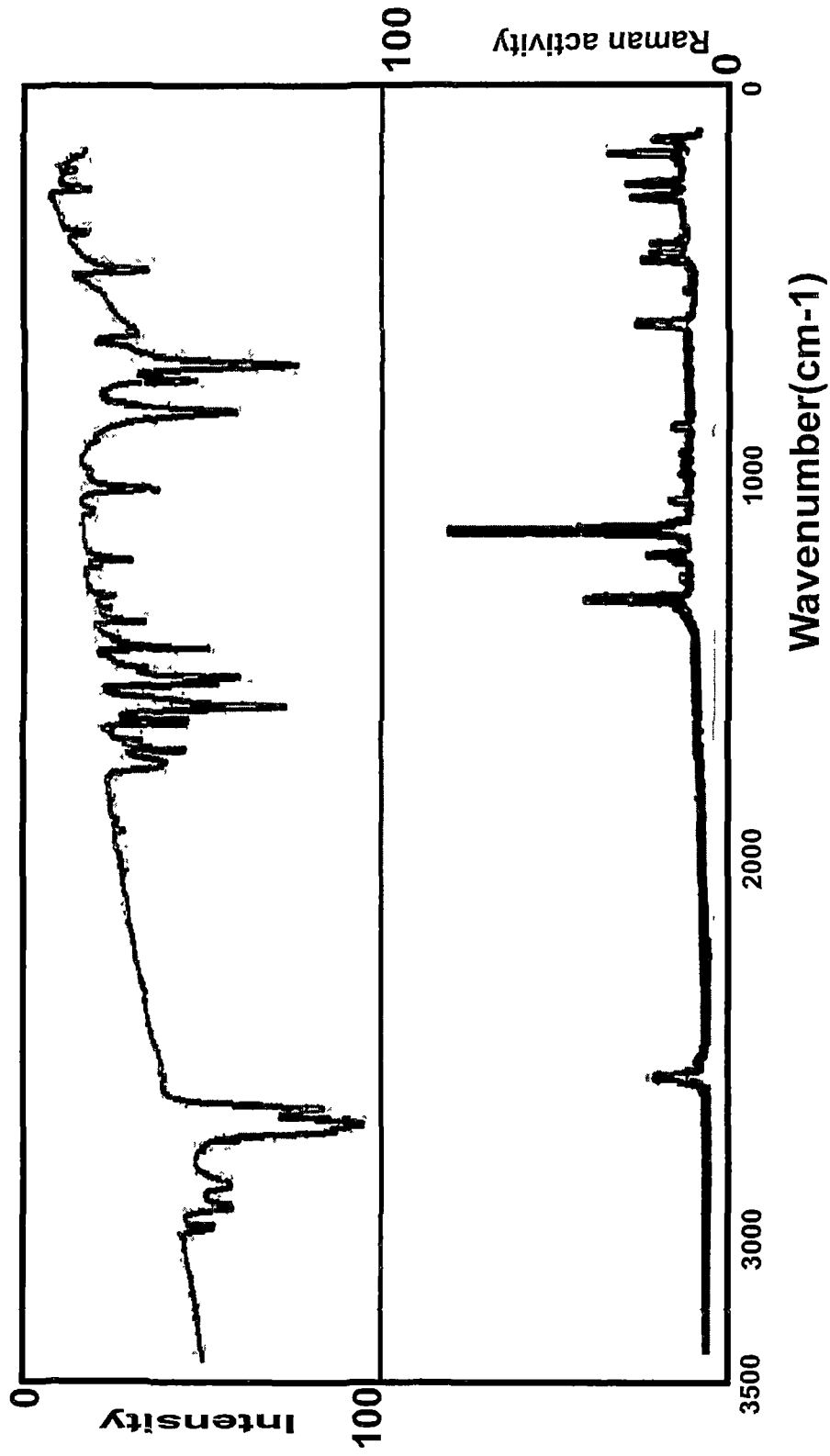


Figure 5.2: Experimental and Simulated IR and Raman spectra

**Table 5.1 Optimized parameters of 1-amnio-4-bromo naphthalene bond length (Å), bond angle (°) and dihedral angle (°)**

Bond length (Å)	HF/ 6-311++ G(d,p)	B3LYP/ 6-311++ G(d,p)	Expt	Bond angle (°)	HF/ 6-311++ G(d,p)	B3LYP/ 6-311++ G(d,p)	Expt	Dihedral angle (°)	HF/ 6-311++ G(d,p)	B3LYP/ 6-311++ G(d,p)
R(1,2)	1.3617	1.3822	1.365	A(2,1,6)	119.2	119.1	118.8	D(6,1,2,3)	-0.8	-0.9
R(1,6)	1.4335	1.4350	1.416	A(2,1,17)	121.2	120.7		D(6,1,2,14)	179.7	179.6
R(1,17)	1.3980	1.3963		A(6,1,17)	119.5	120.1		D(17,1,2,3)	-178.3	-178
R(2,3)	1.4105	1.4068	1.394	A(1,2,3)	121.1	121.3	121.6	D(17,1,2,14)	2.2	2.5
R(2,14)	1.0758	1.0851		A(1,2,14)	120.1	119.8	119.0	D(2,1,6,5)	2.3	2.2
R(3,4)	1.3526	1.3714	1.336	A(3,2,14)	118.8	118.9	119.9	D(2,1,6,8)	-177.2	-177.4
R(3,13)	1.0735	1.0824	0.930	A(2,3,4)	120.6	120.4	120.1	D(17,1,6,5)	179.8	179.4
R(4,5)	1.4259	1.4231	1.405	A(2,3,13)	119.1	119.4	119.9	D(17,1,6,8)	0.3	-0.2
R(4,20)	1.9070	1.9248		A(4,3,13)	120.3	120.2	119.9	D(2,1,17,18)	-137.2	-146.6
R(5,6)	1.4136	1.4374	1.422	A(3,4,5)	120.9	121.2	121.0	D(2,1,17,19)	-9.6	-14.3
R(5,7)	1.4194	1.4192	1.406	A(3,4,20)	118.1	118.0	119.5	D(6,1,17,18)	45.4	36.3
R(6,8)	1.4191	1.4186	1.413	A(5,4,20)	121.0	120.8	119.5	D(6,1,17,19)	173	168.6
R(7,10)	1.3591	1.3743	1.341	A(4,5,6)	118.2	118.1	119.0	D(1,2,3,4)	-1	-0.8
R(7,12)	1.0715	1.0818	0.930	A(4,5,7)	123.3	123.5	121.8	D(1,2,3,13)	178.5	-179.8
R(8,9)	1.3589	1.3751	1.360	A(6,5,7)	118.5	118.4	119.0	D(14,2,3,4)	-0.5	178.7
R(8,15)	1.0730	1.0833	0.930	A(1,6,5)	119.9	119.8	118.8	D(14,2,3,13)	1.3	-0.4
R(9,10)	1.4100	1.4098	1.386	A(1,6,8)	121.3	121.8	123.3	D(2,3,4,5)	-178.9	1.1
R(9,16)	1.0751	1.0840	0.930	A(5,6,8)	118.8	118.5	117.7	D(2,3,4,20)	-179.7	-178.9
R(10,11)	1.0753	1.0841	0.930	A(5,7,10)	121.1	121.4	121.2	D(13,3,4,5)	0.1	-179.8
R(17,18)	0.9964	1.0092		A(5,7,12)	119.1	118.6	119.4	D(13,3,4,20)	0.2	0.2
R(17,19)	0.9962	1.0097		A(10,7,12)	119.8	120.0	119.4	D(3,4,5,6)	179.6	0.2
				A(6,8,9)	121.3	121.5	120.6	D(3,4,5,7)	-179.6	179.7
				A(6,8,15)	119.5	119.6	119.7	D(20,4,5,6)	-0.2	-179.8
				A(9,8,15)	119.2	118.8	119.7	D(20,4,5,7)	-2	-0.2
				A(8,9,10)	119.8	119.9	121.0	D(4,5,6,1)	177.5	-1.9
				A(8,9,16)	120.2	120.0	119.5	D(4,5,6,8)	178.6	177.8
				A(10,9,16)	120.0	120.0	119.5	D(7,5,6,1)	-1.9	178.6
				A(7,10,9)	120.4	120.3	120.3	D(7,5,6,8)	-178.5	-1.8
				A(7,10,11)	119.8	119.8	119.8	D(4,5,7,10)	1.3	-178.8
				A(9,10,11)	119.8	119.9	119.8	D(4,5,7,12)	0.8	1
				A(1,17,18)	114.6	116.2	119.8	D(6,5,7,10)	-179.4	0.8
				A(1,17,19)	113.2	114.5	119.2	D(6,5,7,12)	-178.8	-179.5
				A(18,17,19)	110.2	111.5	119.2	D(1,6,8,9)	2.8	-178.8
								D(1,6,8,15)	1.7	2.9
								D(1,6,8,15)	-176.7	1.6
								D(5,6,8,9)	0.6	-176.7
								D(5,6,8,15)	179.9	0.6
								D(5,7,10,9)	-179.2	179.9
								D(5,7,10,11)	0.1	-179.2
								D(12,7,10,9)		



**Table 5.2 Detailed assignments of fundamental vibrations of 1-amnio-4-bromo-naphthalene based on the HF/6-311++G (d, p) and B3LYP/6-311++G (d, p)**

Species	Observed frequencies( $\text{cm}^{-1}$ )		Calculated frequencies HF/6-311++G(d,p) ( $\text{cm}^{-1}$ )		Calculated frequencies B3LYP/6-311++G (d, p) ( $\text{cm}^{-1}$ )			Assignments		
	IR	Raman	unscaled	scaled	IR intensity	unscaled	scaled		IR intensity	Reduced mass
A'	3510vw		3821	3465	16.08	3660	3506	16.78	1.09	$\nu$ NH
A'	3420m		3728	3380	12.85	3568	3418	16.96	1.04	$\nu$ NH
A'	3070vw		3408	3090	10.39	3206	3071	3.61	1.09	$\nu$ CH
A'		3060m	3403	3086	1.15	3198	3064	2.18	1.09	$\nu$ CH
A'	3050vw		3399	3082	6.66	3192	3058	18.46	1.09	$\nu$ CH
A'		3040vw	3393	3076	10.25	3179	3045	12.19	1.08	$\nu$ CH
A'	3030vw		3381	3066	8.86	3168	3035	0.9	1.08	$\nu$ CH
A'		3025vw	3377	3062	11.04	3162	3029	18.38	1.08	$\nu$ CH
A'	1640m		1785	1618	5.79	1668	1640	136.52	1.28	$\nu$ C=C
A'		1625vw	1754	1590	44.93	1656	1628	5.53	5.04	$\nu$ C=C
A'	1620m		1746	1583	0.4	1626	1598	22.39	4.18	NH <sub>2</sub> sciss
A'		1575m	1679	1522	5.87	1604	1577	6.89	6.46	$\nu$ C=C
A'	1520s		1654	1500	18.74	1547	1521	18.33	3.41	$\nu$ C=C
A'	1460vs		1569	1423	22.33	1485	1460	38.7	2.51	$\nu$ C=C
A'		1440vw	1548	1404	9.09	1467	1442	10.02	2.28	$\nu$ C-C
A'	1390s		1530	1387	52.58	1414	1390	54.25	2.12	$\nu$ C-C
A'	1360vs		1441	1307	8.47	1384	1360	49.83	4.73	$\nu$ C-C
A'		1340vw	1389	1259	20.93	1367	1344	6.08	4.68	$\nu$ C-C
A'	1280vs		1344	1219	12.77	1300	1278	46.94	2.32	$\nu$ C-N
A'	1250vw		1302	1181	1.85	1275	1253	13.67	1.79	$\nu$ C-C
A'	1201vw		1281	1161	13.32	1222	1201	4.42	1.66	$\beta$ C-H

A'	1170vw		1258	1141	14.58	1195	1175	0.08	1.31	$\beta$ NH
A'	1160vw		1215	1102	0.45	1183	1163	1.13	1.36	NH <sub>2</sub> rock
A'	1125w		1199	1087	3.08	1147	1128	11.06	1.82	$\beta$ NH
A'		1115vw	1132	1026	10.04	1137	1118	2.45	1.97	$\beta$ CH
A'		1040vw	1100	997	18.22	1058	1040	6.39	2.13	$\beta$ CH
A''	1025m		1089	987	0.25	1041	1023	16.37	2.84	$\beta$ CH
A''	995vw		1073	973	2.68	997	980	0.07	1.30	$\beta$ CH
A''	955s		1046	948	1.82	966	950	0.48	1.34	$\phi$ CH
A''	925vw		1036	939	1.52	932	916	0.66	1.34	$\phi$ CH
A''	910s		1003	909	53.42	926	910	30.56	5.33	$\phi$ NH
A''	850vw		958	869	1.18	867	852	1.5	1.57	$\phi$ CH
A''	810s		934	847	88.3	826	812	41.88	1.51	$\phi$ CH
A''	790vw		879	797	50.21	801	787	0.65	5.41	$\phi$ CH
A''	760m		860	780	2.96	780	767	41.36	1.97	$\phi$ CH
A'	750s		840	762	3.91	764	751	28.43	2.01	$\beta$ CCC
A''	710vw		835	757	83.73	727	715	3.38	4.73	$\phi$ NH
A''		640vw	758	687	3.22	653	642	40.57	2.70	NH <sub>2</sub> wagg
A'	630m		700	635	2.74	634	623	7.52	5.83	$\nu$ C-Br
A'	580vw		661	599	21	604	594	185.71	1.99	$\beta$ CCC
A'	550vw		645	585	1.98	577	567	65.39	2.22	$\beta$ CCC
A'		525vw	582	528	5.73	533	524	11.23	5.07	$\beta$ CCC
A'	510w		550	499	1.73	513	504	5.19	4.21	$\beta$ CCC
A'		480vw	524	475	0.52	486	478	2.17	6.47	$\beta$ CCC
A'	465w		515	467	0.29	471	463	0.92	3.43	$\beta$ C-Br
A''		420vw	484	439	9.05	424	417	15.61	2.99	$\phi$ CCC
A''		330vw	361	327	3.97	336	330	12.58	2.22	NH <sub>2</sub> twist
A''			347	315	3.32	319	314	2.21	3.91	$\phi$ CCC

A''		287	260	2.79	289	284	17.35	1.63	φ CCC
A''	295vw	242	219	6.93	268	263	0.52	6.31	φ CCC
A''	180vw	209	190	0.21	183	180	5.27	4.19	φ CCC
A''	175vw	168	152	2.21	173	170	0.24	8.64	φ C-Br
A''		109	99	0.18	124	122	0.69	3.57	NH <sub>2</sub> twist
A''		75	68	47.41	91	89	0.47	5.34	Butterfly

VS – very strong; s – strong; m- medium; w – weak; vw-very weak; HF/6-311++G(d,p) scale factor is 0.9050 and B3LYP/6-311++G(d, p) scale factor is 0.950 for the wavenumbers from 4000 to 1700 cm<sup>-1</sup> and 0.983 for wavenumbers below 1700 cm<sup>-1</sup>. γ-stretching, β-in-plane bending, φ-out-of-plane bending

## Scaled quantum ftir and ftraman spectral analysis of 1-amnio-4-bromo naphthalene

M. Govindarajan \*, K. Ganasan # ,S. Periandy @, and R. Madivanan &

\*Department of Physics, Avvaiyar Govt College for Women, Puducherry, Karaikal-609 605

#Department of Physics, T.B.M.L. College, Tamilnadu, Porayar-609 307

@Department of Physics, Tagore Arts College Women, Puducherry, 605 001

& Department of Physics, BGCW, Puducherry, 605 001

### ABSTRACT

---

In this work, the structural and vibrational property of the 1-Amnio-4-bromo naphthalene has been analysed. The fundamental vibrational frequencies and intensity of vibrational bands were evaluated using HF/6-31G (d) basis set and was scaled using various scale factors, which yielded a good agreement between observed and calculated frequencies. The vibrational spectra were interpreted with the aid of normal coordinate analysis. The results of the calculations were applied to simulated spectra of the title compound, which shows excellent agreement with observed spectra. The calculated force constants in vibrational internal coordinates are in closely coincides with the experimentally observed force constants.

---

### INTRODUCTION

Vibrational analysis of molecules are more deep study in organic chemistry, for the confirmation of functional groups, molecular structure and reaction kinetics. Naphthalene and its derivatives are the most important class of organic compounds containing two condensed rings (E. Clar, book 1964). 2-Methoxy naphthalene is used as an intermediate for the synthesis of non steroidal anti-inflammatory drugs. It is also used for soap perfumes and in the preparation of non-steroidal anti-inflammatory agents and bromination process. There are series of ladder-like compounds consisting of linearly fused benzene rings, their technological potential and their intrinsic value as models for more complex conjugated molecules (C. Reese, M. Roberts, M. Ling, and Z. Bao, et al Mater.Today). They have been the subjects of many theoretical and experimental investigations (H. Angliker, E. Rommel, and J. Wirz, et al 2004.). 1-Amnio-4-bromo naphthalene is an intermediate novel therapeutic agents for the treatment of cancer, diabetes, metabolic diseases and skin disorders in mammalian subjects. These compounds are also useful modulators of gene expression. The scaling factors are depending on both the method and basis sets and they are determined

from the mean deviation between the calculated and experimental frequencies (J.W. Finley, P.J. Stephens, J. Mol. Struct. et al 1995). The aim of this work is to study the vibrational analysis of 1-Amnio-4-bromo naphthalene by applying the Hartee-Fock method calculations, based on standard 6-31G(d) basis set. The calculated vibrational frequencies were compared with obtained experimental results. The simulated and the observed spectra were also analysed in detail.

**Experimental:** The compound under investigation namely 1-Amnio-4-bromo naphthalene was purchased from M/S Aldrich chemicals, U.S.A which is of spectroscopic grade and hence used for recording the spectra as such without any further purification. The FTIR spectrum of the compound was recorded in Bruker IFS 66V spectrometer in the range of 4000 to 400  $\text{cm}^{-1}$ . The spectral resolution is  $\pm 2 \text{ cm}^{-1}$ . The FT Raman spectra of the compound was also recorded in the same instrument with FRA 106 Raman module equipped with Nd: YAG laser source operating at 1.064  $\mu\text{m}$  line widths with 200 mW powers. The spectra were recorded with scanning speed of 30  $\text{cm}^{-1} \text{ min}^{-1}$  of spectral width 2 $\text{cm}^{-1}$ . The frequencies of all sharp bands are accurate to  $\pm 1 \text{ cm}^{-1}$ .

**Computational methods:** The quantum chemical calculations were performed for 1-Amnio-4-bromo naphthalene by applying Hartee-Fock (6-31G (d) basis set) method using the Gaussian 03 W program. Scaling of the force field was performed according to the SQM procedure using selective scaling in the natural internal coordinate representation (P. Pulay, G. Fogarasi, G. Pongor, J.E. Boggs, A. Vargha, et al 1983). The optimized bond lengths and bond angles were used for the calculation of vibrational frequencies at the HF levels. The SCF converges to total energy about -3007.68705011 hartrees and zero point energy 104.31402 (Kcal/Mol). The rotational constants values are 1.13994, 0.51154 and 0.35337. GAUSS VIEW program is very helpful for visual interptation of vibrational frequencies assignments with normal modes of vibration (A. Frisch, A.B. Nielson, A.J. Holder, GAUSSVIEW User Manual, Gaussian Inc., Pittsburgh, PA., 2000. 19).

## RESULTS AND DISCUSSION

**Molecular geometry:** The 1-Amnio-4-bromo naphthalene assumed as  $C_s$  point group of symmetry and the optimized geometrical parameters of the title compound are calculated according to labeling of atoms as shown in the fig.1. The most optimized bond lengths and bond angles of this compound were calculated using Gaussian 03 W program.

**Vibrational analysis and theoretical prediction of spectra:** The fifty four modes of vibrations of 1-Amnio-4-bromo naphthalene are distributed by symmetry species as  $\tilde{A}_{\text{vib}} = 35A'$  (in-plane) + 19 $A''$  (out-of-plane)

All vibrations are active both in FTIR and infrared absorption. The detailed vibrational assignments of fundamental modes of 1-amino-4-bromo naphthalene along with the calculated IR, Raman intensities and normal mode descriptions are reported in the Tables.1. The observed and simulated FTIR and FTIR spectra are presented in fig. 2 respectively. Root mean square (RMS) values of frequencies were obtained using the relation

$$n_{\text{RMS}} = \sqrt{\frac{1}{n-1} \sum_i^n (v_i^{\text{calcu}} - v_i^{\text{exp}})^2}$$

The RMS error of unscaled frequencies obtained for 1-amino-4-bromo naphthalene and found to be 194.005 cm<sup>-1</sup>. In order to reproduce the observed frequencies, the refinement through scaling factors was carried out and optimized RMS deviation was reduced to 9.354 cm<sup>-1</sup>

**C-H Vibrations:** In aromatic molecules like 2 naphthalenol C-H vibrations appear in the region 3085 -3040 cm<sup>-1</sup> and in 2-4 diisopropylnaphthalene in the region 3070 - 3030 cm<sup>-1</sup> (Michal. H.Jamroz , Jan.Cz.Dobrowolski, Robert Brzozowski et al 2006). In this compound the C-H stretch vibrations occur in the region 3080-3000 cm<sup>-1</sup>. There are six expected aromatic C-H stretch vibrations, but only five vibrations are observed at 3080, 3065 3050, 3025 and 3015 cm<sup>-1</sup> in IR region. All the vibrations are observed in IR region. Aromatic C-H stretch bands are within in the range shows that, they are not affected by the substitutions. The scaled vibrations are good in agreement with the experimentally reported values of naphthalene derivatives. Here also the above experimental values coincide with the scaled HF/6-31G (d) basis set values. The bands due to C H in-plane bending vibration interact some what with C-C stretching vibrations, are observed as number of bands in the region 1300–1000 cm<sup>-1</sup>( Keresztury .G book , 2002).The C H out-of-plane bending vibrations occur in the region 900–667 cm<sup>-1</sup> (W.D.Bowman, T.G.Spiro,. et al 1980 ).In the present investigation, the bands observed 1300, 1265,1205,1102,1170 cm<sup>-1</sup>and1080 cm<sup>-1</sup> are assigned to C-H in plane bending and C-H out of plane bending bands are assigned at 1012,980,965,879,775,472 and 325cm<sup>-1</sup> within characteristic region except two and is presented.

**C-C Vibrations:** Generally the C-C stretching vibrations in aromatic compounds form the band in the region of 1430-1650 cm<sup>-1</sup>(G.Varasanyi, Vibrational Spectra of Benzene Derivatives). In the present case investigation the bands are observed at 1620, 1595,1520,1455,1390 and 1325 cm<sup>-1</sup>. The last two bands lie below the expected range, this may be due to the substitution of heavy mass elements like Bromine and amino group in the present case. The in plane

**Table 1:** Observed and HF/6-31G (d) level calculated vibrational frequencies of 1-Amnio-4-Bromo Naphthalene.

Symmetry Species	Observed frequency		Calculated frequency		IR Intensity	Raman Activity	Assignments
	IR	Raman	Unscaled	Scaled			
A'	3465		3870	3479	12.1094	71.5608	v NH
A'	3389		3777	3396	14.7694	159.0240	v NH
A'	3080		3420	3075	4.4711	84.4521	v CH
A'	3065		3403	3059	18.7024	125.3469	v CH
A'	3050		3401	3058	6.4394	102.0524	v CH
A'			3380	3039	26.2671	153.5056	v CH
A'	3025		3364	3024	5.4599	79.4733	v CH
A'	3015		3359	3020	25.7299	104.5734	v CH
A'			1850	1663	115.1834	26.4468	v CH
A'			1832	1647	18.4085	2.2153	v CC
A'	1620		1797	1615	32.9159	3.3070	v CC
A'	1595		1775	1596	8.2474	125.0545	v CC
A'	1520		1684	1514	20.4736	9.4630	v CC
A'	1455		1623	1459	22.3533	7.5500	v CC
A'			1596	1435	13.9203	27.9846	$\beta$ CH
A'	1390	1390	1536	1381	34.1255	1.6998	v CC
A'			1485	1335	57.9495	188.8145	v CC
A'	1300		1456	1309	7.5678	103.4532	$\beta$ CH
A'	1265		1395	1254	14.6967	10.8585	$\beta$ CH
A'	1205		1361	1223	35.8804	1.2041	$\beta$ CH
A'	1182		1321	1187	0.9248	3.5349	$\beta$ CH
A'		1170	1295	1164	2.6434	8.6130	$\beta$ CH
A'			1277	1148	2.9790	10.2527	$\beta$ CH
A''	1115		1232	1107	2.0386	6.2828	$\beta$ NH
A'	1080		1194	1073	0.4951	4.3980	$\beta$ CH
A'	1035		1144	1028	7.8855	6.1874	v CCC
A''	1012		1131	1016	0.4212	1.9664	$\phi$ CH
A''	980		1096	985	2.4197	0.3287	$\phi$ CH
A'			1092	981	11.0428	8.3762	$\beta$ CCC
A''	965		1080	971	1.3263	5.4540	$\phi$ CH
A'	900		1003	901	48.0539	1.4694	$\beta$ CCC
A''	879		986	886	4.2173	0.4290	$\phi$ CH
A''			947	851	89.6777	3.8577	$\phi$ CH
A'			885	795	3.1605	3.6154	$\beta$ CCC
A''	775		867	779	46.8427	1.3338	$\phi$ CH
A'			855	768	13.7207	0.8911	$\beta$ CCC
A'	725		818	735	200.3889	10.6935	$\phi$ NH

A'	680	680	769	698	47.3391	12.0502	$\phi$ NH
A''			696	632	21.0668	1.2706	$\phi$ CH
A'			675	613	34.0075	2.9717	$\beta$ CCC
A''			660	599	7.8946	3.5765	$\phi$ CH
A'	510		572	519	3.9520	6.6006	$\nu$ CBr
A''	495	499	552	501	3.3156	6.7788	$\beta$ CCC
A''	472		523	475	1.9114	3.0730	$\phi$ CH
A''			517	469	0.8803	2.4707	$\phi$ CH
A''			466	423	12.1212	3.9107	$\phi$ CH
A''		325	373	339	6.1215	0.6514	$\phi$ CH
A''		295	346	314	8.3215	2.1591	$\phi$ CCC
A'			297	269	17.7837	7.6265	$\nu$ CBr
A''		240	282	256	24.0604	1.1948	$\phi$ CH
A''			201	182	5.5964	0.3645	$\phi$ CCC
A''		170	190	172	0.2974	2.4406	$\phi$ CCC
A''			146	132	0.2443	1.8236	$\phi$ CCC
A'			103	93	0.3996	3.5178	$\beta$ CBr

$\nu$  - Stretching    $\beta$  - in-plane bending    $\phi$  - out-of-plane bending

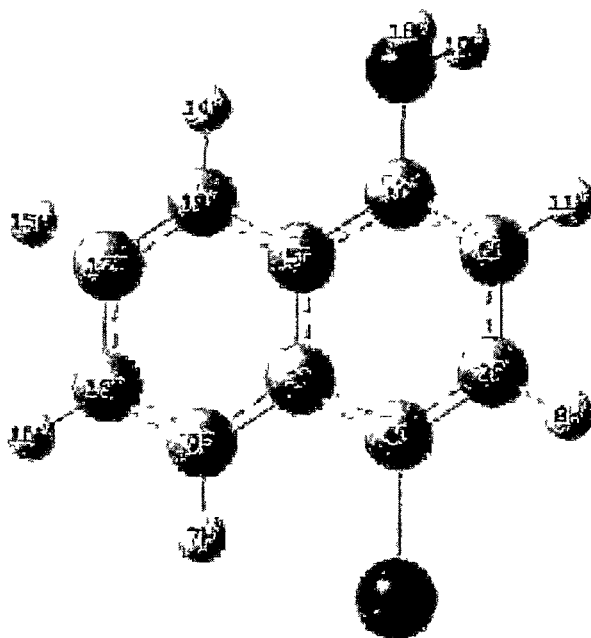


Fig.1: Structure of 1-AMINO-4-BROMO Naphthalene.

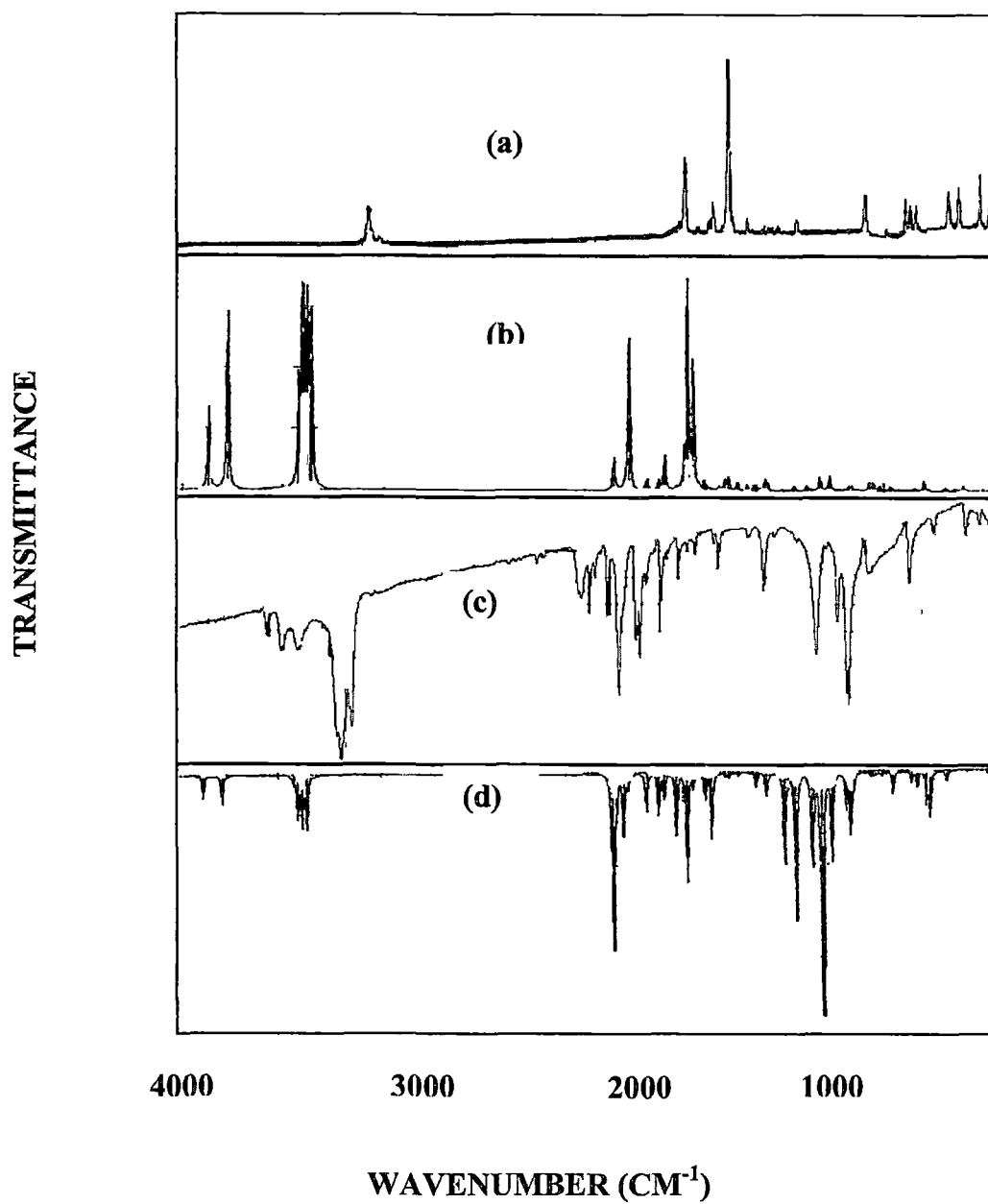


Fig.2: Ftraman (a) Observed (b) Calculated with HF/6-31G (d) 1-AMNIO-4-BROMO Napthalene FTIR  
(c) Observed (d) calculated with HF/6-31G (d) 1-AMNIO-4-BROMO Napthalene

bending C-C vibrations generally occur at higher frequencies than of out-of-plane bending (G. Socrates, *Infrared and Raman Characteristic Group Frequencies*, 3<sup>rd</sup> Ed., John Wiley & Sons, Ltd.). In the present study the bands observed at 900, 765 and 675  $\text{cm}^{-1}$  are assigned to C-C in plane bending modes. The out of plane bending modes of frequencies are attributed to 295, 240 and 170  $\text{cm}^{-1}$  in Raman. Most of the bands are missing in in-plane and out of plane bending due to heavy mass substitutions.

**N-H Vibrations:** N-H stretching vibrations are observed at 3500 – 3300  $\text{cm}^{-1}$ . (Socrates, G. 3<sup>rd</sup> Ed., John Wiley & Sons, Ltd., Chichester., 2001). The N-H in plane deformation bands occur at 1650 -1580  $\text{cm}^{-1}$  in with weak intensity. This observation made by the early workers (R.K. Gupta, R. Prasad, H.L. Bhatnagar, et al 1990), has also been found in the present case. With reference to this, two N-H stretching frequencies are observed at 3465 and 3389  $\text{cm}^{-1}$  in the infrared spectrum are assigned to the N-H asymmetric and symmetric stretching modes respectively. Other vibrations, the N-H in plane bending vibration is found at 1640  $\text{cm}^{-1}$  and the N-H out plane bending vibrations are observed at 725 and 680  $\text{cm}^{-1}$ . Both N-H in plane and out plane bending vibrations are observed in IR region. In N-H in plane bending one band is missing due to the presence of heavy polar bond in this compound.

**C-Br Vibrations:** The vibrations observed to the bond between the naphthalene ring and the Bromine atom are important as mixing of vibrations are possible due to the presence of heavy atoms (M. Bakiler, I.V. Maslov, S. Akyiiz, et al 1999). C-Br bond show lower absorption frequencies as compared to C-H bond due to the decreased force constant and increase in reduced mass. In this titled compound, the C-Br stretching and in plane bending modes are recorded at 510 and 260  $\text{cm}^{-1}$  respectively in IR and Raman. The above two vibrations are in agreement with literature values.

**Conclusion:** A complete vibrational analysis of 1-amino-4-bromo naphthalene was performed on the basis of Hartree Fock functional calculations at 6-31G (d) level. The influences of bromine, amino group in the vibrational frequencies of the title compound were discussed. The observed and simulated spectra are in agreement and show a good frequency fit. The difference between theoretical and experimental wave numbers within 15  $\text{cm}^{-1}$  shows that the assignments of the fundamentals are valid, by the qualitative agreement between the calculated and observed frequencies.

## REFERENCES

- Angliker, H., E. Rommel, and J. Wirz, *Chem. Phys. Lett.*, 7 (1982) 208.  
Bakiler, M., I.V. Maslov, S. Akyiiz, *J. Mol. Struct.* 475 (1999) 83  
Bowman, W.D., T.G. Spiro, *J. Chem. Phys.*, 73 (1980) 5482  
Clar, E., *Polycyclic Hydrocarbons* Academic Press, London., 1964.

**J. Curr. Sci.**

- Finley.J.W., Stephens.P.J , J. Mol. Struct. et al 1995  
Frisch.A, A.B. Nielson, A.J. Holder, GAUSSVIEW User Manual, Gaussian Inc., Pittsburgh, PA., 2000.  
Gupta.R.K, R. Prasad, H.L. Bhatnagar, Indian J. Pure Appl. Phys. 28 (1990)  
533. (42)  
Keresztury .G ,Raman spectroscopy :in : handbook of Vibrational spectroscopy Voll John Wiley & Sons Ltd  
2002.p.71  
Michal. H.Jamroz , Jan.Cz.Dobrowolski, Robert Brzozowski J. Mol. Structure., 787 (2006)  
Pulay.P, G. Fogarasi, G. Pongor, J.E. Boggs, A. Vargha, J. Am. Chem. Soc., 105 (1983) 7037.  
Reese.C, M. Roberts, M. Ling, and Z. Bao, Mater. Today., 20 (2004).  
Socrates.G, Infrared and Raman Characteristic Group Frequencies, 3<sup>rd</sup> Ed., John Wiley & Sons, Ltd., Chichester.,  
2001.  
Varasanyi.G, Vibrational Spectra of Benzene Derivatives, Academic Press, New York, 1969.
-

## CHAPTER-VI

### EXPERIMENTAL (FTIR and FT-RAMAN) AND DFT STUDIES OF 1-METHOXYNAPHTHALENE

#### INTRODUCTION

Naphthalene, which is more reactive than benzene, likes benzene in many of its reactions [1]. The naphthalene which have two six membered rings and its derivatives are of great interest in biological activity and widely used as a parent compound to make many drugs, a precursor for the synthesis of plastics and dyes, also used in dye stuffs, synthetic resins, coatings, tanning agent and celluloid [2]. 1-methoxynaphthalene also known as methy-1-naphtyl ether (abbreviated as MNAP). It is a raw material for the synthesis of some pharmaceuticals and present invention to simulate insulin and used as a therapeutic agent [3, 4].

The aromatic compounds naturally occur higher amount in plants, are used for governing the physiological functions. The vibrational analyses of this molecule would be helpful for understanding the various types of bonding and normal modes of vibration. In recent trends, the quantum chemical computational methods have proved to be an essential tool in analyzing the vibrational spectra [5-8]. Xavier et al [8] investigated the MNAP by using Wilson's F-G matrix method. The potential energy distribution (PED) has been evaluated using the vibrational spectral data and molecular parameters.

Because of spectroscopic properties and chemical significance, in particular, extensive recent studies on vibrational spectra of substituted naphthalene compounds have assigned [10–13] complete vibrational mode and frequency analyses. Krishnakumar et al [9] compared the vibrational spectrum of 2-hydroxy-3-methoxy-5-nitrobenzaldehyde with that of 2-methoxy-1-naphthalaldehyde. Naphthalene and its citations are investigated the infrared and Raman spectra of the condensed and liquid phase by Srivastava et al [10]. Nagabalasubramanian et al [14] studied the FTIR and FT-Raman vibrational spectra of 1, 5-methylnaphthalene molecule. Dimethylnaphthalenes in the gas phase is studied by Das et al. [15].

IR and Raman spectra of MNAP have been examined qualitatively as well as quantitatively. The entire scaled quantum mechanical method and density force fields calculations are performed by combining the experimental and theoretical aspects of Pulay and Rauhut [16]. Their training set and test set have been used to check the reliability of fitting. The overall scaling factors for theoretical harmonic frequencies have been verified with least-square fits [16, 17]. The assignments have also been supported by PED, which is part of the outcomes of the normal coordinate analyses.

Prediction of vibrational frequencies of polyatomic molecules by quantum mechanical method has become important because of its accurate and consistent with experimental data. In the present study, we extend the probing

into the application of DFT employing different types of functional and various basis sets have been evaluated. A close agreement between the observed and calculated wavenumber is achieved by introducing the scale factors. Of all these methods, B3LYP density functional technique with 6-311++G (d, p) has been found to give the most reliable description of vibrational assignments in the present analyses.

## RESULTS AND DISCUSSION

### Molecular geometry

The most optimized geometries by B3LYP of the MNAP with atom numbering are shown in Fig 6.1. By allowing the relaxation of all parameters, the calculations converge to optimized geometries, which correspond to true energy minima, as revealed by the lack of imaginary frequencies in the vibrational mode calculation. The global minimum energy obtained for structure optimization of MNAP with 6-31G, 6-31G (d, p) and 6-311++G(d, p) basis sets is approximately -500 a.u. During the vibrational studies of the title molecule the global lowest energy for B3LYP/3-21G is observed around the value 497 a.u. But the entropy value has been observed as same for all basis sets. All the above observations are made without any symmetric constrains. The total energy, zero point energy, rotational constants, specific heat capacity at constant volume and dipole moment by B3LYP with 3-21G, 6-31G and 6-31G (d, p) basic sets are listed in Table 6.1.

The most optimized bond lengths and bond angles of this compound are calculated by various basis sets listed in Table 6.2. These optimized parameters are slightly overestimated with crystallographic literature values. This overestimation can be explained that the theoretical calculations belong to isolated molecule in gaseous phase and the experimental results belong to similar molecule in solid state. C2–C6, C3–C7, C10–C9, C4–C8 and C5–C4 single– bond lengths are longer than the normal C–C single bond length of about 1.380 Å. As a result of experimental findings and our calculations on C6–C5, C1–C2, C7–C10 and C8–C9 bonds show typical double– bond characteristics. C1–C2 bond length is relatively longer due to the electron– withdrawing effect. Optimized C–H bond lengths are clearly shows that the C–H bonds nearer to the methoxy group C5–H12 and C15–H16 having maximum variation with others. This is undoubtedly due to the impact of methoxy group. It is also evident by the farthest bond C2–H13 with maximum optimized bond length.

The equilibrium structure for the ground state shows that the naphthalene ring is planar, and also the O, C and H atoms of methyl groups are lying approximately in the plane as evident from the torsional angles C1–O18–C19–H20 = 179.99° by using B3LYP/6– 311++G(d,p). The variation in Zero– Point Vibrational Energies (ZPVEs) seems to be significant. The ZPVE energy is much lower in the DFT/B3LYP/6–311++G(d, p) method than by other methods. The biggest value of ZPVE of MNAP is 114.195 kJ mol<sup>-1</sup> obtained at

B3LYP/6-31G whereas the smallest one is  $112.447 \text{ kJ mol}^{-1}$  obtained at BLYP/6-311++G(d, p).

The aromatic C-H bond distances of MNAP are found to have higher values in case of B3LYP/6-31G (d, p) calculation with respect to B3LYP/6-311++G (d, p), B3LYP/6-31G and B3LYP/3-21G computation. But methyl C-H bond distances longer than the aromatic C-H bond distances. An interesting fact that, among three methyl C-H bonds, one bond in the ring of the molecule is shorter than the other two non-planer C-H bonds by angle  $0.0065 \text{ \AA}$ . It also is proved by C19-C21 and C19-C22 bond lengths within all sets are almost equal. The C-O bond lengths are changes with carbon atom attached to the ring and methyl group. The methyl C-O bond length is found larger than the ring C-O bond length about  $0.06 \text{ \AA}$ .

Effective atomic charge calculations have an important role in the application of quantum chemical calculation to molecular system because of atomic charges effect dipole moment, molecular polarizability, electronic structure, acidity-basicity behaviour and more a lot of properties of molecular systems. Mulliken charge distributions were calculated by determining the electron population of each atom as defined by the basis sets. The calculated Mulliken charge values using various levels of theory and basis sets are listed in Table 6.3. The charge changes with basis set presumably occurs due to polarization. For example, the charge of O18 atom is  $-0.556 e^-$  for B3LYP/3-

21G,  $-0.562 e^-$  for B3LYP/6-31G,  $-0.521 e^-$  for B3LYP/6-31G(d, p),  $-0.153 e^-$  for B3LYP/6-311++G(d,p). Considering the all methods and basis sets used in the atomic charge calculation, O18 and C19 atoms exhibit a substantial negative charge, which are donor atom. C3 and C4 atoms exhibit a positive charge, which are acceptor atoms.

### Vibrational analysis

MNAP molecule consists 22 atoms; therefore it has 60 normal modes. The sixty normal modes of vibrations of MNAP are distributed by symmetry species as  $\Gamma_{3N-6} = 41A'$  (in-plane) +  $19A''$  (out-of-plane). It is in agreement with  $C_s$  point group symmetry, all the vibrations are active both in Raman scattering and infrared absorption. Here  $A'$  represents symmetric planer and  $A''$  asymmetric non planer vibrations. The detailed vibrational assignment of the experimental wavenumbers is based on normal mode analyses and a comparison with theoretically scaled wavenumbers by different DFT methods. Since the scaled wavenumbers by following B3LYP/6-311++G(d, p) method is found closer to experimental data than the results obtained using other methods, the PEDs from this set of data are discussed in detail.

The calculated wavenumbers are usually higher than the corresponding experimental quantities, due to the combination of electron correlation effects and basis set deficiencies. After applying, the different scaling factors, the theoretical wave numbers are good in agreement with experimental wave

numbers. The observed (FTIR and FT-Raman) and simulated (B3LYP/6-311++G (d, p)) spectra of MNAP are shown in Fig 6.2. The observed and scaled theoretical frequencies using B3LYP with 3-21G, 6-31G, 6-31G(d, p) and 6-311++G(d, p) basis sets, and PEDs of B3LYP/6-311++G(d, p) basis are listed in the Table 6.4.

### **C-H vibrations**

The substituted benzene like molecule gives rise to C-H stretching, C-H in-plane and C-H out-of-plane bending vibrations. In aromatic hydrocarbons, various C-H stretching absorption occurs in the region  $3050 - 3000 \text{ cm}^{-1}$  [18]. The title molecule (MNAP) has only one O-CH<sub>3</sub> substitution in the naphthalene; hence seven C-H stretching vibrations are expected on naphthalene. The frequencies have appeared within the region  $3085 - 3040 \text{ cm}^{-1}$  in 2-naphthalenol [19, 20] and  $3070 - 3030 \text{ cm}^{-1}$  in 2, 4-diisopropylnaphthalene [19, 21]. In pure naphthalene, the same has occurred in the region  $3080 - 3000 \text{ cm}^{-1}$ . In the present compound, the C-H stretching vibrations have been observed in the infrared spectra at  $3065$  and  $3005 \text{ cm}^{-1}$  with strong intensity. The remaining five bands are observed in Raman with very strong and weak intensities at  $3060$ ,  $3055$ ,  $3050$ ,  $3020$  and  $3010 \text{ cm}^{-1}$ . The upper range of frequency slightly deviated, which may be due to the presence of oxygen atom as the methyl group has altered the wavenumbers in MNAP.

The mean deviations between experimental and calculated scaled wavenumbers are nearly  $8.57 \text{ cm}^{-1}$ .

All bands are medium intensity and in the expected region, but two vibrations are missing in the region due to overtone combinations. The scaled theoretical wavenumbers due to C–H aromatic stretching are lie within the range  $3064 - 3016 \text{ cm}^{-1}$  by B3LYP/6-311++G(d, p). It shows the experimental wavenumbers very good agreement with calculated wavenumbers. In this region the bands are not appreciably affected by the nature of the substituents. The bands due to the C–H in–plane deformation vibrations, which occur in the region  $1390 - 990 \text{ cm}^{-1}$  are very useful for charecterisation and are very strong indeed [22] and the C–H out–of–plane bending vibrations have appeared within the region  $900 - 400 \text{ cm}^{-1}$  [23]. The vibrations are identified at 1325, 1160, 1075 and  $955 \text{ cm}^{-1}$  with weak and  $\text{cm}^{-1}$  very strong intensities in infrared and 1385, 1122, 1051, 1010 and  $990 \text{ cm}^{-1}$  with very strong and weak intensities in Raman are assigned to C–H in–plane bending. Most of the vibrations are observed in the Raman spectrum except two.

Six bands with very strong and medium intensities in infrared at 974, 770, 761, 610 and  $480 \text{ cm}^{-1}$  and three bands with very weak intensities in Raman at 923, 571, 553 and  $460 \text{ cm}^{-1}$  are assigned to C–H out–of–plane bending vibrations also lie within the characteristic region. After scaling procedure, the theoretical C–H vibrations are in good agreement with the

experimental values and literature [24–29]. The change in the frequencies of these deformations from the values in benzene is determined mainly by the relative position of the substituents and is almost independent of their nature

### **Methyl group vibrations**

Whenever a methyl group is present in a compound, it gives rise to two asymmetric and one symmetric stretching vibration. The asymmetric stretching for the  $\text{CH}_3$ ,  $\text{NH}_2$  and  $\text{CH}_2$  has magnitude higher than the symmetric stretching [27]. In the present case, also two asymmetric vibrations at 2990, 2940  $\text{cm}^{-1}$  and one symmetric vibration at 2860  $\text{cm}^{-1}$  are present which is in agreement with literature [21]. The average frequency shift between asymmetric and symmetric stretching vibrations is found to be  $\pm 105 \text{ cm}^{-1}$ . 2-methoxy-1-naphthaldehyde shows methyl vibrations are in the range 2885 – 2803  $\text{cm}^{-1}$ . This may be indicates that the additional substitutions push down the range of vibration.

The asymmetric and symmetric stretching modes of methyl group attached the benzene ring are usually downshifted due to electronic effects and are expected near 2990 and 2940  $\text{cm}^{-1}$  for asymmetric and 2860  $\text{cm}^{-1}$  for symmetric stretching vibrations. This evident that the same electronic effect is also applicable in double ring compound like 1-methoxynaphthalene and the vibrations are observed at 2940 and 2865  $\text{cm}^{-1}$  [23]. Moreover, the symmetrical bands are sharper than the asymmetrical bands. The same trend is also

observed here. The large difference between the asymmetric and symmetric values has been attributed to the electronic effect. Thus, it is evident that the same electronic effect is also applicable in this compound. The CH<sub>3</sub> rocking and torsion vibrations are observed at 960 and 875 cm<sup>-1</sup> and at the lowest frequency 160 cm<sup>-1</sup> respectively. The methyl group assignments proposed in this study is also in agreement with literature values [24–29]

### **C–O vibrations**

The compound under study contains a C–O group and the absorption caused by such C–O stretching is generally very strong [30]. The C–O stretching vibrations of the light substituents [31] lie in the region 1095 – 1310 cm<sup>-1</sup> and in carboxylic acids, the C=O stretching appear at 1725 with  $\pm 65$ cm<sup>-1</sup> [32]. In this compound, C–O stretching vibrations are observed at 1310 and 1260 cm<sup>-1</sup> with very weak intensity in infrared and Raman. The frequencies are certainly lesser than the cited values, which are quite expected as the bond is present between the naphthalene ring and methyl group. The C–O in–plane bending vibrations are observed at 720 and 702 cm<sup>-1</sup> and out–of–plane bending vibrations at 398 and 280 cm<sup>-1</sup>. All these vibrations have appeared with very weak intensity in Raman.

## Ring vibrations

Generally, the C=C stretching vibrations in benzene compounds form the bands in the region 1500 – 1650  $\text{cm}^{-1}$  [33]. Several ring modes are affected by the substitution to the aromatic ring of naphthalene. In the present case, the C=C stretching bands are observed at 1550 and 1495  $\text{cm}^{-1}$  with very strong intensities in infrared and 1640, 1580 and 1456  $\text{cm}^{-1}$  with very weak and strong intensities in Raman. All these bands except the last one are in the expected range. This indicates that the C=C modes are not affected by the substitutions.

In this compound, the six C–C stretching vibrations are observed at 1440, 1435, 1425, 1417, 1220, 1190, 1182 and 1140  $\text{cm}^{-1}$ . All these bands are appeared with weak intensities except one band and most of the bands are laid in the infrared region. The CCC in-plane bending vibrations generally occur at higher frequencies than of out-of-plane bending [18]. In the present study, the bands are observed at 865  $\text{cm}^{-1}$  with very weak intensity in Raman and 845 and 840  $\text{cm}^{-1}$  in IR with medium and very weak intensity are assigned to C–C–C in-plane bending modes. The C–C–C out-of-plane bending wavenumbers are observed at 500  $\text{cm}^{-1}$  with very weak intensity in infrared and 430, 335, 220 and 195  $\text{cm}^{-1}$  with very weak intensities in Raman. The maximum numbers of bands are observed in Raman. Some of the bands are missing in in-plane and out-of-plane bending which may due to heavy mass substitutions.

## CONCLUSION

A complete vibrational analysis of MNAP was performed at B3LYP method with 3-21G, 6-31G, 6-31G(d,p) and 6-311++G(d,p) basis sets. But the results show excellent agreement between experimental and calculated wavenumbers in B3LYP/6-311++G (d, p) basis set. The influences of carbon-oxygen, and methyl group in the vibrational frequencies of the title compound were discussed. The observed and stimulated spectra are in agreement and show a good frequency fit. The difference between the theoretical and experimental wave numbers is found within  $10\text{ cm}^{-1}$ , which indicates validity of the method.

The comparison of the skeletal and C-H vibrations of the naphthalene with benzene indicates that they are almost identical except very small changes. Even the substitution has not influenced these modes much. The global minimum energy between the different sets shows the difference in optimizations between the same sets. Various quantum chemical calculations help us to identify the structural and symmetry properties of the titled molecule. The excellent agreement of the calculated and observed vibrational spectra reveals the advantages of higher basis set for quantum chemical calculations.

**REFERENCES**

- [1] V. Krishnakumar, N. Prabavathi, S. Muthunatesan, *Spectrochim. Acta* 70 (2008) 991.
- [2] M.Arivazhagan, V.Krishnakumar, RJ.Xavier, G.Ilango, V.Balachandran, *Spectrochim. Acta A* 72 (2009) 941.
- [3] Sittig, Marshall, *Pharmaceutical Manufacturing Encyclopedia* (1988)
- [4] Gadamasetti, Kumar, Tamim, Braish, *Process Chemistry in the Pharmaceutical Industry* 2 (2007) 142– 145.
- [5] R.G. Parr, W. Yang, *Density Functional Theory of Atoms and Molecules*, Oxford, New York, 1989.
- [6] R.O. Jones, O.Gunnarson, *Rev. Mol. Phys.* 61 (1989) 689– 746.
- [7] T. Ziegler, *Chem.Rev.* 91 (1991) 651– 667.
- [8] RJ. Xavier, V. Balachandran, M. Arivazhagan, G. Ilango, *Ind. J. Pure and App. Phy.* 48 (2010) 245– 250.
- [9] V. Krishnakumar, V. Balachandran, *Spectrochim. Acta A* 63 (2006) 464–476.
- [10] A. Srivastava, V.B. Singh, *Ind. J. Pure. Appl. Phy.* 45 (2007) 714–720.
- [11] Y. Guo, Y. Xue, X.D. Zhu, G.S. Yana, *J. Mol. Struc. (Theochem)* 40 (2007) 811
- [12] M.R. Jalilian, M.Z. Tabrizi, *Spectrochim. Acta A* 69 (2008) 278–281.
- [13] M.Z. Abrizi, S.F. Tayyari, F. Tayyari, M. Behforouz , *Spectrochim. Acta A* 60 (2004) 111–120.
- [14] P.B. Nagabalasubramanian, S. Periandy, *Spectrochim. Acta A* 77 (2010) 1099.
- [15] P. Das, E. Arunan, P.K. Das, *Vib. Spectrosc.* 47 (2008) 1–9.

- [16] G. Rauhut, P. Pulay, *Phys. Chem.* 99 (1995) 3093–3100.
- [17] A.P. Scott, L. Radom, *J. Phys. Chem.* 100 (1996) 16502–16513.
- [18] G. Socrates, *Infrared and Raman Characteristic Group Frequencies*, 3rd Ed., John Wiley & Sons, Ltd., Chichester, 2001.
- [19] M.H. Jamroz, J.C. Dobrowolski, R. Brzozowski, *J. Mol. Struct.* 787 (2006) 172.
- [20] V. Chis, M. Oltean, A. Pirnau, V. Miclaus, S. Filip, *J Optoelectron Adv Mater.* 8 (2006) 1143.
- [21] S.J. Bunce, H.G. Edwards, A.F. Johnson, I.R. Lewis, P.H. Turner, *Spectrochim. Acta* 49 (1993) 775–783.
- [22] E.B. Wilson, J.C. Decius, P.C. Cross, *Molecular vibrations* McGraw Hill, 1978.
- [23] J. Mohan, *Organic Spectroscopy– Principles and applications*, seconded., Narosa Publishing House, New Delhi, 2001.
- [24] M. Karabacak, D. Karagöz, M. Kurt, *J. Mol. Struct.* 892 (2008) 25.
- [25] A. Altun, K. Gölcük, M. Kumru, *J. Mol. Struct. (Theochem.)* 625 (2003) 17.
- [26] M. Karabacak, M. Kurt and A. Atac, *J. Phys. Org. Chem.* 22 (2009) 321.
- [27] D. Lin–Vien, N.B. Colthup, W.G. Fateley, J.G. Grasselli, *The Handbook of Infrared and Raman Characteristic Frequencies of Organic Molecules*, Academic Press, Boston, MA, 1991.
- [28] M. Silverstein, G. C. Basseler, C. Morill, *Spectrometric Identification of Organic Compounds*, Wiley, New York, 1981.

- [29] M. Govindarajan, K. Ganasan, S. Periandy, M. Karabacak, S. Mohan, *Spectrochim. Acta A* 77 (2010) 1005.
- [30] M. Chalasinski, M. Szczesnaik, *Chem. Rev* 94 (1994) 1723–1765.
- [31] J.A. Pople, A.P. Scolt, M.W. Wong, L. Radom, *Isr. J. Chem.* 33 (1993) 345–350.
- [32] R. Asha, K. Raju, H.T. Varghese, M. Carlos, Granadeiro, I.S. Helena, C. Nogueiradand, Y. Panicker, *J. Braz Chem. Soc* (2009) 549–559.
- [33] G. Varasanyi, *Vibrational Spectra of Benzene Derivatives*, Academic Press, New York, 1969.

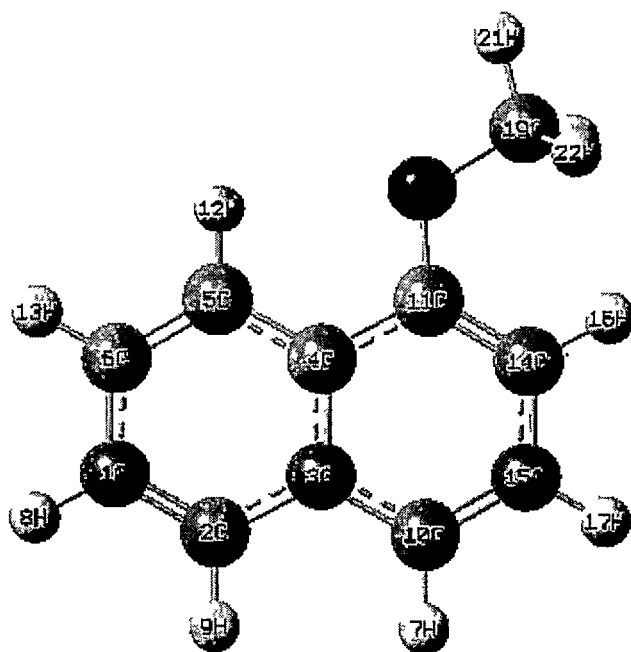


**Fig 6.1 Molecular Structure of 1-methoxynaphthalene**

# 1-methoxynaphthalene

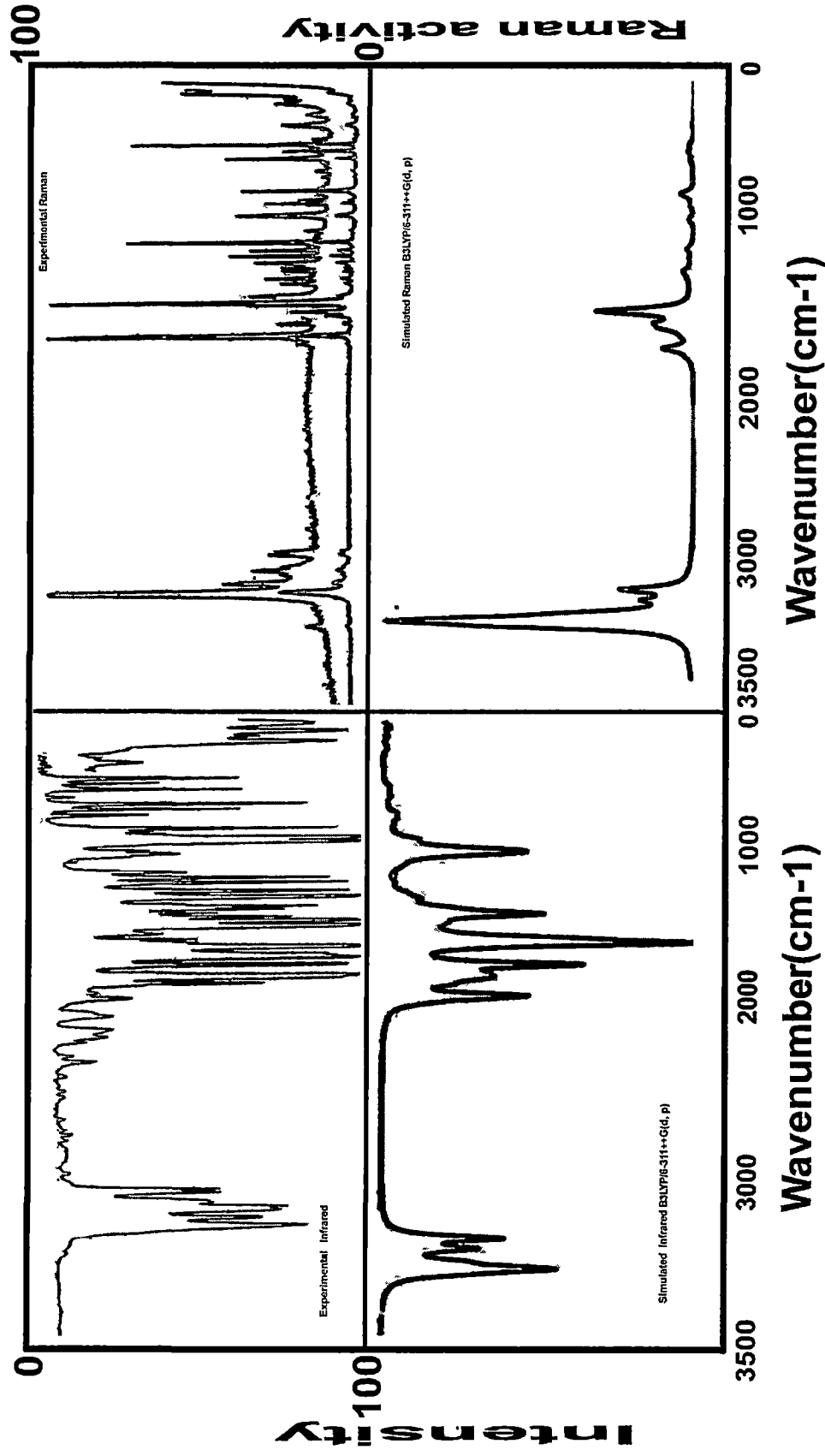


Figure 6.2: Experimental and Simulated IR and Raman spectra

**Table 6.1 Calculated thermo dynamical parameters of 1-methoxynaphthalene**

	<b>B3LYP/ 3-21G</b>	<b>B3LYP/ 6-31G</b>	<b>B3LYP/ 6-31G(d,p)</b>	<b>B3LYP/ 6-311++G(d,p)</b>
SCF Energy(a.u)	-497.6697	-500.2920	-500.4308	-500.5456
Zero point Energy (kcal mol <sup>-1</sup> )	114.0463	114.195	113.193	112.4474
Rotational Constants (GHz)	1.6273 0.8251 0.5494	1.6252 0.8196 0.5467	1.6401 0.8289 0.5525	1.6436 0.8294 0.5532
Specific heat at constant Volume( C <sub>v</sub> ) (cal mol <sup>-1</sup> K <sup>-1</sup> )	37.309	37.44 7	37.957	38.199
Entropy(S) (cal mol <sup>-1</sup> K <sup>-1</sup> )	94.306	94.386	94.594	94.991
Dipole moment(Debye)	1.7824	1.6218	14574.	1.5028

**Table 6.2 Selected optimized parameters of 1-methoxynaphthalene (bond lengths, bond angles and dihedral angles)**

*Parameters	B3LYP/ 3-21G	B3LYP/ 6-31G	B3LYP/ 6-31G(d,p)	B3LYP/ 6-311++G(d,p)
<b>Bond length(Å)</b>				
<b>CH</b>				
R(2,13)	1.0813	1.0828	1.0830	1.0814
R(5,14)	1.0840	1.0856	1.0861	1.0843
R(6,15)	1.0839	1.0854	1.0862	1.0843
R(7,12)	1.0813	1.0829	1.0837	1.0820
R(8,16)	1.0848	1.0863	1.0869	1.0851
R(9,17)	1.0840	1.0856	1.0862	1.0844
R(10,11)	1.0838	1.0854	1.0861	1.0842
R(19,20)	1.0901	1.0894	1.0909	1.0888
R(19,21)	1.0966	1.0963	1.0974	1.0952
R(19,22)	1.0965	1.0964	1.0974	1.0952
<b>CC</b>				
R(6,5)	1.3736	1.3775	1.3729	1.3705
R(1,2)	1.3784	1.3825	1.3811	1.3788
R(7,10)	1.3775	1.3820	1.3780	1.3761
R(8,9)	1.3775	1.3811	1.3769	1.3750
R(2,6)	1.4177	1.4199	1.4170	1.4160
R(3,7)	1.4176	1.4209	1.4184	1.4172
R(10,9)	1.4165	1.4179	1.4142	1.4127
R(4,8)	1.4222	1.4235	1.4203	1.4192
R(5,4)	1.4248	1.4262	1.4227	1.4217
<b>OC</b>				
R(18,1)	1.3845	1.3914	1.3652	1.3635
R(18,19)	1.4588	1.4500	1.4182	1.4208
<b>Bond angle(°)</b>				
<b>CCC</b>				
R(1,2,6)	120.2	119.7	119.9	120.0
R(4,8,9)	120.9	121.0	121.0	121.1
R(6,5,4)	120.1	120.3	120.1	120.1
R(7,10,9)	120.2	120.3	120.3	120.3
R(8,9,10)	120.3	120.2	120.2	120.2
R(2,6,5)	121.1	121.0	121.2	121.1
R(3,7,10)	120.4	120.4	120.5	120.5
R(5,4,8)	122.4	122.1	122.0	122.0
<b>OCC</b>				
R(18,1,2)	125.1	124.1	124.5	124.4
<b>COC</b>				
R(19,18,1)	118.1	118.8	118.3	118.6
<b>HCC</b>				
R(13,2,6)	118.8	119.1	119.1	119.0
R(14,5,6)	120.8	120.7	120.8	120.7
R(15,6,5)	120.1	120.2	120.1	120.1

R(12,7,10)	121.3	120.9	120.7	120.6
R(16,8,9)	120.5	120.4	120.4	120.3
R(17,9,10)	119.5	119.6	119.7	119.7
R(11,10,7)	120.1	119.9	119.9	119.9
<b>HCH</b>				
R(20,19,22)	109.8	109.8	109.3	109.4
R(21,19,20)	109.8	109.8	109.3	109.4
R(22,19,21)	109.2	109.5	109.1	109.4
<b>Dihedral angle(°)</b>				
<b>HCCC</b>				
R(13,2,1,3)	179.9	180.0	179.9	180.0
R(14,5,6,2)	180.0	180.0	180.0	180.0
R(15,6,5,4)	179.9	180.0	180.0	180.0
R(12,7,10,9)	180.0	180.0	180.0	180.0
R(16,8,9,10)	180.0	179.9	180.0	180.0
R(17,9,10,7)	180.0	180.0	180.0	180.0
R(11,10,9,8)	180.0	180.0	180.0	180.0
<b>HCOC</b>				
R(20,19,18,1)	179.9	179.9	180.0	179.9
R(21,19,18,1)	61.2	61.1	61.1	61.2
R(22,19,18,1)	61.0	61.2	61.1	61.2

\* For numbering of atom refers Fig 1.

**Table 6.3 Mulliken charges of 1-methoxynapthalene with different basis levels**

#Atom	B3LYP/ 3-21G	B3LYP/ 6-31G	B3LYP/ 6-31 G(d,p)	B3LYP/ 6-311++ G(d,p)
C1	0.323	0.240	0.313	0.036
C2	-0.214	-0.141	-0.145	0.051
C3	-0.035	0.037	0.040	0.212
C4	-0.007	0.065	0.103	0.170
C5	-0.193	-0.143	-0.130	-0.124
C6	-0.185	-0.144	-0.100	-0.504
C7	-0.168	-0.126	-0.106	-0.185
C8	-0.187	-0.170	-0.139	-0.135
C9	-0.183	-0.122	-0.085	-0.340
C10	-0.185	-0.137	-0.097	-0.315
H11	0.184	0.122	0.083	0.163
H12	0.202	0.154	0.101	0.169
H13	0.185	0.125	0.082	0.150
H14	0.178	0.124	0.078	0.121
H15	0.186	0.123	0.082	0.168
H16	0.182	0.126	0.082	0.135
H17	0.184	0.123	0.083	0.160
O18	-0.556	-0.562	-0.521	-0.153
C19	-0.332	-0.166	-0.078	-0.260
H20	0.221	0.168	0.124	0.175
H21	0.207	0.515	0.114	0.154
H22	0.193	0.151	0.114	0.154

#For numbering of atom refers Fig 1.

**Table 6.4 Detailed assignments of theoretical wave numbers of 1-methoxynaphthalene along with potential energy distribution**

Symmetry species	<sup>a</sup> Experimental frequency		Calculated frequency										PED≥10%	<sup>b</sup> Mode description	
			B3LYP/3-21G		B3LYP/6-31G		B3LYP/6-31G(d,p)		B3LYP/6-311++G(d,p)						
	IR	RAMAN	Unscaled	Scaled	Unscaled	Scaled	Unscaled	Scaled	Unscaled	Scaled	Unscaled	Scaled			
A'	3065vs		3242	3097	3245	3099	3217	3073	3208	3064	3073	3217	3064	γCH(83)	γC-H
A'		3060vs	3235	3090	3238	3093	3209	3065	3207	3063	3065	3209	3063	γCH(91)	γC-H
A'		3055vs	3213	3069	3217	3073	3189	3046	3184	3041	3046	3189	3041	γCH(89)	γC-H
A'		3050vs	3209	3065	3213	3069	3184	3041	3181	3038	3041	3184	3038	γCH(80)	γC-H
A'		3020w	3198	3055	3200	3056	3171	3029	3170	3028	3029	3171	3028	γCH(88)	γC-H
A'		3010vw	3191	3048	3193	3050	3164	3022	3164	3022	3022	3164	3022	γCH(92)	γC-H
A'	3005s		3185	3042	3187	3044	3157	3015	3158	3016	3015	3157	3016	γCH(89)	γC-H
A'		2990vw	3159	3017	3181	3038	3149	3008	3133	2993	3008	3149	2993	γCH(91)	γC-H (CH <sub>3</sub> )
A'		2940s	3086	2948	3106	2967	3074	2936	3065	2928	2936	3074	2928	γCH(100)	γC-H (CH <sub>3</sub> )
A'		2865m	3030	2894	3035	2899	3006	2871	3006	2871	2871	3006	2871	γCH(91)	γC-H (CH <sub>3</sub> )
A'		1640vw	1655	1601	1687	1632	1668	1613	1664	1610	1613	1668	1610	γCC(48)	γC=C
A'		1580vs	1638	1584	1657	1603	1637	1583	1635	1582	1583	1637	1582	γCC(52)+βCH(10)	γC=C
A'	1550vs		1608	1555	1632	1579	1613	1560	1614	1561	1560	1613	1561	γCC(42)+βCC(16)	γC=C
A'	1495vs		1571	1520	1570	1519	1554	1503	1544	1494	1503	1554	1494	γCC(32)+βCH(30)	γC=C
A'		1456vw	1554	1503	1545	1495	1539	1489	1505	1456	1489	1539	1456	βCH(68)+τHCOC(22)	γC=C
A'	1440vw		1549	1498	1531	1481	1523	1473	1494	1445	1473	1523	1445	γCC(12)+βCH(52)	γC-C
A'		1435w	1519	1469	1523	1473	1511	1462	1491	1442	1462	1511	1442	βCH(74)+τHCOC(23)	γC-C
A'	1425vw		1505	1456	1503	1454	1494	1445	1476	1428	1445	1494	1428	βCH(62)	γC-C
A'		1417vw	1496	1447	1498	1449	1489	1440	1470	1422	1440	1489	1422	γCC(12)+βCH(51)	γC-C
A'		1385vs	1453	1406	1454	1407	1444	1397	1425	1378	1397	1444	1378	βCH(35)	βC-H
A'	1325w		1408	1362	1436	1389	1412	1366	1402	1356	1366	1412	1356	βCH(59)	βC-H
A'	1310w		1373	1328	1405	1359	1384	1339	1375	1330	1339	1384	1330	γCO(22)+βCH(18)	γC-O
A'		1260w	1318	1275	1319	1276	1309	1266	1293	1251	1266	1309	1251	γCO(19)+βCH(10)	γC-O
A'	1220vs		1286	1244	1283	1241	1271	1230	1264	1223	1230	1271	1223	γCC(17)+βCH(14)+βCCC(10)	γC-C
A'	1190m		1254	1213	1268	1227	1253	1212	1238	1198	1212	1253	1198	γCC(12)+βCH(36)+βCCC(15)	γC-C
A'		1182vw	1241	1201	1236	1196	1225	1185	1215	1175	1185	1225	1175	βCH(14)+γCC(49)	γC-C
A'	1160vs		1221	1181	1219	1179	1208	1169	1195	1156	1169	1208	1156	βCH(47)+τHCOC(10)	βC-H
A'		1155vw	1202	1163	1204	1165	1197	1158	1180	1142	1158	1197	1142	βCH(60)	βC-H
A'		1140m	1191	1152	1196	1157	1185	1146	1168	1130	1146	1185	1130	βCH(20)+γCC(74)	γC-C
A'		1122vw	1161	1123	1166	1128	1160	1122	1166	1128	1122	1160	1128	γCO(12)+βCH(13)+βCCC(26)	βC-H

A'	1075vs		1130	1093	1129	1092	1120	1084	1128	1091	βCH(61)	βC-H
A'		1051m	1095	1059	1105	1069	1093	1057	1092	1056	γCC(12)+βCH(27)	βC-H
A'		1010vs	1045	1011	1058	1024	1044	1010	1043	1009	γCC(14)+βCH64)	βC-H
A'		990s	1032	998	1029	996	1027	994	1010	977	τHCCC(66)	βC-H
A'	974vs		1017	984	1002	969	1002	969	997	965	τHCCC(73)	φC-H
A'	955vs		1006	973	1001	968	994	962	976	944	βCH(64)	βC-H(CH <sub>3</sub> ) rock
A''			997	965	990	958	991	959	963	932	βCCC(58)	φC-H (CH <sub>3</sub> ) rock
A'			930	900	915	885	910	880	881	852	τHCCC(63)	βC-C-C
A''	845m		909	880	896	867	891	862	871	843	τHCCC(42)	βC-C-C
A''	840vw		877	849	877	849	869	841	863	835	γCO(14)+βCCC(47)	βC-C-C
A'	770vs		841	814	828	801	820	793	804	778	φCH(21)+βOCCC(36)	φC-H
A''	761vs		824	797	821	794	817	791	801	775	φCH(63)+βOCCC(13)	φC-H
A''	760s		807	781	806	780	797	771	786	761	γOC(12)+βCCC(25)	βC-C-C
A'			759	734	762	737	756	732	739	715	φCH(81)	βC-O
A'			729	705	729	705	724	701	726	703	βCCC(50)	βC-O
A''	610s		681	659	660	639	654	633	648	627	φCH(61)	φC-H
A''			623	603	620	600	617	597	615	595	φCH(12)+βCCC(59)	φC-H
A'			603	584	594	575	593	574	584	565	βCCC(70)	φC-H
A''	500vw		558	540	552	534	551	533	541	524	γCC(12)+φCCC(51)	φC-C-C
A''	480s		506	490	502	486	499	483	493	477	φCCC(68)	φC-H
A''			491	475	491	475	488	472	474	459	βCCC(58)	φC-H
A''		460m	465	450	450	436	457	442	455	440	φCCC(74)	φC-C-C
A''		430vw	440	426	437	423	435	421	427	413	βCCC(68)	φC-O
A''		398vs	336	325	336	325	333	323	338	327	φCCC(77)	φC-C-C
A''		335vw	292	283	288	279	285	276	282	273	φCCC(79)	φC-O
A'		280w	224	217	227	220	225	218	225	218	βCOC(63)	φC-C-C
A''		220vw	200	194	202	196	200	194	206	200	φCCC(67)	φC-C-C
A''		195vw	183	177	185	179	183	177	178	173	φCCC(79)	CH <sub>3</sub> torsion
A''		160vw	144	140	143	139	141	137	135	131	φCOC(10)+φCCC(66)	φC-C-C
A''			79	77	81	79	80	78	78	76	φCCC(51)	Butterfly

<sup>a</sup> s: strong; vs: very strong; m: medium; w: weak; vw: very weak.

<sup>b</sup> γ: stretching; β: in-plane bending; φ: out-of-plane bending.

Scale factor over 1800 cm<sup>-1</sup> 0.955

Scale factor below 1800 cm<sup>-1</sup> 0.967



<http://www.e-journals.net>



ISSN: 0973-4945; CODEN ECJHAO  
E-Journal of Chemistry  
2010, 7(2), 457-464

## Scaled Quantum FT-IR and FT-Raman Spectral Analysis of 1-Methoxynaphthalene

M. GOVINDARAJAN\*, S. PERIANDY<sup>§</sup> and K. GANESAN

\*Department of Physics, Avvaiyar Govt College, Karaikal-609 602, India.

<sup>§</sup>Department of Physics, Tagore Arts College, Puducherry-605 001, India.

Department of Physics, TBML College Porayar-609 307, India.

*govindarajan64@gmail.com*

Received 12 September 2009; Accepted 5 November 2009

**Abstract:** The structural and vibrational property of 1-methoxynaphthalene has been studied. The fundamental vibrational frequencies and intensity of vibrational bands were evaluated using B3LYP/6-31G (d, p) basis set and was scaled using various scale factors, which yielded a good agreement between observed and calculated frequencies. The vibrational spectra were interpreted with the aid of normal coordinate analysis. The results of the calculations were applied to simulated spectra of the title compound, which shows excellent agreement with observed spectra. The calculated force constants in vibrational internal coordinates are in closely coincides with the experimentally observed force constants.

**Keywords:** Scaled quantum FT-IR, FT-Raman Spectra, 1-Methoxynaphthalene, Vibrational property.

### Introduction

Vibrational analyses of molecules are more deep study in organic chemistry, for the confirmation of functional groups, molecular structure and reaction kinetics. The naphthalene and its derivatives<sup>1,2</sup> are the most important class of organic compounds containing two condensed rings. 1-Methoxynaphthalene is used as an intermediate for the synthesis of nonsteroidal anti-inflammatory drugs. It is also used for soap perfumes and in the preparation of non-steroidal anti-inflammatory agents and bromination process. There are series of ladder-like compounds consisting of linearly fused benzene rings<sup>1,2</sup>, their technological potential<sup>3-5</sup> and their intrinsic value as models for more complex conjugated molecules have been the subjects of many theoretical and experimental investigations<sup>6-14</sup>.

## Experimental

The compound under investigation namely 1-methoxynaphthene was purchased from M/S Aldrich chemicals, U.S.A which is of spectroscopic grade and hence used for recording the spectra as such without any further purification. The FT-IR spectrum of the compound was recorded in Bruker IFS 66V spectrometer in the range of 4000 to 400  $\text{cm}^{-1}$ . The spectral resolution is  $\pm 2 \text{ cm}^{-1}$ . The FT-Raman spectra of this compound was also recorded in the same instrument with FRA 106 Raman module equipped with Nd: YAG laser source operating at 1.064  $\mu\text{m}$  line widths with 200 mW powers. The spectra were recorded with scanning speed of 30  $\text{cm}^{-1} \text{ min}^{-1}$  of spectral width 2  $\text{cm}^{-1}$ . The frequencies of all sharp bands are accurate to  $\pm 1 \text{ cm}^{-1}$ .

### *Computational methods*

The quantum chemical calculations were performed for 1-methoxynaphthalene by applying B3LYP/6-31G (d,p) basis set method using the Gaussian 03 W program<sup>15</sup>. The Cartesian representation of the theoretical force constants has been computed at the fully optimized geometry by assuming  $C_s$  point group symmetry. Scaling of the force field was performed according to the SQM procedure<sup>16</sup> using selective scaling in the natural internal coordinate representation<sup>17</sup>. The optimized bond lengths and bond angles were used for the calculation of vibrational frequencies at the B3LYP levels. The SCF converges to total energy about -500.430925363 and zero point energy 113.19344 (kcal/mol). The rotational constants values are 1.64020, 0.82882 and 0.55253. GAUSSVIEW program<sup>18</sup> is very helpful for visual interpretation of vibrational frequencies assignments with normal mode of vibration.

## Results and Discussion

### *Molecular geometry*

The 1-methoxynaphthalene assumed as  $C_s$  point group of symmetry and the optimized geometrical parameters of the title compound are calculated according to labeling of atoms as shown in the Figure 1. The most optimized bond lengths and bond angles of this compound were calculated and shown in Table 1.

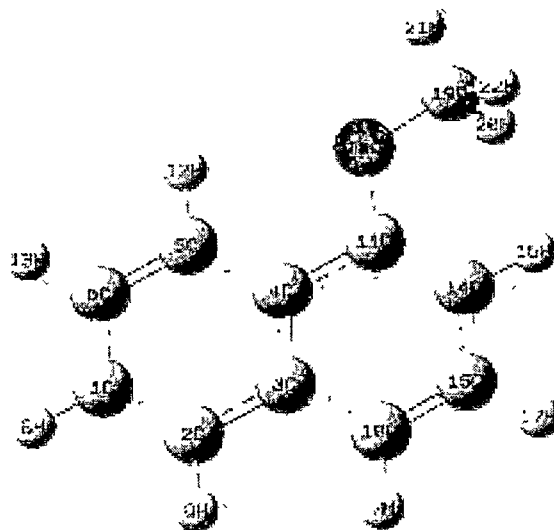


**Figure 1.** Molecular structure of 1-methoxynaphthalene.

**Table 1.** Optimized parameters of 1- methoxynaphthalene.

Bond length	Value (Å <sup>0</sup> )	Bond angle	Value (°)
C1-C2	1.3769	C2-C1-C6	120.2083
C1-C6	1.4143	C1-C2-H8	120.0527
C1-H8	1.0862	C6-C1-H8	119.739
C2-C3	1.4203	C1-C2-C3	121.0797
C2-H9	1.0869	C1-C2-C9	120.405
C3-C4	1.4309	C3-C2-C9	118.5153
C3-C10	1.4227	C2-C3-C4	118.4281
C4-C5	1.4184	C2-C3-C10	122.0275
C4-C11	1.4336	C4-C3-C10	119.5444
C5-C6	1.378	C3-C4-C5	119.3869
C5-C12	1.0837	C3-C4-C11	118.5468
C6-C13	1.0861	C5-C4-C11	122.0663
H7-C10	1.0861	C4-C5-C6	120.5573
C10-C15	1.3729	C4-C5-H12	118.6985
C11-C14	1.3811	C6-C5-H12	120.7442
C11-O18	1.3652	C1-C6-C5	120.3396
C14-C15	1.417	C1-C6-H13	119.7196
C14-H16	1.083	C5-C6-H13	119.9407
C15-H17	1.0862	C3-C10-H7	119.0627
O18-C19	1.4182	C3-C10- C15	120.1449
C19-H20	1.0973	H7- C10-C15	120.7924
C19-H21	1.0909	C4-C11-C14	120.6224
C19-H 22	1.0973	C4-C11-O18	114.8672
		C14-C11-O18	124.5104
		C11=C14-C15	119.925
		C11-C14-H16	120.9587
		C15-C14-H16	119.1163
		C10-C15-C14	121.2165
		C10-C15-H17	120.1347
		C14-C15-H17	118.6488
		C11-O18-C19	118.2875
		O18-C19-H20	111.5413
		O18-C19-H21	106.0622
		O18-C19-H22	111.5386
		H20-C19-H21	109.2863
		H20-C19-H22	109.0488
		H21-C19-H22	109.2914

*Vibrational analysis and theoretical prediction of spectra*

The sixty normal modes of vibrations of 1-methoxynaphthalene are distributed by symmetry species as

$$\Gamma_{\text{vib}} = 41A'(\text{in-plane}) + 19A''(\text{out-of-plane})$$

It is in agreement with C<sub>s</sub> point group symmetry, all vibrations are active both in FT-Raman and infrared absorption. The detailed vibrational assignments of fundamental modes of 1-methoxynaphthalene along with the calculated frequencies, IR intensities, Raman activities and polarization ratios are reported in the Table 2. The observed and simulated FT-IR and laser Raman spectra are presented in Figures 2 & 3 respectively.

**Table 2.** Observed and B3LYP 6-31G (d,p) level calculated vibrational frequencies of 1-methoxynaphthalene.

Symmetry	IR	Raman	Unscaled	scaled	Reduced mass	Force constants	IR intensity	Raman activity	Depolar ratio(P)	Depolar ratio(U)	Assignments
A'	3065		3227	3065	1.09	6.69	7.59	201.60	00.11	0.20	C-H stretch
A'		3060	3226	3064	1.09	6.69	12.39	46.33	0.58	0.73	C-H stretch
A'		3055	3201	3040	1.09	6.61	28.85	268.79	0.14	0.24	C-H stretch
A'		3050	3198	3037	1.09	6.59	31.92	212.82	0.39	0.56	C-H stretch
A'		3020	3187	3027	1.09	6.52	15.12	127.75	0.74	0.85	C-H stretch
A'		3010	3180	3021	1.08	6.47	1.76	48.82	0.74	0.85	C-H stretch
A'	3005		3175	3015	1.08	6.44	1.14	42.82	0.63	0.78	C-H stretch
A'		2990	3150	2992	1.10	6.43	22.29	106.12	0.52	0.68	C-H stretch
A'	2940		3080	2925	1.10	6.18	40.46	62.39	0.75	0.85	C-H stretch
A'	2860		3017	2865	1.03	5.54	60.81	136.48	0.03	0.06	C-H stretch
A'		1640	1682	1631	6.29	10.49	7.1218	6.98	0.54	0.70	C-O stretch
A'	1595		1653	1586	5.09	8.20	19.53	1.93	0.28	0.44	C-C stretch
A'		1580	1633	1567	6.75	10.60	64.91	57.52	0.60	0.75	C-C stretch
A'		1505	1562	1499	3.54	5.08	21.39	7.82	0.29	0.46	C-C stretch
A'	1465		1520	1461	1.09	1.49	13.74	8.50	0.59	0.74	C-H in plane bend
A'	1460		1509	1451	2.03	2.73	32.80	14.17	0.49	0.66	C-H in plane bend
A'	1459		1503	1442	1.04	1.39	5.49	24.98	0.75	0.85	C-C stretch
A'	1440		1489	1431	1.50	1.96	3.23	9.00	0.28	0.43	C-H in plane bend
A'		1435	1483	1426	1.81	2.34	19.20	45.48	0.37	0.54	C-H in plane bend
A'		1385	1438	1380	2.21	2.69	97.08	19.94	0.19	0.33	C-C stretch
A'	1325		1418	1325	5.65	6.70	0.99	178.62	0.18	0.31	C-O stretch
A'	1310		1391	1334	3.54	4.04	1.27	4.46	0.34	0.51	C-C stretch
A'		1260	1305	1255	2.56	2.57	149.46	2.00	0.67	0.80	C-H in plane bend
A'	1220		1274	1225	1.73	1.66	51.44	2.65	0.60	0.75	C-C in plane bend
A'	1190		1247	1199	2.08	1.90	3.05	1.81	0.54	0.70	C-H in plane bend
A'	1175		1223	1176	1.41	1.24	4.39	5.11	0.64	0.78	C-H in plane bend
A'	1160		1203	1156	1.42	1.21	6.75	4.90	0.72	0.84	C-H in plane bend
A'		1155	1185	1139	1.14	0.95	8.96	3.12	0.70	0.82	C-H out plane bend
A'		1140	1178	1132	1.27	1.04	0.85	4.56	0.75	0.85	C-H in plane bend
A'	1105		1175	1129	1.33	1.08	2.61	9.79	0.68	0.81	C-H in plane bend
A'	1075		1138	1092	2.66	2.03	74.68	2.95	0.20	0.33	C-C stretch
A'	1025		1101	1042	2.19	1.56	15.22	5.63	0.13	0.24	C-C stretch
A'	995		1052	1011	2.37	1.54	11.00	12.63	0.15	0.27	C-H in plane bend
A'		990	1019	978	6.07	3.72	5.85	1.44	0.74	0.85	C-H out plane bend
A'	974		994	977	1.26	0.73	0.00	0.12	0.75	0.85	C-C-C in plane bend
A'	971		969	952	1.30	0.72	1.70	0.10	0.75	0.85	C-C-C in plane bend
A''		960	960	921	1.29	0.70	0.09	0.39	0.75	0.85	C-H out plane bend
A'		875	888	872	1.57	0.73	0.71	4.91	0.75	0.85	C-C-C in plane bend
A''	863		874	839	4.63	2.08	2.00	4.78	0.11	0.20	C-H out plane bend

*Contd...*

A''	840	866	831	1.47	0.65	1.28	0.71	0.75	0.85	C-H out plane bend
A'	795	806	792	1.88	0.72	45.95	1.43	0.75	0.85	C-C-C in plane bend
A''	775	802	770	5.23	1.98	1.46	1.73	0.12	0.22	C-H out plane bend
A''	760	788	757	1.68	0.61	40.60	2.43	0.75	0.85	C-H out plane bend
A'	720	746	733	1.36	0.44	0.45	5.57	0.75	0.85	C-C-C in plane bend
A'	710	729	716	5.41	1.69	11.25	24.81	0.10	0.19	C-C-C in plane bend
A''	640	649	638	3.48	0.86	1.97	0.62	0.75	0.85	C-C-C in plane bend
A''	580	615	590	5.47	1.22	4.33	1.91	0.48	0.65	C-H out plane bend
A'	554	585	561	3.38	0.68	4.89	1.86	0.75	0.85	C-H out plane bend
A''	500	541	519	6.45	1.11	0.73	5.50	0.48	0.65	C-H out plane bend
A''	465	494	474	6.45	0.92	2.91	9.92	0.28	0.44	C-C-C out plane bend
A''	460	481	461	3.45	0.47	0.10	0.31	0.75	0.85	C-H out plane bend
A''	430	456	430	5.06	0.61	1.99	6.97	0.42	0.59	C-C-C out plane bend
A''	420	432	407	3.23	0.35	2.15	2.31	0.75	0.85	C-C-C out plane bend
A''	335	341	321	3.71	0.25	0.50	4.16	0.21	0.35	C-C-C out plane bend
A'	280	291	274	2.20	0.11	0.02	0.87	0.75	0.85	C-O in plane bend
A''	220	235	221	1.44	0.04	0.21	0.91	0.75	0.85	C-H out plane bend
A''	195	208	196	3.71	0.09	2.44	1.88	0.72	0.84	C-C-C out plane bend
A''	160	181	170	3.67	0.07	0.03	0.23	0.75	0.85	C-C-C out plane bend
A''		138	130	3.73	0.04	2.38	2.20	0.75	0.84	C-C-C out plane bend
A''		81	76	3.09	0.01	3.84	1.99	0.75	0.85	C-C-O out plane bend

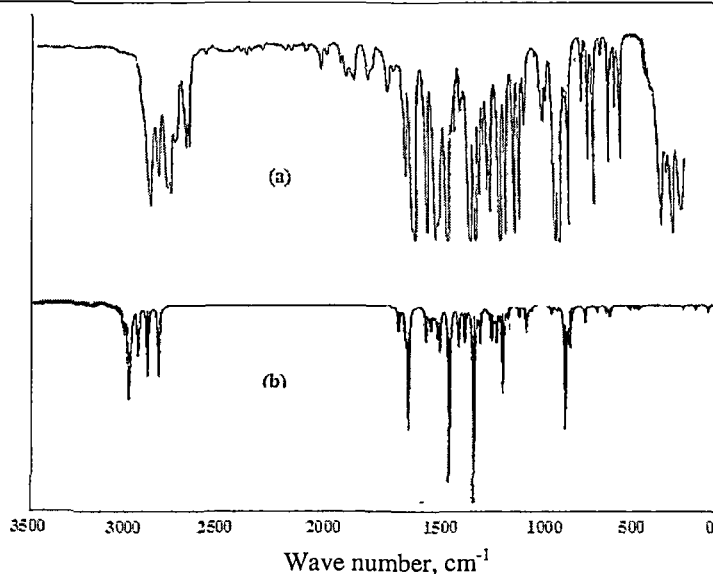


**Figure 2.** Comparison of observed and calculated FT-Raman 1-methoxynaphthalene. (a) Observed (b) calculated with B3LYP/6-31G (d,p).

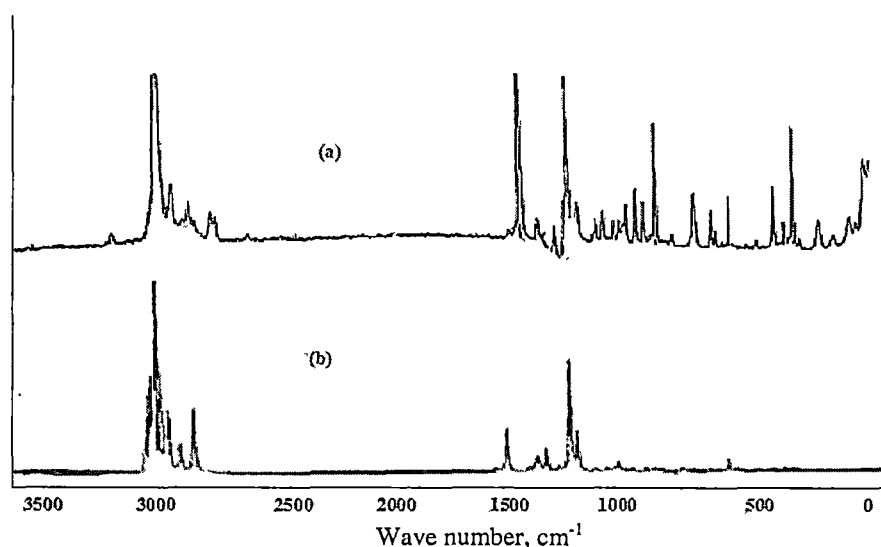


**Figure 3.** Comparison of observed and calculated FT-Raman 1-methoxynaphthalene (a) Observed (b) calculated with B3LYP/6-31G (d,p).

Root mean square (RMS) values of frequencies were obtained using the relation

$$v_{\text{RMS}} = \sqrt{\frac{1}{n-1} \sum_i^n (v_i^{\text{calcu}} - v_i^{\text{exp}})^2}$$

The RMS error of unscaled frequencies is obtained for 1-methoxy naphthalene and found to be  $77.04 \text{ cm}^{-1}$ . In order to reproduce the observed frequencies, the refinement through scaling factors was carried out and optimized RMS deviation was reduced to  $12.1 \text{ cm}^{-1}$ .

#### *C-H Vibrations*

In aromatic molecules like 2 naphthalenol C-H vibrations appear<sup>19</sup> in the region  $3085\text{--}3040 \text{ cm}^{-1}$  and in 2,4 diisopropyl naphthalene<sup>20</sup> in the region  $3070\text{--}3030 \text{ cm}^{-1}$ . In this compound the C-H stretch vibrations occur in the region  $3065\text{--}3000 \text{ cm}^{-1}$ . The upper limit of frequency comparatively decreases may be due to the presence of oxygen and methyl group. There are seven aromatic C-H stretching vibrations, are observed at  $3060, 3055, 3050, 3020$  and  $3010 \text{ cm}^{-1}$  in FT-Raman and  $3065$  and  $3005 \text{ cm}^{-1}$  are in IR region. The maximum and minimum frequencies are lies in the IR region. The mean deviations between experimental and scaled calculated frequencies are nearly  $8.57 \text{ cm}^{-1}$ . The scaled vibrations are good in agreement with the experimentally reported values of naphthalene derivatives. Optimized C-H bond lengths are clearly shows that the C-H bonds nearer to the methoxy group  $\text{C}_5\text{-H}_{12}$  and  $\text{C}_{15}\text{-H}_{16}$  having maximum variation with others. This is undoubtedly due to the impact of methoxy group. It is also evident by the farthest bond  $\text{C}_2\text{-H}_{13}$  with maximum optimized bond length.

#### *Methyl group vibrations*

The methyl group stretching vibrations are in the region  $3000\text{--}2980 \text{ cm}^{-1}$ . In this compound, there two asymmetric and one symmetric C-H stretching vibrations are appeared at  $2990, 2940$  and  $2860 \text{ cm}^{-1}$  respectively. These assignments are also evidenced by literature values<sup>21</sup>. The calculated frequencies are at  $2992, 2940$  and  $2865 \text{ cm}^{-1}$ . Usually the symmetrical bands are sharper than the asymmetrical bands. The same trend is appeared here also.

2-methoxy-1-naphthaldehyde shows methyl vibrations are in the range 2885-2803  $\text{cm}^{-1}$ . This may indicate that the additional substitutions push down the range of vibration. The asymmetric and symmetric stretching modes of methyl group attached to the benzene ring are usually downshifted due to electronic effects and are expected near 2925 and 2865  $\text{cm}^{-1}$  asymmetric and symmetric stretching vibration. This is evident that the same electronic effect is also applicable in double ring compound like 1-methoxynaphthalene and the vibrations are observed<sup>22</sup> at 2940 and 2865  $\text{cm}^{-1}$ . Here also the above experimental values coincide with the scaled B3LYP/6-31G (d, p) basis set values. There is an appreciable change in one calculated C<sub>19</sub>-H<sub>21</sub> bond due to its orientation and very near to the oxygen atom.

The bands due to C-H in-plane bending vibration interact somewhat with C-C stretching vibrations, are observed as number of bands in the region 1300–1000  $\text{cm}^{-1}$ . The C-H out-of-plane bending vibrations occur<sup>23</sup> in the region 900–667  $\text{cm}^{-1}$ .

In the present investigation, the bands observed at 1465, 1460, 1440, 1435, 1260, 1220, 1190, 1175, 1160, 1155, 1140, 1105 and 1075  $\text{cm}^{-1}$  and 1025  $\text{cm}^{-1}$  are assigned to C-H in plane bending vibration. The C-H out of plane bending modes were also assigned at 995, 974, 971, 875, 863, 795, 775, 720, 640, 290 and 220  $\text{cm}^{-1}$  within characteristic region except three and is presented.

#### *C–O vibrations*

The compounds contain a carbonyl group; the absorption caused by the C–O stretching is generally very strong<sup>24</sup>. In *p*-anisaldehyde, the C-O vibration with B3LYP/6-31G(d,p) predicted frequencies at 1332 and 1305  $\text{cm}^{-1}$  are in agreement with experimental frequencies<sup>25</sup> at 1322 and 1291  $\text{cm}^{-1}$ . The characteristic infrared absorption frequencies of carbonyl group in cyclic ketones are normally strong in intensity and found in the region 1685–1660  $\text{cm}^{-1}$ . Carboxylic acids, the C=O stretching observation<sup>26</sup> observed at 1725±65. In this compound C=O and C-O stretching vibrations are observed at 1640 and 1325  $\text{cm}^{-1}$ . The bands are strong and medium appeared in Raman and IR. The scaled calculated values obtained from B3LYP/6-31G (d,p) are 1631 and 1325  $\text{cm}^{-1}$ . The in plane bending vibration is observed at 280  $\text{cm}^{-1}$ .

#### *C–C vibrations*

Generally the C-C stretching vibrations in aromatic compounds form<sup>27</sup> the band in the region of 1430 to 1650  $\text{cm}^{-1}$ . In the present case investigation the bands are observed at 1640, 1595, 1580, 1505, 1440, 1325 and 1310  $\text{cm}^{-1}$ . The last two bands lie below the expected range, this may be due to the substitution of heavy elements oxygen and methyl group in the present case. The in-plane bending C-C vibrations generally occur at higher frequencies than of out-of-plane bending<sup>28</sup>. In the present study the bands observed at 760, 720, 580, 500, 465 and 430 are assigned to C-C in plane bending modes. The out of plane bending modes of frequencies are attributed to 554, 460 and 420  $\text{cm}^{-1}$  in Raman and 175, 140 and 85  $\text{cm}^{-1}$  in IR.

### **Conclusions**

A complete vibrational analysis of 1-methoxynaphthalene was performed on the basis of DFT functional calculations at B3LYP/6-31G (d, p) basis level. The influences of carbon-oxygen, and methyl group in the vibrational frequencies of the title compound were discussed. The observed and simulated spectra are in agreement and show a good frequency fit. The difference between theoretical and experimental wave numbers within 10  $\text{cm}^{-1}$  shows that the assignments of the fundamentals are valid, by the qualitative agreement between the calculated and observed frequencies.

### **References**

1. Clar E, Polycyclic Hydrocarbons, Academic Press, London, 1964.

2. Havey R G, Polycyclic Aromatic Hydrocarbons, Wiley-VCH, New York, 1997.
3. Geerts Y, Klärner G and Mullen K, in *Electronic Materials: The Oligomer Approach*, Edited by Mullen K and Wagner G, Wiley-VCH, Weinheim, 1998, p. 48.
4. Dimitrakopoulos C D and Malenfant P R L, *Adv Mater.*, 2002, **14**, 99.
5. Reese C, Roberts M, Ling M and Bao Z, *Mater Today*, 2004, **7**, 20
6. Bendikov M, Wudl F and Perepichka D F, *Chem Rev.*, 2004, **104**, 4891
7. Angliker H, Rommel E and Wirz J, *Chem Phys Lett.*, 1982, **87**, 208.
8. Kertesz M and Hoffmann R, *Solid State Comm.*, 1983, **47**, 97.
9. Kivelson S and Chapman O L, *Phys Rev B.*, 1983, **28**, 7236.
10. Wiberg K B, *J Org Chem.*, 1997, **62**, 5720.
11. Houk K N, Lee P S and Nendel M, *J Org Chem.*, 2001 **66**, 5517-5521.
12. Bendikov M, Duong H M, Starkey K, Houk K N, Carter E A and Wudl F, *J Am Chem Soc.*, 2004, **126**, 7416.
13. Mondal R, Shah B K and Neckers D C, *J Am Chem Soc.*, 2006, **128**, 9612.
14. Reddy A R and Bendikov M, *Chem Commun.*, 2006, **1179**.
15. Frisch M J, Trucks G W, Schlegel H B, Scuseria G E, Robb M A, Cheeseman J R, Montgomery J A, Jr, Vreven T, Kudin K N, Burant J C, Millam J M, Iyengar S S, Tomasi J, Barone V, Mennucci B, Cossi M, Scalmani G, Rega N, Petersson G A, Nakatsuji H, Hada M, Ehara M, Toyota K, Fukuda R, Hasegawa J, Ishida M, Nakajima T, Honda Y, Kitao O, Nakai H, Klene M, Li X, Knox J E, Hratchian H P, Cross J B, Adamo C, Jaramillo J, Gomperts R, Stratmann R E, Yazyev O, Austin A J, Cammi R, Pomelli C, Ochterski J W, Ayala P Y, Morokuma K, Voth G A, Salvador P, Dannenberg J J, Zakrzewski V G, Dapprich S, Daniels A D, Strain M C, Farkas O, Malick D K, Rabuck A D, Raghavachari K, Foresman J B, Ortiz J V, Cui Q, Baboul A G, Clifford S, Cioslowski J, Stefanov B B, Liu G, Liashenko A, Piskorz P, Komaromi I, Martin R L, Fox D J, Keith T, Al-Laham M A, Peng C Y, Nanayakkara A, Challacombe M, Gill P M W, Johnson B, Chen W, Wong M W, Gonzalez C and Pople J A, Gaussian Inc., Wallingford, CT, 2004.
16. Pulay P, Fogarasi G, Pongor G, Boggs J E and Vargha A, *J Am Chem Soc.*, 1983, **105**, 7037.
17. Fogarasi G, Zhov X, Taylor P W and Pulay P, *J Am Chem Soc.*, 1992, **114**, 8191.
18. Fogarasi G and Pulay P in: Durig J R (Ed.), *Vibrational Spectra and Structure*, Elsevier, Amsterdam, 1985, **14**, 125.
19. Chis V, Oltean M, Pirnau A, Miclaus V and Filip S, *J Optoelectron Adv Mater.*, 2006, **8(3)**, 1143.
20. Michal. H Jamroz, Jan Cz Dobrowolski and Robert Brzozowski, *J Mol Struct.*, 2006, **787**, 172-183.
21. Bunce S J, Edwards H G, Johnson A F, Lewis I R and Turner P H, *Spectrochim Acta.*, 1993, **49A**, 775.
22. Jag Mohan, *Organic Spectroscopy-Principles and applications*, second Ed., Narosa publishing House, New Delhi, 2001.
23. Bowman W D and Spiro T G, *J Chem Phys.*, 1980, **73**, 5482.
24. Chalasinski M and Szczesnaik M, *Chem Rev.*, 1994, **94**, 1723.
25. Gunsekaran S, Seshadri S, Muthu S, Kumaresan S and Arunbalaji R, *Spectrochim Acta A, Mol Biomol Spectrosc.*, 2008, **70(3)**, 550-556.
26. Asha Raj, Raju K, Hema Tresa Varghese, Carlos M, Granadeiro, Helena I S, Nogueira and C, Yohannan Panicker, *J Braz chem Soc.*, 2009, **20(3)**, 549-559
27. Varasanyi G, *Vibrational Spectra of Benzene Derivatives*, Academic Press, New York, 1969.
29. Socrates G, *Infrared and Raman Characteristic Group Frequencies*, 3<sup>rd</sup> Ed., John Wiley & Sons, Ltd., Chichester, 2001.

## CHAPTER –VII

### LSDA, B3LYP and B3PW91 COMPARATIVE VIBRATIONAL SPECTROSCOPIC ANALYSIS OF $\alpha$ -ACETONAPHTHONE

#### INTRODUCTION

The naphthalene and its derivatives are of great interest in biological activity and widely used as a parent compound to make drugs.  $\alpha$ -acetonephthone is a raw material for the synthesis of some pharmaceuticals and present invention to simulate of insulin and used as a therapeutic agent [1–2]. The aromatic compounds naturally occur higher amount in plants, are used for governing the physiological functions. The vibrational analyses of this molecule would be helpful for understanding the various types of bonding and normal modes of vibration. In recent trends, the quantum chemical computational methods have proved to be an essential tool in analyzing the vibrational spectra [3–6]. KrishnaKumar [7] compared the vibrational spectrum of 2-hydroxy-3-methoxy-5-nitrobenzaldehyde with that of 2-methoxy-1-naphthalaldehyde.

Alka Srivastava has investigated the infrared and Raman spectrum of the condensed and liquid phase naphthalene and its cation. Extensive recent studies on vibrational spectra of substituted naphthalene compounds have assigned [8–11] complete vibrational mode and frequency analyses. IR and Raman spectra of  $\alpha$ -acetophenone have been examined qualitatively as well as quantitatively. The entire scaled quantum mechanical method and density force

fields calculations are performed by combining the experimental and theoretical aspects of Pulay and Rauhut. Their training set and test set have been used to check the reliability of fitting. The overall scaling factors for theoretical harmonic frequencies have been verified with least-square fit [12–13]. The assignments have also been supported by the potential energy distribution, which is part of the outcomes of the normal coordinate analyses.

Prediction of vibrational frequencies of polyatomic molecules by quantum mechanical method has become important because of its accurate and consistent with the experimental data. In the present study, we extend the probing into the application of density functional theory (DFT) employing different types of functional and various basis sets have been evaluated. A close agreement between the observed and calculated wavenumber is achieved by introducing the scale factors. Of all these methods, B3PW91 density functional technique with 6–311G has been found to give the most reliable description of vibrational assignments in the present analyses.

## **RESULTS AND DISCUSSION**

### **Molecular geometry**

The most optimized DFT geometries by B3PW91/6–311G of the  $\alpha$ -acetonephthone with atom numbering are shown in Fig 7.1. By allowing the relaxation of all parameters, the calculations converge to optimized geometries, which correspond to true energy minima, as revealed by the lack of imaginary

frequencies in the vibrational mode calculation. The global minimum energy obtained for structure optimization of  $\alpha$ -acetonephthone with 6-31G/6-311G basis sets is approximately -538 a.u. for both DFT B3LYP and B3PW91. With the 3-21G basis set the minimum energy becomes -532 a.u. and -535 a.u. for LSDA and B3LYP/B3PW91 methods respectively. During the vibrational studies of the titled molecule the global lowest energy for LSDA/3-21G and 6-311G methods are observed around the value -532 a.u. The difference in energy between the methods is 3 a.u. only. The same trends have been observed in entropy calculations. All the above observations are made without any symmetric constrains.

The total energy, zero point energy, rotational constants, specific heat capacity at constant volume and dipole moment by LSDA, B3LYP and B3PW91 with 3-21G, 6-311G and 6-311G methods are listed in Table 7.1. The most optimized DFT geometrical parameters of the title compound according to labeling of atoms are shown in Fig 7.1. The most optimized bond lengths and bond angles of this compound are calculated by various methods listed in Table 7.2. These optimized parameters are slightly overestimated with crystallographic literature values. The aromatic C-C bond distances of  $\alpha$ -acetonephthone are found to have higher values in case of B3LYP/B3PW91 calculation with respect to LSDA computation. But the C-H aromatic bond distances are in opposite trend, with relatively larger distances in LSDA. An interesting fact that, among three methyl C-H bonds, one bond in the ring of

the molecule is shorter than the other two non-planer C–H bonds by angle 0.004 Å. It also is proved by C20–C21 and C20–C23 bond lengths within all sets are equal except LSDA/3–21G. The substitutional C–C bond is larger in length with aromatic C–C bond and its higher most value in B3LYP computation.

The C–O bond length is almost equal in B3LYP/B3PW91 methods, but less value in LSDA method. An interesting conjugation effect of is observed between the bond angles C3–C2–C8 and C9–C18–O19 in the methods LSDA and B3PW91 with 3–21G and 6–311G basis. The bond angles are calculated using various methods shows the same trends as significant variation in bond lengths. The elaborate descriptions of vibrational modes can be given by means of normal coordinate analysis. The local symmetry coordinates have been constructed with suitable combinations of internal coordinates recommended by Fogarasi and Pulay [14] are listed in Table 7.3.

### **Vibrational analysis**

The sixty three normal modes of vibrations of  $\alpha$ -acetonaphthone are distributed by symmetry species as

$$\Gamma_{\text{vib}} = 43A' (\text{in-plane}) + 20A'' (\text{out-of-plane})$$

It is in agreement with Cs point group symmetry, all vibrations are active both in FTRaman and infrared absorption. Here A' represents symmetric planer and A'' asymmetric non planer vibrations. The detailed vibrational

assignment of the experimental wavenumbers is based on normal mode analyses and a comparison with theoretically scaled wavenumbers with PED by LSDA, B3LYP and B3PW91 methods. Since the scaled wavenumbers following B3PW91/6-311G method are found closer to experimental data than the results obtained using other methods, The PEDs from this set of data are discussed in detail.

The calculated frequencies are usually higher than the corresponding experimental quantities due to the combination of electron correlation effects and basis set deficiencies. After applying, the overall uniform scaling factor theoretical calculations reproduce the experimental data well in agreement. The observed and simulated FTIR and laser Raman spectra of  $\alpha$ -acetonaphthone are shown in figs 7.2. The observed and scaled theoretical frequencies using methods LSDA, B3LYP and B3PW91 with 3-21G,6-31G and 6-311G basis sets, IR intensities, and Raman activities of B3PW91/6-311G basis with PEDs are listed in Table 7.4

### **C–H vibrations**

The acetyl substituted naphthalene like molecules gives rise to C–H stretching, C–H in-plane and C–H out-of-plane bending vibrations. Aromatic compounds commonly exhibit multiple weak bands in the region 3100 – 3000  $\text{cm}^{-1}$  [15] due to aromatic C–H stretching vibrations. In the present study the C–H vibrations of the title compound are observed at 3098, 3055 and 3049

$\text{cm}^{-1}$  in FTIR spectrum and the same type of vibrations are observed at 3072 and  $3010 \text{ cm}^{-1}$  in FT-Raman. All bands are medium intensity and within the expected region, but two vibrations are missing in the region due to overtone combinations. The theoretical wave numbers due to C–H aromatic stretching are lie within the range  $3119 - 3063 \text{ cm}^{-1}$  by B3PW91/6–311G and agreement with the results of Sundraganesan et. al.[16]. In this region the bands are not appreciably affected by the nature of the substituents.

The bands due to C–H in-plane bending vibration interact with C–C stretching vibrations, are observed as a number of bands in the region  $1465 - 1281 \text{ cm}^{-1}$  [17]. In this compound, the above vibrations are observed at  $1419 - 1016 \text{ cm}^{-1}$  in FTIR and  $1447- 1061 \text{ cm}^{-1}$  in FT-Raman. The theoretically scaled vibrations by B3PW91/6–311G level methods also shows good agreement with experimentally recorded data. The C–H out-of-plane bending vibrations are appeared within the region  $900 - 667 \text{ cm}^{-1}$  [18]. The vibrations identified at 1447, 1389, 1230,1170,1165,1147 and  $1061 \text{ cm}^{-1}$  are assigned to C–H in-plane bending. Most of the vibrations are observed in the Raman spectrum except two. The C–H out-of-plane bending vibrations are also lie within the characteristic region.

### **Methyl group vibrations**

The methyl substituted C–H stretching vibrations usually appears below the range of aromatic C–H stretching The  $\text{CH}_3$  stretching and bending

modes appear in pure mode of vibrations. The methyl substitution shows strongly two C-H stretching vibrations bands identified at  $2977\text{ cm}^{-1}$  in Raman and  $2920\text{ cm}^{-1}$  in IR and Raman. But one band appeared at  $3005\text{ cm}^{-1}$  in IR. All these C-H stretching vibrations are asymmetric with weak intensity. The theoretically calculated values by B3PW91/6-311G method at 3024, 2978 and  $2908\text{ cm}^{-1}$  shows good agreement with experimental values. The asymmetric and symmetric deformation vibrations of methyl group appear within the region  $1465 - 1440\text{ cm}^{-1}$  and  $1390 - 1370\text{ cm}^{-1}$  [19]. In the present investigation, the bands at  $1435\text{ cm}^{-1}$  in infrared with medium intensity and  $1365\text{ cm}^{-1}$  in Raman with strong intensity are observed as  $\text{CH}_3$  asymmetric deformation and symmetric deformation vibrations. The methyl rocking mode vibration usually appears within the region  $1070 - 1010\text{ cm}^{-1}$  [20]. With reference to literature data, a band observed at  $1016\text{ cm}^{-1}$  in infrared spectrum is assigned  $\text{CH}_3$  rocking vibration. The theoretically calculated value in this mode is deviated only by  $6\text{ cm}^{-1}$ . The  $\text{CH}_3$  torsional modes of vibrations are observed at very low frequencies. In our study also, a band at  $209\text{ cm}^{-1}$  in Raman is assigned to torsional mode of vibration.

### **C=O vibrations**

The characteristic infrared absorption frequency of C=O in acids are normally strong in intensity and found in the region  $1800 - 1690\text{ cm}^{-1}$  [21]. This position of C=O stretching more effective to analyze the various factors in ring aromatic compounds. The C=O bond formed by  $\pi-\pi$  bond between C and O

intermolecular hydrogen bonding, reduces the frequencies of the C=O stretching absorption to a greater degree than does intermolecular H bonding because of the different electro- negativities of C and O, the bonding are not equally distributed between the two atoms. The lone pair of electrons on oxygen also determines the nature of the carbonyl groups. In carboxylic acids C=O band shows a strong absorption between 1710 and 1760  $\text{cm}^{-1}$  in IR. The C=O stretching bands of acids are considerably more intense than ketonic C=O stretching bands. The characteristic ketonic frequency C=O in the present study appears at 1675  $\text{cm}^{-1}$  in FT-Raman spectrum. This C=O vibration appears in the expected range shows that it is not much affected by other vibrations. Unfortunately, the theoretically calculated values are differing a lot from experimental value.

### **Ring vibrations**

The naphthalene ring modes are influenced more C–C bands. The ring stretching vibrations are expected within the region 1620 – 1390  $\text{cm}^{-1}$  [22]. Most of the ring modes are altered and missing by the substitutions to aromatic ring of naphthalene. Generally the C–C stretching vibrations in aromatic compounds form the strong bands. In present study, the bands are of different intensity and are observed at 1564, 1490, 1417, 1340, 1261, 1212 and 1114  $\text{cm}^{-1}$  have been assigned to C–C stretching vibrations. The theoretically calculated values are at 1570, 1496, 1424, 1354, 1269, 1213 and 1120  $\text{cm}^{-1}$  by B3PW91/6–311G method and the values shows excellent agreement with experimental

data. The ring in-plane bending and out-of-plane bending modes are also good agreement with experimental data

### **Analysis of different vibrational calculations**

The execution of different methods with different basis sets are calculated and listed in Table 4. The unscaled theoretical wavenumbers are overestimated and scaled by overall scaling factors. The overall scaling factors computed by using a linear least square fitting [12]. A disadvantage of all selective scaling procedures is the necessity to transform the force constants to nonredundant valance coordinates. But it is a tedious process for larger molecules. So the overall scaling is able to produce reasonably accurate force constants by simple procedure. The values of the estimated scale factors are nearly the same as those of Scott and Random [13]. The theoretical values in different methods are in harmonic nature.

A close agreement between the experimental and scaled wabvenumbers is mostly achieved in the fingerprint region. A very strong IR band is assigned as C=O stretching vibration in conformity with the PED distribution. Only LSDA/3-21G describes the mode accurately than the other methods. In B3LYP and B3PW91 methods reproduces improved results after scaling, though B3PW91 method performs more accurately than B3LYP. The correlation between the calculated (unscaled and scaled) and observed results of B3PW91/6-311G method shown in Fig. 4. It is evident from figure that by the

introduction of scaling factors, the large deviations are remarkably reduced and larger error for the C=O stretching mode is also indicated. This may be due to uniform scaling factor.

## CONCLUSION

A complete vibrational analysis of  $\alpha$ -acetone naphthone is by performed B3PW91 method at 6-311G basis set level. The influences of carbon-oxygen bond and methyl group to the vibrational frequencies of the title compound were discussed. The observed and stimulated spectra are agreed for the good frequency fit. The difference between theoretical and experimental wave numbers within  $10\text{ cm}^{-1}$  is confirmed by the qualitative agreement between the calculated and observed frequencies. In B3LYP/6-31G over estimates the C=O wave number, which in turn underestimates in B3LYP/6-311G. The same trend is also reflected in the optimized parameters. The global minimum energy between the different methods shows the difference in optimizations between the same and the different sets. Various quantum chemical calculations help us to identify the structural and symmetry properties of the titled molecule. The excellent agreement of the calculated and observed vibrational spectra reveals the advantages of higher basis set for quantum chemical calculations.

**REFERENCES**

- [1] Sittig, Marshall, *Pharmaceutical Manufacturing Encyclopedia*, (1988), pp 39,177
- [2] Gadamasetti, Kumar, Tamim, Braish, *Process Chemistry in the Pharmaceutical Industry*, Volume 2, 2007, pp 142– 145.
- [3] R.G. Parr, W.Yang, *Density Functional Theory of Atoms and Molecules*, Oxford, New York, 1989.
- [4] R.O. Jones, O.Gunnarson, *Rev. Mol. Phys.* 61 (1989) 689.
- [5] T. Ziegler, *Chem.Rev.* 91 (1991) 651.
- [6] W. Kohn, L.J. Sham, *Phys. Rev. A* 140 (1965) 1133.
- [7] V.Krishnakumar, V.Balachandran, *Spectrochim. Acta A* 63 (2006) 464.
- [8] AlkaSrivastava, V.B.Singh, *Indian J.Pure.Appl.Physics.* 45 (2007) 714.
- [9] Yong Guo, Ying Xue, Xian De Zhu, Guo Sen Yana, *Theochem.* 820 (2007) 40.
- [10] M.R.Jalilian, Mansoureh Zahedi– Tabrizi, *Spectrochimica. Acta A* 69 (2008) 278.
- [11] MZ. Tabrizi, SF. Tayyari, F. Tayyari, M. Behforouz, *Spectrochim. Acta A* 60 (2004) 111.
- [12] G.Rauhut, P.Pulay, *Phys. Chem.* 99 (1995) 3093.
- [13] A.P. Scott, L. Radom, *J. Phys. Chem.* 100 (1996) 16502.
- [14] G. Fogarasi, P. Pulay, *J.Am.Chem.Soc.* 114 (1992) 8191.
- [15] V.Krishnakumar, R.John Xavier, *Indian J. Pure. Appl Phys*, 41 (2003) 597.
- [16] S.Chandra, H.Saleem, N.Sundaraganesan, S.Sebastian, *Sectrochim. Acta A* 74 (2009) 704.
- [17] M.H. Jamroz, Jan Cz. Dobrowolski, Robert Brzozowski, *J.Mol. Struct.* 787(2006) 172.

- [18] George. Socrates, *Infrared and Raman Characteristic Group Frequencies*, John Wiley, Chichester, 2001. House, New Delhi, 2001.
- [19] J. Mohan, *Organic Spectroscopy Principles and Applications*, Narosa Publishing
- [20] B. Karthikeyan, *Spectrochim. Acta* 64 A (2006) 1083.
- [21] M.Silverstein, G.Clayton Bassler, C.Morrill, *Spectrometric Identification of organic compounds*, Wiley, New York, 1981.
- [22] M.Arivazhagan, V.Krishnakumar, G.John Xavier, V.Ilango, K.Balachandran, *Spectrochim. Acta* A 72 (2009) 941.

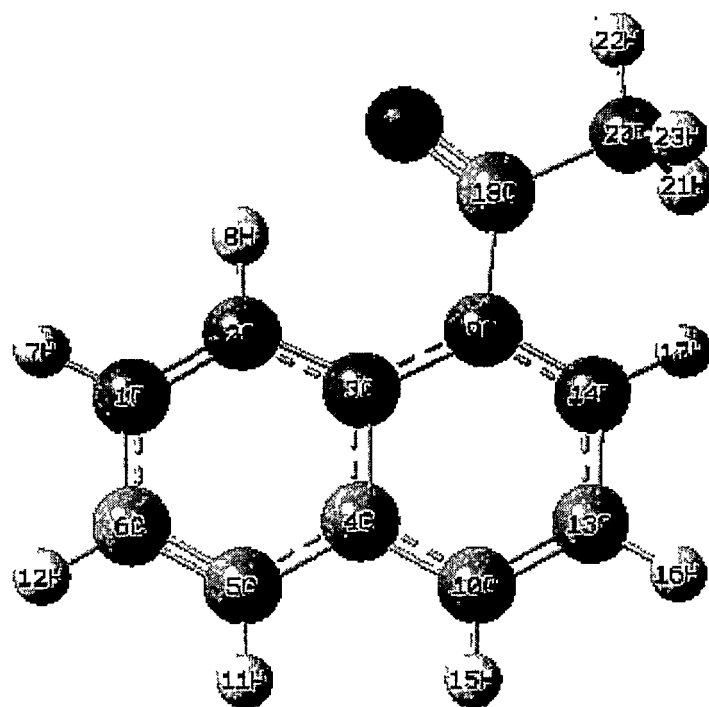


**Fig 7.1 Molecular structure of  $\alpha$ -acetonaphthone**

# $\alpha$ -acetonephthone

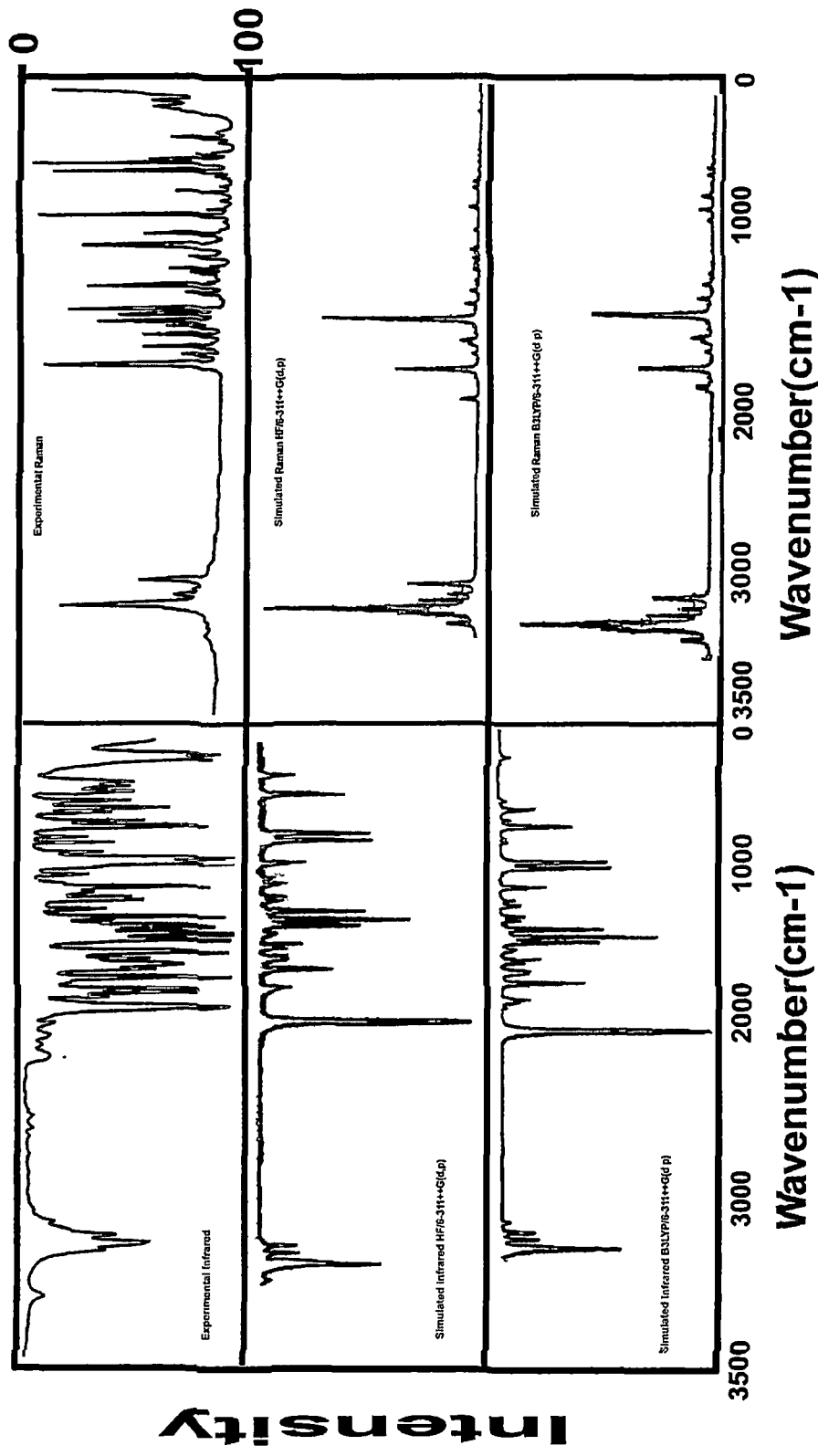
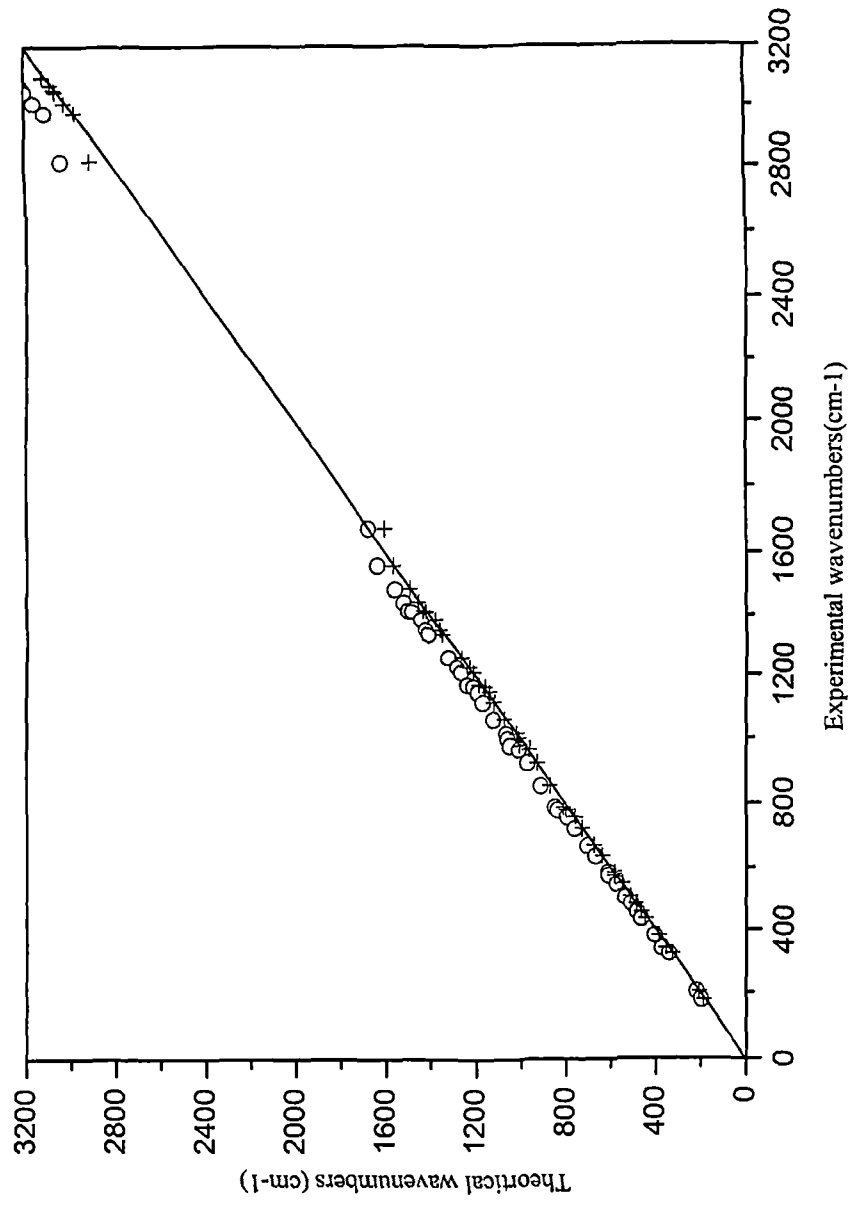


Figure 7.2: Experimental and Simulated Infrared spectra



**Fig 7.3 Unscaled (o) and scaled (x) B3PW91/6-311G vibrational wavenumbers in comparison to experimental data  $\alpha$ - acetonaphthone**

**Table 4**  
Detailed assignments of theoretical wavenumbers  $\alpha$  acetanaphthone along with potential energy distribution

Symmetry species	Experiment value		DFT theoretical value												PED $\geq 10\%$	Mode of description		
	IR	Raman	LSDA <sup>a</sup>						B3LYP <sup>b</sup>								B3PW91/6-311G	
			3-21G	6-31G	6-311G	3-21G	6-31G	6-311G	3-21G	6-31G	6-311G	I <sub>i</sub>	R <sub>act</sub>					
A	3098		3131	3147	3118	3151	3155	3129	3135	3145	3119	1412	56.54	$\gamma$ CH (98)	$\gamma$ CH			
A		3072	3126	3144	3115	3112	3106	3088	3101	3110	3084	15.62	155.74	$\gamma$ CH (95)	$\gamma$ CH			
A'	3055		3116	3136	3107	3090	3083	3088	3085	3093	3069	36.32	257.59	$\gamma$ CH (86)	$\gamma$ CH			
A'	3049		3115	3128	3088	3087	3080	3063	3080	3089	3063	25.33	112.07	$\gamma$ CH (94)	$\gamma$ CH			
A'			3106	3118	3089	3074	3088	3050	3068	3075	3049	24.41	113.95	$\gamma$ CH (90)	$\gamma$ CH			
A'			3094	3108	3075	3065	3060	3041	3059	3067	3041	3.01	68.54	$\gamma$ CH (86)	$\gamma$ CH			
A			3093	3105	3075	3062	3056	3037	3055	3063	3037	0.74	37.56	$\gamma$ CH (83)	$\gamma$ CH			
A'		3010	3092	3104	3074	3041	3047	3019	3039	3053	3024	12.22	85.07	$\gamma$ CH <sub>3</sub> (99)	$\gamma$ CH <sub>3</sub>			
A		2977	3048	3055	3024	3001	2998	2971	3002	3006	2978	11.50	50.23	$\gamma$ CH <sub>3</sub> (100)	$\gamma$ CH <sub>3</sub>			
A'	2818		2973	2974	2946	2943	2939	2911	2935	2932	2908	3.21	146.01	$\gamma$ CH <sub>3</sub> (99)	$\gamma$ CH <sub>3</sub>			
A	1675		1670	1665	1647	1627	1712	1598	1633	1624	1607	24.25	8.57	$\gamma$ CC (53) + $\beta$ CH (12)	$\gamma$ C=O			
A			1630	1649	1621	1587	1612	1580	1590	1612	1588	50.68	24.67	$\gamma$ CO (34) + $\gamma$ CC (29) + $\beta$ CH (12)	$\gamma$ C=C			
A'		1564	1603	1623	1602	1572	1589	1566	1571	1589	1570	51.28	28.54	$\gamma$ CO (37) + $\gamma$ CC (21) + $\beta$ CH (17)	$\gamma$ C=C			
A'			1581	1614	1594	1536	1564	1546	1540	1570	1555	35.81	180.88	$\gamma$ CC (52)	$\gamma$ C=C			
A'		1490	1516	1545	1528	1494	1502	1494	1484	1508	1496	46.68	20.42	$\gamma$ CC (29) + $\beta$ CH (36)	$\gamma$ C=C			
A'		1447	1472	1482	1471	1488	1455	1468	1480	1461	1457	15.45	19.40	$\beta$ CH (36) + $\tau$ HCCC (21)	$\beta$ CH <sub>3</sub>			
A'			1470	1461	1446	1470	1452	1457	1458	1460	1452	18.67	15.21	$\beta$ CH (57)	$\gamma$ C=C			
A	1435		1446	1448	1443	1456	1444	1447	1446	1445	1438	14.77	8.99	$\beta$ CH (46) + $\tau$ HCCC (13)	CH <sub>3</sub> asym-metric def			
A'		1417	1443	1446	1425	1435	1427	1428	1428	1434	1424	16.03	26.89	$\beta$ CH (44)	$\gamma$ C=C			
A	1389		1408	1433	1422	1389	1381	1388	1380	1393	1384	7.13	15.23	$\beta$ CH (50)	$\beta$ CH			
A		1365	1400	1428	1410	1371	1355	1374	1359	1374	1364	32.55	21.49	$\beta$ CH (82)	CH <sub>3</sub> symm def			
A	1340		1381	1402	1389	1325	1344	1336	1334	1367	1354	10.68	188.71	$\gamma$ CC (67)	$\gamma$ CC			
A'			1344	1350	1348	1319	1333	1328	1327	1352	1336	0.91	0.89	$\gamma$ CC (34) + $\beta$ CH (13)	$\gamma$ CC			
A	1261		1292	1305	1296	1273	1258	1271	1267	1278	1269	57.66	9.92	$\gamma$ CC (10) + $\beta$ CH (31)	$\gamma$ CC			
A		1230	1253	1267	1256	1226	1220	1230	1224	1240	1231	133.94	37.52	$\gamma$ CC (15) + $\beta$ CH (18)	$\beta$ CH			
A'	1212		1245	1250	1242	1202	1203	1210	1207	1226	1213	10.96	4.30	$\gamma$ CC (45) + $\beta$ CH (12)	$\gamma$ CC			
A'		1170	1210	1212	1204	1192	1178	1189	1189	1196	1188	18.04	2.22	$\beta$ CH (36)	$\beta$ CH			
A'	1165		1177	1169	1163	1178	1151	1167	1172	1170	1162	3.91	0.62	$\beta$ CH (71)	$\beta$ CH			
A'		1147	1167	1164	1156	1154	1136	1145	1150	1154	1143	11.64	11.11	$\gamma$ CC (29) + $\beta$ CH (22)	$\beta$ CH			
A	1114		1138	1141	1135	1122	1112	1121	1119	1127	1120	21.22	0.28	$\beta$ CH (20) + $\tau$ HCCC (10) + $\tau$ CH (10)	$\gamma$ CC			
A'		1061	1102	1111	1100	1070	1074	1071	1071	1085	1074	9.80	9.14	$\gamma$ CC (44) + $\beta$ CH (15)	$\beta$ CH			

	1016	1052	1053	1042	1045	1019	1028	1038	1027	1022	1.93	0.78	$\beta\text{CH}_3$ rock
A'													$\tau\text{CH}$ (63)+ $\phi\text{CCC}$
A'	1000	1041	1026	1024	1035	1011	1013	1031	1026	1015	8.54	13.58	$\gamma\text{CC}(43)+\beta\text{CH}$ (16)
A'	979	1040	1024	1020	1012	986	1012	1011	1014	1006	1.58	0.49	$\tau\text{CH}(81)$ (17)
A'	1011	1011	1009	1005	1004	975	1003	1000	1005	998	9.59	30.36	$\beta\text{CCC}$ (21)+ $\tau\text{CH}(34)$
A'	975	975	981	984	985	947	983	983	985	980	2.07	0.40	$\tau\text{CH}$ (67)+ $\tau\text{CCC}$ (15)
A'	967	963	963	968	971	931	967	968	965	964	0.53	0.27	$\tau\text{CH}(63)$ (13)
A'	921	939	948	945	920	913	929	919	933	928	25.78	14.21	$\gamma\text{CC}(54)+\tau\text{CH}$ (13)
A''		906	922	917	918	899	921	914	923	918	0.02	1.27	$\tau\text{CH}(83)$ (10)
A''		880	888	880	882	859	876	879	880	872	0.10	0.39	$\tau\text{CH}(74)$ (10)
A'	790	837	845	840	814	804	809	809	817	812	0.40	8.17	$\gamma\text{CC}$ (32)+ $\beta\text{CCC}$ (12)
A'		817	820	809	803	794	805	805	810	801	89.69	0.09	$\tau\text{CH}$ (67)+ $\phi\text{CCC}$ (10)
A'		810	804	804	791	773	788	789	788	785	0.05	0.19	$\beta\text{OCC}$ (62)
A'	761	774	784	770	778	763	768	775	776	762	35.54	0.76	$\tau\text{CH}$ (32)+ $\phi\text{CCC}$ (29)
A'	725	731	742	737	737	725	736	733	738	732	0.01	0.74	$\phi\text{CH}$ (73)+ $\tau\text{CCC}$ (13)
A'	672	697	697	696	680	670	678	677	679	677	1.45	17.18	$\gamma\text{CC}$ (20)+ $\beta\text{CCC}$ (42)
A'		673	663	655	667	636	644	663	650	641	0.04	0.75	$\tau\text{CCC}$ (42)+ $\beta\text{OCC}$ (13)+ $\beta\text{CCC}$ (14)
A'	587	610	600	601	604	583	589	602	589	587	35.61	0.47	$\tau\text{CCC}$ (35)+ $\phi\text{CCC}$ (20)
A'		597	597	596	581	579	588	581	587	586	1.48	1.03	$\gamma\text{CC}$ (20)+ $\beta\text{OCC}$ (46)+ $\beta\text{CCC}$ (15)
A'	550	566	566	565	551	544	552	550	553	551	1.26	15.15	$\gamma\text{CC}$ (38)+ $\beta\text{CCC}$ (11)
A'	507	525	522	523	519	506	517	514	514	514	0.61	11.29	$\beta\text{OCC}$ (16)+ $\beta\text{CCC}$ (41)

Table 4 (Continued)

Symmetry species	Experiment value		DFI theoretical value												PED $\geq 10\%$	Mode of description		
	IR	Raman	LSDA <sup>a</sup>			B3LYP <sup>b</sup>			B3PW91 <sup>c</sup>			B3PW91/6-311G						
	3-21G	6-31G	6-31G	495	497	495	3-21G	6-31G	6-311G	488	488	488	6-31G	6-311G	$I_r$	$R_{act}$		
A''		485	495	497	495	483	492	483	490	488	488	488	488	488	16.43	0.43	$\tau$ CCC (12)+ $\beta$ OCC (25)+ $\beta$ CCC (19)	$\phi$ CCC
A''		458	466	473	469	462	469	462	469	467	463	467	465	465	0.12	0.19	$\tau$ CH (10)+ $\tau$ CCC (71)	$\phi$ CCC
A''		436	457	457	457	440	448	440	420	448	447	448	447	447	1.95	5.77	$\gamma$ CC (13)+ $\beta$ OCC (36)	$\phi$ CCC
A''	381	398	397	397	395	388	397	388	393	391	392	391	390	390	0.44	1.88	$\tau$ CCC (62)+ $\beta$ OCC (11)+ $\beta$ CCC (13)	$\phi$ CCC
A''	340	373	371	370	370	355	361	355	360	360	358	360	358	358	0.15	4.09	$\gamma$ CC (26)+ $\beta$ OCC (15)+ $\beta$ CCC (19)	$\phi$ CCC
A''	323	346	341	341	341	325	332	325	329	330	332	330	328	328	0.83	4.47	$\beta$ CCC (56)	$\phi$ CCC
A''	204	242	233	232	232	215	225	215	218	217	224	217	216	216	5.38	0.96	$\beta$ CCC (67)	$\phi$ CCC
A''		225	212	209	209	206	219	206	209	208	224	208	207	207	0.79	0.71	$\tau$ CCC (48)+ $\beta$ CCC (23)	$\phi$ CCC
A''	178	209	201	194	194	199	209	199	188	199	206	199	190	190	0.01	0.14	$\tau$ CH (50)+ $\beta$ CCC (14)	$\tau$ CH <sub>3</sub>
A''		177	177	174	174	171	175	171	171	172	174	172	170	170	2.20	0.01	$\tau$ CH (21)+ $\tau$ CCC (28)+ $\beta$ CCC (31)	$\phi$ CCC
A''		113	101	97	97	89	103	89	92	92	102	92	90	90	0.24	4.01	$\tau$ CCC (48)+ $\beta$ CCC (26)	$\phi$ CCC
A''		64	49	40	40	19	52	19	21	28	50	28	17	17	4.91	0.10	$\tau$ CCC (88)	Butterfly

$\gamma$ , Stretching;  $\beta$ , in-plane bending;  $\phi$ , out-of-plane bending;  $\tau$ , torsion;  $I_r$ , IR intensity;  $R_{act}$ , Raman activity.

<sup>a</sup> Scaling factor = 0.9934.

<sup>b</sup> Scaling factor = 0.9679.

<sup>c</sup> Scaling factor = 0.9631.

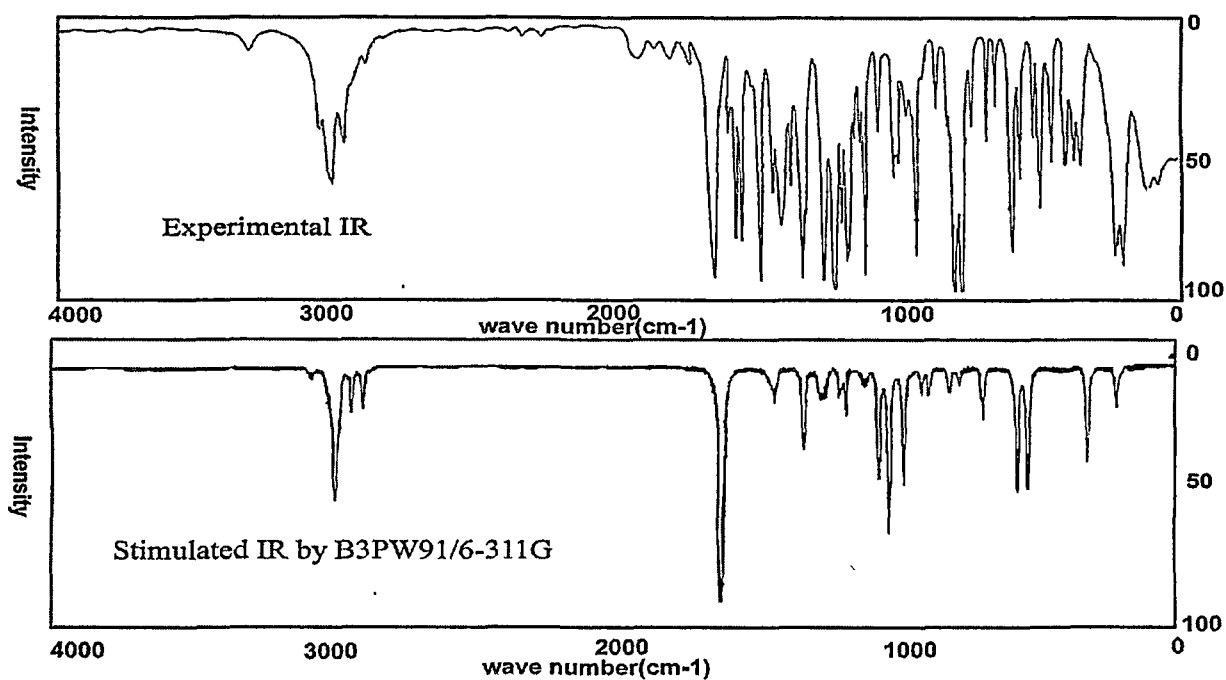


Fig. 2. Comparison of experimental and theoretical FT-IR spectrum of  $\alpha$ -acetonaphthone.

above vibrations are observed at 1419–1016  $\text{cm}^{-1}$  in FT-IR and 1447–1061  $\text{cm}^{-1}$  in FT-Raman. The theoretically scaled vibrations by B3PW91/6-311G level method also shows good agreement with experimentally recorded data. The C–H out-of-plane bending vibrations are appeared within the region 900–667  $\text{cm}^{-1}$  [22]. The vibrations identified at 1447, 1389, 1230, 1170, 1165, 1147 and 1061  $\text{cm}^{-1}$  are assigned to C–H in-plane bending. Most of the vibrations are observed in the Raman spectrum except two. The

C–H out-of-plane bending vibrations are also lie within the characteristic region.

#### 4.4. Methyl group vibrations

The methyl substituted C–H stretching vibrations usually appears below the range of aromatic C–H stretching. The  $\text{CH}_3$  stretching and bending modes appear in pure mode of vibrations.

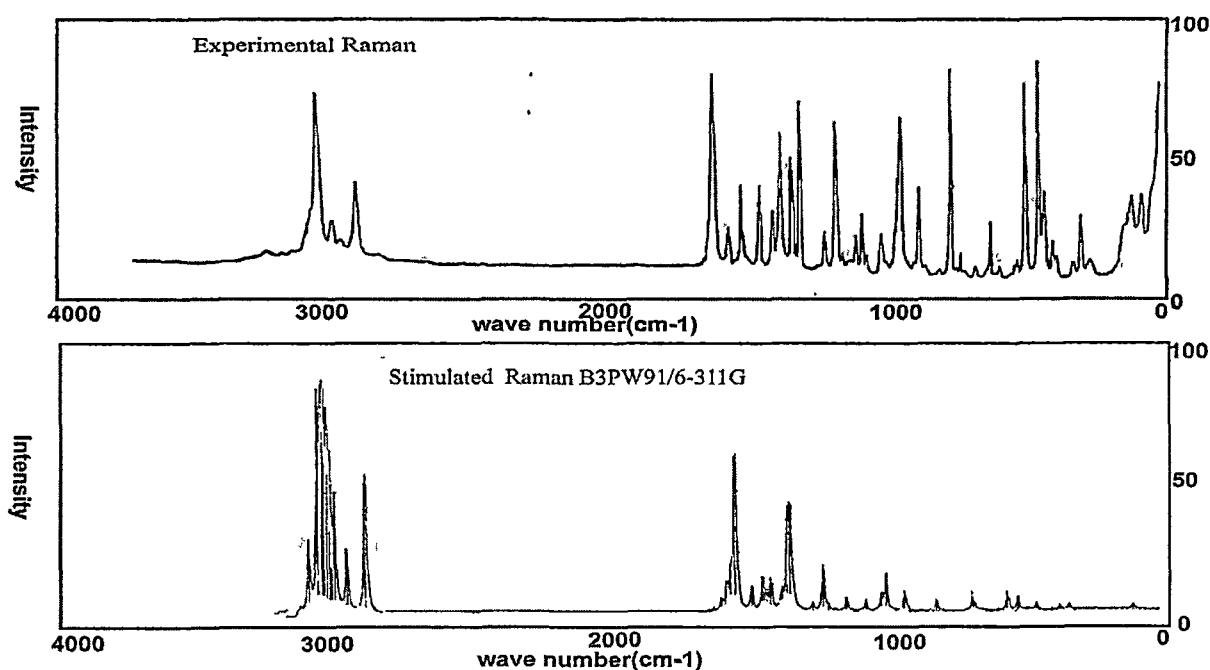


Fig. 3. Comparison of experimental and theoretical FT-Raman spectrum of  $\alpha$ -acetonaphthone.

The methyl substitution shows strongly two stretching vibrations bands identified at  $2977\text{ cm}^{-1}$  in Raman and  $2920\text{ cm}^{-1}$  in IR and Raman. But one band appeared at  $3005\text{ cm}^{-1}$  in IR. All these  $\text{CH}_3$  stretching vibrations are asymmetric with weak intensity. The theoretically calculated values by B3PW91/6-311G method at 3024, 2978 and 2908 shows good agreement with experimental values. The asymmetric and symmetric deformation vibrations of methyl group appear within the region  $1465\text{--}1440\text{ cm}^{-1}$  and  $1390\text{--}1370\text{ cm}^{-1}$  [23]. In the present investigation, the bands at  $1435\text{ cm}^{-1}$  in infrared with medium intensity and  $1365\text{ cm}^{-1}$  in Raman with strong intensity are observed as  $\text{CH}_3$  asymmetric deformation and symmetric deformation vibrations. The methyl rocking mode vibration usually appears within the region  $1070\text{--}1010\text{ cm}^{-1}$  [24]. With reference to literature data, a band observed at  $1016\text{ cm}^{-1}$  in infrared spectrum is assigned  $\text{CH}_3$  rocking vibration. The theoretically calculated value in this mode is deviated only by  $6\text{ cm}^{-1}$ . The  $\text{CH}_3$  torsional modes of vibrations are observed at very low frequencies. In our study also, a band at  $209\text{ cm}^{-1}$  in Raman is assigned to torsional mode of vibration.

#### 4.5. C=O vibrations

The characteristic infrared absorption frequency of C=O in acids are normally strong in intensity and found in the region  $1800\text{--}1690\text{ cm}^{-1}$  [25]. This position of C=O stretching more effective to analyze the various factors in ring aromatic compounds. The C=O bond formed by  $\pi\text{--}\pi$  bond between C and O intermolecular hydrogen bonding, reduces the frequencies of the C=O stretching absorption to a greater degree than does intermolecular H bonding because of the different electro-negativities of C and O, the bonding are not equally distributed between the two atoms. The lone pair of electrons on oxygen also determines the nature of the carbonyl groups. In carboxylic acids C=O band shows a strong absorption between  $1710$  and  $1760\text{ cm}^{-1}$  in IR. The C=O stretching bands of acids are considerably more intense than ketonic C=O stretching bands. The characteristic ketonic frequency C=O in the present study appears at  $1675\text{ cm}^{-1}$  in FT-Raman spectrum. This C=O vibration appears in the expected range shows that it is not much affected by other vibrations. Unfortunately, the theoretically calculated values are differing a lot from experimental value.

#### 4.6. Ring vibrations

The naphthalene ring modes are influenced more C–C bands. The ring stretching vibrations are expected within the region  $1620\text{--}1390\text{ cm}^{-1}$  [26]. Most of the ring modes are altered and missing by the substitutions to aromatic ring of naphthalene. Generally the C–C stretching vibrations in aromatic compounds form the strong bands. In present study, the bands are of different intensity and are observed at  $1564, 1490, 1417, 1340, 1261, 1212$  and  $1114\text{ cm}^{-1}$  have been assigned to C–C stretching vibrations.

The theoretically calculated values are at  $1570, 1496, 1424, 1354, 1269, 1213$  and  $1120\text{ cm}^{-1}$  by B3PW91/6-311G method and the values shows excellent agreement with experimental data. The ring in-plane bending and out-of-plane bending modes are also good agreement with experimental data.

#### 4.7. Analysis of different vibrational calculations

The execution of different methods with different basis sets are calculated and listed in Table 4. The unscaled theoretical wavenumbers are overestimated and scaled by overall scaling factors. The overall scaling factors computed by using a linear least-square fitting [12]. A disadvantage of all selective scaling procedures is the necessity to transform the force constants to nonredundant valance coordinates. But it is a tedious process for larger molecules. So

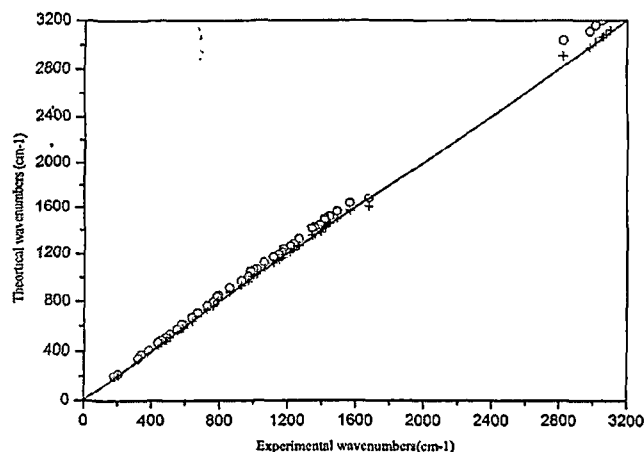


Fig. 4. Unscaled (O) and scaled (x) B3PW91/6-311G vibrational wavenumbers in comparison to experimental data of  $\alpha$ -acetonephthone.

the overall scaling is able to produce reasonably accurate force constants by simple procedure. The values of the estimated scale factors are nearly the same as those of Scott and Radom [13]. The theoretical values in different methods are in harmonic nature. A close agreement between the experimental and scaled wavenumbers is mostly achieved in the fingerprint region. A very strong IR band is assigned as C=O stretching vibration in conformity with the PED distribution. Only LSDA/3-21G describes the mode accurately than the other methods. In B3LYP and B3PW91 methods reproduces improved results after scaling, though B3PW91 method performs more accurately than B3LYP. The correlation between the calculated (unscaled and scaled) and observed results of B3PW91/6-311G method is shown in Fig. 4. It is evident from figure that by the introduction of scaling factors, the large deviations are remarkably reduced and larger error for the C=O stretching mode is also indicated. This may be due to uniform scaling factor.

## 5. Conclusion

A complete vibrational analysis of  $\alpha$ -acetonephthone is by performed DFT-B3PW91 method at 6-311G basis set level. The influences of carbon-oxygen bond and methyl group to the vibrational frequencies of the title compound were discussed. The observed and stimulated spectra are agreed for the good frequency fit. The difference between theoretical and experimental wavenumbers within  $10\text{ cm}^{-1}$  is confirmed by the qualitative agreement between the calculated and observed frequencies. In B3LYP/6-31G over estimates the C=O wavenumber, which in turn underestimates in B3LYP/6-311G. The same trend is also reflected in the optimized parameters. The global minimum energy between the different methods shows the difference in optimizations between the same and the different sets. Various quantum chemical calculations help us to identify the structural and symmetry properties of the titled molecule. The excellent agreement of the calculated and observed vibrational spectra reveals the advantages of higher basis set for quantum chemical calculations.

## References

- [1] E. Sittig, R. Marshall, Pharm. Manuf. Encycl. 39 (1988) 177.
- [2] G. Kumar, B. Tamim, Process Chemistry in the Pharmaceutical Industry, vol. 2, 2007, pp. 142–145.
- [3] R.G. Parr, W. Yang, Density Functional Theory of Atoms and Molecules, Oxford, New York, 1989.
- [4] R.O. Jones, O. Gunnarson, Rev. Mol. Phys. 61 (1989) 689.
- [5] T. Ziegler, Chem. Rev. 91 (1991) 651.
- [6] W. Kohn, L.J. Sham, Phys. Rev. A 140 (1965) 1133.

- [7] V. Krishnakumar, V. Balachandran, *Spectrochim. Acta A* 63 (2006) 464.
- [8] A. Srivastava, V.B. Singh, *Indian J. Pure. Appl. Phys.* 45 (2007) 714.
- [9] Y. Guo, Y. Xue, X. De Zhu, Y. Guo Sen, *J. Mol. Struct. (Theochem.)* 820 (2007) 40.
- [10] M.R. Jalilian, M. Zahedi-Tabrizi, *Spectrochim. Acta A* 69 (2008) 278.
- [11] M.Z. Tabrizi, S.F. Tayyari, F. Tayyari, M. Behforouz, *Spectrochim. Acta A* 60 (2004) 111.
- [12] G. Rauhut, P. Pulay, *J. Phys. Chem.* 99 (1995) 3093.
- [13] A.P. Scott, L. Radom, *J. Phys. Chem.* 100 (1996) 16502.
- [14] M.J. Frisch, G.W. Trucks, H.B. Schlegel, G.E. Scuseria, M.A. Robb, J.R. Cheeseman, J.A. Montgomery Jr., T. Vreven, K.N. Kudin, J.C. Burant, J.M. Millam, S.S. Iyengar, J. Tomasi, V. Barone, B. Mennucci, M. Cossi, G. Scalmani, N. Rega, G.A. Petersson, H. Nakatsuji, M. Hada, M. Ehara, K. Toyota, R. Fukuda, J. Hasegawa, M. Ishida, T. Nakajima, Y. Honda, O. Kitao, H. Nakai, M. Klene, X. Li, J.E. Knox, H.P. Hratchian, J.B. Cross, C. Adamo, J. Jaramillo, R. Gomperts, R.E. Stratmann, O. Yazyev, A.J. Austin, R. Cammi, C. Pomelli, J.W. Ochterski, P.Y. Ayala, K. Morokuma, A. Voth, P. Salvador, J.J. Dannenberg, V.G. Zakrzewski, S. Dapprich, A.D. Daniels, M.C. Strain, O. Farkas, D.K. Malick, A.D. Rabuck, K. Raghavachari, J.B. Foresman, J.V. Ortiz, Q. Cui, A.G. Baboul, S. Clifford, J. Cioslowski, B.B. Stefanov, G. Liu, A. Liashenko, P. Piskorz, I. Komaromi, R.L. Martin, D.J. Fox, T. Keith, M.A. Al-aham, C.Y. Peng, A. Nanayakkara, M. Challacombe, P.M.W. Gill, B. Johnson, W. Chen, M.W. Wong, C. Gonzalez, J.A. Pople, Gaussian 03, Gaussian, Inc., Pittsburgh, PA, 2003.
- [15] H. Arslan, Ö. Algül, *Int. J. Mol. Sci.* 8 (2007) 760.
- [16] M.H. Jamróz, *Vibrational Energy Distribution Analysis VEDA 4*, Warsaw, 2004.
- [17] R.I. Dennington, T. Keith, J. Millam, K. Eppinnett, W. Hovell, Gauss View Version 3.09, 2003.
- [18] G. Fogarasi, P. Pulay, *J. Am. Chem. Soc.* 114 (1992) 8191.
- [19] V. Krishnakumar, R. John Xavier, *Indian J. Pure. Appl. Phys.* 41 (2003) 597.
- [20] S. Chandra, H. Saleem, N. Sundaraganesan, S. Sebastian, *Spectrochim. Acta A* 74 (2009) 704.
- [21] M.H. Jamroz, J.C. Dobrowolski, R. Brzozowski, *J. Mol. Struct.* 787 (2006) 172.
- [22] G. Socrates, *Infrared and Raman Characteristic Group Frequencies—Tables and Charts*, third ed., Wiley, New York, 2001.
- [23] J. Mohan, *Organic Spectroscopy—Principles and Applications*, Narosa Publishing House, New Delhi, 2001.
- [24] B. Karthikeyan, *Spectrochim. Acta A* 64 (2006) 1083.
- [25] M. Silverstein, G. Clayton Bassler, C. Morrill, *Spectrometric Identification of Organic Compounds*, Wiley, New York, 1981.
- [26] M. Arivazhagan, V. Krishnakumar, R. JohnXavier, V. Ilango, K. Balachandran, *Spectrochim. Acta A* 72 (2009) 941.

## CHAPTER VIII

### BIBLIOGRAPHY

#### REFERENCES

- [1] I.Chalakkal. Jose, A.Anagha Belhkar and S.Mangala. Agashe, Spectrochim Acta aMolecular spectroscopy, 44, 899 (1988)
- [2] M.Pagannone, B.Formari, G.Mattel, Spectrochim Acta A Molecular spectroscopy, 43,621 (1987)
- [3] K.Yesook, M.Katsunosuke, Spectrochim Acta A Molecular spectroscopy, 42, 881 (1986)
- [4] P.Tarakeshwar, S.Manogaran, Spectrochim Acta A Molecular spectroscopy, 50, 2327 (1994)
- [5] M.Ramalingam, N.Sundaraganesan, H.Saleem, J.Swaminathan,Spectrochim Acta A 71 (2008) 23-30
- [6] N.Sundaraganesan, B.Anand, B.Dominic Joshua;Spectrochim Acta A;65 (2006) 1053-62
- [7] N.Sundaraganesan, C.Meganatha, B.Anand, C.Lapouge, Spectrochim Acta A 66(2006)773-8025.
- [8] N.Sundaraganesan, S.Ilakiamani, B.Dominic Joshua, Spectrochim Acta A 67 (2007)287-97
- [9] Y.Ye, M.Ruan, Y.Song,, YY.Li, W.Xie, Spectrochim Acta A 68(2007) 85-93
- [10] M.Karabacak, M.Kurt, Spectrochim Acta A 71(2008) 876-83
- [11] M.Kurt, TR.Sertbakan, M.Ozduran, Spectrochim Acta A (2008 ) 664-73
- [12] Y.Sarrafi, M. Mohadeszadeh, K. Alimohammadi, Chin. Chem. Lett. 20 (2009) 784.
- [13] W. Zhang, G. Pugh, Tetrahedron 59 (2003) 3009;
- [14] G. Rauhut, P. Pulay, J. Phys. Chem. 99 (1995) 3093-3100.
- [15] A.P. Scott, L. Radom, J. Phys. Chem. 100 (1996) 16502-16513.

- [16] P.K. Verma, A. Rashid, S. Tariq, *Ind. J. Pure Appl. Phys.* 25 (1987) 203.
- [17] S. Mohan, D. Arul Dhass, *Ind. J. Phys.* 67B (1993) 403.
- [18] J. Swaminathan, M. Ramalingam, H. Saleem, V. Sethuraman, M.T. Noorul Ameen, *Spectrochimica Acta Part A* 74 (2009) 1247–1253
- [19] J.H.S.Green, D.J.Harrison, M.R.Kipis, *Spectrochim. Acta*, 29A, (1973)1177.
- [20] B.K.Wiberg , A.V.Waltrus, N.K.Wong and D.S.Colson, *J. Phys. Chem.*, 88, 6067 (1984).
- [21] G.Ponger, P.Pulay, G.Fogarsi and E.J.Boggs, *J. Am. Chem. Soc.*, 106 2765 (1984).
- [22] R.K.Goel and M.L.Agarwal, *Indian J. Pure & Appl. Phys.*, 20 164 (1982).
- [23] S.Mohan and R.Murugan, *Indian J. Pure & Appl. Phys.*, 30 283 (1992).
- [24] S.Gunasekaran, R.S.Vardhan and K.Manoharan , *Indian J. Phys.*, 67B(1), 95 (1993).
- [25] L.Wang, Y.Fang *J.Chemical Physics* 323, 376 (2006).
- [26] N.Sundaraganesan, S.Ilakiamani , B.Anand, H.Saleem , B.Dominic Joshua, *Spectrochimica Acta A* 64 586 (2006)
- [27] Adnan Sağlam, Fatih Uçun, Vesile Güçlü , *Spectrochimica Acta A* 67 465 (2007).
- [28] Z.Zhuang, *Spectrochim. Acta*, 72, 954 (2009).
- [29] V.Krishnakumar, R.John Xavier , *Spectrochim acta A*61 253 (2005).
- [30] M.K.Subramanian, P.M.Anbarasan, S.Manimegalai, *Spectrochim acta A*73 642 (2009).
- [31] J.Swaminathan, M.Ramalingam, V.Sethuraman, N.Sundaraganesan, S.Sebastian, *Spectrochimica Acta A* 73 593 (2009).
- [32] Yu-Xi Sun, Qing-Li Hao , Zong-Xue Yu , Wen-Jun Jiang, Lu-De Lu, XinWang *Spectrochimica Acta A*73 892 (2009).
- [33] Y.Umar , *Spectrochimica Acta A*71 1907 (2009).
- [34] V.Karthikeyan, *Indian journal of chemistry* 46A 929 (2007).

- [35] B.S.Yadav, I.Ali, Pradeep Kumar,Preeti Yadav,Indain , Journal of Pure and Applied Physics 45979(2007).
- [36] <http://www.p-chloroaniline.com/> (2007).
- [37] R.B .Sing, D.R.Rai. Indian J. Pure and Appl.Phys. 20 (1982) 596.
- [38] J.A.Faniran, H.F Sharvell, Spectrochim acta, part A 38A (1982) 1155.
- [39] R.A.Kydd, A.R.C.Dunham, J. Mol. Struct. 98 (1983) 39.
- [40] P.K.Mallick, S.B.Banergee, J. Pure and Appl.Phys. 12 (1974) 296.
- [41] E.Allenstein, P.Kimle, E.Schlipf, W.Podzun, Spectrochim acta, 34A, 423(1978).
- [42] S.L Srivastava, Specroscopic studies of some distr. Substituibuted benzenes, Ph.d. Thesis , Gorkhapur university , Gorkhapur.
- [43] Y.Anantharama, Spectrochim Acta 34 A (1978) 852.
- [44] Y.Abdulla, Obaid and Mamdouh S. Soliman. Spectrochim acta, 46A (1990) 1779.
- [45] R.B.Sing , D.K.Ray, Indian J. Pure and Appl.Phys. 20 (1982) 330.
- [46] Iqbal, Krishnan, Indian J. Pure and Appl.Phys. 12 (1974) 598.
- [47] G.Quillard, G.Lourn, S.Lefrant, Phys.Rev.B50 (1994) 12496.
- [48] K.Sree Ramulu & Ramana Rao, Indian J pure & Appl Phys, 20 (1982) 372 .
- [49] E.Krishnamoorthy & Ramana Rao, J. Raman Spectrosc. 19 (1988) 359.
- [50] J.Baran, A.PawlukojÄ, I.Majerz, Z.Malarski, L.Sobczyk, E.Grech. Spectrochim Acta A 56(2000 ) 1801
- [51] A.PawlukojÄ ,I Natkaniec , G.Bator,L. Sobczyk , E.Grech , J.Nowicka-Scheibe , Spectrochim Acta A 63(2006) 766
- [52] V, Balachandran V ,Krishnakumar. ,Spectrochim Acta A 61(2005)1811.
- [53] R.Mathammal, V.Krishnakumar, S.Muthunatesan,Spectrochim Acta A70 (2008)210

- [54] D.Sajan, J.Binoy, B.Pradeep, K.Venkata Krishna, VB. Kartha, Hubert Joe I, Jayakumar VS., Spectrochim Acta A60 (2004)173
- [55] RJ.Xavier, V.Krishnakumar, Spectrochim Acta A 61(2005)1799
- [56] V.Krishnakumar, John Xavier R. Spectrochim Acta A63( 2006) 454
- [57] N.Prabavathi , V.Krishnakumar , S. Muthunatesan, Spectrochim Acta A 70(2008) 991
- [58] S.Muthunatesan, V.Krishnakumar, R.Mathammal, Spectrochim Acta A 70 (2008) 201
- [59] N.Prabavathi, V.Krishnakumar, S.Muthunatesan, Spectrochim Acta A69 (2008) 528
- [60] M.Karabacak, D.Karagöz, M. Kurt, , Spectrochim Acta A 72(2009)1076
- [61] G.Keresztury, VK.Kumar, T.Sundius, RJ.Xavier, Spectrochim Acta A 61(2005)261.
- [62] V.Krishnakumar, N. Prabavathi, S.Muthunatesan, Spectrochim Acta A 9(2008) 853
- [63] V.Balachandran, V.Krishnakumar, Spectrochim Acta A 63(2006)464
- [64] S.Muthunatesan, V.Krishnakumar, N.Prabavathi, Spectrochim Acta A70(2008)991
- [65] V.Krishnakumar, N.Prabavathi ,S. Muthunatesan , Spectrochim Acta A9(2008) 853
- [66] V, Balachandran , V.Krishnakumar ., Spectrochim Acta A 61(2005)2510
- [67] F,Ucun ,A. Sağlam A, V,Güçlü., Spectrochim Acta A 67(2007)342
- [68] V.Krishnakumar , V.Balachandran ., Spectrochim Acta A61(2005)2510
- [69] G. Keresztury, V.Krishnakumar, S.Muthunatesan, T.Sundius. Spectrochim Acta A 62(2005) 1081
- [70] J.Swaminathan, M.Ramalingam, N.Sundaraganesan, Spectrochim Acta A71 (2009)1776
- [71] HM. Badawi , W. Förner. Spectrochim Acta A 59(2003)335

- [72] V.Krishnakumar, G.Seshadri, S.Muthunatasen., *Spectrochim Acta A* 68(2007)811
- [73] V.Arjunan , N.Puviarasan, S.Mohan., *Spectrochim Acta A* 64(2006)233
- [74] SP.Jose ,S. Mohan ., *Spectrochim Acta A* 64(2006)205
- [75] R.G. Parr, W. Yang, *Density Functional Theory of Atoms and Molecules*, Oxford, New York, 1989.
- [76] R.O. Jones, O.Gunnarson, *Rev. Mol. Phys.* 61 (1989) 689-746.
- [77] T. Ziegler, *Chem.Rev.* 91 (1991) 651-667.
- [78] RJ.Xavier, V. Balachandran, M. Arivazhagan, G. Ilango, *Ind. J. Pure and App.Phy.* 78 (2010) 245-250.
- [79] V. Krishnakumar, V. Balachandran, *Spectrochim. Acta A* 63 (2006) 464-476.
- [80] A. Srivastava, V.B. Singh, *Ind. J .Pure. Appl. Phy.* 45 (2007) 714-720.
- [81] P.B. Nagabalasubramanian, S. Periandy, *Spectrochim. Acta A* 77 (2010) 1099.
- [82] P. Das, E. Arunan, P.K. Das, *Vib. Spectrosc.* 47 (2008) 1–9.
- [83] G. Rauhut, P. Pulay, *Phys. Chem.* 99 (1995) 3093-3100.
- [84] AlkaSrivastava,V.B.Singh,*Indian J.Pure.Appl.Physics.* 45 (2007) 714.
- [85] Yong Guo, Ying Xue, Xian De Zhu, Guo Sen Yana, *Theochem.* 820 (2007)
- [86] M.R.Jalilian, Mansoureh Zahedi– Tabrizi, *Spectrochimica. Acta A* 69 (2008) 278.
- [87] MZ.Tabrizi, SF.Tayyari, F.Tayyari, M.Behforouz,,*Spectrochim. Acta A* 60 (2004) 111.